Aix*Marseille université
Socialement engagée

NNT : 0000AIXM0000

# THÈSE DE DOCTORAT

Soutenue à Aix-Marseille Université
Le 18 septembre 2024 par

**Maëva DAOUD**

# Effets Cliniques et Neurophysiologiques de la Stimulation Electrique Transcrânienne Multi-canaux dans l'Epilepsie

**Discipline**

Biologie Santé

**Spécialité**

Neurosciences

**École doctorale**

ED 62 – Science de la vie et de la santé

**Laboratoire**

Institut de Neurosciences des Systèmes

**Composition du jury**

| | |
|---|---|
| Riëm EL TAHRY<br>UC Louvain (Belgique) | Rapporteuse |
| Serge VULLIEMOZ<br>Université Genève (Suisse) | Rapporteur |
| Fabrice WENDLING<br>Université Rennes (France) | Examinateur |
| Martine GAVARET<br>Université Paris (France) | Présidente du jury |
| Fabrice BARTOLOMEI<br>Université Aix Marseille | Directeur de thèse |
| Christian-George BENAR<br>Université Aix Marseille | Co-directeur de thèse |

galvani

DYNAMAP

APHM
Assistance Publique Hôpitaux de Marseille

# Affidavit

I, undersigned, Maëva DAOUD, hereby declare that the work presented in this manuscript is my own work, carried out under the scientific supervision of Fabrice BARTOLOMEI and Christian-George BENAR, in accordance with the principles of honesty, integrity and responsibility inherent to the research mission. The research work and the writing of this manuscript have been carried out in compliance with both the French national charter for Research Integrity and the Aix-Marseille University charter on the fight against plagiarism.

This work has not been submitted previously either in this country or in another country in the same or in a similar version to any other examination body.

Place Marseille, France, date 6 juin 2024



Cette œuvre est mise à disposition selon les termes de la Licence Creative Commons Attribution - Pas d'Utilisation Commerciale - Pas de Modification 4.0 International.

*« Plus dolet quam necesse est qui ante dolet quam necesse est. »*

*Seneca, Epistulae, Epistula XCVIII*

# List of Publications and Conferences

## 1) List of publications:

**Articles in Press:**

1. **Daoud, M**.*, Durelle, C.*, Fierain, A., Wendling, F., Ruffini, G., Benquet, P., & Bartolomei, F. (2024). Long-term Effect of Multichannel tDCS Protocol in Patients with Central Cortex Epilepsies Associated with Epilepsia Partialis Continua. *Brain topography*, 10.1007/s10548-024-01045-3.

2. Simula, S.*, **Daoud, M.***, Ruffini, G., Biagi, M. C., Bénar, C. G., Benquet, P., Wendling, F., & Bartolomei, F. (2022). Transcranial current stimulation in epilepsy: A systematic review of the fundamental and clinical aspects. *Frontiers in neuroscience*, 16, 909421

3. **Daoud, M**., Salvador, R., El Youssef, N., Fierain, A., Garnier, E., Biagi, M. C., Medina Villalon, S., Wendling, F., Bénar, C., Ruffini, G., & Bartolomei, F. (2022). Stereo-EEG based personalized multichannel transcranial direct current stimulation in drug-resistant epilepsy. *Clinical neurophysiology*, 137, 142–151.

**Articles Submitted:**

1. **Daoud, M**., Medina Villalon, S., Salvador, R., Fratello, M., Kanzari, K., Damiani, G., Garnier, E., Badier, Pizzo, F., Wendling, F., Ruffini, G., Bénar, C. G., Bartolomei, F. Local and Network Changes after Multichannel Transcranial Direct Current Stimulation Using Magnetoencephalography in Patients with Refractory Epilepsy. (In review in *Epilepsia*)

2. **Daoud, M**., Medina Villalon, S., Garnier, E., Bratu, F., Damiani, G., Salvador, R., Wendling, F., Ruffini, G., Bénar, C. G., Pizzo, F.*, Bartolomei, F.* The extent and depth of the epileptogenic zone network impact the response to transcranial direct current stimulation (tDCS). (Submitted)

## 2) Conferences and Workshops:

1. ILAE Europe Epilepsy Congress 2024, Rome, Italy. Oral Speaker: "Personalized multichannel transcranial direct current stimulation". **Daoud, M**., …, Bartolomei, F.

2. American Epilepsy Society Congress 2023, Orlando, USA. Poster: "Effects of tDCS on Source Functional Connectivity Measured with Magnetoencephalography in Patients with Refractory Epilepsy". **Daoud, M**., …, Bartolomei, F.

3. ILAE International Epilepsy Congress 2023, Dublin, Ireland. Poster: "Effects of Transcranial Direct Current Stimulation on Source Functional Connectivity Measured with MEG in Patients with Drug Resistant Epilepsy". **Daoud, M**., …, Bartolomei, F.

4. European Congress of Clinical Neuroscience (ECCN) 2023, Marseille, France. Poster: "Effects of Transcranial Direct Current Stimulation on Source Functional Connectivity Measured with Magnetoencephalography in Patients with Drug-Resistant Epilepsy: Preliminary Findings". **Daoud, M**., …, Bartolomei, F.

5. Practical MEEG Workshop 2022, Aix-en-Provence, France.

6. ILAE Europe Epilepsy Congress 2022, Geneva, Switzerland. Poster: "Personalized Multichannel Transcranial Direct Current Electrical Stimulation Guided by SEEG in Epilepsy: Clinical and Neurophysiological Effects". **Daoud, M**., …, Bartolomei, F.

7. Journées Françaises de l'Epilepsie 2021, Strasbourg, France. Oral Speaker: "Multichannel tDCS Personnalisée à partir d'Enregistrements SEEG dans l'Epilepsie Pharmacorésistante: Evaluation des Effets Thérapeutiques et Neurophysiologiques". **Daoud, M**., …, Bartolomei, F.

8. European Congress of Clinical Neuroscience (ECCN) 2021 (online). Poster

9. ILAE International Epilepsy Congress (online). Poster

# Résumé

La stimulation transcrânienne à courant continu (tDCS) est une nouvelle thérapie non invasive proposée aux patients atteints d'épilepsie pharmacorésistante (EPR). Cette méthode consiste à délivrer un courant de faible intensité au niveau du crâne à l'aide de deux (conventionnelle) ou plusieurs électrodes (multicanaux). Cette thèse vise à élucider les mécanismes peu connus de la tDCS sur le cerveau et à optimiser son efficacité dans l'épilepsie. Les objectifs étaient les suivants :

1) Evaluer les effets cliniques d'un protocole de tDCS optimisé par stimulation multicanaux personnalisée à partir des résultats SEEG.

2) Explorer les mécanismes sous-jacents à la tDCS, en se focalisant sur les modifications de connectivité fonctionnelle à partir d'enregistrements cérébraux non invasifs.

Les résultats ont confirmé l'efficacité de la tDCS pour réduire la fréquence des crises chez les patients atteints d'EPR. Nous avons observé des modifications dynamiques de la connectivité cérébrale après tDCS, avec une diminution chez les répondeurs et une augmentation chez les non-répondeurs, suggérant ainsi que la modulation des réseaux joue un rôle essentiel dans l'efficacité de la tDCS. La reconstruction des sources sur les données MEG a révélé des modifications étendues de la connectivité dans l'ensemble des régions cérébrales, indiquant un impact global de la tDCS multicanaux sur les réseaux épileptogènes.

Nos résultats ont également montré que la connectivité fonctionnelle initiale pourrait être un marqueur prédictif de la réponse à la tDCS. De plus, nous avons examiné les facteurs influençant cette réponse, variant d'un patient à l'autre. Donc, l'efficacité de la tDCS variait selon l'étendue et la profondeur de la zone épileptogène ciblée, montrant une meilleure efficacité pour des régions focales et superficielles. Les réponses à la tDCS différaient également selon les types de crises étudiées, soulignant la complexité de ses mécanismes d'action dans l'épilepsie. Cela suggère l'intégration future de l'apprentissage automatique (machine learning) pour l'identification de biomarqueurs prédictifs intégrant les caractéristiques spécifiques de chaque patient.

**Mots clés** : Stimulation Transcrânienne à Courant Continu, Epilepsie, Connectivité fonctionnelle, Réseau épileptogène, Electroencéphalographie, Magnétoencéphalographie, Traitement personnalisé.

# Abstract

Transcranial direct current stimulation (tDCS) is a new non-invasive therapy for patients with drug resistant epilepsy (DRE), based on delivering a low-intensity current through two (conventional) or multiple electrodes (multichannel). Despite promising initial clinical trials, the mechanisms underlying tDCS effects remain unclear. This PhD thesis aimed to address these gaps and enhance the effectiveness and duration of tDCS after-effects. Our objectives were:

1) To assess the clinical effects of an optimized tDCS protocol using personalized multichannel stimulation based on SEEG results.

2) To explore the mechanisms behind tDCS, focusing on functional connectivity changes on non-invasive brain recordings.

We confirmed tDCS efficacy in reducing seizure frequency in DRE patients. We have shown dynamic changes in brain connectivity induced by tDCS, with a decrease in connectivity for responders, and an increase for non-responders, suggesting that network modulation is key to tDCS efficacy. Source reconstruction on MEG data revealed widespread connectivity changes, suggesting a large-scale impact of multichannel tDCS on epileptogenic networks.

Furthermore, we underscored the potential of baseline functional connectivity as a predictive factor for tDCS responsiveness and explored factors influencing the variable response to tDCS across patients. We found that tDCS efficacy varies with the extent and depth of the targeted epileptogenic area, being more effective in focal and superficial regions. Our investigations also revealed varying responses to tDCS across different seizure types, highlighting the complexity of its mechanisms of action on epileptic brains. Our work shows the importance of considering functional connectivity as a marker for assessing tDCS impact. It paves the way to the future integration of machine learning to identify predictive biomarkers and patient-specific factors.

**Keywords**: Transcranial Direct Current Stimulation, Epilepsy, Functional Connectivity, Epileptogenic Network, Electroencephalography, Magnetoencephalography, Personalized Treatment

# Remerciements

Je tiens tout d'abord à remercier mes deux superviseurs de thèse, le Professeur Fabrice Bartolomei et le Docteur Christian Bénar pour leur confiance en me choisissant pour ce projet de thèse. Merci à Fabrice de m'avoir guidée durant ce travail de recherche, de s'être rendu disponible pour m'éclairer, et de m'avoir enrichie de tous ses enseignements, toujours avec une bienveillance extraordinaire et un humour sans pareil. Merci à Christian d'avoir su rendre didactiques les aspects les plus techniques de ce projet, et d'avoir toujours eu la patience et l'enthousiasme de nous les inculquer le mieux possible. Je n'aurais pas pu espérer de meilleurs encadrants pour ce Ph.D. ; c'est une chance d'avoir eu l'opportunité d'apprendre à vos côtés et de bénéficier de votre expérience, de votre esprit critique et de votre soutien sans faille.

Je souhaite également remercier très chaleureusement les membres de mon jury de thèse, qui marquent le point final de ce travail en apportant leur expertise et leur regard critique. Mes remerciements vont au Pr Riëm El Tahry, au Dr Fabrice Wendling, au Pr Martine Gavaret, et au Pr Serge Vulliémoz, avec qui j'ai la chance de pouvoir poursuivre ma carrière de chercheuse.

Ce travail, réalisé dans le cadre d'un essai clinique, m'a permis de vivre une expérience humaine très enrichissante grâce aux patients des différentes études, que je remercie sincèrement. Tous ont fait preuve d'une gentillesse et d'une volonté de bien faire exceptionnelles, et ils sont pour moi des exemples de résilience et de courage.

Je voudrais également remercier toute l'équipe médicale qui a travaillé à mes côtés sur ce projet, et plus particulièrement Dr Francesca Pizzo et Dr Julia Makhalova qui m'ont toujours encouragée et conseillée durant ces denières années. Merci aussi à Pauline, Mégane, et Sophie Semidei avec qui j'ai eu grand plaisir à collaborer.

Merci à l'équipe de la MEG avec qui j'ai partagé de très bons moments tout au long de cette thèse. Merci à Bruno pour ta disponibilité et ton aide précieuse avec AnyWave et BIDS quand je faisais des bêtises… Merci à Jean-Michel, véritable puits de connaissances, pour tes anectodes et pour toutes nos discussions équestres. Merci à Khoubeib d'avoir rendu les enregistrements MEG beaucoup plus funs.

Cette thèse n'aurait jamais été la même sans l'open space, ces amis avec qui j'ai partagé des rires quotidiens, des discussions sans fin, des débats mémorables, ainsi que des afterworks et même des vacances ! Merci à vous d'avoir été là durant tous les moments importants de ma vie ces quatre dernières années. Merci à toi, Sara, ma binôme de thèse, avec qui j'ai commencé et terminé cette aventure unique. Merci pour ton soutien, pour tes anectodes toujours incroyables, et aussi pour tes tiramisus (trop rares hélas). Merci à Sam pour ton aide technique sans limite, pour ton humour et pour avoir tout rendu possible. Merci à Elodie pour tellement de choses que je ne pourrais pas tout

énumérer, mais particulièrement pour ton aide avec les statistiques, pour avoir répondu à toutes mes requêtes, toujours dans la bonne humeur et les rires. J'ai adoré détester découvrir les résultats avec toi ! Merci aussi à Eya, d'avoir été la meilleure voisine de bureau durant ces derniers mois. Merci à Victor de trouver si aisément des solutions à tous les problèmes. Merci à Zoé pour ton soutien indéniable et pour nos galères partagées. Merci à Maria (même pour BIDS…), Aurore, Flavius, Nicolas, Safia, Lisa, pour rendre le quotidien si léger et lumineux. Et merci à mes copines Aude et Emma avec qui la thèse avait déjà si bien commencé ; vous m'avez beaucoup manqué par la suite.

Je tiens aussi à remercier mes copines du Lion d'Or, qui ont été une partie essentielle de mon quotidien depuis 2020. Merci à Solenne, Laure, Fred, Aurélie, Eva, Julie, Léa, pour tous ces moments hors du temps, remplis de joie, et de confidences. Merci aussi à Nanou de m'apprendre à me dépasser et à ne jamais baisser les bras.

Une pensée à mes amis de longue date : Lucas, Charles, Marie, qui m'ont toujours entourée et suivie au fil des années. Un grand merci à toi, Marie, tu es la meilleure des amies que l'on puisse avoir. Merci pour ton soutien inconditionnel, et pour être toujours présente à mes côtés. Je me souviens encore, il y a presque 20 ans, quand on réfléchissait à nos futurs métiers… et nous voilà Docteures !

Enfin, je tiens à remercier ma famille. Merci à ma sœur, à mes oncles et tantes, et à mes grands-parents pour leurs encouragements, et pour tous les moments de bonheur partagés ensemble. Un merci spécial à Manoue et Michel pour leurs précieux conseils et pour m'avoir soutenue tout au long de mes études. Merci à mes parents de m'avoir écoutée et guidée, de m'avoir inculqué le goût de la réflexion, et de m'avoir appris les valeurs du travail et de la persévérance. J'espère que ce travail vous rendra fiers.

# Abbreviations

*tDCS: Transcranial Direct Current Stimulation*

*DRE: Drug-resistant epilepsy*

*MEG: Magnetoencephalography*

*EEG: Electroencephalography*

*SEEG: Stereoelectroencephalography*

*EI: Epileptogenicity Index*

*IED: Interictal Epileptiform Discharge*

*DBS: Deep Brain Stimulation*

*VNS: Vagus Nerve Stimulation*

*TMS: Transcranial Magnetic Stimulation*

*tACS: Transcranial Alternating Current Stimulation*

*PZ: Propagation Zone*

*FC: Functional Connectivity*

*SC: Structural Connectivity*

*TLE: Temporal Lobe Epilepsy*

*PSD: Power Spectral Density*

*ICA: Independent component Analysis*

*R: Responders*

*EF: Electric Field*

*MRI: Magnetic Resonance Imaging*

*MSI: Magnetic Source Imaging*

*ESI: Electric Source Imaging*

*SOZ: Seizure Onset Zone*

*NR: Non-responders*

*EZ: Epileptogenic Zone*

*VEP: Virtual Epileptic Patient*

*SF: Seizure Frequency*

*icoh: Imaginary Coherence*

*C1, C2, C3: Cycle 1, Cycle 2, Cycle 3*

*tES: Transcranial Electrical Stimulation*

*AE: Adverse Events*

*TI: Temporal Interference*

*TEP: Positron Emission Tomography*

*EPC: Epilepsia Partialis Continua*

*FDR: False Discovery Rate*

*EPZN: Epileptogenic and early Propagation Networks*

*FCD: Focal Cortical Dysplasia*

*SGTC: Secondarily Generalized tonic-clonic*

*HFO: High Frequency Oscillation*

*ASM: Antiseizure Medication*

# Table of Contents

**AFFIDAVIT** ..... **2**

**LIST OF PUBLICATIONS AND CONFERENCES** ..... **4**

**RÉSUMÉ** ..... **6**

**ABSTRACT** ..... **7**

**REMERCIEMENTS** ..... **8**

**ABBREVIATIONS** ..... **10**

**TABLE OF CONTENTS** ..... **11**

**1. CHAPTER I: INTRODUCTION AND THEORETICAL PRINCIPLES** ..... **14**

1.1. FOCAL EPILEPSY ..... 15

*1.1.1. Definition of epilepsy and focal epilepsy* ..... *15*

*1.1.2. Pharmacological treatments and pharmacoresistance* ..... *18*

*1.1.3. Presurgical evaluation and epilepsy surgery* ..... *19*

1.2. NEUROSTIMULATION METHODS AS AN ALTERNATIVE TO EPILEPSY SURGERY ..... 23

*1.2.1. Invasive neuromodulatory treatments* ..... *23*

*1.2.2. Non-invasive neuromodulatory treatments* ..... *25*

*1.2.3. Transcranial Electrical Stimulation (tES)* ..... *26*

1.3. NON-INVASIVE EXPLORATION OF BRAIN ACTIVITY IN EPILEPSY ..... 35

*1.3.1. Non-invasive neurophysiological recordings* ..... *35*

*1.3.2. Source localization* ..... *38*

*1.3.3. Local markers of brain activity* ..... *41*

*1.3.4. Functional connectivity* ..... *46*

1.4. THESIS OBJECTIVES AND PLAN OF INVESTIGATION ..... 51

**2. CHAPTER II: FUNDAMENTAL AND CLINICAL ASPECTS OF TRANSCRANIAL CURRENT STIMULATION IN EPILEPSY** ..... **53**

2.1. INTRODUCTION ..... 55

2.2. MATERIALS AND METHODS ..... 58

2.3. RESULTS ..... 59

*2.3.1. Clinical studies ..... 59*

*2.3.2. Network effects of application of weak electric current in epilepsy ..... 66*

*2.3.3. Neurobiological aspects ..... 68*

2.4. DISCUSSION ..... 81

**3. CHAPTER III: PERSONALIZED MULTICHANNEL TDCS PROTOCOL IN DRUG-RESISTANT EPILEPSY: A PRELIMINARY STUDY ..... 85**

3.1. INTRODUCTION ..... 87

3.2. MATERIALS AND METHODS ..... 88

3.3. RESULTS ..... 94

3.4. DISCUSSION ..... 97

3.5. SUPPLEMENTARY MATERIAL ..... 100

**4. CHAPTER IV: LOCAL AND NETWORK CHANGES AFTER MULTICHANNEL TDCS USING MEG IN EPILEPSY ..... 105**

4.1. INTRODUCTION ..... 107

4.2. MATERIALS AND METHODS ..... 107

4.3. RESULTS ..... 112

4.4. DISCUSSION ..... 117

4.5. SUPPLEMENTARY DATA ..... 120

**5. CHAPTER V: DECODING TDCS EFFICACY: UNRAVELING THE IMPACT OF EPILEPTOGENIC ZONE NETWORK EXTENT AND DEPTH IN DRUG-RESISTANT EPILEPSY ..... 126**

5.1. INTRODUCTION ..... 128

5.2. MATERIALS AND METHODS ..... 129

5.3. RESULTS ..... 132

5.4. DISCUSSION ..... 137

5.5. SUPPLEMENTARY DATA ..... 139

**6. CHAPTER VI: LONG-TERM TDCS IN EPILEPSIA PARTIALIS CONTINUA CASES ..... 142**

6.1. INTRODUCTION ..... 144

6.2. MATERIALS AND METHODS ..... 145

6.3. Results ..... 148

6.4. Discussion ..... 151

**7. CHAPTER VII: GENERAL DISCUSSION AND PERSPECTIVES ..... 154**

Summary of studies' findings ..... 155

7.1. A personalized protocol of multichannel tDCS to decrease the seizure frequency ..... 156

7.2. Functional changes in whole brain networks are related to tDCS efficacy ..... 159

7.3. Why do patients respond differently to tDCS effectiveness? ..... 161

**GENERAL CONCLUSION ..... 165**

**REFERENCES ..... 166**

**APPENDICES ..... 198**

Appendix A ..... 198

Appendix B ..... 199

**INDEX ..... 201**

# 1. Chapter I: Introduction and Theoretical Principles

The first chapter provides an introduction on the main topics related to the PhD thesis: medical context, brain stimulation mechanisms, the macroscopic brain functioning, and detailing the various methodologies employed for studying brain excitability within the scope of epilepsy.

# 1.1. Focal epilepsy

## 1.1.1. Definition of epilepsy and focal epilepsy

### *Definitions and prevalence*

Epilepsy is one of the oldest known conditions in humanity. While epilepsy had been documented since antiquity, it was not until the 20th century that international organizations, including the International League Against Epilepsy (ILAE) and the World Health Organization (WHO), formalized a comprehensive definition for the condition. Epilepsy was defined as a neurological disorder characterized by an enduring predisposition to generate epileptic seizures caused by abnormal electrical activity in the brain (Fisher *et al.*, 2005).

Epilepsy stands as a prevalent neurological condition, affecting more than 50 million people worldwide. The specific prevalence of epilepsy is approximately 6.38 per 1000 individuals, with an annual cumulative incidence of 67.77 per 100,000 people per year (Fiest *et al.*, 2016). There is a notable rise in mortality rates among individuals with epilepsy compared to the general population (Thurman *et al.*, 2017). The principal immediate causes of this elevated mortality include sudden unexpected death in epilepsy (SUDEP), status epilepticus, injuries, and suicide (Trinka *et al.*, 2023). Furthermore, comorbidities are common in epilepsy patients, impacting diagnosis, treatment, costs, and quality of life. These include medical conditions (e.g., migraine), psychiatric disorders (e.g., depression), and cognitive challenges (e.g., attention-deficit) (Seidenberg, Pulsipher and Hermann, 2009). Patients suffering from epilepsy commonly face scholar difficulties and tend to have a lower socio-professional status compared to the general population. The economic burdens encompass direct healthcare costs and indirect costs such as lost earnings due to work absence and reduced productivity. In 2019, global healthcare costs for epilepsy alone were approximately $78.95 billion (Begley *et al.*, 2022). Additionally, individuals with epilepsy face not only the potential side effects of medication and necessary lifestyle adjustments but also with the compounded vulnerability arising from the pervasive societal stigma, adding to their psychosocial burden (Thomas and Nair, 2011).

Comprehensively understanding the underlying causes of epilepsy remains challenging due to the multifaceted nature of the condition, despite its widespread prevalence and significant impact. The etiology of epilepsy can be classified into six distinct categories (Scheffer *et al.*, 2017):

- Structural: Visible abnormalities on neuroimaging, like stroke or cortical malformations.
- Genetic (idiopathic): Known or presumed genetic mutations, such as channelopathies.
- Infectious: Resulting from infections like meningitis or encephalitis.

- Metabolic: Arising from metabolic disorders like porphyria or uremia.
- Immune: Originating from immune disorders causing CNS inflammation.
- Unknown (or cryptogenic): Cause remains unidentified in about 50% of cases.

### *Seizures and epilepsy types*

An epileptic seizure is defined as a "*transient occurrence of signs and symptoms due to abnormal excessive or synchronous neuronal activity of a population of neuronal cells in the brain*" (Fisher *et al.*, 2005).

The ILAE provides guidelines for categorizing seizures types depending on the onset manifestation of the seizure which can be focal, generalized, or unknown if the available clinical data cannot identify the onset (Fisher *et al.*, 2017). The framework of epilepsy classification is illustrated in Figure I.1. Focal seizures are initiated in localized brain regions confined to one hemisphere, while generalized seizures originate from widespread brain regions in both hemispheres. Focal seizures are more commonly observed than generalized seizures, with a median incidence rate of 30.4 per 100,000 per year, in contrast to 19.6 per 100,000 per year for generalized seizures (Kotsopoulos *et al.*, 2002).

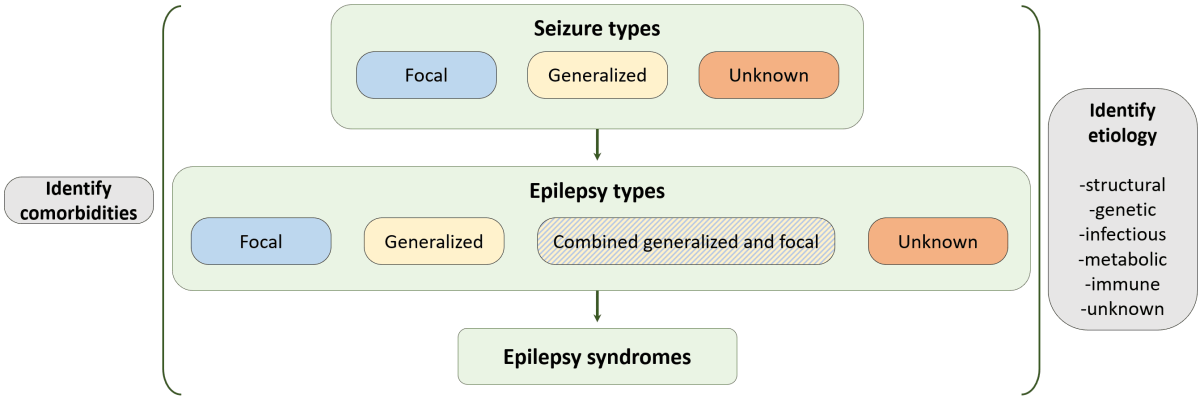


**Figure I.1. Framework of epilepsy classification.** Adapted from (Devinsky *et al.*, 2018).

Focal seizures are due to the involvement of localized brain regions, with more or less widespread start, followed by a dynamic spread of seizure activity. When considering semiology and its connection to cerebral organization, the network basis of epilepsy contrasts fundamentally with the epileptic focus model. Clinicians are increasingly recognizing the abundant evidence supporting epilepsy as a disorder of neural networks (McGonigal, Bartolomei and Chauvel, 2021). Thus, the initial concept of the focus in the case of focal epilepsy has evolved into a more complex model considering potential interactions within the neural networks involved during seizures (Wendling *et al.*, 2010; Laufs, 2012; Bartolomei, Guye and Wendling, 2013). In focal epilepsy, the epileptogenic

network is viewed as a hierarchical organization defining brain regions implicated in seizure onset and propagation (see (Bartolomei *et al.*, 2017) for a review). This conceptual model relies on spatiotemporal dynamics to govern the emergence of both ictal and interictal activities across diverse brain regions involved from the start. Within this framework, brain regions are categorized based on epileptogenicity into the epileptogenic zone network, the propagation zone network, and the non-involved zone network (Wendling *et al.*, 2010; Bartolomei *et al.*, 2017; Lagarde *et al.*, 2022) (Figure I.2). These critical zone networks also exhibit specific patterns of synchrony and desynchrony. The functional and spatiotemporal characteristics defining the epileptogenic network are outlined below in section 1.3.4.

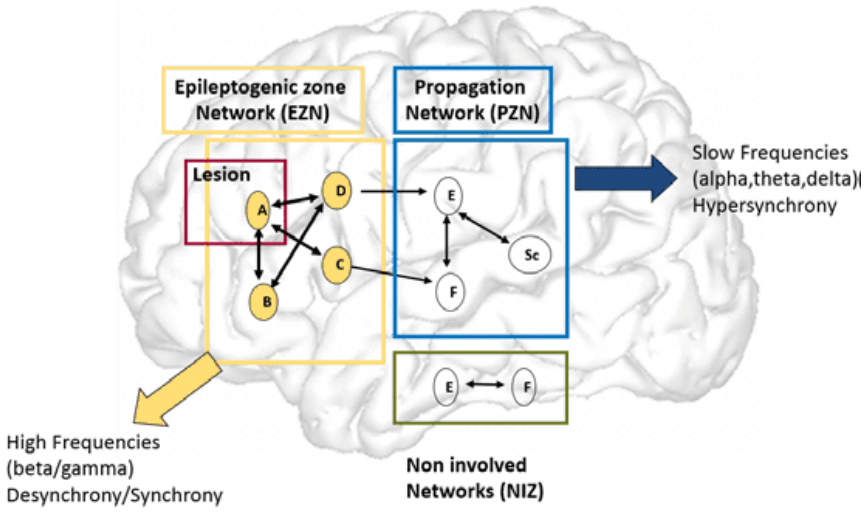


**Figure I.2. Illustration of the concept of epileptogenic networks in focal epilepsies.** Cerebral regions are designed by letters (A, B,..). The epileptogenic zone (EZ) includes brain regions capable of generating seizures, labeled as part of the EZ Network (A, B, C, and D). The EZ Network displays a distinct synchrony-desynchrony pattern. Less epileptogenic regions form the "propagation zone network" (E, F, SC, and H), with SC representing subcortical involvement. Certain regions remain uninvolved during seizure propagation, constituting the noninvolved network (NIN, G, H). From (Bartolomei *et al.*, 2017).

Focal seizures can be divided into two subtypes: those with preserved awareness, referred as focal aware seizures, and the seizures with impaired awareness (Devinsky *et al.*, 2018). Motor focal seizures can exhibit various manifestations determined by the onset brain areas, including automatisms, epileptic spasms, atonic, myoclonic, and tonic movements (Devinsky *et al.*, 2018). Non-motor focal seizures may present behavior arrest, cognitive impairment (such as transient language deficit) and may also induce an emotional or sensory component (Devinsky *et al.*, 2018). Importantly, focal seizures can spread, potentially culminating in the occurrence of a secondarily generalized seizure.

Early diagnosis is essential for effective and prompt management of seizures, resulting in better treatment outcomes, enhanced quality of life, and an overall improved

prognosis for patients with epilepsy. This multistep approach includes a thorough review of the patient's medical history, a detailed physical examination, and brain activity recordings through electroencephalogram (EEG) and neuroimaging data based on magnetic resonance imaging (MRI) (Chadwick, 1990; Kuzniecky, 2005; Nascimento *et al.*, 2023). In patients suspected of having epilepsy, the interictal EEG can reveal epileptiform activity and non-specific abnormalities. Interictal epileptiform discharges (IEDs) are brief transient increases in brain voltage and may manifest as spikes, sharp waves, and paroxysmal fast activity. These events extend to include distinctive combinations with slow waves, such as spike-and-wave complexes (characterized by a spike followed by a slow wave). The electrophysiological signatures of epileptic events are detailed below (in section 1.3.3). In the context of neuroimaging data, MRI scans enable the identification of various conditions such as malformations, vascular or traumatic lesions, tumors and more. These insights are essential for guiding targeted and effective treatment strategies (Kuzniecky, 2005; Roy and Pandit, 2011).

### 1.1.2. Pharmacological treatments and pharmacoresistance

The primary objectives in epilepsy management are to minimize or eliminate seizures, alleviate treatment-related adverse effects, address medical and neuropsychiatric comorbidities, and enhance overall quality of life. Antiseizure medication (ASM) constitute the mainstay therapeutic approach, serving as a symptomatic treatment that can reduce the occurrence and the severity of seizures (Devinsky *et al.*, 2018). Even after trying various ASMs, either as monotherapy or in combination, 36% of patients continue to experience uncontrolled seizures (Devinsky *et al.*, 2018). The ILAE defined drug-resistant epilepsy (DRE) as *"failure of adequate trials of two tolerated, appropriately chosen and used anti-epileptic drugs schedules (whether as monotherapies or in combination) to achieve sustained seizure-freedom"* (Kwan *et al.*, 2010). Moreover, DRE is associated with an increased risk of mortality compared to patients responding well to anti-epileptic treatments. Despite the emergence of many new ASMs with diverse mechanisms of action, the clinical outcomes in newly diagnosed epilepsy have not been improved (Chen *et al.*, 2018). Treatment options for DRE include trying alternative ASMs, epilepsy surgery, neurostimulation devices, and dietary therapies. Among these options, epilepsy surgery stands out as the most promising path to achieving prolonged seizure control. Epilepsy surgery aims at removing or disconnecting a part of the brain, with the objective for these patients to be seizure-free. A comprehensive evaluation is crucial to determine the most suitable surgery strategy for each patient.

## 1.1.3. Presurgical evaluation and epilepsy surgery

In patients with focal DRE, the surgical objective is to address and remove the epileptogenic zone (EZ), potentially leading to seizure freedom. According to the concept of the EZ, as introduced during the sixties by Bancaud and Talairach, it is defined as the "*site of the beginning of the epileptic seizures and of their primary organization*" (Bancaud and Talairach, 1965; Bartolomei *et al.*, 2002; Kahane *et al.*, 2006). The presurgical evaluation enables the precise identification of the EZ while ensuring its non-overlapping with eloquent brain regions. The evaluation is divided into two phases: a non-invasive and an invasive phases (Figure I.3).

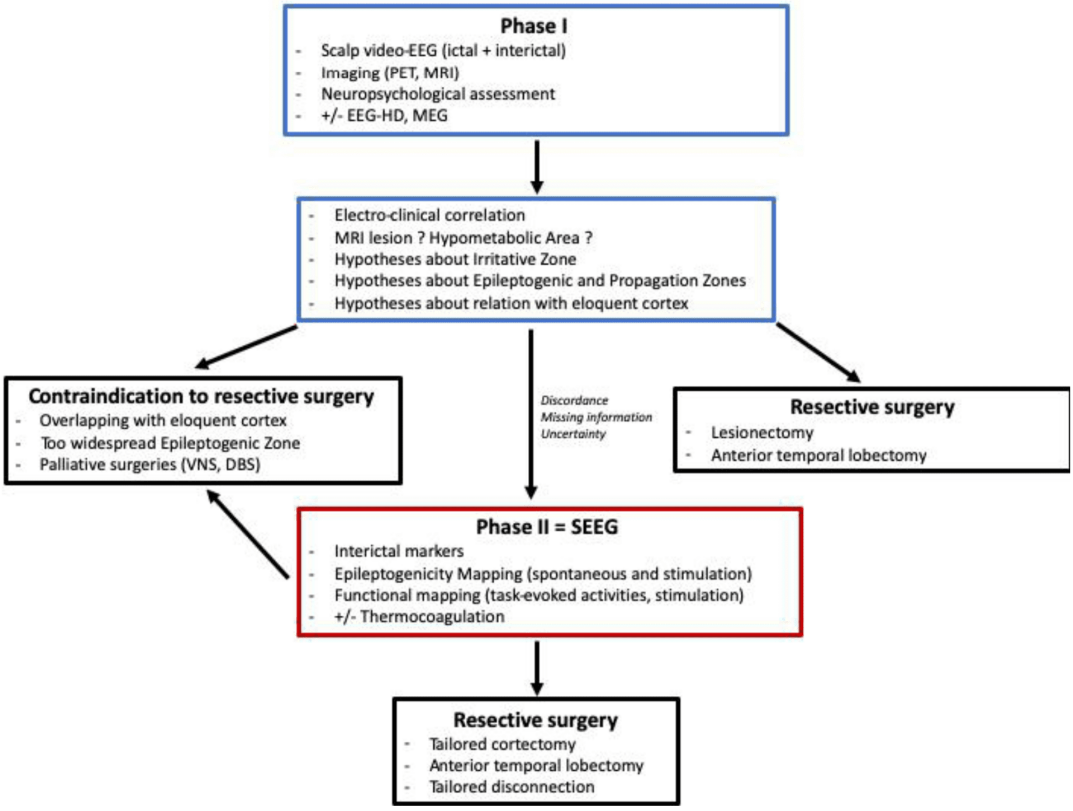


**Figure I.3. Pre-surgical assessment of focal drug-resistant epilepsy**. From (Bartolomei *et al.*, 2002).

### *Non-invasive assessment of presurgical evaluation*

During the first phase of presurgical evaluation, the patients with focal DRE undergo electrophysiological investigation combining EEG recordings with video monitoring, a procedure referred to video-electroencephalography (V-EEG). It enables clinicians to establish correlations between clinical manifestations of potential seizures and the corresponding electrophysiological activity captured by EEG (Cascino, 2002; Bartolomei *et al.*, 2004). This non-invasive exam is intended to identify initial clues regarding the affected area, such as a specific brain lobe or hemisphere, responsible for generating seizures or interictal epileptiform activities

Neuroimaging techniques also play a significant role in the pre-surgical evaluation of refractory epilepsy cases. MRI is the preferred imaging modality due to its superior capability in detecting subtle lesions such as mesial temporal sclerosis, cortical dysplasia, and small tumors (Kuzniecky, 2005; Roy and Pandit, 2011). However, cost and limited access to MRI require the use of CT scan as an alternative. By detecting metabolic abnormalities, positron emission tomography (PET) scanner also contributes to the identification of the EZ (Engel *et al.*, 1982; Lamusuo *et al.*, 2001). In cases of temporal lobe epilepsy, interictal PET reveals hypometabolism in the epileptogenic region in most patients (see review in (Verger *et al.*, 2018)).

Originally used for cognitive research, magnetoencephalography (MEG) has evolved into a powerful tool within clinical routine. Given its minimal susceptibility to magnetic field distortion from surrounding anatomical structures, including the brain, the cerebrospinal fluid, the skull, and the skin, MEG stands out as an advanced technique for recording the brain's magnetic activity. This distinctive feature provides MEG with high spatiotemporal resolution, offering insights that are complementary to EEG and MRI exams. Thus, interictal MEG recordings contribute to enhanced focus localization and functional mapping, which are essential for pre-surgical assessment (Rampp and Stefan, 2007; Stefan, 2009). MEG and EEG techniques are further described below (1.3.1) within the scope of non-invasive signal analysis methods.

Finally, the neuropsychological assessment aims at identifying any specific intellectual deficits, which can help direct attention towards a particular EZ localization, and assess the risk of cognitive deficits following surgery. When all the pieces of information gathered from these examinations converges on a specific area of the brain and indicate minimal involvement of eloquent cortex, surgical intervention may be considered for the patient. However, when there is inconsistency between electro-clinical hypotheses and MRI findings, or if the data obtained are ambiguous or conflicting, further invasive investigations are warranted to provide additional clarity and guidance in decision-making (Bartolomei *et al.*, 2002; Isnard *et al.*, 2018).

### *Invasive assessment of presurgical evaluation and surgery*

During phase 2 of presurgical evaluation, invasive EEG recordings are performed using either electrocorticography (ECoG) or stereo-electroencephalography (SEEG). In the ECoG procedure, brain surgery involves a craniotomy, where a portion of the skull is temporarily removed to access the brain surface. Subsequently, grids or strips of electrodes are positioned on the exposed cortex (Figure I.4). ECoG is preferred for mapping functional areas due to its extensive cortical coverage (Mercier *et al.*, 2022), while SEEG provides access to and monitors activity within deep cortical structures and sulci from multiple sites, encompassing both mesial and lateral brain regions.

The SEEG technique was conceived and pioneered in the 1960s by J. Talairach and J. Bancaud in France (Bancaud and Talairach, 1965; Talairach and Bancaud, 1966). The term '*strereo*' refers to the positioning of electrodes through the use of a 3D stereotactic frame. Using all non-invasive data available for a particular patient, a preoperative planning is performed. During the surgical procedure, the surgeon drills small openings in the skull and inserts needle-like multi-lead electrodes deep into the brain (Figure I.4). This approach enables a three-dimensional examination of the brain regions involved in seizure generation. The aim is to accurately characterize ictal manifestations and conduct detailed functional mapping of the explored brain areas. SEEG facilitates this by providing precise recording capabilities for both interictal and ictal discharges. Additionally, direct brain electrical stimulation is employed to trigger seizures (Chauvel *et al.*, 1993; Isnard *et al.*, 2018). The SEEG approach allows understanding of seizure onset and propagation, particularly by examining the spatiotemporal organization of epileptic discharges within the brain for each patient. By the end of this phase, detailed three-dimensional maps of the epileptogenic zone (EZ), propagation zone, irritative zone, and eloquent areas are constructed. Based on this data, clinicians can define the optimal surgical strategy, aiming at the best possible outcome while minimizing functional deficits. The SEEG can also serve as a therapeutic option thanks to SEEG-guided radiofrequency thermocoagulation (SEEG-guided RF-TC). This therapy is particularly indicated when surgical resection is contraindicated due to anatomical or functional constraints defining the EZ (Isnard *et al.*, 2018). It also permits to verify that the conclusions on the EZ are correct.

Signal analysis is crucial for interpreting SEEG data. One biomarker consists in quantifying spiking activity across different states such as wakefulness, sleep, pre-ictal, and post-ictal periods (Bartolomei *et al.*, 2017). Rapid discharges observed during seizures are key in identifying the EZ in focal epilepsy (Allen, Fish and Smith, 1992; Wendling *et al.*, 2003). The timing and spectral content of fast ictal activity are crucial for EZ determination, guiding the development of specialized signal processing methods for clinical use. Various computational tools have been developed to localize the EZ, including the Epileptogenicity Index (EI) (Bartolomei, Chauvel and Wendling, 2008), Epileptogenicity maps (Job *et al.*, 2019), the Labview tool (Gnatkovsky *et al.*, 2011), the Connectivity Epileptogenicity Index (cEI) (Balatskaya *et al.*, 2020), and methods based on graph theory or machine learning (Wang *et al.*, 2017; Grinenko *et al.*, 2018). Notably, the EI provides a quantitative assessment of the epileptogenicity of brain structures recorded with depth electrodes. This index evaluates both spectral aspects, such as the emergence of fast oscillations replacing background activity, and temporal properties, such as the delay of appearance of fast discharge in a given region (Bartolomei, Chauvel and Wendling, 2008). High EI values are indicative of structures that are involved early in the ictal process, i.e., generating rapid discharges at the onset of a seizure. Thus, this method provides additional support to clinicians for precisely identifying the specific brain region for resection in patients undergoing epilepsy surgery.

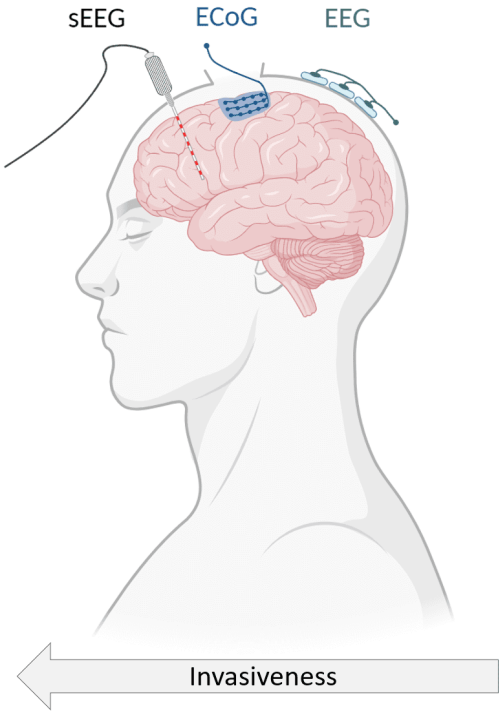


**Figure I.4. Illustration of electrophysiological recording methods used for presurgical assessment in refractory focal epilepsy**. The non-invasive method is EEG with electrodes positioned on the scalp. Invasive methods include: SEEG electrodes implanted from the skull into the cortex and ECoG subdural grid electrodes placed on the brain surface beneath the dura *(created with BioRender.com)*.

Despite the available set of pre-surgical examinations and the sophisticated methods assisting in the identification of the EZ, resection surgery is not a fail-safe solution. Epilepsy surgery involving resection can achieve sustained seizure control in 53.4–70.9% of patients considered for the procedure. Thus, even with surgical intervention, a notable proportion, approximately 30–50% of patients, may continue to experience recurrent seizures post-surgery (Baud *et al.*, 2018; Cardinale *et al.*, 2019; Lagarde *et al.*, 2019). In cases where surgical outcomes fail to achieve seizure freedom with no prospect for reoperation or when the patient is ineligible for epilepsy surgery (due to factors such as generalized epilepsy, surgical risks, multifocal or inconclusive evaluation findings, or the inability to spare eloquent areas) (El Tahry and Wang, 2017), clinicians turn to alternative treatments. These approaches, aiming to improve seizure control in difficult cases, are based on neuromodulation.

## 1.2. Neurostimulation methods as an alternative to epilepsy surgery

### 1.2.1. Invasive neuromodulatory treatments

Over recent decades, neuromodulation techniques have emerged as an alternative therapeutic strategy for individuals with focal DRE. These methods involve the application of electrical stimulation to targeted brain regions with the aim of reducing cortical excitability, which is linked to seizure generation and propagation. This approach can target various anatomical sites, using different stimulation settings, and operate via distinct mechanisms of action. Invasive neuromodulatory techniques for epilepsy involve surgical procedures where stimulation devices are implanted directly into the brain or are placed at its surface. There are three possible invasive neuromodulatory devices for focal DRE: Vagus Nerve Stimulation (VNS), Responsive Neurostimulation (RNS) and Deep Brain Stimulation (DBS) (Figure I.5).

#### *Vagus Nerve Stimulation (VNS)*

The VNS device comprises a bipolar electrode and a pulse generator, surgically implanted within the left chest wall (Figure I.5). The device stimulates the vagus nerve, inducing sufficient depolarization to generate action potentials. The exact mechanisms remain incompletely understood but likely involve a complex network connecting brainstem centers to subcortical and cortical regions (Hachem, Wong and Ibrahim, 2018). The "vagus afferent network" transmits sensory signals to various brainstem nuclei, modulating subcortical and cortical circuitry, potentially inducing changes in blood flow and neurotransmitters, likely forming the neural basis for the anti-seizure effects of VNS. This occurs through the induction of desynchronization in epileptiform activity (Fraschini *et al.*, 2013; Bartolomei *et al.*, 2016), and the modulation of thalamocortical circuits (Warsi *et al.*, 2023).

Long-term VNS therapy has proven effective in reducing seizure frequency, with approximately half of patients classified as responders experiencing a substantial reduction in seizures (Englot *et al.*, 2011). Moreover, other studies have indicated that VNS leads to a sustained improvement in the quality of life of patients with epilepsy (Ryvlin *et al.*, 2014; Englot *et al.*, 2017). Patient-specific optimal parameters, including output current, pulse width, frequency, and stimulation timing, play a crucial role in VNS effectiveness (Fahoum *et al.*, 2022). Recent devices offer additional settings for tailored stimulation. VNS is generally safe and well-tolerated, with moderate side effects such as infection, voice alteration, and sleep disturbance reported (Kuba *et al.*, 2009; Meng *et al.*, 2015).

### *Responsive Neurostimulation (RNS)*

RNS, available only in the United States, operates as a "closed-loop" neuromodulation system, responding directly to electrocorticographic signs of epileptic abnormalities to prevent seizures (Morrell, 2011). Surgically implanted, components of the RNS System include a neurostimulator and two electrode arrays, which may be depth arrays and/or strip arrays (Inaji *et al.*, 2020) (Figure I.5). Each array is equipped with four contacts positioned at epileptogenic foci. The neurostimulator is localized under the skull surface. The RNS device continuously monitors ECoG data and provides responsive electrical stimulation upon detecting abnormal patterns near the epileptogenic foci. Physicians configure stimulation parameters such as frequency, current, pulse width, and burst duration, with typical settings applied in clinical practice (Geller, 2018; Skarpaas, Jarosiewicz and Morrell, 2019). Clinical trials have shown positive outcomes with RNS, including a sustained reduction in seizure frequency of 53% after two years (Heck *et al.*, 2014). Quality of life assessments revealed meaningful improvements for 44% of patients after two years (Meador *et al.*, 2015), with limited data on pediatric effectiveness. Adverse events related to RNS may include surgical complications, changes in seizure patterns, and moderate side effects such as pain, headache, and memory impairment (Touma *et al.*, 2022).

### *Deep Brain Stimulation (DBS)*

The DBS emerged first as a treatment for movement disorders, and was applied later to epilepsy. DBS shows promises for epilepsy, targeting the thalamus, which is a central hub in epileptic activity (Pizzo *et al.*, 2021; Fisher, 2023). While various targets have shown positive outcomes, the anterior nucleus of the thalamus (ANT) is a prominent target (Fisher, 2023; Yan *et al.*, 2023). The surgical procedure involves inserting an implantable pulse generator beneath the skin in the subclavicular region, and intracranial electrodes into the ANT (Figure I.5). Stimulation parameters, typically around 130 Hz, are based on the SANTE trial, which demonstrated the efficacy and safety of ANT-DBS in reducing seizure frequency (Fisher *et al.*, 2010). Subsequent studies have confirmed its clinical benefits and cognitive improvements (Lee, Shon and Cho, 2012; Oh *et al.*, 2012). Despite its widespread use, the precise mechanism of how DBS electrically influences the central nervous system remains unclear. It is believed that the fundamental mechanisms of DBS may involve network modulation, wherein it overrides neural circuitry by effectively blocking pathological activity, and replacing efferent output (Bouwens Van Der Vlis *et al.*, 2019). Common adverse effects include implant site infection and milder symptoms like pain, paresthesia, and mood fluctuations (Bouwens Van Der Vlis *et al.*, 2019).

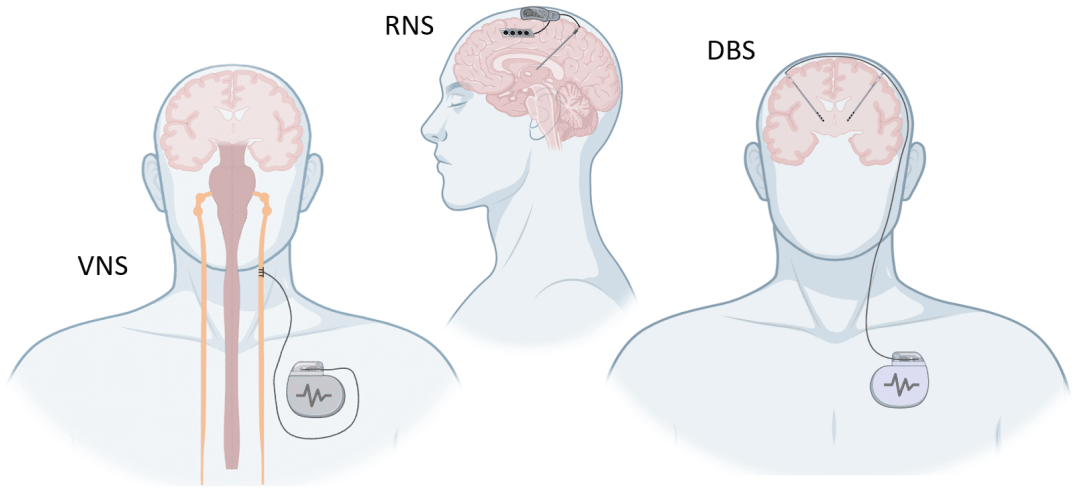


**Figure I.5. Invasive neuromodulatory devices for epilepsy.** The vagus nerve stimulation (VNS) device includes an electrode with three helical contacts attached to the vagus nerve and connected with a subclavicular implantable pulse generator. The responsive neurostimulation (RNS) device comprises a depth electrode, cortical strips, and a cranial implantable pulse generator. In the deep brain stimulation (DBS) device, depth electrodes implanted bilaterally in the thalamus are linked to a subclavicular implantable pulse generator *(created with BioRender.com)*.

## 1.2.2. Non-invasive neuromodulatory treatments

Non-invasive brain stimulation (NIBS) methods are based on transcranial stimulation involving the application of an induced or direct electrical current to modulate the underlying brain excitability. Common NIBS methods include transcranial magnetic or electric stimulation. These approaches serve as potential alternative treatment for patients with epilepsy when conventional pharmacological interventions have proven ineffective. Notably, NIBS techniques offer the advantage of avoiding the risks associated with surgical procedures (hemorrhage, infection), which exist in the case of implantable neurostimulation devices.

### *Magnetic stimulation*

Transcranial magnetic stimulation (TMS) consists in applying an electric current through a coil near the skull, generating a dynamic magnetic field that induces an electrical current within the brain (Figure I.6). Used in epilepsy for diagnosis and therapy, TMS can probe cortical excitability, evaluate ASM effects, map eloquent cortex for surgery guidance, and adjust cortical excitability (VanHaerents *et al.*, 2020). While repetitive TMS (rTMS) may influence synaptic plasticity (Reithler, Peters and Sack, 2011), its effectiveness in reducing seizure frequency remains uncertain, with inconsistent findings across studies, some reporting significant reductions and others showing no difference

compared to control groups (e.g., in (Walton *et al.*, 2021)). Clinical data generally confirms TMS safety, with minor side effects like temporary headache and muscle discomfort (VanHaerents *et al.*, 2020). Reports have documented that induced seizures can occur in patients with complex focal seizures and even be triggered spontaneously in healthy volunteers (VanHaerents *et al.*, 2020).

### *Electric stimulation*

Transcranial electrical stimulation (tES) is considered safer, less expensive and more portable compared to rTMS. tES involves applying a weak direct current (between 1 mA and 2 mA) to the brain through scalp electrodes (Figure I.6), aiming to modify cortical excitability by influencing ion channels and gradients, thereby changing the resting membrane potentials. tES has shown promising clinical effectiveness, leading to a reduction in seizure frequency in multiple studies involving patients with refractory epilepsy of diverse etiologies (San-juan *et al.*, 2015; Lefaucheur *et al.*, 2017). Despite the potential benefits of this non-invasive treatment for assisting patients facing therapeutic failures, the neurophysiological mechanisms underlying tES remain poorly understood. Clarifying the nature of tES-related effects on brain network dynamics and its local impacts could streamline the implementation of predictive biomarkers for clinical efficacy. The following section 1.2.3 provides an overall description of tES concepts, history, mechanisms of action and applications in epilepsy.

## 1.2.3. Transcranial Electrical Stimulation (tES)

### *Concepts and origins of Transcranial Electrical Stimulation (tES)*

The method of current delivery in tES determines its specific type (Figure I.6):

- **Transcranial direct current stimulation (tDCS)**: constant and unidirectional electric currents to either inhibit or excite a targeted brain area consistently.
- **Transcranial alternating current stimulation (tACS)**: alternating currents with a defined frequency, stimulating the same region with both positive and negative currents based on the waveform phase.
- **Transcranial random noise stimulation (tRNS)**: employs alternating current with random-noise frequencies for stimulation.

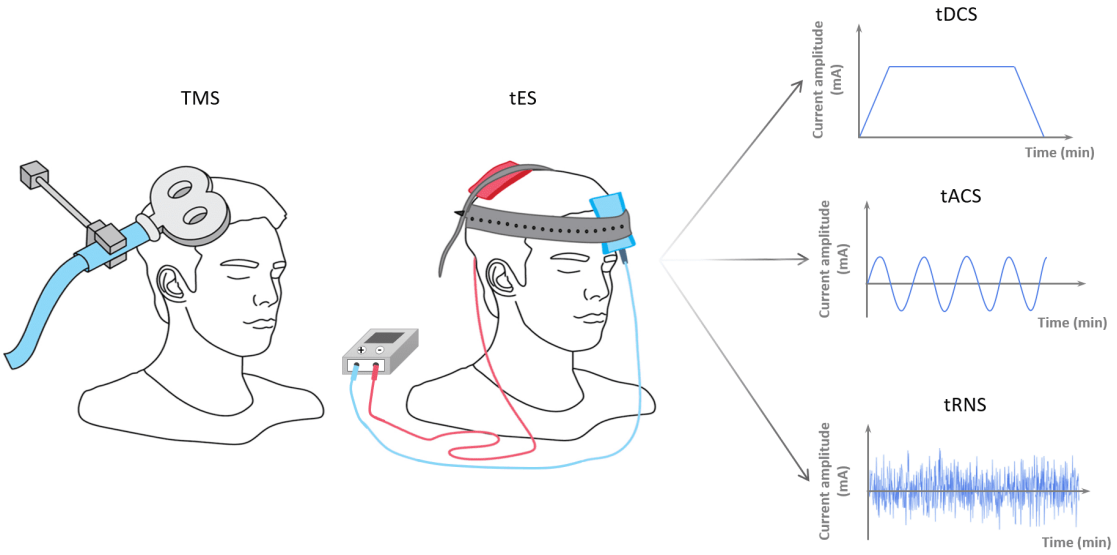


**Figure I.6. Non-invasive brain stimulation (NIBS) techniques for epilepsy.** Transcranial magnetic stimulation (TMS) and transcranial electrical stimulation (tES) are the two main non-invasive neuromodulatory methods. tES includes: Transcranial direct stimulation (tDCS), transcranial alternating current stimulation (tACS) and transcranial random-noise stimulation (tRNS). Adapted from (Ekhtiari *et al.*, 2019).

Electricity has been used for medical purposes since ancient times. In ancient Egypt, fishermen on the Nile observed that touching catfish could cause intense shocks inducing temporary numbness or anesthesia. However, it remains uncertain whether and how Egyptians used them for clinical purposes. The first documented use of electrical stimulation for therapeutic purposes appeared in ancient Greece, where Plato and Aristotle noted the healing properties of the electric ray (torpedo fish) (Sarmiento, San-Juan and Prasath, 2016). During the Roman Empire, Scribonius Largus, physician for the Emperor Tiberius Claudius Nero Caesar, successfully relieved headaches by placing a live torpedo fish over the patient's head. During the late 11$^{th}$ century, Ibn-Sidah, a prominent Muslim physician from Persia, proposed using torpedo fish as a treatment for epilepsy by placing the live fish on the patient's brow (Priori, 2003).

The use of electric fish for medical treatment continued for centuries, with the first significant developments in the late 18th and 19th centuries. Luigi Galvani and Alessandro Volta made pioneering discoveries about electricity and its interaction with muscles. Galvani's experiments on frogs showed that electricity could induce muscle contractions, suggesting the concept of "animal electricity". Volta, disagreeing with Galvani's interpretation, and conducted experiments that resulted in the creation of the first battery in 1800. Giovanni Aldini, Galvani's nephew, later, treated a patient with melancholia (depression) using galvanic currents applied to the head. Aldini postulated that galvanic scalp currents held potential benefits for the management of mental disorders. His research played a crucial role in the early development of electrotherapy.

An important advancement in the evolution of neurostimulation as a therapy occurred in the early 20th century with the introduction of electroconvulsive therapy (ECT) by the Italian psychiatrist Ugo Cerletti. In 1938, he reported that administering ECT to a patient diagnosed with schizophrenia triggered epileptic seizures, but ultimately resulting in the clinical improvement of the patient's mental illness (Patriarca *et al.*, 2021). In 1998, the adoption of direct current (DC) paved the way for the emergence of modern tES. Priori and his colleagues delved into the effects of DC on cerebral cortex excitability using TMS. Their research findings provided the first direct evidence that even a minimal electric field could penetrate the skull and influence brain excitability (Priori *et al.*, 1998). Nitsche and Paulus subsequently confirmed these findings. They also specified the effects of applying a low DC through the skull, showing that anodal stimulation increased the excitability of the motor cortex, while cathodal stimulation, on the contrary, induced inhibition (Nitsche and Paulus, 2000). From their research, they inferred that tDCS held promise as a tool for clinical neuroplasticity research. Indeed, this approach offered a painless, selective, focal, non-invasive, and reversible modulation of cortical excitability.

In the present era, tES has been explored as a potential therapeutic intervention in various pathologies and conditions including depression, chronic pain, Parkinson's disease, Alzheimer's disease, stroke rehabilitation, cognitive enhancement, and more recently, in epilepsy (San-juan *et al.*, 2015). This thesis primarily centers on tDCS, with some consideration given to tACS, as alternative therapies for DRE.

### *tDCS principles*

In the conventional tDCS system, a battery-powered controlled current generator is linked by stimulation cables to two large electrodes—one functioning as the anode and the other as the cathode—each with an area of 25–35 $cm^2$. These two large rectangular electrodes are applied to the scalp using a conducting gel. A constant current ranging between 1-2 mA is applied through scalp electrodes (usually one anode and one cathode) to either enhance or reduce neural excitability (Nitsche and Paulus, 2000). The anode refers to the scalp electrode through which conventional current flows into the brain, increasing cortical activity (Figure I.7.A). Conversely, the cathode is an electrode through which current flows out of the brain, decreasing cortical activity (Figure I.7.A). Following the application of a current, neural cells can exhibit differential polarization patterns (Figure I.7.B). The impact of the electric field thus may vary across different neuronal components, including soma, dendrites, axon initial segment, and axon tree. The specific morphology and orientation of neurons, as well as individual neuronal compartments, play a crucial role in determining whether the overall effect on the neuron will result in net depolarization or hyperpolarization (Liu *et al.*, 2018). In a typical cortical pyramidal neuron, the soma is deeper while the axon is closer to the gyrus surface. During tDCS anodal stimulation, the axon becomes hyperpolarized while the soma depolarizes. Conversely, switching the cathode with the anode results in axonal depolarization and

somatic hyperpolarization. Additionally, neurons oriented parallel to the electric field experience either hyperpolarization or depolarization, while those perpendicular to it undergo simultaneous hyperpolarization and depolarization across all compartments, resulting in minimal net polarization effects (Figure I.7.B).

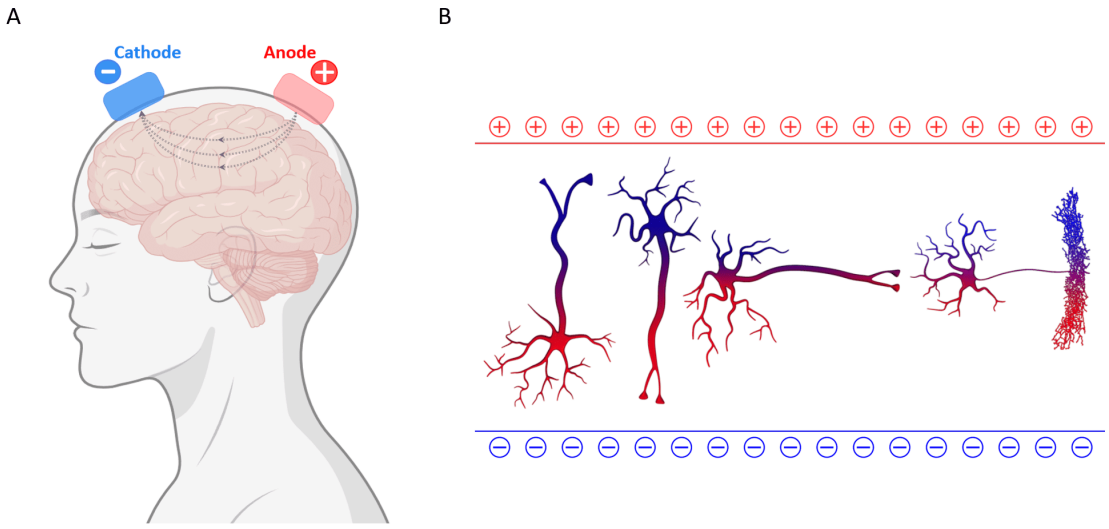


**Figure I.7. Polarization effects on neurons induced by transcranial direct current stimulation.** A) Illustration showing bipolar tES setup with two electrodes, one functioning as an anode and the other as a cathode, with current flowing from the anode to the cathode. B) Influence of neuronal compartment orientation on tES-induced excitability.

The electrical field that reaches the underlying nervous tissue is not strong enough to elicit neuronal action potentials. Instead, the immediate effects of tDCS on neurons are believed to originate from induced shifts in resting membrane potential, which subsequently influences the likelihood of action potential discharge (Polanía, Nitsche and Ruff, 2018). When a sufficient amount of current is applied, the effects on cortical excitability may persist beyond the stimulation period. These long-term changes are believed to rely on synaptic plasticity mechanisms, such as long-term potentiation (LTP) and long-term depression (LTD). Thus, anodal tDCS typically induces long-term modulatory effects that promote increased cortical facilitation, while cathodal tDCS tends to enhance inhibition (Sudbrack-Oliveira *et al.*, 2021). The effects of tDCS extend beyond electric field polarization and neuronal orientation, encompassing various factors such as stimulation duration, current intensity, number of repetitions, interval between stimulations, electrode placement, and the number of stimulation electrodes.

Differing from the constant and unidirectional electric current used in tDCS, tACS applies sinusoidal current over time (Bikson *et al.*, 2019). Through scalp electrodes, a single peak current amplitude is administered transcranially to the cortex, exhibiting a unidirectional flow from anode to cathode in one half-cycle and reversing direction in the subsequent half-cycle. Thus, in tACS, cells alternate between hyperpolarization and

depolarization depending on the phase of the sinusoidal wave. Therefore, reversing the direction of the external electric field does not significantly alter the polarization effects on neurons. Several studies have examined tACS effects on memory, sleep and other functions but its impact on epilepsy remains poorly investigated (Antal *et al.*, 2022). Recently, San-Juan et al. investigated the safety and efficacy of tACS protocols for multifocal refractory epilepsy (San-Juan *et al.*, 2022). The study found no significant reduction in seizure frequency compared to placebo and only minor adverse events, indicating a lack of evidence supporting the potential of tACS as a treatment for epilepsy. Currently, tDCS is the main non-invasive neurostimulation technique for epilepsy.

### *Application of tDCS in epilepsy*

The clinical and neurobiological effects induced by tES in epilepsy are described more precisely in Chapter 2. through a systematic review. Here, I briefly introduce the main effects of tDCS as an alternative anti-epileptic treatment and outline the key limitations observed in prior studies. In clinical practice, the use of tDCS as a non-invasive therapy for focal DRE is relatively recent, yet its usage is increasingly prevalent. In the case of epilepsy, the cathode is localized over the EZ to deliver direct currents, causing hyperpolarization and, thus, inhibition of pyramidal cells. The anode, placed over a non-involved area, completes the circuit, allowing the current to flow and targeting non-involved regions (usually the contralateral hemisphere, the supra-orbital region, or an external target such as the shoulder). Typically, the potential changes in seizure frequency and in IEDs are evaluated pre- and post-stimulation.

The first controlled clinical trial using tDCS for epilepsy treatment was conducted by Fregni et al. in 2006, involving 19 patients with refractory epilepsy. The study found that a single session of cathodal tDCS (1 mA for 20 minutes) led to a significant 44% decrease in seizure frequency (Fregni *et al.*, 2006). Further trials with higher current intensities and more sessions have shown that the method is feasible, safe, and effective for epilepsy treatment in both adults and children. By 2021, 27 studies had investigated the effect of tDCS in patients with DRE. According to a recent comprehensive review, 84% of these studies (21 out of 25) reported a significant reduction in clinical seizures (Sudbrack-Oliveira *et al.*, 2021). Importantly, out of the 27 studies, 9 employed a sham-control design, providing greater validity and reliability in assessing tDCS effects. In these trials, sham stimulation serves as a control method, involving the placement of electrodes on the scalp similar to active tDCS. During sham stimulation, only a brief, transient stimulation lasting a few seconds is administered, mimicking active tDCS without inducing the intended neurophysiological effects. Patients may initially experience similar sensations during both active and sham stimulation, as sensations of stimulation tend to diminish after a few minutes during active sessions.

Moreover, to assess the effects of tDCS on epilepsy, most study protocols incorporate scalp EEG recordings before and after tDCS sessions to measure their impact on interictal epileptiform discharges (IEDs). In line with animal and *in vitro* research, 43% of clinical trials in humans with epilepsy (6 out of 14 studies) indicated a decrease in interictal EEG abnormalities, showing the potential of cathodal stimulation in reducing the occurrence of IEDs (Sudbrack-Oliveira *et al.*, 2021). However, other studies have reported no significant EEG changes after tDCS (Varga *et al.*, 2011; Assenza *et al.*, 2017; Karvigh *et al.*, 2017; Marquardt *et al.*, 2019). Given the variability of scalp EEG data and the uncertain link between IEDs and seizure risk, exploring additional electrophysiological metrics to assess the impact of tDCS is crucial. A broader approach could provide deeper insights into the neural changes induced by tDCS, enhancing our understanding of its therapeutic mechanisms, and improving its clinical application in epilepsy management.

tDCS has been shown to be safe, with no reports of serious adverse events for both pediatric and adult cases. Mild side effects, such as itching, tingling, or skin rash at the electrode sites, are the most commonly observed events. These side effects are temporary and resolve soon after the tDCS session. More details about clinical results and side effects in tDCS trials are provided in 2.3.1.

### *Stimulation electrode montages*

In recent years, the tDCS technique has evolved with the introduction of multichannel tDCS (or HD-tDCS), which employs several pairs of smaller electrodes (~1 cm radius). Multichannel tDCS offers more precise targeting of the generated electric field over the desired area, whereas bipolar (conventional) tDCS modulates cortical activity in a larger area than that covered by the target electrode (Figure I.8). In epilepsy, employing multichannel tDCS may be favorable to enhance stimulation precision, minimizing the risk of unintended excitation in non-target regions. Multichannel tDCS offers a potential advantage in reaching deeper brain regions compared to conventional tDCS. Indeed, modeling studies have suggested that adjusting the number and positioning of scalp electrodes during tDCS could enhance both the intensity and focusing of stimulation, even for deep brain targets (Sadleir *et al.*, 2012; Ruffini *et al.*, 2014; Wagner, Burger and Wolters, 2016; Huang and Parra, 2019). Human studies have corroborated these results using tES during intracranial recordings. They proposed that tES could induce an electric field capable of reaching deep structures like the hippocampus thanks to the proximity of cerebrospinal fluid (CSF)-filled ventricles (Datta *et al.*, 2009; Huang *et al.*, 2017). However, to date, none of these studies have been clinically validated (Huang *et al.*, 2017; Louviot *et al.*, 2022).

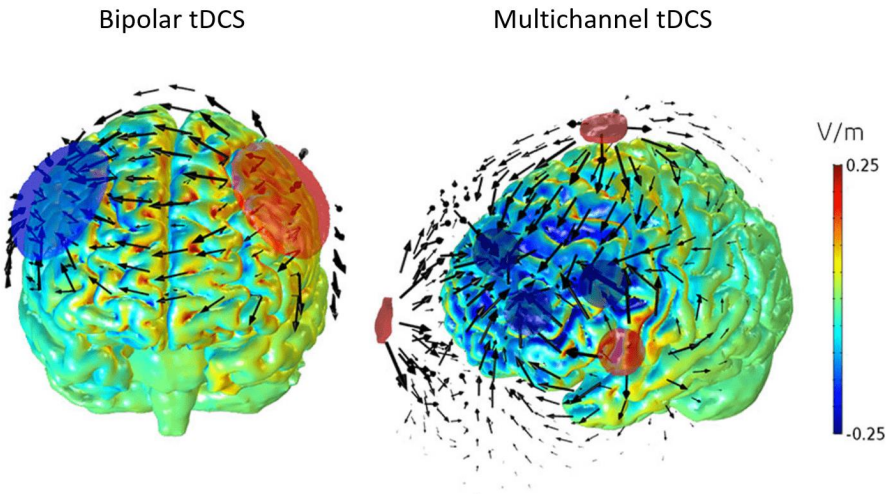


**Figure I.8. Electric field propagation on a realistic brain model generated by a conventional bipolar tDCS montage (left) and by Multichannel tDCS (right).** Cathodes are represented in blue and anodes in red. The colormap denotes the component of the electric field directed perpendicular to the cortical surface (or normal electric field, scale in V/m). The arrows depict the current density field in the brain. On the left, conventional bipolar stimulation creates a widespread field affecting a significant area of the brain. Conversely on the right, multichannel stimulation generates a more targeted field through the optimized arrangement of anodes and cathodes (*Illustration provided by NeuroElectrics®).*

Finally, using multichannel tDCS offers the opportunity to use biophysical modeling and electrophysiological and/or imaging data for optimizing electrode montage. This process is facilitated by the implementation of individualized head models, ensuring greater accuracy and effectiveness in stimulation. Indeed, it is widely accepted that even small deviations between the simulated and real brain target can result in significant variations in the distribution of electric field during transcranial electrical stimulation (Opitz *et al.*, 2018). Additionally, considering the individual cortical anatomy with patient-specific geometry of sulci and gyri is essential for accurately evaluating the correct electric field components on the brain (Miranda *et al.*, 2013). Due to the complex nature of DRE, assigning target weights to specific cortical regions can greatly enhance the effects of tES and help mitigate safety risks associated with stimulation. Notably, epilepsy studies may involve individuals with craniotomies, scars, skull defects, and varying ages. Individualizing the tDCS montage ensures the safety and reliability, and maximizes the effectiveness of the stimulation process. The outcomes of studies using multichannel tDCS are detailed in the following section, found in 2.3.1.

Despite the widespread use of tDCS in epilepsy and the emergence of innovative methodologies, the neurophysiological mechanisms underlying tDCS effects remain poorly understood. To unravel the mechanisms underlying the effects of transcranial

current stimulation on brain activity, external weak electrical fields have been applied to *in vitro*, *in vivo*, and *in silico* (computational) models, as presented in next section.

### *tDCS mechanisms*

Multiple *in vitro* and *in vivo* animal investigations have demonstrated the efficacy of both direct current (DC) and alternating current (AC) in reducing epileptiform activity. While tDCS does not directly trigger action potentials, it modulates cell firing rates, changing cortical excitability. The peak response triggered by the current, delivered at 1-2 mA, reaches approximately 1 V/m, resulting in a membrane polarization change of 0.12 mV – too low to trigger action potentials (Bikson *et al.*, 2004; Reato *et al.*, 2010). Applying transcranial direct current stimulation tDCS for several minutes can lead to long-lasting effects that are similar to long-term potentiation or depression, largely involving NMDA receptors effects (see review about tDCS mechanisms in (Lefaucheur *et al.*, 2017). The impact on individual neurons is minimal, but the effect is amplified through interaction with local endogenous fields and the cumulative activity of thousands of neurons (Francis, Gluckman and Schiff, 2003). This amplification could affect ion conductance, membrane integrity, and cytoskeletal structure exposure (San-juan *et al.*, 2015; Lefaucheur *et al.*, 2017). Beyond neurons, tDCS also influences non-neuronal brain cells like endothelial cells, lymphocytes, and glial cells, potentially impacting inflammation, neuroprotection, axogenesis, neurogenesis, neuroplasticity, and angiogenesis (Nitsche *et al.*, 2008; Rahman *et al.*, 2013) (see Table I.1). The *in vitro*, *in vivo* and computational studies of tES (tACS and tDCS separately) are further detailed in section 2.3.3.

| ACUTE EFFECTS | LONG-TERM EFFECTS |
|---|---|
| Neuronal facilitation | Neuroplasticity (Long-term Depression LTD) |
| Postsynaptic hyperpolarization | Cell migration and orientation (growth cone direction), differentiation |
| Increase potential membrane threshold | |
| Decrease of firing rate | Anti-Inflammation, migration of immune cells |
| Reduction of presynaptic input | Neurogenesis |
| Changes in ionic concentrations (decrease of intracellular $Ca^{+}$, $Na^{+}$ influx) | Transmembrane protein migration |
| Depression of synaptic force mediated by the NMDA receptors | Angiogenesis |

**Table I.1. Potential neurobiological mechanisms of cathodal transcranial direct current stimulation in epilepsy**. Adapted from (Pelletier and Cicchetti, 2015; San-juan *et al.*, 2015).

### *The Galvani project approach*

The GALVANI project (ERC Synergy, 2020-2026) focuses on optimizing tES parameters to improve epilepsy treatment. It aims to understand the impact of low-level electric fields on brain activity, exploring the best stimulation parameters, session timing, and electrode placement to identify suitable candidates for treatment. Most previous tDCS studies in epilepsy employed generic bipolar montage with large sponges (Figure I.8 on the left), with stimulation applied over one or a few treatment sessions. This approach lacks personalization and does not account for individual variations in brain anatomy. Since the effectiveness of tES relies on specific electric field patterns, a patient-specific method is needed to effectively target the desired brain regions (Miranda *et al.*, 2013; Ruffini *et al.*, 2014; Laakso *et al.*, 2015). Briefly, the approach involves creating computational models of each patient's brain, based on mathematical finite-element modeling based on MRI scans, in order to better predict current flow. In cases where patients have skull defects, individualized models are particularly important for increased accuracy. With this information, and with localization of the epileptogenic zones through SEEG data, the placement of electrodes can be optimized (Figure I.9). Using a genetic algorithm, up to eight independent electrodes can be positioned on the scalp to achieve the most effective levels and orientation of currents. The ultimate goal of this tailored approach is to inhibit a medium-sized area surrounding the epileptic focus while minimizing the impact on other brain regions. By customizing the electrode configuration to each patient's unique anatomy, the project aims to enhance tES effectiveness in treating epilepsy, offering a more personalized and potentially more successful treatment.

This Ph.D. thesis is part of the Galvani European project, aiming to explore the clinical translation of research into mapping epileptogenic networks and validating computational models and established protocols. My work investigates the clinical and neurophysiological effects of tDCS in patients, using non-invasive brain activity recordings. The last part of this general introduction covers the non-invasive electrophysiological recordings used in this thesis, along with the signal analysis methods applied in my work.

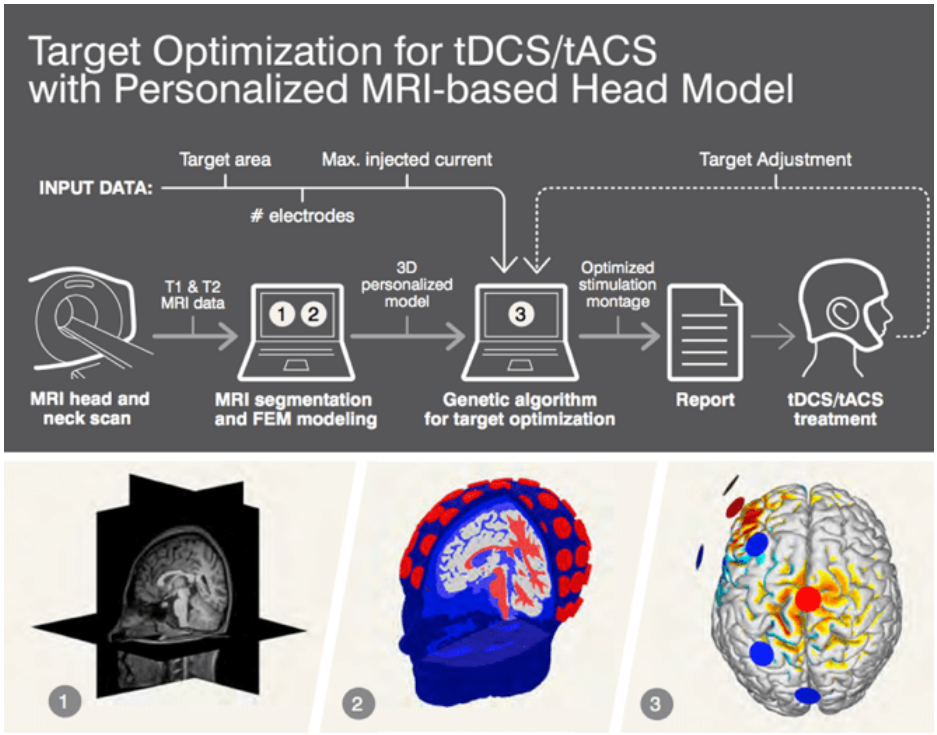


**Figure I.9. Illustration of the process for creating a personalized biophysical model of the head for transcranial electrical stimulation (tES) optimization.** (1) An anatomical MRI is used to create a finite element model (FEM) of the head. (2) Electrodes are then placed according to the 10-10 EEG system. The Stimweaver software optimizes the electrode positions and currents based on a specified target electric field and weight map, which prioritize certain brain regions. The optimization also considers other factors, such as the maximum number of electrodes and current limits. Accurate target definition requires a detailed understanding of cortical function, including network properties (Illustration provided by *Neuroelectrics ®).*

# 1.3. Non-invasive exploration of brain activity in epilepsy

## 1.3.1. Non-invasive neurophysiological recordings

### *Electroencephalography (EEG)*

Electroencephalography (EEG) measures differences in electrical potential between electrodes on the scalp, typically with conductive gel to improve contact. The EEG signal amplitude ranges from 10 to 100 µV. The 10-20 system has been classically used to record the EEG (Jasper, 1958) based on anatomical landmarks such as the nasion, inion, and pre-auricular points for electrode placement (Figure I.10). Electrodes are named according to their locations—frontopolar (Fp), frontal (F), central (C), temporal (T), parietal (P), and

occipital (O)—with even numbers for the right hemisphere and odd for the left. The standard setup uses 20 electrodes, but high-resolution EEG (HR-EEG) or high-density EEG (HD-EEG) configurations may use 64, 128, or even 256 electrodes, adding electrodes between standard points. Three common EEG montages for visualizing signals are:

- **Common Reference Montage**: Measures the potential difference between an active electrode and a shared reference point, which can be cephalic or non-cephalic.
- **Average Reference Montage**: Calculates the average from all electrodes to serve as a common reference, requiring a larger number of electrodes to be effective.
- **Bipolar Montage**: Measures the potential difference between two active electrodes on the scalp, useful for localized brain activity detection and specific patterns or anomalies.

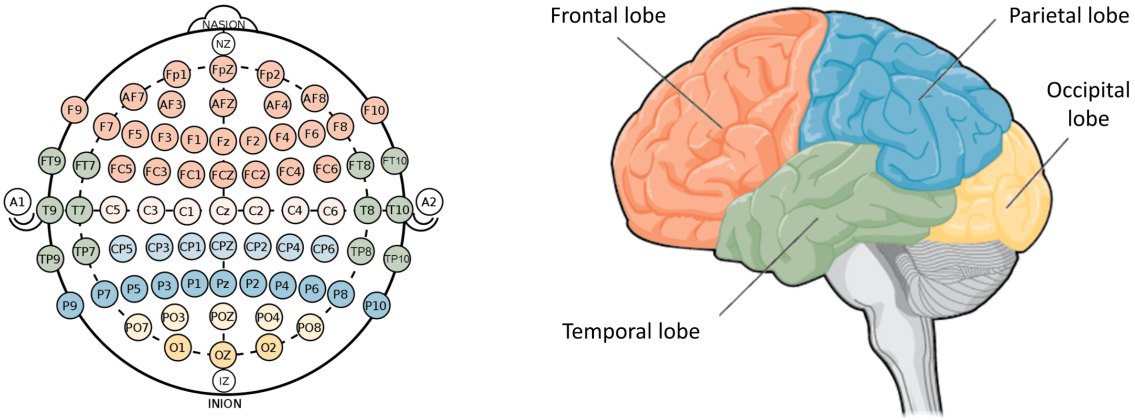


**Figure I.10. High-resolution EEG based on the extension within the 10-10 system (74 channels) (left) and the corresponding brain regions (right).** The electrode letter labeling, from front to back, is as follows: Fp (pre-frontal or frontopolar), F (frontal), C (central line of the brain), T (temporal), P (parietal), and O (occipital).

### *Magnetoencephalography (MEG)*

Magnetoencephalography (MEG) detects brain magnetic fields that are extremely faint, or the order of a few hundred of femtoteslas (10-13 fT), which is ten billion times weaker than the Earth's magnetic field. Recording these signals requires highly sensitive sensors based on low-temperature superconductors called SQUIDs (Superconducting Quantum Interference Devices), which convert magnetic flux into electrical voltage. The array of sensors is submerged in liquid helium to maintain the superconducting components at optimal operating temperatures. MEG setups also need a shielded room to minimize the influence of external magnetic fields. Modern MEG systems typically encompass between 64 to over 300 magnetometers or gradiometers in order to measure brain magnetic activity, and are configured within a helmet-shaped machine (Figure I.11).

There are different types of coils in MEG sytems:

- **Pure magnetometers**: use a single coil to measure the magnetic field (such as in Marseille, see Figure I.11).
- **Gradiometers**: use two coils to measure the gradient of the magnetic field.

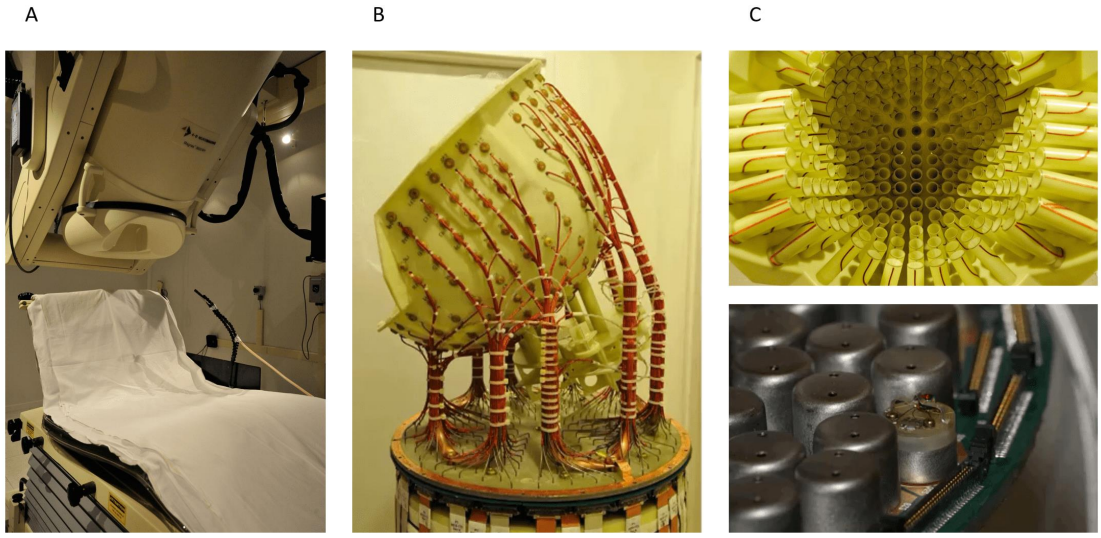


**Figure I.11. The magnetoencephalography system used at the Marseille platform.** A) The MEG system in Marseille is a 4D Neuroimaging™ 3600 whole head system equipped with 248 magnetometers operating at a sampling rate of 2034.51 Hz (4D Neuroimaging Inc., San Diego CA). B) Head helmet with Sensing coils. C) on the top: Sensing coils seen inside. Bottom right panel: SQUID sensors.

While M/EEG signals arise from similar neurophysiological processes, they exhibit notable distinctions (see Table I.2). The conductivity of brain tissue, cerebrospinal fluid, scalp, and skull affects electrical currents, reducing EEG spatial resolution, while MEG, unaffected by conductivity, has a higher spatial resolution. However, both EEG and MEG offer excellent temporal resolution (about 1 ms). EEG captures signals from both tangential and radial currents, while MEG is exclusively sensitive to tangential currents, making MEG more sensitive to activity originating in cortical sulci. EEG is less affected by head movement compared to MEG, which can suffer from imprecise localization due to movement during examination. Finally, MEG is considerably more expensive than EEG due to the complexity of its instrumentation.

| ELECTROENCEPHALOGRAPHY (EEG) | MAGNETOENCEPHALOGRAPHY (MEG) |
|---|---|
| Measures electric potentials | Measures magnetic fields |
| Field generated by primary and secondary currents | Voltage differences generated by secondary currents |
| Large signal (10 mV) | Tiny signal (10 fT) |
| Temporal resolution 0.1 ms | Temporal resolution 0.1 ms |
| Spatial resolution 1-2 cm | Spatial resolution 0.2-0.5 cm |
| Captures both tangential and radial sources | Selective for tangential sources |
| Signal distorted by skull and brain tissues (conductivity) | No distortion of signal |
| Less sensitive to head movement | Significantly sensitive to movements |
| Affordable equipment | Expensive equipment |

**Table I.2: Comparison of EEG and MEG recording features.**

In the pre-surgical assessment of epilepsy, MEG has shown effectiveness in non-invasively localizing the EZ. The standard procedure involves visually detecting IEDs, also known as "interictal spikes", followed by dipole source modeling to identify the brain's source generators (Gavaret, Badier and Chauvel, 2008).

## 1.3.2. Source localization

MEG and EEG signals capture, respectively, the magnetic and the electrical fields generated by epileptiform activities, enabling the identification of their sources through the resolution of as inverse problem—magnetic source imaging (MSI) for MEG and electric source imaging (ESI) for EEG. These techniques allow estimating the actual brain source underlying patterns of epilepsy measured at the surface, including IEDs or seizures. Large-scale studies underscore the importance of IED source localization in epilepsy presurgical evaluation (see (Mégevand and Seeck, 2018) for a comprehensive review). Below is a summary of common source reconstruction methods.

### *Forward Problem*

To identify the brain's source generators responsible for the activity detected through sensors in non-invasive brain recordings, the initial step is to solve the forward problem that link the brain sources to the sensor measurements. This involves simulating M/EEG signals mostly based on a source model, and a tissue model. The forward problem accounts for brain tissue geometry and conductivity, helping to determine how sources

are projected onto sensors. The basic spherical model considers the head as concentric spheres, each representing different tissues with specific conductivities, typically comprising scalp, skull and brain tissues (Figure I.12 on the left) (Frank, 1952), review in (Hallez *et al.*, 2007; Næss *et al.*, 2017). Some models include an extra layer representing the cerebrospinal fluid (CSF) (Næss *et al.*, 2017). For EEG, the skull low conductivity, heavily affecting electrical current flow, requires accurate modeling (Figure I.12). Realistic models, derived from anatomical MRI scans, offer a more individualized approach by segmenting MRI images to identify distinct tissue layers. Realistic models come in two types: surface models, assuming uniform conductivity within each tissue type (brain, skull, scalp) based on surface elements (boundary element model, BEM) (He *et al.*, 1987; Kybic *et al.*, 2006) and volume models based on volume finite element models (FEM) that use tetrahedral meshes to represent heterogeneous conductivities and potentially tissue anisotropy (Yan, Nunez and Hart, 1991; Wolters *et al.*, 2006).

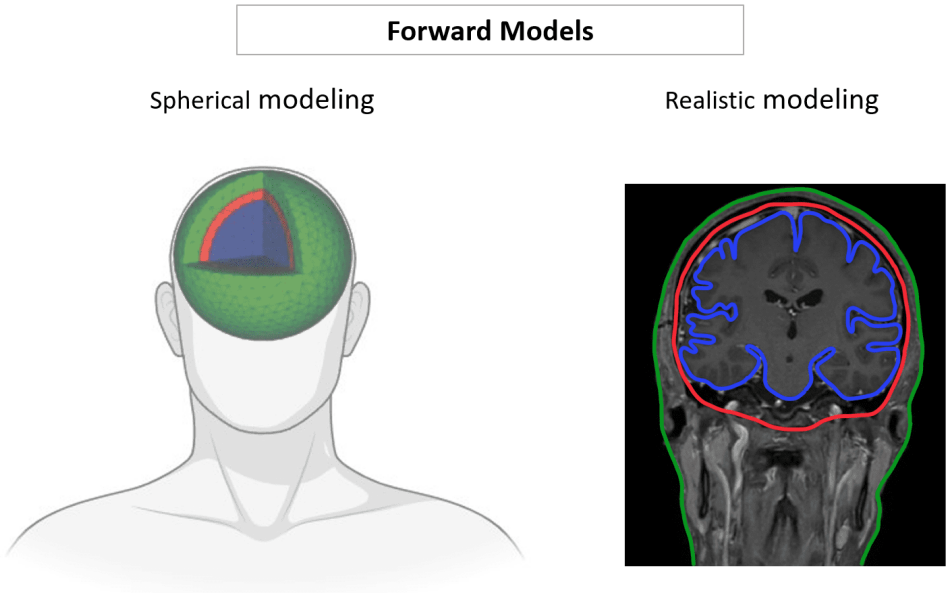


**Figure I.12. Forward modeling**. Spherical modeling (left) is based on concentric spheres, while realistic modeling involves extracting brain tissues using MRI segmentation (here, surfacic BEM modeling is used).

Unlike EEG, MEG recordings are less influenced by tissue conductivity, simplifying the forward problem approximation. Consequently, sources can be modeled using either a single sphere model or a realistic model focusing on the interior of the cranial cavity.

### *Inverse solutions*

The inverse problem in M/EEG refers to identifying the brain sources responsible for recorded signals after solving the direct problem. It requires understanding how a brain source is represented at a given sensor location, with no single solution due to the various physiological and mathematical constraints (based on fundamental laws of

physics, (Helmholtz, 1853)). Source reconstruction in M/EEG, employs various techniques to locate signal sources. These methods have different assumptions, benefits, and limitations, and are selected mostly based on signal characteristics, and required spatial resolution.

Dipole fitting or equivalent current dipole (ECD) is one of the earliest and commonly used parametric methods for source localization in M/EEG (Brazier, 1966; Schneider and Gerin, 1970). This non-linear technique assumes that cerebral electrical activity is concentrated in a few small regions relative to the sensor distance (He *et al.*, 1987; Benar *et al.*, 2005). The aim of ECD is to identify dipole parameters that minimize the residual variance – the difference between measured and estimated fields computed through the forward problem. While a single dipole is often considered, multiple dipoles may be necessary for more accurate modeling. Each dipole has six parameters: three for position, two for orientation, and one for amplitude. ECD models typically involve instantaneous localizations, often at wave peaks, and can also track activity trajectories over time in a 'moving dipole' model (He and Musha, 1992). This approach is effective in identifying early generators of evoked. Moreover, it requires specifying the number of sources in advance, which can limit its flexibility and accuracy.

Distributed source models (or distributed inverse solutions) are also a prominent approach to solving the inverse problem in M/EEG. This method identifies brain activity by considering multiple dipole sources with fixed positions and fixed or free orientations, distributed in the whole brain volume or on the cortex (Dale and Sereno, 1993; Lin *et al.*, 2006; Baillet, 2014). These models do not require deciding in advance on the number of sources. Yet, they need to address the challenge of estimating the parameters of thousands of elementary dipoles with limited data by incorporating prior information to constrain the potentially infinite solution space. The most popular model is the minimum norm estimate (MNE), which estimates the amplitudes of all source locations to reconstruct a distribution with minimal overall energy while explaining the measured data. MNE models are robust against noise and head-modeling approximations, providing computational efficiency and centimeter-level resolution (Ou, Hämäläinen and Golland, 2009; Baillet, 2014).

Scanning methods differ from previous approaches by evaluating every volume element in the brain to estimate the plausibility of presence of a dipole, rather than focusing on identifying the best dipole position to fit the data. The Multiple-SIgnal Classification (MUSIC) algorithm estimates this plausibility by assessing to which extent the contribution of a given source is consistent with the data within the selected time interval (Mosher, Lewis and Leahy, 1992). MUSIC requires defining the dimension of the signal subspace, which is an upper bound to the number of sources that are searched for. Spatial filtering techniques, referred to as "beamformers" can also be classified as scanning methods. They work by computing a filter at each spatial point to isolate the contribution of a source at that specific point while suppressing signals from other sources (Hillebrand *et al.*, 2005). Beamforming does not require prior assumptions

regarding the number of dipoles. The linearly constrained minimum variance (LCMV) beamformer enhances the signal-to-noise ratio by creating a spatial filter that minimizes the influence of noise and interference (output variance) while ensuring that the signal from the target source is accurately captured without distortion (linear constraints).

Independent Component Analysis (ICA) is a blind source separation technique, that decomposes the observed EEG and MEG signal into components. As there is an infinity of possible decomposition, one also needs to use mathematical constraints. ICA can separate and reconstruct the time-courses of EEG and MEG source signals ('*source*' is used here in the sense of blind source separation BSS, not in the sense of source localization), distinguishing between weak and strong sources and providing a unique spatial signature for each source (Jonmohamadi *et al.*, 2014). Unlike power-based previous methods that may struggle with stronger interfering signals, ICA isolates statistically independent components from multi-channel M/EEG data, aiming for temporal independence among components. The goal of the ICA algorithm is to estimate an unmixing matrix that project the original data (which is a mixture of sources) into components. The unmixing matrix reflects a linear combination of original channels, with weights adjusted to maximize the temporal independence of the output sources. The independent components can reflect synchronized or partially synchronized neural activities from one or more cortical regions, or artifacts like eye movements, muscle or cardiac activities, or technical interferences (e.g., line noise) (Vigário, 1997; Jung *et al.*, 2000). In MEG research involving epilepsy patients, ICA has been shown to be effective in identifying epileptic activities and networks (Kobayashi *et al.*, 1999; Ossadtchi *et al.*, 2004; Malinowska *et al.*, 2014; Pellegrino *et al.*, 2020).

## 1.3.3. Local markers of brain activity

### *Neural oscillations*

Brain function relies on the interactions of neural oscillations, which are characterized by their repetitive, rhythmic, and synchronized frequency patterns produced by large clusters of neurons. Neural oscillations arise from various mechanisms, including neuron excitation-inhibition cycles, pacemaker cells, resonance, and subthreshold membrane oscillations (McCormick and Bal, 1997; Buzsaki and Draguhn, 2004; Pevzner *et al.*, 2016). In the decomposition of brain sinusoidal oscillations (as depicted in Figure I.13), some parameters are important for understanding neural activity dynamics:

- Amplitude: Indicates the signal strength with variations reflecting changes in neuronal synchronization. Lower frequencies usually exhibit higher amplitudes, indicating stronger and more synchronized signal components. Conversely, higher

frequencies tend to have lower amplitudes, reflecting faster and more desynchronized oscillatory activity.

- Frequency: Measured in Hertz (Hz), indicating cycles per second. Brain oscillations are categorized into five main frequency bands: delta (0.5-4Hz), theta (4-8 Hz), alpha (8-15 Hz), beta (15-30 Hz), and gamma (>30 Hz).
- Period: represents the duration of a complete cycle of the oscillatory signal. It is inversely related to frequency.
- Phase: Denotes the position within an oscillatory cycle, measured in degrees or radians, ranging from 0° to 360° or from 0 to 2π. Phase synchronization among different brain regions is crucial for coordinating information processing and communication across the brain.

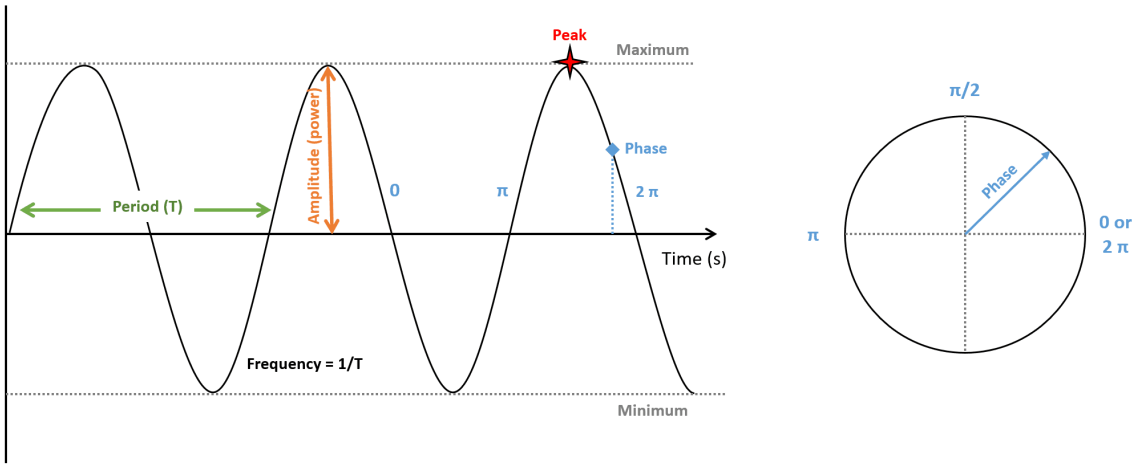


**Figure I.13. Oscillation parameters.** Frequency: Number of cycles per unit of time (s). Amplitude: Strength of the signal (size of deflections from the mean). Phase: Current position on the cycle at a given time. Period: Time duration of one cycle. Within a single cycle, the phase spans from 0 to 2 π, with the peak representing maximum activity and the trough indicating minimum activity.

### *Epilepsy biomarkers*

Studying brain oscillations and their parameters is highly relevant in epilepsy. Identifying distinct patterns in brain signals and specific alterations in neural activity could potentially serve as biomarkers for epilepsy. The accurate identification and validation of biomarkers for epileptogenesis and ictogenesis could help predict seizure susceptibility, localize seizure-generating brain tissues, and evaluate treatment efficacy. Some biomarkers can be detected through scalp recordings, such as interictal IEDs, while others may require intracerebral recordings via SEEG, such as high-frequency oscillations (HFOs). IEDs can be detected in scalp EEG recordings within the sensor space or in the source space after applying computational methods. They are also detectable through invasive brain recordings. The International Federation of Clinical Neurophysiology defined 6 criteria for IEDs, requiring at least 4 to classify a sharp transient as epileptiform (see Figure I.14) (Nascimento and Beniczky, 2023). Key characteristics for identifying

IEDs include: (1) sharp or spiky di- or tri-phasic waves with a pointed peak, (2) wave durations that are either shorter or longer than the background activity, (3) asymmetric waveforms with a sharply rising phase and a slowly decaying phase, or vice versa, (4) transient waves followed by slow after-waves, (5) disruption of the surrounding background activity by the IEDs, and (6) scalp distributions of negative and positive potentials indicating a brain source with radial, oblique, or tangential orientation (Kural *et al.*, 2020). IEDs, consisting of spike waves and sharp waves, are closely linked to epilepsy, with a strong correlation between interictal spikes and spontaneous seizures (Ayala *et al.*, 1973; Greiner *et al.*, 2016), for a review see (Ramantani *et al.*, 2023). However, many EEG recordings from epilepsy patients show no signs of IEDs, even in cases of high seizure activity (Gallotto and Seeck, 2023).

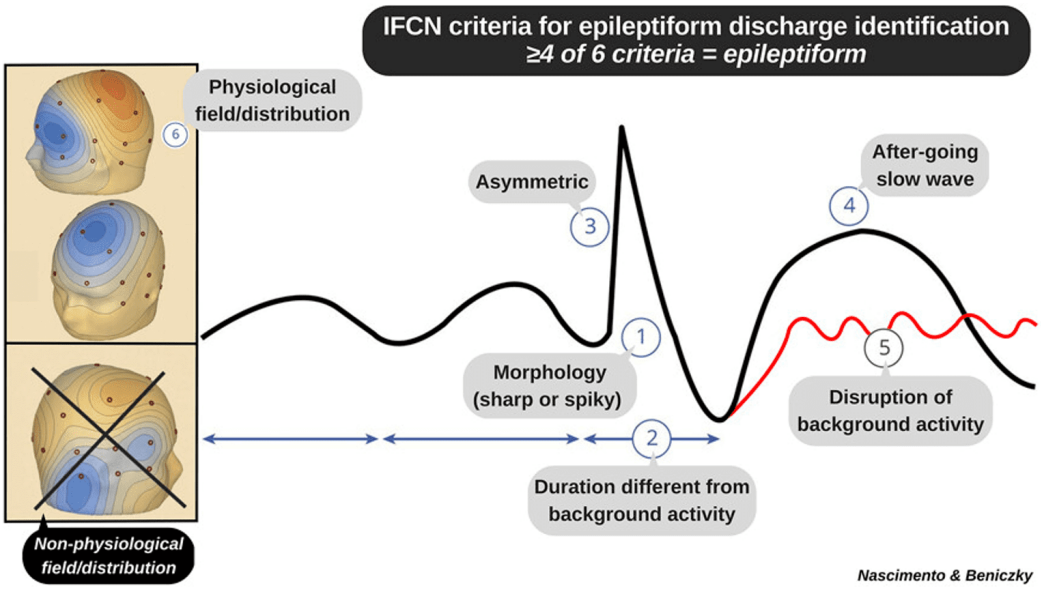


**Figure I.14. Criteria for identifying Interictal Epileptiform Discharges on EEG.** From (Nascimento and Beniczky, 2023).

High-frequency oscillations (HFOs) are brief field potential oscillations in the 80-500 Hz range, identified in epileptic brain tissue through in vitro studies, animal models, and human patients (Zijlmans *et al.*, 2012, 2017). They occur during ictal, pre-ictal, and interictal periods (Jacobs *et al.*, 2010; Zijlmans *et al.*, 2011), with two main categories (Figure I.15):

- **Ripples**: HFOs 80-250 Hz, physiological or pathological, detectable with MEG and EEG.
- **Fast ripples**: 250-500 Hz, often detected with intracranial EEG, commonly during interictal periods, especially during slow-wave sleep or waking quiescence. They can also occur at the onset of some seizures.

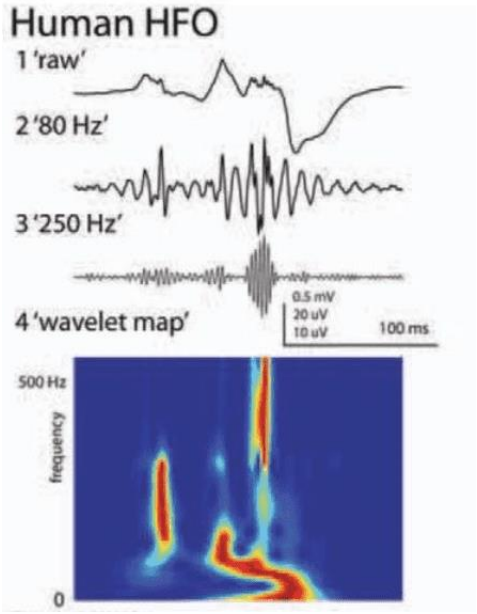


**Figure I.15. Examples of HFOs recorded with depth macroelectrode in human.** (1) Raw intracranial EEG with sharp wave from human hippocampal area (macroelectrode). (2 and 3) Filtered with high-pass filter of 80 Hz and 250 Hz. Note the differences in amplitude scales. Such an event would not stand out in normal EEG. (4) Wavelet transform of frequencies up to 500 Hz. From (Zijlmans *et al.*, 2012).

Clinical studies have identified HFOs as potential markers of epileptogenicity (see the review of (Frauscher *et al.*, 2017)). Indeed, correlations have been observed between brain areas showing HFOs and successful outcomes after epilepsy surgery (Ochi *et al.*, 2007; Jacobs *et al.*, 2010; Wu *et al.*, 2010; Akiyama *et al.*, 2011). A difficulty of HFO identification is the fact that filtering spikes may produce '*falses ripples*' (Bénar *et al.*, 2010). However, research by Roehri et al. found highlights the ongoing challenge of distinguishing between physiological and pathological HFOs, indicating that fast ripples alone may not provide sufficient predictive power for epileptogenic regions (Roehri and Bartolomei, 2019). Combining HFOs with IEDs may improve accuracy.

### *Signal analysis of brain oscillations*

EEG signals consist of sinusoidal waves and a non-oscillatory component, with each wave exhibiting distinct frequency, collectively shaping the EEG spectrum. To estimate the amplitudes of these oscillations and determine the signal spectral power, there are two main approaches: the time and the frequency domains. The temporal approach involves analyzing EEG signal values at specific time intervals or within different temporal windows. For instance, Hilbert analysis is a temporal method used to determine the envelope and the instantaneous phase of the signal. The frequency or spectral approach evaluates changes in EEG signal power across various frequency bands.

This often involves the Fourier transform, which decomposes a signal into its sinusoidal components. The resulting power spectrum shows the distribution of power across frequencies, allowing the identification of dominant frequencies and understand neural dynamics. EEG spectrum estimation can be valuable for identifying how events or stimuli affect power levels, with decreases in oscillation amplitude indicating desynchronization among neurons, and increases indicating synchronization (Pfurtscheller and Lopes Da Silva, 1999).

In epilepsy research, electrophysiological power spectral densities (PSD) are examined as biomarkers for seizure detection and to understand epileptogenicity. High-frequency activity may indicate regions of seizure onset (Bragin *et al.*, 2002; Bartolomei, Chauvel and Wendling, 2008). Moreover, EEG spectral power analysis has proven effective in tracking transitions between interictal and ictal periods (Cerf and El Ouasdad, 2000; Mormann *et al.*, 2005; Park *et al.*, 2011) and in predicting seizure onset (Ayala *et al.*, 2011; Bandarabadi *et al.*, 2015; Chen *et al.*, 2021). Additionally, scalp and intracranial EEG studies demonstrate that PSD values can differentiate between epileptogenic and non-epileptogenic structures across various types of epilepsy (Zaveri *et al.*, 2001; Bettus *et al.*, 2008; Pan *et al.*, 2009). The electrophysiological signals exhibit a dual nature: a periodic component including the oscillatory activity at specific frequencies like theta, alpha, beta, and gamma bands, and an aperiodic background component characterized by a $1/f^{\alpha}$ distribution (Donoghue *et al.*, 2020; Gerster *et al.*, 2022). The measurement of the periodic component of the signal involves assessing the power of specific frequency peaks against the aperiodic background (Figure I.16). Aperiodic activity varies within and across individuals. The aperiodic component can be characterized by the exponent $\alpha$, defining the slope of the background, and an offset parameter (Figure I.16). Research suggests that this component is often associated with the balance between excitation and inhibition or the overall spiking activity of the neural population generating the signals (He *et al.*, 2010). Specifically, the aperiodic offset may be linked to neuronal population spiking (Manning *et al.*, 2009), while the aperiodic exponent, which reflects the integration of underlying synaptic currents, influences the 1/f-like nature of the PSD (Buzsáki, Anastassiou and Koch, 2012; Donoghue *et al.*, 2020). Notably, lower exponent values, indicating a flatter PSD, are associated with higher excitability relative to inhibition, and conversely (Gao, Peterson and Voytek, 2017). The FOOOF algorithm analyzes the electrophysiological power spectrum by identifying and quantifying the periodic and aperiodic components (Donoghue *et al.*, 2020). Normalizing the logarithmic transform of the PSD can reduce the influence of the aperiodic component, but achieving a complete elimination of this influence remains challenging.

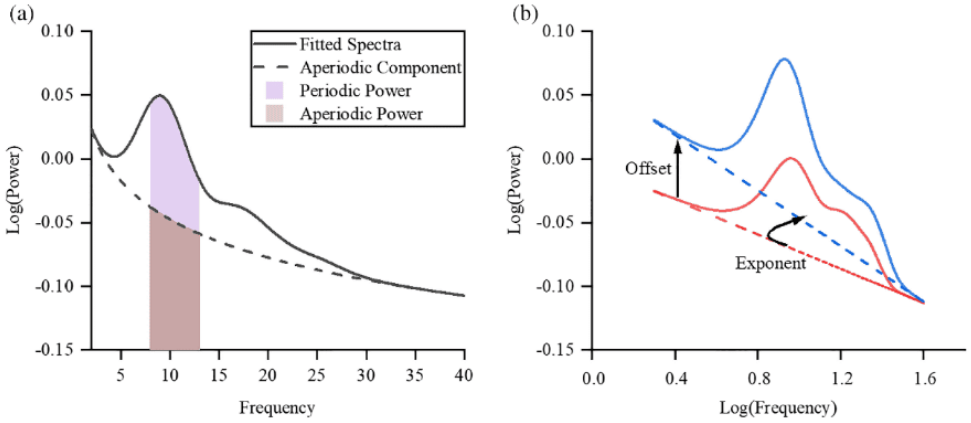


**Figure I.16. Schematic illustration of neural power spectrum parameters.** a) Schematic representation of the aperiodic component (dashed line) and one or more periodic component (full line 'bump') of a power spectrum. Total power is equal to the sum of periodic power (light purple shadow) and aperiodic power (light brown shadow). b) Fitting examples before a treatment (red line) and after a treatment (blue line) in a patient. From (Wang *et al.*, 2022).

## 1.3.4. Functional connectivity

### *Brain connectivity*

Oscillatory synchronization is a key mechanism for neural populations to transmit information and form larger networks. Recent advances in neuroimaging have increased interest in exploring brain functions in both healthy and pathological states, advancing the concept of brain connectivity. Brain connectivity reveals pathways between brain regions, showing how information is processed, transmitted, received, and exchanged across the brain (Bullmore and Sporns, 2012; Stam and Van Straaten, 2012; Bassett and Sporns, 2017). Brain connectivity involves neural networks across various spatial and temporal scales. In this Ph.D. thesis, we focus on large-scale (macroscopic) connectivity. For studying macroscopic brain connectivity, the main methods are mainly MRI (functional and diffusion), MEG, EEG and intracranial EEG. Connectivity measures often derive from both phase and power, using various linear and nonlinear techniques. A network is a mathematical model for complex systems, with nodes and links (or edges) connecting pairs of nodes. In large-scale brain networks, nodes usually represent distinct brain regions. These regions are interconnected by links, representing their connections. In neuroimaging, brain connectivity is classified into two primary types (Bullmore and Sporns, 2009; Friston, 2011) (Figure I.17):

- Structural connectivity (SC) or anatomical connectivity, is the network of fiber tracts linking neuron pools across spatially distant brain regions, forming the white matter. SC is usually studied using diffusion tensor imaging (DTI) with MRI scans.
- Functional connectivity (FC) refers to the temporal correlation of neural activation patterns across anatomically distant brain regions. It focuses on the statistical dependencies within neural populations involved in information processing. FC can be study through functional magnetic resonance imaging (fMRI), MEG and EEG, revealing the dynamics and synchronization of brain networks during different cognitive tasks and states.

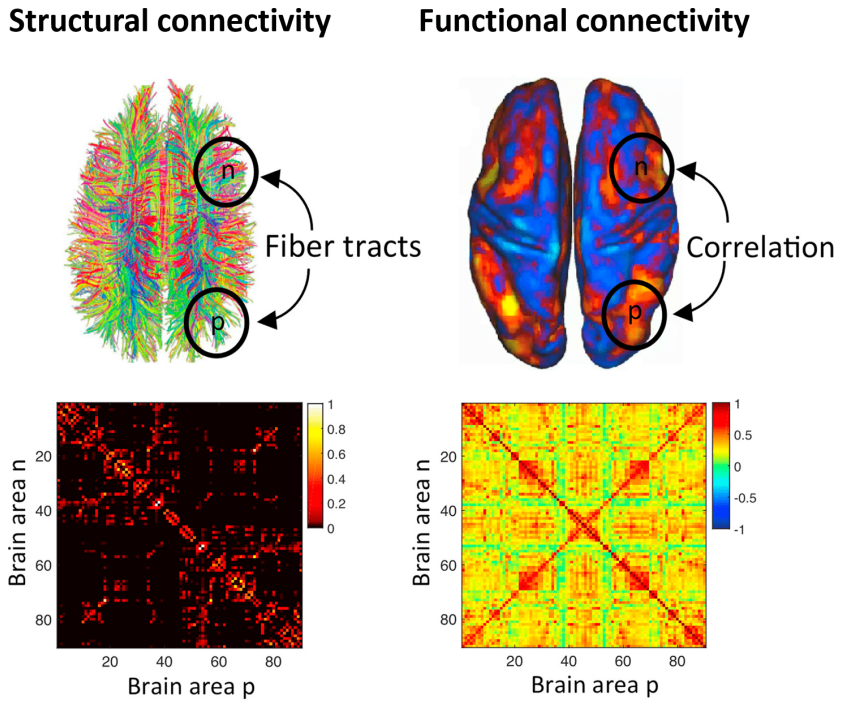


**Figure I.17. Structural vs functional brain connectivity**. (Left) White matter fiber tracts from diffusion-MRI. The structural connectivity matrix SC(n,p) estimates the fiber tracts between brain areas n and p, while the functional connectivity matrix FC(n,p) computes the correlation of brain activity (e.g., BOLD signal) in these areas during recording. From (Cabral, Kringelbach and Deco, 2017).

FC measures can be directed or not, depending on whether an attempt is made to estimate the flow of information from one region to another. For example, the delay in cross correlation or the phase profile in coherence can be used to infer the time of propagation from one region to another (Gotman, 1983). Friston has proposed to use a modeling approach in order to estimate the 'effective connectivity', defined as the direct causal influence between activated brain regions (David *et al.*, 2008; Friston, 2011). Another method for assessing the causal influence between regions is the Granger Causality (Brovelli *et al.*, 2004). Effective connectivity identifies communication direction without necessarily implying physical connection.

SC reflects stable anatomical pathways over longer time scales, whereas FC shows dynamic patterns over shorter time scales, reflecting flexible neural organization between

brain regions. MEG, scalp and intracranial EEG are frequently used to assess FC in epilepsy due to their high temporal resolution. Connectivity is visualized as graphs or matrices with nodes representing brain regions and edges representing connections (Figure I.18). Traditional FC measures include correlation, which evaluates similarity between signals in the time domain, and coherence, which measures similarity in the frequency domain (see (Bastos and Schoffelen, 2016) for a review). Additionally, synchronization measures focus on the phase of oscillations in electrophysiological signals (Palva, Palva and Kaila, 2005; Stam, Nolte and Daffertshofer, 2007). When two signals oscillate synchronously, they share the same phase at the same time. Analyzing phase differences, or phase lag, offers insights into signal propagation and is used to study directed connectivity (Stam, Nolte and Daffertshofer, 2007).

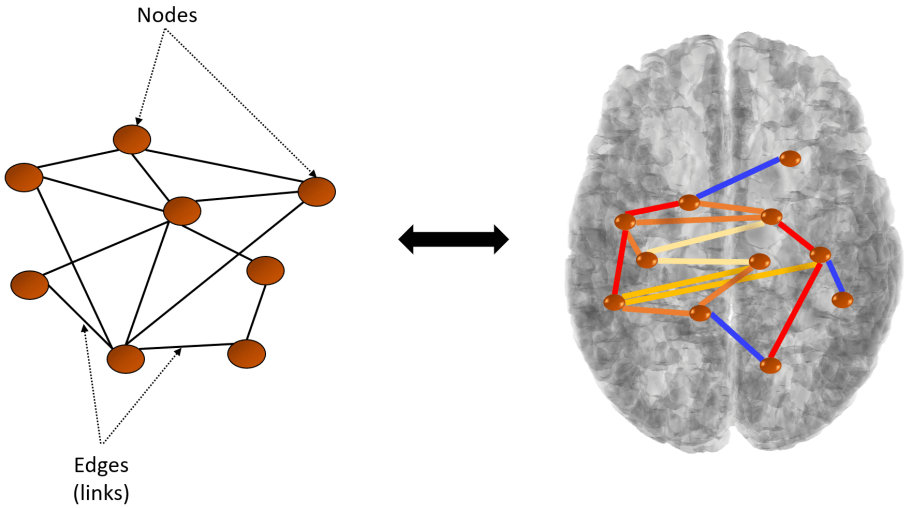


**Figure I.18. Schematic representation of complex brain network with an undirected graph.** The nodes represent different brain regions, while the edges represent the connections (connectivity) between them.

Neurological diseases affecting synaptic plasticity can disrupt communication within and between neuronal populations. Several studies highlight these effects (Bettus *et al.*, 2008; Warren *et al.*, 2010; van Diessen *et al.*, 2013; Lagarde *et al.*, 2018). Measuring and localizing brain processes provides insight into critical features of pathological networks. Previous research has underlined the usefulness of FC in predicting seizures and localizing epileptogenic focus within both ictal and interictal recordings and using both invasive and non-invasive data (see review (Van Mierlo *et al.*, 2014)).

### *Functional connectivity in epileptic brain*

The epileptogenic zone (EZ) is typically organized as a network of hyperexcitable and hypersynchronized neuronal populations distributed across different brain

structures (Wendling *et al.*, 2010; Bartolomei *et al.*, 2017; Lagarde *et al.*, 2018). Seizure propagation is a complex process, distinct from classical nerve flux propagation, characterized by significant changes in FC. The propagation zone (PZ) typically comprises regions with lower epileptogenicity compared to the EZ during seizure onsets. Intracerebral recording studies focusing on the PZ have shown the role of cortico-subcortical loops, suggesting that synchronized thalamocortical oscillations can amplify and synchronize seizures (Bertram *et al.*, 2001; Guye, 2006; Bartolomei *et al.*, 2017). Invasive ictal studies indicate that while seizure onset often involves a decline in synchrony across brain structures, the most significant changes, marked by increased network synchrony, occur during seizure spread and termination (Wendling *et al.*, 2003; Jiruska *et al.*, 2013; Bartolomei *et al.*, 2017). These alterations in the propagation network likely contribute to the emergence of clinical symptoms. The functional epileptogenic network is summarized in Figure I.19. An SEEG study during the interictal state confirmed previous findings by showing a gradual decrease in FC within the whole network (EZ, PZ, NIZ), with higher FC in the EZ and PZ and lower in non-involved zones (NIZ) (Lagarde *et al.*, 2018). The study also reported preferential coupling within the EZ and between EZ and PZ. Patients with higher FC in the NIZ had poorer post-surgical outcomes, suggesting that even during the interictal state, stronger FC within epileptic cortices is associated with worsening surgical prognosis.

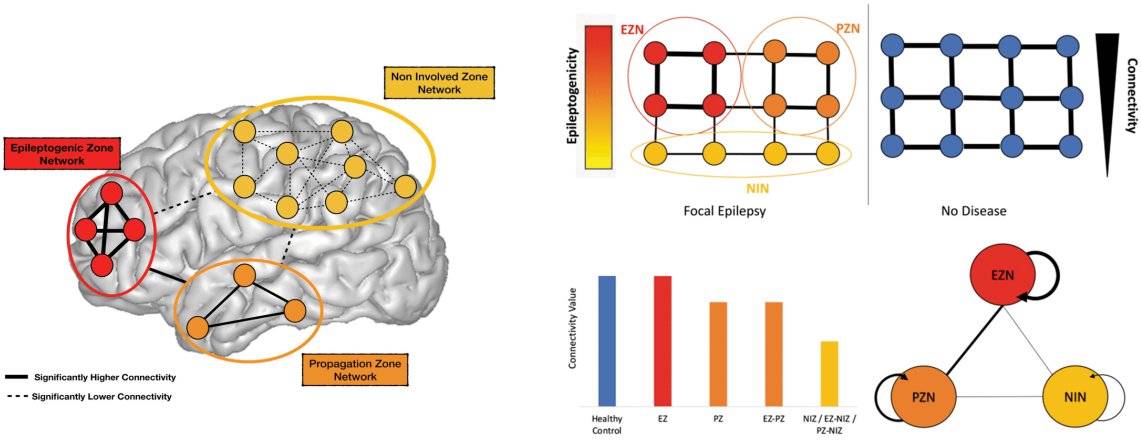


**Figure I.19. Changes of functional connectivity in epileptogenic brain networks.** Lines between small circles depict the functional connectivity within structures of a zone. The lines between large-circles represent the functional connectivity between zones. Plain lines correspond to a significantly higher functional connectivity and the dashed lines represent lower functional connectivity. From (Lagarde *et al.*, 2018, 2022).

Moreover, FC studies using M/EEG signals have been conducted at the sensor level or through source reconstruction methods. These studies confirmed a heightened connectivity within the EZ and a widespread hypoconnectivity outside the EZ (Malinowska *et al.*, 2014; Wu *et al.*, 2014; Englot *et al.*, 2015; Nissen *et al.*, 2016). Analyzing scalp signals provides insights into M/EEG connectivity in source space, but is limited by the spatial resolution of the surface signals and presents challenges when investigating deep structures (Pizzo *et al.*, 2019). The volume conduction effect complicates scalp

recording analysis by simultaneously detecting a given brain source on many M/EEG sensors, leading to potential false connections and impacting connectivity results (Van Mierlo *et al.*, 2019). To address these issues, source-reconstructed data offers a more accurate representation of connectivity. However, careful selection of connectivity measures—such as using the imaginary part of coherence—is required to reduce source leakage artifacts (Brookes, Woolrich and Barnes, 2012). The standard process for M/EEG source connectivity involves several steps: recording M/EEG sensor signals, preprocessing to clean data and remove artifacts, projecting M/EEG signals from sensor to source space using M/EEG source imaging (MSI/ESI), and estimating activity within regions of interest (ROIs) using an anatomical atlas parcellation (Figure I.20). Connectivity measures are then applied to obtain the source space connectivity pattern, allowing for further graph analysis to extract local and global network properties.

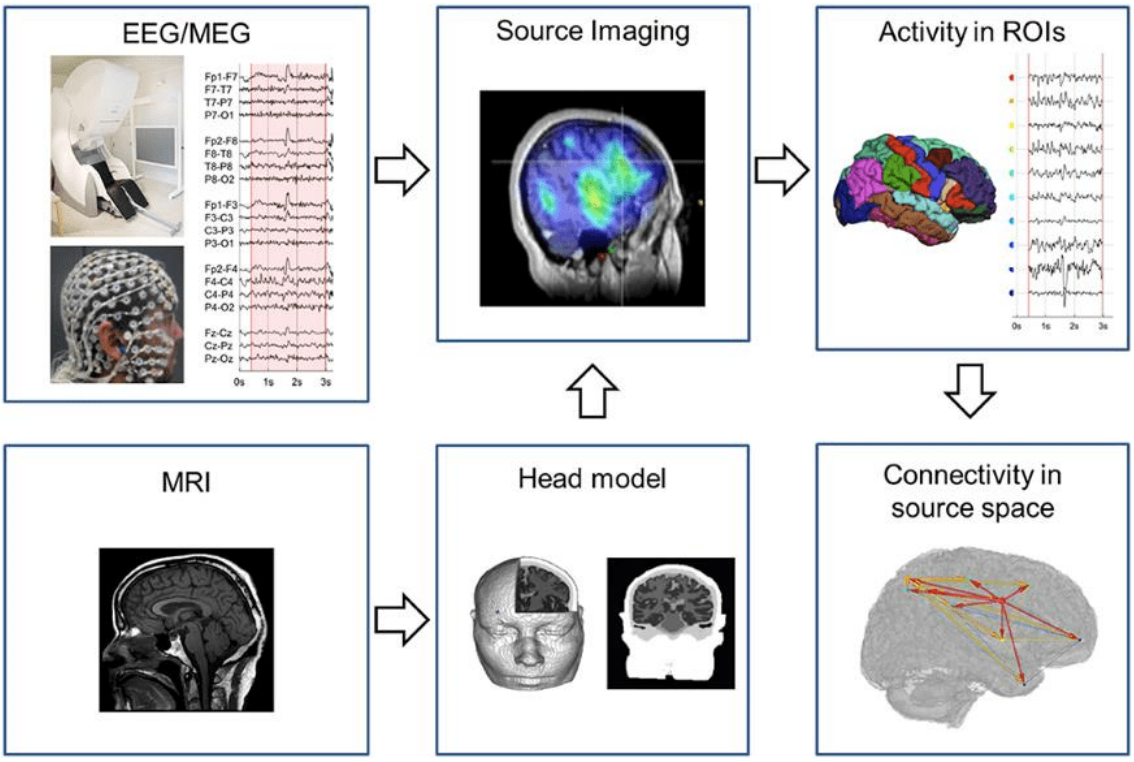


**Figure I.20. Pipeline to obtain M/EEG source connectivity.** From (Van Mierlo *et al.*, 2019).

Overall, studies applying M/EEG source imaging have reported hyperconnectivity within the EZ during seizures ((Ding *et al.*, 2007; Lu *et al.*, 2012), for a review see (Van Mierlo *et al.*, 2019)). This hyperconnectivity is characterized by outgoing information flow, suggesting that the EZ acts as the initial source of network activation. Interictal studies have shown that directed connectivity can trace spike propagation patterns, indicating their origin (Coito *et al.*, 2015), which was also observed on SEEG (Courtens *et al.*, 2016; Azeem *et al.*, 2021). Furthermore, source connectivity analyses revealed distinct patterns that differentiate epilepsy patients from healthy subjects, even in the absence of epileptiform activity (Clemens *et al.*, 2011; Coito *et al.*, 2016). Connectivity studies in focal epilepsies using fMRI have also uncovered distributed connectivity changes during the

interictal period showing both increased and decreased connectivity. This provides insights into pathological and potentially compensatory processes in epilepsy. Additionally, fMRI and M/EEG FC analysis can help identify the key drivers of epileptic activity and predict postsurgical outcomes (Centeno and Carmichael, 2014; Pittau and Vulliemoz, 2015; Bartolomei *et al.*, 2017).

In summary, the range of findings regarding alterations in functional networks within epileptic brains shows a strong relationship between abnormal synchrony and epileptogenicity. These results may guide therapeutic interventions including surgical procedures and neuromodulatory therapies. By studying changes in functional brain networks resulting from these treatments, we could better understand their mechanisms of action and improve the customization of patient-specific plans.

## 1.4. Thesis objectives and plan of investigation

This doctoral thesis explores the application of tDCS in patients with DRE, using a multichannel stimulation protocol optimized and individualized for each patient. This research had two main objectives:

1) To assess the clinical effects of the treatment, by monitoring potential changes in seizure frequency after the stimulation treatment and by documenting the adverse events reported after multiple sessions of stimulation.

2) To examine the induced neurophysiological changes within brain networks. To explore he mechanisms behind tDCS and understand its efficacy, the long-term changes in functional connectivity have been studied through non-invasive electrophysiological brain recordings (EEG, MEG).

Chapter 2 presents **study 1**, a systematic review on the effects of tES in treating DRE. This review explores tDCS and tACS mechanisms, addressing neurobiological and clinical aspects, and emphasizes the importance of analyzing pathological brain networks to understand the impact of tDCS on epilepsy.

Chapter 3 presents the results of **study 2**, which evaluated an optimized, personalized multichannel tDCS protocol for epilepsy patients. This study addressed limitations found in prior research on tDCS in epilepsy. It tested the feasibility of this personalized protocol in 10 DRE patients, targeting the EZ based on SEEG findings. Study 2 also examined changes in functional connectivity using EEG before and after tDCS sessions.

Chapter 4 consists in **study 3**, which replicated the protocol used in Study 2 with 17 DRE patients. Study 3 used MEG to assess functional changes at the source level,

focusing on spectral analysis and connectivity patterns. An objective was to determine if functional connectivity could serve as a predictive biomarker for tDCS efficacy in epileptic patients.

Chapter 5 details **study 4**, a retrospective analysis exploring why tDCS was effective for some epileptic patients but not for others. This study examined the anatomical characteristics of the EZ and how they might impact tDCS efficacy, including the extent and depth of the EZ targeted regions. This study included the patients of studies 2 and 3.

Chapter 6 describes **study 5**, which investigated tDCS effects on epilepsia partialis continua, a severe epilepsy syndrome characterized by continuous partial seizures. The study assessed the long-term impact of tDCS on different seizure types and etiologies.

And Chapter 7 is a general discussion of the findings, offering insights into future research perspectives.

# 2. Chapter II: Fundamental and Clinical Aspects of Transcranial Current Stimulation in Epilepsy

This chapter was published in:

Simula, S.*, **Daoud, M**.*, Ruffini, G., Biagi, M. C., Bénar, C. G., Benquet, P., Wendling, F., & Bartolomei, F. (2022). Transcranial current stimulation in epilepsy: A systematic review of the fundamental and clinical aspects. Frontiers in neuroscience, 16, 909421. https://doi.org/10.3389/fnins.2022.909421

* These authors have contributed equally to this work and share first authorship

# Rationale

As mentioned in the introduction, the first-line therapeutic approach for patients with epilepsy involves pharmacological treatments to control seizure activity. However, one-third of patients experience resistance to antiseizure medications, a condition termed drug-resistant epilepsy (DRE) (Kwan *et al.*, 2010). In such cases, the surgical resection of the epileptogenic zone (EZ) may be considered for focal epilepsy. Nevertheless, this option may not always be applicable due to the localization of the EZ and the potential functional risks associated. Moreover, surgical intervention does not always lead to successful outcomes, and seizures may persist despite the procedure (Jehi *et al.*, 2015).

In recent years, brain stimulation methods based on neuromodulation have emerged as alternative treatments, or at least palliative techniques. Among the non-invasive stimulation techniques, the application of low-intensity transcranial electrical currents has been proposed in treating patients with DRE. However, due to its relatively recent introduction into clinical practice, studies yield varying results, likely influenced by differences in protocols and by a lack of consensus. Moreover, despite its increasing use, the neurophysiological mechanisms underlying antiepileptic activity of stimulation remain poorly understood.

Study 1 presents a systematic review of transcranial electrical stimulation (tES) application in epilepsy, exploring its effects on biological, neurophysiological, functional, and clinical aspects. This review provides a comprehensive overview of existing research, highlighting the strengths and limitations of previous studies and pinpointing unresolved questions. Additionally, the studies referenced in this literature review have served as the basis of the stimulation protocol employed in our own investigations. Lastly, analyzing the existing literature helped shedding light on the underlying mechanisms and on the biomarkers associated with tES efficacy.

# 2.1. Introduction

Epilepsy is one of the most common chronic neurologic disorders affecting 70 million people worldwide. It is characterized by unpredictable seizures caused by abnormal neuronal activity in the brain (Devinsky *et al.*, 2018). One-third of epileptic patients experience seizures that are refractory to pharmacotherapy. The complications of drug-resistant epilepsy (DRE) are devastating with severely diminished quality of life. Surgical resection of the epileptogenic zone (EZ) is not always indicated, in particular for patients with multifocal or diffuse disease or those with inaccessible EZ. In addition, surgery is associated with a relatively high number of failures (Baud *et al.*, 2018).

Consequently, alternative treatments based on neurostimulation methods represent a promising therapeutic approach decreasing cortical excitability. On the one hand, various types of invasive neuromodulation are available: Vagus Nerve Stimulation (VNS), responsive neurostimulation (RNS), and deep brain stimulation (DBS). These three therapies involve the implantation of a neurostimulator device with potential surgical complications, and uncertainty regarding the clinical benefit for the patients. VNS consists in an implanted electrode located around the left vagus nerve and an implanted generator in subclavicar region to obtain alternation of stimulations for desynchronizing network activity modulating neurotransmitter release. DBS involves electrical stimulation with pulse-train delivered chronically, intermittently in a closed loop manner using intracerebral electrodes located precisely with stereotaxic surgery. The principle of RNS is to detect ongoing epileptiform activity using a combination of electrocorticogram recording electrodes and stimulation electrodes.

On the other hand, non-invasive brain stimulation techniques have emerged since several years for epilepsy treatment with the advantage of being safe, well tolerated, and reversible. The first technique used for treating seizures refractory to pharmacotherapies was repetitive transcranial magnetic stimulation (rTMS) (Tergau *et al.*, 1999). The technique of rTMS uses an external electromagnetic coil inducing an electrical current flow in the targeted cortical area. However, further studies reported a lack of evidence in seizure frequency decrease using this technique and a risk of inducing seizures in patients and in healthy subjects (see reviews (Tsuboyama, Kaye and Rotenberg, 2020; VanHaerents *et al.*, 2020)).

The quite recent technique of transcranial current stimulation (tCS or tES) appears to be safer, less expensive, and more portable than rTMS, which also opens the potential for "at home" usage. This is a non-invasive neuromodulatory technique which modulates brain excitability by applying low intensity, controlled currents (~1 mA and < 2mA) on the brain via scalp electrodes (Nitsche and Paulus, 2000; Modolo *et al.*, 2018). In particular, tES protocols can be designed to either increase or decrease neural excitability. The terms anodal and cathodal stimulation are often used in the field and are a source of confusion. An anode, in the context of tES, is a scalp electrode through which conventional

current (positive charge, opposite to the flow of negatively charged electrons) flows into the brain from the stimulation device. On the other hand, a cathode is an electrode through which current flows out of the brain. It has been observed that anodal stimulation over a brain area increases cortical activity (i.e., it is excitatory) while cathodal stimulation can decrease it (i.e., it is inhibitory) (Nitsche and Paulus, 2000). In epilepsy, cathodal electrodes can be placed over the epileptogenic region to inhibit the underlying tissues. When the electrical current applied is constant and unidirectional, from anodal electrode to cathodal one, it is referred to transcranial direct current stimulation (tDCS). Otherwise, if the applied electrical current is sinusoidally changing in time, it is referred to as transcranial alternating current stimulation (tACS). So far, for treating DRE, tDCS has been preferentially used.

### *General overview of tES and clinical settings in epilepsy*

A classical generic tDCS device employs a battery powered controlled current generator connected to two large surface electrodes (one anode and one cathode, approximately 25-35 $cm^2$ each) localized on the scalp. A constant current with a maximum output in the milliamp range (1-2 mA) is delivered through an electrode (cathode) over epileptogenic zone to hyperpolarize pyramidal cells in this region (inhibition) and the circuit is completed by an electrode (the anode) localized preferentially over a non-involved zone in epileptic patients.

The tES effects depend on several factors, including stimulation duration, current intensity, repetition, number of electrodes (bipolar or multichannel tDCS), and electrode position (Figure II.1.A).

The tES currents are associated with electric fields (EF) by a linear relation that depends on electrode positions, current (measured in mA), anatomy and conductivity (units of S/m). This is crucial, because the effects of tES are assumed to be mediated by the electrical fields in the cortex – with both intensity and direction being important (Ruffini *et al.*, 2013). The electric field is vectorial, and its magnitude has units of V/m (or equivalently, mV/m). It is a force field that induces ions to displace and accumulate across the membrane. The charge accumulation effect is larger in the dendritic-soma direction of long elongated neurons, such as the pyramidal neurons (*in vitro* studies: (Ghai, Bikson and Durand, 2000; Lian *et al.*, 2003; Bikson *et al.*, 2004; Chang, Lu and Shyu, 2015), or see (Ruffini *et al.*, 2014)). The EF can be obtained by calculating the gradient of the voltage measured on each contact of a same SEEG electrode. Therefore, studies can estimate the amount of EF reaching the explored brain areas when using tES with a given current. Since cortical pyramidal neurons are preferentially aligned in a normal direction to the cortical surface, the normal component of the electric field seems to be the most crucial for cortical modulation. If the current (and thus the electric field) are directed out of the cortex, as in

the case of cathodal stimulation, the soma is made slightly hyperpolarized, i.e., less excitable (Figure II.1.B).

The direction of the electrical field components is loosely related to the nature of nearby electrodes, with cathodal electrodes predominantly inducing outward pointing (inhibitory) fields in the brain region underneath, although this is heavily influenced by the cortical folding (Figure II.1.A). Realistic head models can be used to analyze the electric fields associated to a montage (Miranda *et al.*, 2013) and even to optimize them provided that a cortical target is at hand (Ruffini *et al.*, 2014). In a clinical perspective, it is desirable to optimize stimulation focality and to prolong therapeutic after-effects. Thus, the understanding of underlying mechanisms could help us to determine the optimal parameters for tES in epilepsy. Although there is a growing body of research on tES, the stimulation parameters and the experimental designs are not consistent between studies and the resulting findings are at times contradictory.

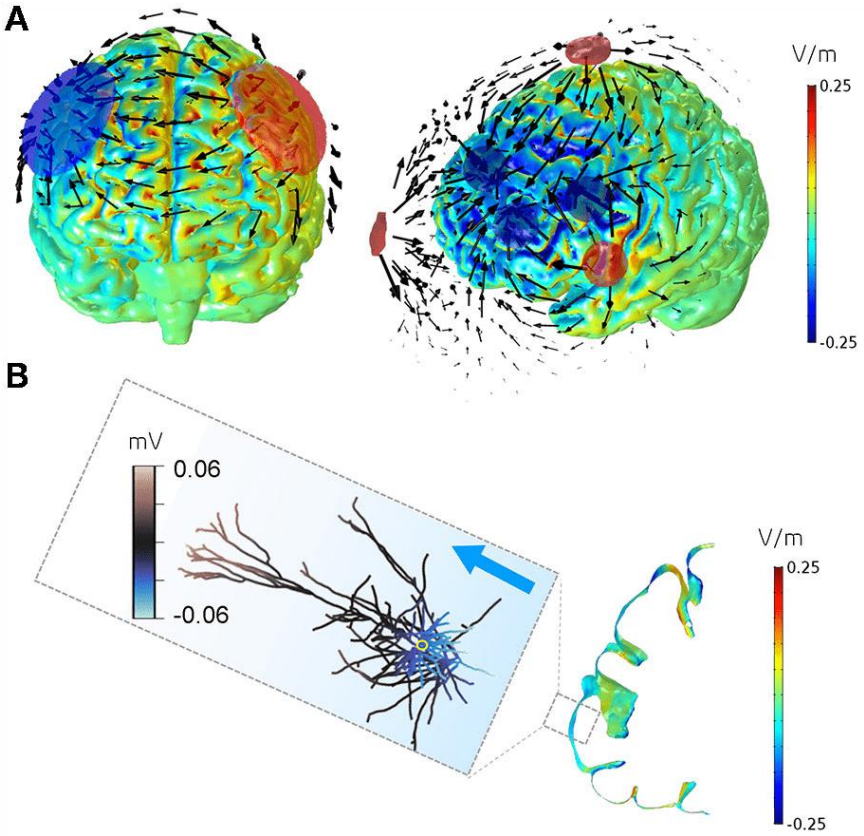


**Figure II.1. Simulation of tES-induced electric field on realistic brain model.** (A) Electric field on a realistic brain model, generated by a bipolar montage with large sponge electrodes (left) and a multichannel montage employing six smaller electrodes (right). Cathodes are shown in blue, and anodes in red. Fields are shown for a total applied stimulation current of 1mA for the bipolar and 4mA for the multichannel montages. The colormap represents the component of the electric field directed perpendicularly to the cortical surface (or normal electric field, scale in V/m). The arrows display the current density field in the brain (not in scale). In our convention, the cortical normal vector points from the cortex surface to deeper brain regions, therefore outward currents give rise to negative values of the normal electric field component (in blue) and inward currents to positive values (in red). Normal electric fields are strongest under the

electrode and in regions where the cortical gyration aligns the cortical column with the electric field between the electrodes. In multielectrode focal montages (right figure), the outward fields are particularly predominant under the cathodes. (B) Normal electric field and induced soma polarization for a total applied stimulation current of 1 mA. Detail of the membrane polarization induced by an electric directed outwardly from the cortex on a realistic pyramidal neuron. The neuron morphology was reconstructed from Blue Brain Project. It is approximately located in the area in the dashed box, oriented perpendicularly to the cortex and exposed to an electric field value of 0.15 V/m along its axo-somatic axis and directed outwardly (blue arrow). The electric field causes a net polarization, or hyperpolarization, of the soma (located inside the yellow circle) of about −0.06 mV from the resting potential.

The purpose of this systematic review is to provide an up-to-date summary of tES development in clinical epilepsy treatment and its effects on the underlying basic neurophysiology. Indeed, the neuro-modulatory mechanisms involved during the application of a weak current remain to be clarified.

## 2.2. Materials and methods

### *Review planning and searches*

This systematic review was performed in accordance with the Preferred Reporting Items for Systematic Reviews and Meta-Analyses (PRISMA) guidelines (Page *et al.*, 2021). A database search was performed in November 2021 via the databases PUBMED, MEDLINE, Web of Science and Cochrane CENTRAL by two independent reviewers. Articles whose title, abstract or keywords contained the keywords "epilepsy AND (transcranial current stimulation OR transcranial electrical stimulation)" were screened. Figure II.2 shows the Prisma flowchart of the selection process.

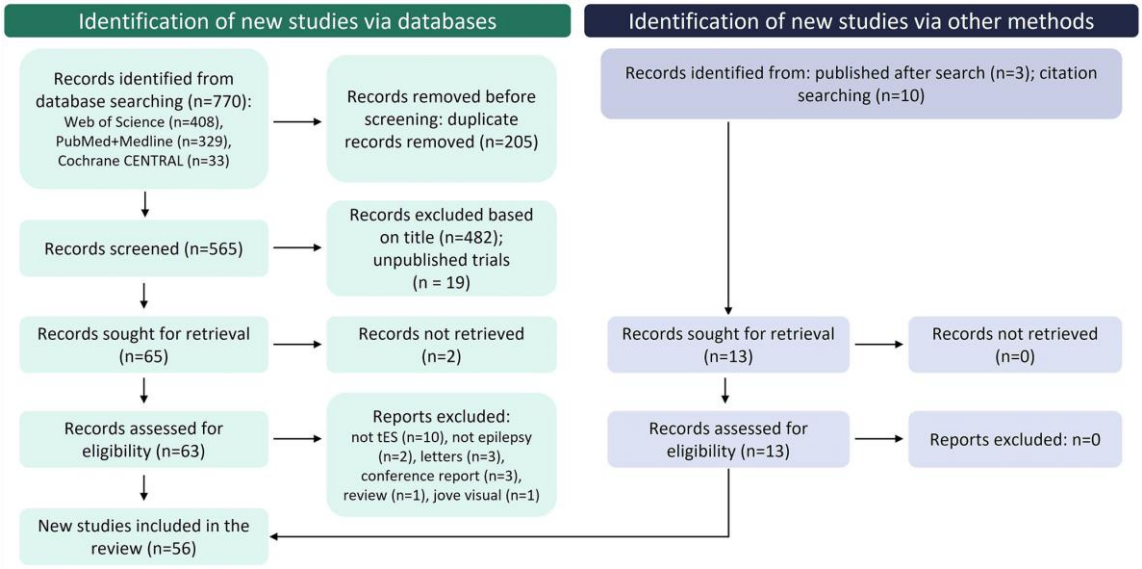


**Figure II.2. Flowchart of PRISMA record selection process.**

### *Screening and eligibility criteria*

In the first place, duplicate records were excluded. After a screening based on title and abstract and performed by two independent reviewers, both clinical and fundamental research records regarding tES and epilepsy were submitted to eligibility. Articles not fulfilling the eligibility criteria (full-text records, original research concerning epilepsy and focusing on tES, English text available) were excluded. Selected articles are presented in the form of summary tables and of qualitative description of the main results described in the original studies.

# 2.3. Results

### *Retrieved papers*

From a total of 770 records identified from the database search, 718 were excluded for several reasons, specified in the flowchart shown in Figure II.2. A total of 49 studies fulfilled eligibility criteria and 13 studies were subsequently added through complementary methods. Among the included records, 23 were clinical studies with 17 clinical trials (Table II.1) and 6 clinical cases (Table II.2), 6 analyzed tES-related brain network changes and 27 focused on the physical and neurobiological effects of tES (9 records using animal models of epilepsy, 5 on epileptic patients, 7 *in vitro* and 6 studying computational models).

## 2.3.1. Clinical studies

### *Seizure Frequency*

Cathodal tDCS has been used in several clinical studies with pediatric and adult patients suffering from DRE. Table I.1 shows a summary of clinical trials of patients ($n \geq 5$ patients) with epilepsy treated with cathodal tDCS and Table II.2 summarizes the clinical cases ($n < 5$) using tDCS for treating epilepsy. The first controlled clinical trial using cathodal tDCS on patients suffering from refractory epilepsy was conducted by Fregni et al. in 2006 (Fregni *et al.*, 2006). This study investigated the effects of one cathodal tDCS active session stimulation of 20 min at 1 mA in 19 patients with DRE compared to sham stimulation. They showed that cathodal direct-current polarization decreased seizure frequency (mean decrease of −44%) compared to the baseline. Most studies are consistent with these results, reporting positive effects of cathodal tDCS in epileptic patients reducing seizure frequency (SF). Indeed, focusing on SF change due to cathodal tDCS, 15 clinical trials (15/17) reported a decrease or a trend to a decrease in

SF. Auvichayapat et al. reported a slight decrease in SF one month after one session of 20 min of cathodal tDCS at 1 mA in children suffering from DRE (n = 36 children, 27 with active stimulation and 9 with sham stimulation), highlighting the safety of this technique for young population and its clinical usefulness (Auvichayapat *et al.*, 2013). Two other studies reported significant (>50%) decrease in SF in patients suffering from Rasmussen's encephalitis, a rare and progressive inflammatory disease that reaches one cerebral hemisphere, leading to intractable partial onset seizures (San-Juan *et al.*, 2011; Tekturk, Erdogan, Kurt, Kocagoncu, *et al.*, 2016). Another clinical pediatric trial conducted by Auvichayapat et al. (2016) has shown reduction in SF of 55.9% in patients with epileptic spasms and Lennox Gastaut syndrome (LGS) compared to sham group one month after five consecutive days of 20 min tDCS at 2 mA (Auvichayapat *et al.*, 2016). Then, 28 patients suffering from mesial temporal lobe epilepsy with hippocampal sclerosis have been enrolled in a randomized placebo-controlled, double-blinded clinical trial where they received one session of tDCS at 2 mA for three or five days (San-Juan *et al.*, 2017). Two months after the cathodal tDCS session, they obtained a decrease of −43% in SF for the group with three days of stimulation and a decrease of −55% in SF for the group receiving tDCS for five days compared to baseline. Thus, the heterogeneity of epilepsy types among studies demonstrates the potential efficacy of cathodal tDCS for treating several etiologies of refractory focal epilepsy.

The tDCS technique has been improved over the last few years with the recent use of several pairs of smaller electrodes (multichannel tDCS), contrasting with conventional tDCS using two large rectangular electrodes (see Figure II.1.A). Indeed, conventional tDCS, using one electrode (cathode) placed over the epileptogenic region and one anodal electrode placed on the scalp over a non-involved zone, allowed a modulation of cortical activity in a relatively larger area than that covered by the target electrode (Nitsche *et al.*, 2007). In addition to more precise targeting of the generated electric field over the desired area, an enhanced stimulation focality would avoid unwanted excitation of non-target areas. Thus, neurophysiological and modeling studies have shown that smaller multiple electrodes produce more targeted outcomes and that their placement is crucial for the effects of stimulation (Ruffini *et al.*, 2014; Hannah, Iacovou and Rothwell, 2019). This focal method has been previously used in the clinical field with encouraging results. A recent study confirmed the safety of multichannel tDCS applying 20 min of stimulation (4-Ring configuration) each day for 10 days in a 30-month-old child suffering from neonatal epileptic encephalopathy (Meiron *et al.*, 2018). Then, a clinical trial enrolling 10 patients with intractable lateral frontal lobe epilepsy has shown changes in SF with a decrease of −38.1% 1 month after the multichannel tDCS at 2 mA applied for 10 consecutive days (Karvigh *et al.*, 2017). Another interest of using multifocal tDCS is to use biophysical modeling and electrophysiological or imaging data to optimize electrode montage to target and avoid specific brain regions depending on their degree of epileptogenicity. Recently, an open label study has been conducted on epileptic pediatric population using personalized multichannel tDCS (max 8 electrodes) for 10 sessions of 20 min of cathodal tDCS over 2 weeks (Kaye *et al.*, 2021). Multi-electrode montages were designed using a realistic head model-driven approach to apply an inhibitory electric field to the target

cortical seizure foci and surrounding cortex to suppress excitability and reduce seizure rate. They demonstrated the feasibility and the efficacy of a customized multichannel cathodal tDCS as antiepileptic protocol with a −44% seizure reduction and a responder rate of 40%.

If the clinical benefit of tES is further demonstrated, one of the main objectives of future studies will be to prolong the positive after-effects on SF. In this regard, performing several tDCS sessions is expected to decrease SF in the long-term. Indeed, previous studies only performed one tES session with promising short-term results whereas a clinical case conducted by Yook et al. highlighted that the repetition of stimulation allows to prolong and enhance the effects of tDCS. They showed a decrease in SF lasting for two months after two consecutive weeks of daily stimulations (Yook *et al.*, 2011). San-Juan et al. observed greater clinical improvement in patients with mesial temporal lobe epilepsy after five consecutive days of tDCS than those who received the treatment for three days (San-Juan *et al.*, 2017). Interestingly, the duration of after-effects is dependent on the length of the interval between stimulation sessions. Thus, Monte-Silva et al. explored the effects of different break durations between cathodal tDCS stimulation sessions in healthy subjects (Monte-Silva *et al.*, 2010). They showed that the magnitude of cathodal tDCS-induced inhibition was enhanced after a break interval of 20 min between two 9 min stimulation sessions but not after a 3 min break. This specific timing effect seems to be important for optimizing cumulative effects due to tDCS. Further recent studies also tried to lengthen tDCS after-effect modifying the interval duration. Recently, a multicentric controlled study conducted by Yang et al. in 2020 showed a significantly greater reduction in SF (64.98–66.32%) in the group of epileptic patients receiving 2 × 20 min of stimulation with 20 min off compared to the group receiving only 20 min of stimulation at five weeks follow-up (Yang *et al.*, 2020). Then, another clinical trial performing 2×9 min stimulation with 20 min break at 2 mA in epileptic patients has shown a mean decrease of SF about 48% (n = 15) immediately after one session of cathodal tDCS (Kaufmann *et al.*, 2021). Regarding the main limitations of previous clinical studies, we noticed a lack of data regarding a potential improvement of quality of life and of seizure severity after tES, as the majority of studies focused on seizure frequency only.

Furthermore, the most common limit of previous studies is the lack of long-term follow-up, the small sample size of patients and the large and heterogeneous epilepsy types. To date, only one randomized, double-blind, sham-controlled, multicentric study on tES in epilepsy has been conducted (Yang *et al.*, 2020), including 70 patients suffering from DRE and divided into three groups: group 1 with sham stimulation, group 2 with 20 min of stimulation and group 3 with 2×20 min stim at 2 mA during 14 consecutive days. They obtained a significant decrease in SF in active groups compared to sham group, with better results for group 3 compared to group 2 at 8 weeks follow-up. They reported a decrease in SF in group 2 of −50% the first 4-weeks of follow-up compared to baseline and a decrease of −25% in SF the second 4-weeks of follow-up. The group 3 obtained also a −50% decrease in SF in the first 4-weeks of follow-up but a decrease of −45% in SF after the second 4-weeks of follow-up. Regarding the sham group, they observed a decrease in

SF in group of −25% the first 4-weeks of follow-up compared to baseline and a decrease of −12.5% in SF the second 4-weeks of follow-up. Thus, the beneficial effects lasted longer when the patients received 2 × 20 min of tDCS. However, they did not find any difference in quality-of-life scale (QOLIE) after tDCS treatment.

| References | Number of subjects | Epilepsy type | Methodology | Duration | Method outcome | Effects | Side effects |
|---|---|---|---|---|---|---|---|
| Fregni et al. (2006) | 19 | Focal, malformation of cortical development (MCD) | Cathodal tDCS at 1 mA, 20 min ($n = 10$), sham ($n = 9$) Max follow-up: 1 month | 1 session | EEG (21 electrodes), number of EDs, SF | Decrease of −64.3% of EDs −44% SF decrease at 1 month follow-up | Itching sensation |
| Varga et al. (2011) | 5 (children) | Focal DRE, continuous spike-wave discharges during slow sleep (CSWS) | Small tDCS electrodes at 1 mA, 20 min before sleep + sham | 2 sessions before sleep (1 active, 1 sham) | EEG (19 electrodes), EDs during slow sleep (spike-index) | Cathodal tDCS did not reduce EDs | No adverse event |
| Faria et al. (2012) | 15 healthy subjects + 2 epileptic patients | DRE, CSWS | Heathy subjects: active 0.5 mA, 5 min + 1 mA, 5 min + sham Epileptic patients: 3 sessions (1 mA, 10 min during sleep for 3 days) | 3 sessions | EEG (24 electrodes), EDs | Decrease of −45% EDs | 93% of the participants did not feel anything |
| Auvichayapat et al. (2013) | 36 (children) | Focal DRE | Cathodal tDCS at 1 mA, 20 min ($n = 27$), sham ($n = 9$) Max follow-up: 1 month | 1 session | EEG (32 electrodes), EDs, SF, "Quality of life in childhood epilepsy questionnaire" (QOLCE) | Decrease of EDs (−45.3%) at 48 h, small decrease of SF at 1 month | 1 patient had transient skin erythema |
| Tekturk et al. (2016a) | 5 | Rasmussen encephalitis | Cathodal and anodal tDCS: at 2 mA, 20 min + sham after 2 months | 3 consecutive days | SF | >50% of decrease in SF | No adverse effects |
| Auvichayapat et al. (2016) | 22 (children) | Lennox-Gastaut syndrome | Randomized double-mind-controlled Each day: active cathodal tDCS ($n = 15$) at 2 mA, 20 min, sham ($n = 9$) Follow-up: 4 weeks | 5 consecutive days | EEG (32 electrodes), EDs, oxygen saturation | −8% decrease of ED at 1 month, more after 48 h, −55.9% decrease of SF | 1 patient had superficial skin burn |
| Tekturk et al. (2016b) | 12 | Mesial temporal lobe epilepsy with hippocampal sclerosis (MTLEHS) | Cathodal tDCS at 2 mA, 30 min, + sham | 3 days | SF | 83% of responders (>50% of SF decrease) | Tingling sensation |
| Zoghi et al. (2016) | 29 | Focal temporal lobe epilepsy (TLE) | Cathodal tDCS active group ($n = 20$): 1 mA 9 min stim-20 min break-9 min stim + sham group ($n = 9$) Max follow-up 1 month | 1 session | EEG, Paired-pulse transcranial magnetic stimulation: short interval intracortical inhibition (SICI) calculated from motor evoked potentials MEP, SF | Increase in SICI for experimental group compared to sham, Decrease of −42% of SF in active group | Itching, burning sensation, transient headache, neck pain |
| Assenza et al. (2017) | 10 | Focal TLE | Randomized controlled, Cathodal tDCS at 1 mA, 20 min + Sham | 2 sessions (1 active, 1 sham) | EEG (19 electrodes), interictal epileptiform activity (EA) | No change in EA, decrease of SF: −71 ± 33% in active group vs. 25 ± 125% for sham | Itching sensation |
| San-Juan et al. (2017) | 28 | MTLEHS | Randomized placebo-controlled, double-blinded clinical trial Cathodal tDCS at 2 mA, 30 min for 3 days ($n = 12$) + Cathodal tDCS, 30 min for 5 days ($n = 8$) + Sham ($n = 8$) Max follow-up: 60 days | 1 session | EEG, interictal epileptiform discharges (IEDs) | Decrease of IEDs immediately after tDCS, decrease in SF at 1 and 2 months after tDCS (3 days: −43%; 5 days: −55%) compared to baseline | Mild itching sensation, moderate headache |
| Karvigh et al. (2017) | 10 | Lateral frontal lobe epilepsy | HD-tDCS 2 mA, 20 min, no sham Max follow-up: 1 month | 10 consecutive days | EEG (18 electrodes), EDs, SF, neurocognitive functions (neuropsychological tests) | Decrease of EDs (−35% for $n = 5$), increase of EDs (+48% for $n = 5$), decrease of 38.1% of SF at 1 month, improvement of attention and working memory after HD-tDCS | Mild headache |
| Lin et al. (2018) | 9 | Partial refractory epilepsy | 2 mA, 20 min Max follow-up: 1 month | 6 sessions of stim per month for 2 months | EEG (21 electrodes), EDs, Phase-lag-index (PLI), SF | No change in ED, decrease of PLI correlated to decrease of SF, Decrease of SF (−48 ± 31.2%) compared with baseline | Transient erythematous rash |
| Yang et al. (2019) | 7 | Epileptic spasms | Cathodal tDCS at 1 or 2 mA for 40 min (2 × 20 min with different electrode's positions) Follow-up: 28 days min, 4 months max | 14 consecutive days of stim (for 1 or several times) | SF | Decrease in SF for short or long-term duration compared to the baseline (−46% at 4 months follow-up) | NA |
| Yang et al. (2020) | 70 | Focal DRE | Randomized, double-blind, sham-controlled, three-arm (Group 1: Sham, Group 2: 20 min stim, Group 3: 2 × 20 min stim), parallel multicentric study Cathodal tDCS at 2 mA Follow-up: 56 days | 14 consecutive days | SF, QOLIE-31 | Decrease in SF in Group 2 (−50.73–21.91%) compared to sham, decrease in SF in Group 3 (−63.19–49.79%) compared to sham Decrease in SFs in Group 3 (64.98–66.32%) compared with group 2 at 5 weeks follow-up No difference in QOLIE | Mild itching sensation |

| | | | | | | | |
|---|---|---|---|---|---|---|---|
| Kaufmann et al. (2021) | 15 | DRE | Cathodal tDCS at 2 mA for 9 min stim- 20 min break–9 min stim No follow-up | 1 session | EEG (32–64-channels) IEDs, SF, Comfort Rating Questionnaire (CRQ) | Reduction in IEDs (−30.4 ± 21.1%), decrease of −48% in SF | Tingling feeling, burning sensation, slight tiredness |
| Kaye et al. (2021) | 20 | DRE | 2-center, open-label study, personalized multichannel tDCS (max 8 electrodes) 10 sessions of 20 min of cathodal tDCS over 2 weeks Max follow-up: 8–12 weeks | 10 sessions over 2 weeks | SF | SF reduction of −44% compared to baseline, 40% of responders | Increase in SF for 3 patients, tingling, itching sensation, transient dizziness, moderate and transient headache |
| Daoud et al. (2022) | 10 | Focal DRE | Personalized multichannel tDCS (max 8 electrodes) based on SEEG recordings, cathodal tDCS at 2 mA for 20 min stim- 20 min break–20 min stim Max follow-up: 6 months | 3 sessions of 5 consecutive days, each separated by 2 months | EEG (19-channels), R2 strength, IEDs, SF | Decrease in R2 strength in responders in alpha and beta frequency bands, SF reduction of −48% compared to baseline at 2 months follow-up | Slight itching, slight dizziness during the stimulation |

**Table II.1 Clinical trials with tDCS in epilepsy (n ≥ 5).** Abbreviations: tDCS, Transcranial direct current stimulation; MCD, Malformation of cortical development; EEG, Electroencephalography; ED, Epileptiform discharges; CSWS, Continuous Spike-Wave Discharges During Slow Sleep; DRE, Drug-resistant epilepsy; SF, Seizure frequency; QOLCE, Quality of Life in Childhood Epilepsy Questionnaire; MTLEHS, Mesial temporal lobe epilepsy with hippocampal sclerosis; TLE, Temporal lobe epilepsy; SICI, Short interval intracortical inhibition; MEP, Motor evoked potentials; EA, Epileptiform activity; IEDs, Interictal epileptiform activities; HD-tDCS, High-definition tDCS; PLI, Phase-lag index; QOLIE-31, Quality of life in epilepsy.

| References | Number of subjects | Age | Epilepsy type | Age epilepsy onset | Seizure semiology | EZ | Methodology | Duration | Method outcome | Effects | Side effects |
|---|---|---|---|---|---|---|---|---|---|---|---|
| Yook et al. (2011) | 1 (F) | 11 | Focal cortical dysplasia | 4 years | NA | Right temporo-parietal | Cathodal tDCS at 2 mA, 20 min, 5 times a week for 2 weeks Follow-up: 2 months | 5 consecutive day for 2 weeks | Sleep EEG | Decrease of seizure duration Decrease of SF (-50%) | NA |
| San-Juan et al. (2011) | 2 (2M) | P1: 31 P2: 17 | Rasmussen encephalitis | P1: 28 P2: 15 | P1: Generalized tonic-clonic seizures, epilepsia partialis continua, aphasia P2: Generalized tonic-clonic seizures, epilepsia partialis continua | | P1: cathodal tDCS at 1 mA, 60 min in 4 sessions Follow-up: 12 months P2: cathodal tDCS at 2 mA, 60 min in 4 sessions Follow-up: 6 months | 4 sessions | SF | P1: seizure free, improvement of attention P2: improvement of seizure intensity, improvement of motor functions, mild improvement of partial seizures | NA |
| San-Juan et al. (2016) | 1 (F) | 16 | Pharmaco- resistant juvenile myoclonic epilepsy | 12 years | Myoclonic absence | Anterior quadrant | tACS 1 mA at 3 Hz pulse train during 60 min Follow-up: 1-2 months | 4 consecutive days | EEG, SF | 75% increase of SF 15-day seizure free at 2 months follow-up | NA |
| Meiron et al. (2017) | 1 (M) | 30 months | Neonatal epileptic encephalopathy | 5 days | Continuous tonic spasms, focal motor seizures, hemiconvulsions, generalized tonic-clonic seizures, focal myoclonus, suppression-burst pattern | Right temporal lobe | HD-tDCS 4 × 1-Ring configuration, 20 min each day for 10 days, at 0.1–1.0 mA | 10 days | Video-EEG (32-channels), Paroxysmal epileptiform activity, hypsarrhythmic sharp waves, SF | No decrease in SF but lower sharp wave amplitude vs. baseline, vital signs, and blood chemistry stables | No adverse event |
| San-Juan et al. (2018) | 1 (F) | 28 | Focal cortical dysplasia | 9 years | Clonic and sensory right hemi-body seizures | Left frontal | 2 mA for 30 min, long-term follow-up: 1 year | 7 sessions over 9 weeks | EEG, counting spikes, SF | No change in the number of spikes, cumulative decrease in SF at long-term follow-up | Mild itching sensation |
| Marquardt et al. (2019) | 1 (F) | 15 | POLG-related mitochondrial disease, multifocal epilepsia partialis continua | NA | Status epilepticus multifocal seizures with multiple semiology, epilepsia partialis continua | Right occipital region | 2 mA for 20 min each day for 4 or 5 days | 5 consecutive days | EEG (25- channels), spike frequency, jerk frequency | No change in jerk frequency and spike | NA |

**Table II.2. Clinical cases with tES in epilepsy.** Abbreviations: tDCS, Transcranial direct current stimulation; EEG, Electroencephalography; SF, Seizure frequency; HD-tDCS, High-definition tDCS; tACS, Transcranial alternative current stimulation.

### *Epileptiform discharges*

Studying clinical outcomes, one of the main techniques to quantitatively measure the benefit of tES in epileptic patients is focusing on change in the count of interictal epileptiform discharges (IEDs) using electrophysiological recordings.

Among clinical studies, six clinical trials reported a decrease in interictal epileptic discharges using scalp EEG recordings (Fregni *et al.*, 2006; Faria *et al.*, 2012; Auvichayapat *et al.*, 2013, 2016; San-Juan *et al.*, 2017; Kaufmann *et al.*, 2021). First, Fregni et al. showed significant reduction in IEDs (64.3%) in epileptic patients receiving the active tDCS treatment (n = 10) compared to the sham group (n = 9) (Fregni *et al.*, 2006). Then, Auvichayapat et al. reported improvement in EEG abnormalities in 36 children suffering from intractable focal epilepsy (reduction in IEDs of 45.3% for 48 h) after one active stimulation session of cathodal tDCS at 1 mA for 20 min (n = 27) compared to sham group (n = 9)(Auvichayapat *et al.*, 2013).

In contrast to these findings, three clinical trials (Varga *et al.*, 2011; Assenza *et al.*, 2017; Lin *et al.*, 2018) and two clinical cases (San-Juan *et al.*, 2018; Marquardt *et al.*, 2019) reported no effect of cathodal tDCS on IEDs and one clinical study revealed an increase of 48% in interictal epileptiform discharges after cathodal tDCS (Karvigh *et al.*, 2017). Indeed, in a pediatric clinical study conducted by Varga et al. in five children suffering from refractory continuous spike and waves during slow sleep, they found no reduction of spike-index and they assigned this result to the use of smaller tDCS electrodes than those usually used in conventional tDCS (Varga *et al.*, 2011).

Furthermore, focusing on multichannel tDCS studies, Karvigh et al. reported a change in IEDs after repeated multichannel tDCS in epileptic patients (Karvigh *et al.*, 2017). However, the change of IEDs was different between patients. They indeed reported an increase in IEDs in five patients, while IEDs had decreased in the five others immediately and one month after high-definition tDCS (HD-tDCS). Thus, several clinical trials of tES in epilepsy did not report information regarding potential change in IEDs (Tekturk, Erdogan, Kurt, Kocagoncu, *et al.*, 2016; Tekturk, Erdogan, Kurt, Vanli-yavuz, *et al.*, 2016; Yang *et al.*, 2019; Kaye *et al.*, 2021).

These discrepancies may come from the variability of study designs, stimulation protocols and parameters such as the current intensity, stimulation duration, repetition of sessions, interval between sessions, electrode size, number, and localization of electrodes on the scalp. Further studies should standardize the stimulation parameters in order to optimize the clinical benefit of this technique by being more reproducible and efficient in epilepsy therapy.

Finally, despite the vast number of studies investigating the effects of tACS in memory, sleep and other functions, there is little account for tACS effects on epilepsy. One study conducted by Holmes et al. implemented a slow pulsed tACS protocol in seven adult DRE

patients with MRI-based personalized head models (Holmes *et al.*, 2019). The study consisted of five consecutive days of tES protocol combined with 256-channel dense EEG recordings before and after stimulation. Each tES pulse measured 100 ms in duration, with a 0.5 Hz stimulation frequency. They reported spike suppression without worsening of epileptiform activity, highlighting the safety and the efficacy of tACS to suppress IEDs. The use of IEDs as a quantifying marker for tES studies is a matter of debate. Indeed, since the presence of IEDs in scalp EEG recordings is not systematic and is not always related to seizure risk, the use of alternative electrophysiological methods for quantifying tES effects on the brain should be developed and explored in further trials.

### *Safety*

Cathodal tES is a safe, non-invasive method of neuromodulation showing only mild adverse events and transient side effects. To date, no serious adverse event has been reported in studies using cathodal tDCS as epilepsy treatment. The more common effects are slight itching (Fregni *et al.*, 2006; Zoghi *et al.*, 2016; Assenza *et al.*, 2017; San-Juan *et al.*, 2017; Yang *et al.*, 2020; Kaye *et al.*, 2021), tingling (Tekturk, Erdogan, Kurt, Kocagoncu, *et al.*, 2016; Kaufmann *et al.*, 2021; Kaye *et al.*, 2021), mild skin erythema (Faria *et al.*, 2012), and less frequently transient and moderate headache post-session (Zoghi *et al.*, 2016; Karvigh *et al.*, 2017; San-Juan *et al.*, 2017; Kaye *et al.*, 2021), slight tiredness (Kaufmann *et al.*, 2021) and burning sensation during the current application (Auvichayapat *et al.*, 2016; Zoghi *et al.*, 2016). Numerous studies reported no side effects at all (San-Juan *et al.*, 2011; Varga *et al.*, 2011; Faria *et al.*, 2012; Tekturk, Erdogan, Kurt, Vanli-yavuz, *et al.*, 2016; Meiron *et al.*, 2018). Kaye et al. reported that three participants in their study experienced an increase in seizure frequency (>50%) during treatment (Kaye *et al.*, 2021). In one participant, the cause might have been the presence of several undetected seizure foci. Their results suggest that high certainty regarding the epileptic focus for appropriate targeting is desirable and that stimulation should be stopped immediately if convincing evidence of a worsening of seizures is seen. Their data also suggested that if stimulation is stopped, a return to the baseline seizure frequency will occur.

The use of tACS in epilepsy is still limited. As for tDCS, previous studies using tACS only reported minor side effects. The safety and effects of tACS have been assessed in 13 DRE patients undergoing stereo-EEG investigation during NREM sleep and waking rest by (Lafon *et al.*, 2017). Sinusoidal tES was applied at either 0.75 Hz or 1 Hz with standard stimulation intensities (up to 2.5 mA; maximum induced field: 0.43 V/m). Although tACS failed to entrain spindle, gamma, or theta activity during neither NREM sleep nor waking rest, this study has proven the safety of low frequency tACS in epilepsy patients implanted with intracranial electrodes. Moreover, the tACS safety has also been proven with simultaneous tACS-SEEG recordings in both animal and human studies. Opitz et al. investigated the electric field distribution in non-human primates and human epileptic

patients during tACS and tDCS with variable frequencies and current intensities (Opitz *et al.*, 2016). Thus, they positively assessed the safety and the possibility of reaching subcortical structures.

### 2.3.2. Network effects of application of weak electric current in epilepsy

The human brain is characterized by specific structural and functional interconnection patterns linking cortical regions on short or long-distance. Neurological diseases inducing changes in synaptic plasticity may affect the communication within and between neuronal populations (Bettus *et al.*, 2008; Warren *et al.*, 2010; van Diessen *et al.*, 2013; Lagarde *et al.*, 2018). Critical features of pathological networks can be captured by measuring and localizing brain segregation and integration processes. Functional connectivity (FC) is typically used to define statistical temporal dependencies among neuronal signals measured from different brain regions. Thus, several methods (both linear and non-linear) have been developed for estimating FC. Synchrony of signals obtained from imaging and electrophysiological studies allow to characterize FC between different, distant brain regions.

Previous investigations have provided increasing evidence that epilepsy is a large-scale brain network disorder, not limited to a focal epileptogenic area (Pittau and Vulliemoz, 2015; Bartolomei *et al.*, 2017). Thus, even focal drug-resistant epilepsies are associated with interictal alteration in FC involving the nodes of the epileptogenic network. Using EEG, SEEG, magnetoencephalography (MEG), and functional magnetic resonance imaging (fMRI) data, previous studies have shown that the functional disturbances are characterized by reinforced FC within epileptic cortices [epileptogenic zone (EZ) and propagation zone (PZ)] compared to the non-involved zone (NIZ) (Bettus *et al.*, 2008; Warren *et al.*, 2010; van Diessen *et al.*, 2013; Bartolomei *et al.*, 2017), whereas the connectivity between EZ and the NIZ is lower. These studies also showed that an increased FC within the NIZ is associated with a poorer post-surgical outcome. The reduced synchrony observed between EZ and the surrounding NIZ indicates that the EZ may be functionally disconnected from surrounding brain regions (Warren *et al.*, 2010).

Observations of enhanced connectivity within the EZ suggested that this disturbance within the epileptogenic network may facilitate seizure occurrence and propagation by generating the exacerbated synchronization during seizures. This hypothesis defines new pathways for treatment. Thus, it seems reasonable to hypothesize that an efficient antiepileptic therapy would restore the normal FC decreasing abnormal coupling within EZ and between EZ and PZ. Recent studies indeed demonstrated that global brain network dynamics are linked to clinical outcome of pharmacological antiepileptic treatments and that such epilepsy-related FC changes are reversible and can be controlled by AEDs

(Clemens *et al.*, 2014; Anderson, Madhavan and Swaminathan, 2020). As far as neurostimulation is concerned, clinical studies using invasive neuromodulatory devices, such as vagus nerve stimulation (VNS) have shown a decreased synchrony induced by VNS as anti-epileptic mechanism in patients with good response (Fraschini *et al.*, 2013; Bodin *et al.*, 2015; Sangare *et al.*, 2020).

Recent clinical studies applying tES on epilepsy patients have as well found tES-induced FC modifications, which could accompany the decrease in epilepsy features after tES. In this section, we analyze the recent findings on tES induced network changes in epilepsy patients and their relation to the clinical outcome of stimulation. Stimulation via tDCS can modulate the whole brain networks, rather than just the stimulated cortical area localized under the scalp electrode (Luft *et al.*, 2014). Indeed, some studies performing cathodal tDCS on healthy participants have been conducted. Polanía et al. investigated the tDCS-induced effects on cortical network function using high-resolution EEG (62 channels). They found interhemispheric and interhemispheric connectivity changes in several frequency bands (4–90 Hz) after excitatory anodal tDCS over the primary motor cortex (Polanía *et al.*, 2011). Then, in a simultaneous high definition tDCS-EEG study, they reported that cathodal stimulation had induced significant changes in global broadband cortical activity compared to sham stimulation (Roy, Baxter, and Bin He, 2014). Applying cathodal stimulation resulted in lower global synchronization across frequency bands compared to sham and anodal stimulation, interpreted as an inhibitory action of cathodal stimulation.

Furthermore, in the clinical field, a recent double-blind sham-controlled study focused on FC changes after tDCS in epileptic patients has been performed (Tecchio *et al.*, 2018). This study aimed to explain part of cathodal tDCS clinical effects in six DRE patients with FC changes. Both cathodal tDCS and sham stimulations have been performed in each patient at 1 mA for 20 min for the active stimulation. They reported that the decrease of SF due to tDCS was correlated with an increase of coherence measures in epileptogenic focus in the whole frequency band and in theta band, compared with sham stimulation. Thus, the clinical improvement of epileptic patients was correlated with functional changes of EZ. On the contrary, another clinical trial, conducted by Lin et al., investigated the effects of repeated sessions of cathodal tDCS in nine patients suffering from partial refractory epilepsy (Lin *et al.*, 2018). Here, they estimated FC changes studying modifications of phase-lag index (PLI) and they obtained a negative correlation of PLI in alpha band and the SF decrease-induced by tDCS. They considered that tDCS induced a cumulative clinical benefit with reduction in SF in epileptic patients, associated with a decrease in synchronization. A more recent study aimed to evaluate and predict the potential clinical efficacy of cathodal tDCS by analyzing the induced functional network alterations (Hao *et al.*, 2021). The 27 epileptic patients were separated in two groups of stimulation: sham group and active cathodal tDCS group with 20-min stimulation at -1 mA, for five consecutive days, targeting the regions with higher IEDs rate. Graph theoretical analysis has been based on fMRI data performed before the tDCS treatment and after the 5-days stimulation. They reported tDCS-induced functional alterations with

a significant decrease of graph theoretical measures only for the patients presenting a good response to tDCS, acknowledging the potential of fMRI-based graph theoretical measures for clinical prediction of tDCS outcome in epileptic patients. Furthermore, using EEG data, another controlled tDCS trial conducted on 25 DRE patients has shown an attenuation of the functional network's connectivity (Luo *et al.*, 2021). Indeed, they estimated changes in FC between brain networks using graph-theory metrics such as average clustering coefficient, characteristic path length and small-world index calculated from scalp EEG recorded at baseline, at the end of 5-days cathodal tDCS at -1 mA for 20 min, and at four weeks follow-up. They observed a decrease in neural transfer efficiency after cathodal tDCS and a slight increase in characteristic path-length. The measure of characteristic path-length is controversial in most studies in epilepsy. Thus, they hypothesized that the increase in path length may be explained by the loss of connectivity between the nodes, and that the change in small-world index after cathodal tDCS is more meaningful to reflect functional induced changes. In this study, the alterations in FC were only associated with significant IED reduction and may be responsible for the electrophysiological protection of the brain limiting seizure onset and seizure propagation. Recently, we have studied the link between EEG functional connectivity changes and the response to multichannel tDCS (Daoud *et al.*, 2022). This study included ten drug resistant epilepsy patients. Multichannel tDCS was applied during three cycles (one cycle every two months) of stimulation. Each cycle consisted of five consecutive days where patients received tDCS daily in two 20 min sessions separated by 20 min. After the last tDCS session, five patients experienced a SF decrease of 50% or more compared with baseline (R: responders). FC changes between cycles and across R and non-responder (NR) patients was estimated using linear correlation. R presented a significant decrease in FC at the third session in alpha and beta frequency bands.

To conclude, since some studies suggested that cathodal tDCS showed long-term cumulative effects of functional disturbances, a possible mechanism underlying this electrophysiological plasticity focused on network's changes might be explained by inhibition and long-term depression (LTD). Consequently, cellular, and molecular studies are needed to shed light on the involved underlying mechanisms due to tES. Thus, *in vivo*, *in vitro*, and computational studies are needed to address this gap in knowledge.

### 2.3.3. Neurobiological aspects

The inter-subjects and inter-studies variability in clinical efficacy and in network changes underlie the need for a better identification of the basic mechanisms of tES. To discover the underpinnings of tES on brain activity, external weak electrical fields have been applied to *in vitro*, *in vivo*, and *in silico* (computational) models. Moreover, to identify the actual current flow inside the brain during tES and evaluate its potential to reach deep brain structures, various studies have taken advantage of intracranial recordings from

DRE patients during tES stimulation (Opitz *et al.*, 2016; Huang *et al.*, 2017; Louviot *et al.*, 2022). Here, we present the main findings on tES modulation of epileptic activity from *in vitro*, *in vivo*, *in silico* and human models. Since the objective of this review is to summarize the findings on the use of tES in epilepsy, we will not present studies on rhythm entrainment on normal brain activity. For comprehensive reviews on such topics, the reader is referred to (Reato *et al.*, 2013; Liu *et al.*, 2018).

### *In vitro* studies

*In vitro* studies have been useful to observe the cellular effects of tES via the application of either alternating (AC) or direct current (DC) electric fields (EF) on brain slices. The most common setup consists in placing two parallel Ag-AgCl plates or wires in the bath containing hippocampal or cortical slices and applying a certain current across the slice. Therefore, it is possible to record both intracellularly and extracellularly. To reproduce epilepsy *in vitro* (creating hyperexcitability), the standard artificial cerebrospinal fluid bath is modified by adding or reducing specific components. The main models use either bicuculline, 4-aminopyridine, picrotoxin, low-$Ca^{2+}$ or high-$K^{+}$ concentration changes to induce epileptiform activity. To offer a clearer overview of the used methods, Table II.3 summarizes the epilepsy model, stimulation methods and electric field intensities of all *in vitro* studies here included.

Most *in vitro* studies employed DC fields to demonstrate its ability in controlling epileptogenic biomarkers and seizure features. Applied cathodal EFs show suppression of burst activity in hippocampal (Ghai, Bikson and Durand, 2000; Lian *et al.*, 2003; Bikson *et al.*, 2004) and thalamo-cingulate slices (Chang, Lu and Shyu, 2015). The efficacy of DC fields in acute suppression of epileptiform-like activity depends on EF polarity (Ghai, Bikson and Durand, 2000; Lian *et al.*, 2003; Bikson *et al.*, 2004; Chang, Lu and Shyu, 2015). Chang et al. demonstrated how cathodal DC stimulation, if oriented parallel to the dendritic-somatic axis, can control seizure duration and propagation in slices of mice anterior cingulate cortex (Chang, Lu and Shyu, 2015). Ghai et al. demonstrated that cathodal DC application suppresses bursts more efficiently when they are parallel to the cell dendritic-somatic axis (Ghai, Bikson and Durand, 2000). Moreover, they showed how the *in vitro* low-$Ca^{2+}$ model of epilepsy requires lower EF intensities than those required for epileptiform activity suppression in the low-$K^{+}$ model. Such finding could be due to the induced cell swelling of the low-$Ca^{2+}$ cellular environment, which in turn leads to reduced extracellular volume and higher tissue resistance. Thus, DC fields efficacy depends not only on the cellular orientation with respect to the EF, but also on the model of epilepsy and osmolarity. A possible limitation to the use of DC fields is the post-stimulation rebound that was shown to occur even after short DC pulses (Lian *et al.*, 2003). Nevertheless, this rebound was caused by an electric field magnitude of up to 160 V/m, which is unrealistically obtained in human brains during tES (where, from both measurements and models we know that EF intensity is of the order of 1 V/m) and thus

should not have an impact on clinical tES protocols. Moreover, DC fields do not modulate all cortical layers uniformly, which might be the reason for the variable cathodal-tDCS clinical efficacy (Sun *et al.*, 2020).

Cathodal DC fields show both short- and long-term effects on epileptic-like activity, which would be supported, respectively, by neuronal hyperpolarization (Ghai, Bikson and Durand, 2000) and long-term depression (LTD)—like mechanisms (Lian *et al.*, 2003; Chang, Lu and Shyu, 2015). Regarding long-term effects of stimulation, cathodal tDCS (cathodal tDCS) was shown to induce post-synaptic depression even after 15 min of stimulation, but only when combined with background spontaneous synaptic activity (Chang, Lu and Shyu, 2015). In this study, such effects did not apply to the pre-synaptic currents and lasted more than 1 h, suggesting the involvement of LTD mechanisms. Indeed, Chang et al. demonstrated that the application of the N-methyl-D aspartate (NMDA) receptor antagonist abolished tDCS-induced LTD, highlighting the fundamental role of NMDA-mediated plasticity in tES long-term effects. Nevertheless, contradicting results of NMDA's role in long-term DC modulation comes from (Sun *et al.*, 2020). In this study, the authors demonstrate how cathodal DC stimulation coupled with NMDA receptor block produces LTD in different cortical layers, both in mouse primary motor cortex and human neocortex *in vitro* slices. Such contradicting findings may be due to differences in brain slices (thalamo-cingulate in Chang et al., motor cortex and neocortex in Sun et al.) or type of stimulation paradigm (see Table II.3 for details on the stimulation parameters).

Although less investigated than DC fields, AC stimulation has been studied in various in vitro studies. Like DC fields, AC stimulation can suppress burst activity in epilepsy models (Bikson *et al.*, 2001; Lian *et al.*, 2003). Differently from DC stimulation, AC stimulation-induced polarization does not depend on orientation (Bikson *et al.*, 2001; Lian *et al.*, 2003) and does not show any post-stimulation rebound (Lian *et al.*, 2003). Instead, AC stimulation induces different effects depending on the stimulus frequency. Bikson et al. showed that AC stimulation at 500 and 5,000 Hz could not suppress burst activity at any field strength, while 20 and 50 Hz had very similar effects and significantly reduced epileptiform discharges (Bikson *et al.*, 2001). In the same study, they further showed that neither stimulus waveform nor cell morphology influenced the EF-induced polarization. Interestingly, Bikson et al. reported the first direct measurement of membrane time constant (ranging from 14 to 70 ms), crucial for understanding the induced polarization of external EF (Bikson *et al.*, 2004). This result indicates that neurons should be less sensitive to relatively fast AC electric fields (>15 Hz) because of the quite slow polarization recovery of the membrane.

*In vitro* studies are particularly suited for understanding the mechanisms underlying the effects of electric fields on brain tissue, as induced by tES stimulation. Concerning DC fields, studies have shown that stimulation induces linear polarization in neurons. For EF magnitudes below 40 V/m, every 1 V/m of stimulation intensity will typically induce a membrane polarization of about 0.12 V/m in pyramidal cells (Bikson *et al.*, 2004). While

the underlying mechanisms of DC fields in epileptiform bursts suppression appear to be represented by membrane hyperpolarization (Ghai, Bikson and Durand, 2000; Rahman *et al.*, 2017), the mechanisms underlying AC effects would be more complex (Bikson *et al.*, 2001; Lian *et al.*, 2003). Indeed, AC stimulation induces an increase (2.5 mM ± 0.5, n = 5) in extracellular $K^+$ concentration lasting for the whole stimulus duration and related to burst suppression (Lian *et al.*, 2003). These authors moreover showed that bursts started again after a decrease in $K^+$ extracellular concentration.

It is nevertheless important to notice how the abovementioned studies were carried out with EF intensities significantly stronger than the standard intensities observed intracranially in tES human studies. It is estimated that a tDCS intensity of 1 mA generates electrical fields at the level of cortical neurons in the 0.2–0.5 V/m range (Datta *et al.*, 2009; Miranda *et al.*, 2013), while 2 mA produce an EF of about of 1 V/m (the reader is referred to the review summarizing studies non-involving epilepsy models such as (Jackson *et al.*, 2016; Vöröslakos *et al.*, 2018). Indeed, only Ghai et al. and Chang et al. use EF intensities ranging 2–16 V/m, which are nevertheless at least twice higher than the EF produced by a 2 mA tDCS (217,219). Therefore, more efforts should be made to characterize the translation of *in vitro* studies to *in vivo* ones, evaluating the reliability of seizure models, quantifying the differences between thin slices and real brains with gyri and sulci (the EF is uniformly distributed in slices, but not uniformly distributed in real brains), and adapting EF intensities to the ones realistically used in human studies. *In vivo* studies are pivotal for implementing more realistic stimulation parameters within *in vitro* investigations.

| References | Model | AC/DC | Stimulation | EF magnitude |
|---|---|---|---|---|
| Ghai et al. (2000) | Low-Ca2+ rat model of epilepsy *in vitro*, hpc CA1 region brain slices | DC only | 2 parallel AgCl-coated wires placed on the surface of the ACSF in the interface chamber. Changes in EF orientation angles. | 1–5 V/m, min 3.7 V/m for suppression activity |
| Bikson et al. (2001) | Rat hpc CA1 and CA3 brain slices, 3 different ACSF models of spontaneous bursting (low Ca, high K) and picrotoxin | AC only | AgCl-coated wires on surface of ACSF, square biphasic wave or 50 Hz sin wave + 20,50,500 and 5,000 Hz stim only in spontaneous low-Ca2+ bursting | Min ±25 V/m, Max ±200 V/m |
| Lian et al. (2003) | Rat hpc CA1 or CA3 brain slices, 3 different ACSF models of spontaneous bursting (low Ca, high K) and picrotoxin | DC and AC | Same as above (uniform external EF) + local monopolar stimulation to mimic DBS, 50 Hz | ±160 V/m |
| Bikson et al. (2004) | Rat hpc slices, intracellular and voltage-sensitive dye recordings | DC and AC | AgCl wires >40 mm long, placed >15 mm apart or sintered Ag–AgCl cylindrical pellet electrodes 12 mm long and placed >5 mm apart (for stronger fields) | Min ±40 V/m |
| Chang et al. (2015) | Mouse thalamocingulate slices, 4-aminopyridine and bicuculline. | DC only | 2 V/m cathodal DC + higher EF magnitude (max 16 V/m) to induce an immediate effect on seizure-like activity. For LTD analysis: 15 min of 4 V/m cathodal DC stimulation applied after 15 min of baseline | 2–16 V/m |
| Rahman et al. (2017) | Rat primary motor cortex slices; anodal DC stimulation: EF > 0 on M1, opposite for cathodal | DC only | 15 (adaptation) or 200 (post-adaptation) constant-current pulses (0.2 ms, 10-150 uA) or uniform extracellular EFs. Pre-synaptic afferent axons were stimulated at 5, 10, 20, and 40 Hz to simulate synaptic activity with c-DCS or a-DCS | ±10 and ±20 V/m |
| Sun et al. (2020) | *In vitro*: mouse M1 and human post-operative neocortex slices, *in vivo*: mouse kainic acid (KA)-seizure model. Drug: NMDAR blockers (memantine/D-AP5) | DC only | cDCS: 400 μA, 25 min; cathode: proximal to the cortical pial surface, anode: beneath the subcortical WM. | 9.2 V/m in the ACSF; 2.3 V/m at the recording surface |

**Table III.3. Models and stimulation methods used in *in vitro* studies.** Abbreviations: AC, Alternating Current; DC, Direct Current; hpc, hippocampus; CA1, CA3, hippocampus Cornu Ammonis 1 and 3; $Ca^{2+}$, calcium; $K^{+}$, potassium; ACSF, artificial cerebrospinal fluid; Ag, silver; AgCl, silver chloride; M1, primary motor cortex; LTD, long term depression.

### *In vivo studies*

Animal models of epilepsy (depicting epilepsy features such as spike and wave discharges, generalized epilepsy-like seizures, focal epilepsy, status epilepticus models) can be genetic or obtained from various electrical or chemical procedures. For a comprehensive overview on these models, not subject of the current review, we refer the reader to (Pitkänen *et al.*, 2017). All records included in this review used rat models of epilepsy. More precisely, the used models consisted in: cortical-ramp stimulation to induce focal epilepsy (one record, (Liebetanz *et al.*, 2006); spontaneous recurring spike-wave patterns (two records, (Berényi *et al.*, 2012; Kozák and Berényi, 2017)); WAG/Rij genetically modified rats (one record, (Zobeiri and Van Luijtelaar, 2013)) as model of absence epilepsy; lithium-pilocarpine (one record, (Kamida *et al.*, 2011)) and kainic acid (1 record: (Wu *et al.*, 2020)) as status epilepticus models; pentylenetetrazol (two records: (Dhamne *et al.*, 2015; Regner *et al.*, 2020)) as a model of either acute or chronic generalized seizures.

Cathodal tDCS efficiently increased the threshold of seizure triggering and latency of the first seizure after epilepsy induction (Liebetanz *et al.*, 2006; Dhamne *et al.*, 2015; Regner *et al.*, 2020; Wu *et al.*, 2020). Other outcomes concerned decrease in seizure duration, frequency, and severity (Kamida *et al.*, 2011; Dhamne *et al.*, 2015; Wu *et al.*, 2020). In addition, cathodal tDCS led to changes in epileptiform discharges such as decrease of number and duration of spike-and-wave complexes (Zobeiri and Van Luijtelaar, 2013; Wu *et al.*, 2020), and reduction of epileptic bursts (Dhamne *et al.*, 2015). Despite the positive results in seizure rate and epileptiform discharges reduction when applied interictally, tES does not seem to be able to stop ongoing seizures (Dhamne *et al.*, 2015). Nevertheless, some studies have shown the potential of tES combined with pharmacological treatment, demonstrating that adding either lorazepam (Dhamne *et al.*, 2015) or diazepam (Regner *et al.*, 2020) to the tDCS stimulation can efficiently increase the antiepileptic effects of stimulation (abortion of seizures, threshold increase for the first seizure). Therefore, association of tDCS with pharmacological treatment may potentially reduce drug doses and thus, the drug's side effects.

Moreover, cathodal tDCS induces changes of signal frequency content: during stimulation, power in delta band was increased and power in alpha, beta and theta bands decreased (Zobeiri and Van Luijtelaar, 2013; Dhamne *et al.*, 2015). Wu et al. found that applying cathodal tDCS before status epilepticus induction *via* kainic acid injections led to a small increase of low frequency power (3–6Hz) and an important decrease of high frequency content (35–37Hz) in the cathodal tDCS treated group with respect to sham (Wu *et al.*, 2020). In the study, they show that the high frequency content is associated with epileptic polyspikes, while the low frequency content would represent spike and wave patterns. Therefore, frequency power changes would indicate that tDCS inhibits neuronal networks by the inhibition of polyspike initiation, while shifting the tendency toward spike and wave patterns. Consistently with *in vitro* and human studies, *in vivo* stimulation effects are intensity dependent. More specifically, whereas a 100 μA current can cause a reduction in number of spike-and-wave patterns, only a 150 μA current could affect the duration of spike and wave episodes during cathodal tDCS and for about 1 h after stimulation (Zobeiri and Van Luijtelaar, 2013). Similarly, Liebetanz et al. showed that, whereas 30 min of cathodal tDCS at 100 μA had no effect on the seizure threshold, a stimulation of 60 min led to seizures threshold changes up to 120 min after tDCS (Liebetanz *et al.*, 2006). In contrast, a stimulation of 200 μA resulted in significant effects even after only 30 min of stimulation.

Besides changes in seizure activity or epileptiform discharges, studies show either non-significant or very small changes in animal behavior during tES stimulation. Zobeiri and van Luijtelaar show a small increase in rats behavioural activity as recorded by passive infrared registration, but only for 150 μA and not 100 μA stimulation (Zobeiri and Van Luijtelaar, 2013). Concerning the cognitive changes possibly induced by tDCS, Kamida et al. found that long-term tDCS treatment (30 min daily sessions for two weeks) rescued spatial memory impairment, measures *via* the Morris water maze test, in a rodent model of status epilepticus (Kamida *et al.*, 2011). Regarding the impact of tES on brain tissue, no

histological abnormalities were found (Liebetanz *et al.*, 2006; Zobeiri and Van Luijtelaar, 2013). However, various molecular changes have been reported after tES. Importantly, several studies demonstrated a reduction in hippocampal mossy fiber sprouting (Kamida *et al.*, 2011; Wu *et al.*, 2020), associated with seizure severity and cognitive impairment after status epilepticus induction. Since seizures can lead to microglia activation and thus produce inflammatory cytokines, Regner et al. investigated the immunomodulatory effects of cathodal tDCS (Regner *et al.*, 2020). Indeed, tDCS induced changes in interleukin 1 beta (IL-1β, one of the main pro-inflammatory cytokines) and Tumor Necrosis Factor alpha (TNF-α) levels. While IL-1β decreased in the hippocampus and increased in the cortex of cathodal tDCS treated animals, TNF-α displayed changes only at cortical level (increase in the cathodal tDCS group, decrease in the anodal tDCS group). Moreover, cathodal tDCS alone or associated with diazepam increased the cortical nerve growth factor (NGF) and brain-derived neurotrophic factor (BDNF) levels, which might be linked to the improved convulsive behavior of the tDCS-treated animals (Regner *et al.*, 2020). Oppositely to cortical BDNF, hippocampal BDNF levels were reduced after cathodal tDCS treatment (Regner *et al.*, 2020; Wu *et al.*, 2020). Decrease of BDNF was moreover correlated to reduction of seizure severity (Wu *et al.*, 2020).

Two studies moreover investigated the effects of tACS on epileptogenic activity *in vivo*. Berényi et al. showed the ability of standard 1 Hz tACS to modulate multi-unit activity firing and spike amplitude in a thalamocortical epilepsy rodent model (Berényi *et al.*, 2012). However, such open loop stimulation was unable to modulate spike and wave duration. Approaches using trigger-based stimulation, for instance sending a train of stimulation pulses when the system automatically detects a spike and wave pattern (closed loop stimulation), might be more efficient in modulating epileptogenic events. Closed loop tACS stimulation could indeed efficiently reduce spike and wave episodes duration by more than 60% with respect to sham (Berényi *et al.*, 2012; Kozák and Berényi, 2017). Again, this effect is highly intensity-dependent: only a 10 V/m tACS, but not a 0.8 V/m one, could successfully modulate spike and wave patterns. Although applying an intracranial EF intensity of 10 V/m would pose safety concerns in humans, this study also shows that tES starting from 1 V/m can effectively entrain neurons by phase modulation. Nevertheless, it is important to notice that such closed loop studies used a triphasic stimulus pulse, which is hard to use in clinical settings for humans and needs high stimulation intensity to be effective. Although the closed loop treatment was highly effective in reducing time spent in seizures and seizure durations, its effects did not outlast the stimulation period, and the parameters that were effectively controlled by tES returned to baseline right after the end of the treatment (Kozák and Berényi, 2017).

Furthermore, since epilepsy is a chronic disease, understanding the long-term effects of tES is fundamental to better shape a stimulation paradigm for epileptic patients. Despite this, most of the studies investigated acute tES effects. Zobeiri and van Luijtelaar (2013) partially answered this issue by adding an EEG recording 24 h after one day of tES stimulation (four sessions of 15 min cathodal tDCS) but found no difference in number or duration of spike and wave events compared to baseline pre-tDCS (Zobeiri and Van

Luijtelaar, 2013)(Zobeiri and van Luijtelaar, 2013). Real long-term effects of tES were evaluated by Kozák and Berényi (2017) in an unsupervised closed loop tES experiment. When tES was applied chronically on demand for six weeks continuously (four months and half for one rat), the decrease of seizure duration was constant over the weeks but returned to baseline right after the end of the treatment (Kozák and Berényi, 2017). The long-term effects of tES may as well depend on the time in which stimulation is applied. Indeed, Wu et al. (2020) found only acute effects when applying stimulation on epileptic rats but reported longer-lasting effects (up to few days after kainic acid injection) when tDCS was applied before the induction of epilepsy (Wu *et al.*, 2020). Thus, tDCS might establish neuroprotective mechanisms which could have more long-term effects than stimulation protocols aimed at reducing ongoing seizure-like activity.

Overall, *in vivo* models of tES and epilepsy solve some of the issues of *in vitro* models, such as the need for more realistic brain anatomy and EF intensities. On the other hand, they still present some limitations. For instance, most of the studies here reported used epicranial electrodes (fixated onto the temporal bone) instead of transcranial electrodes (Liebetanz *et al.*, 2006; Kamida *et al.*, 2011; Berényi *et al.*, 2012; Zobeiri and Van Luijtelaar, 2013). This, coupled to relatively strong EF intensities and the differences in brain anatomy (rodents have smaller brains and lack gyrification), pose issues to the translation to human studies. Computational models of tES can provide partial solutions to such issues by using realistic human brain models and stimulation parameters.

### *Human studies: electrical fields distributions*

Although *in-vitro* and *in-vivo* studies have fully demonstrated the ability of weak electric fields to affect the firing patterns and excitability of neuronal populations, the study of tES mechanisms in patients with epilepsy is not straightforward. Indeed, to elucidate the underpinnings of weak EF in human brains, invasive recording techniques and innovative computational simulations are needed. A great step toward the understanding of EF propagation in the human brain has been made by tACS studies in DRE patients, using intracranial electrodes to measure the effects of stimulation in deep structures.

Thanks to such invasive recordings, tACS stimulation has been found to produce EF up to about 0.4 V/m when applying a 1 mA current through two scalp electrodes (Opitz *et al.*, 2016; Huang *et al.*, 2017; Louviot *et al.*, 2022). Importantly, it has been shown that EF can reach structures as deep as the hippocampus and the amygdala (Huang *et al.*, 2017; Lafon *et al.*, 2017; Louviot *et al.*, 2022). In such structures, Louviot et al. (2022) recorded maximal EF magnitudes of 0.38 and 0.49 V/m, respectively (Louviot *et al.*, 2022). Generally, EF peak intensities were achieved underneath the stimulation electrodes, but also in deep midline structures such as the anterior cingulate cortex (Huang *et al.*, 2017; Lafon *et al.*, 2017).

Reported EF magnitudes differ between records. Indeed, the measured EF in SEEG electrodes highly depends on the direction of the electrode with respect to the local EF vector and the way in which the EF is calculated. Although current models suggest that the EF magnitude should not depend strongly on frequency (for frequencies below a few kHz, (Ruffini *et al.*, 2013)), Opitz et al. (2016) described an inverse correlation between frequency and EF magnitude, while the correlation was direct in Louviot et al. (2022). Indeed, the former study reported a 10% drop in EF magnitude at 150 Hz, the latter found that EF magnitudes at 1 Hz were 15% lower than at 300 Hz. Such discrepancies may be explained by instrumental or experimental conditions. Lafon et al. (2017) found that tACS at 2.5 mA peak intensity—above the 2 mA maximal current normally used on human subjects—gives rise to a maximal electrical field intensity of only 0.16 V/m across recording electrodes (Lafon *et al.*, 2017). Including details such as anisotropic white matter and inhomogeneous bone compartments does not improve prediction performance (Huang *et al.*, 2017).

In conclusion, these studies not only demonstrate the ability of tES in reaching deep brain structures in human brains, but they also largely validate realistic modeling of electric fields. Since non-epilepsy *in vitro* models found that EF intensities of 0.2–0.5 V/m are sufficient for modifying spike timing and excitability (see *in vitro* section and (Liu *et al.*, 2018)), the EF intensities found in the human brain would be able to modify neural activity even at 1 mA stimulation (Opitz *et al.*, 2016; Huang *et al.*, 2017; Louviot *et al.*, 2022). Moreover, such reports confirm the importance of using computational models and provide important information for their future improvement. Nevertheless, there still are limitations. Firstly, the location of intracranial electrodes is sparse and corresponds to clinical needs, not to research ones. This restrains the measurements only to specific brain locations (mainly the ones involved in epilepsy) and prevents recordings from the brain surface, where the highest field intensity is expected. Secondly, there is no possible evaluation of differences between epileptic and healthy brains, restricting these results only to patients with epilepsy. The lack of cognitive, molecular, and pharmacological characterizations of such simultaneous tACS-intracranial recordings studies makes it hard to extrapolate the pure physical effects of field distributions from the physiological perturbations of epilepsy and cognitive states.

### *Computational models*

In recent years, the development of mathematical and computational tools has allowed for the modeling of electric fields on realistic brain representations. Using biophysical models, various parameters of tES stimulation and brain composition may be analyzed, enabling to target brain regions with more accuracy (Sadleir *et al.*, 2012). Computational head models allow for analysis of EF intensities and electrode positions which optimize the stimulation efficacy taking into account the unique geometry and conductive properties of individual heads. In this section, we review the main studies

aimed at improving and clarifying the underpinnings of tES stimulation protocols in epilepsy patients *via in silico* models (Denoyer *et al.*, 2020; Giannakakis *et al.*, 2020). We summarize the findings of studies which analyzed the optimal stimulation montage parameters for reaching the highest EF spatial focality and intensity on target brain areas (Datta *et al.*, 2009; Miranda *et al.*, 2013; Parazzini *et al.*, 2014; Ruffini *et al.*, 2014; Opitz *et al.*, 2018). Individualized head models are fundamental for defining the optimal stimulation montage. Even small deviations between the simulated and real brain target can in fact result in strong differences in the EF distributions applied during tES stimulation (Opitz *et al.*, 2018). Moreover, modeling the presence of skull defects and the precise location of subdural or intracranial electrodes leads to significantly higher similarity between the predicted and the measured intracranial EF distribution (Opitz *et al.*, 2018). In addition, the patient-specific geometry of sulci and gyri is crucial to evaluate the correct EF components on the brain surface (Miranda *et al.*, 2013).

Using intracranial recordings during tES stimulation in ten DRE patients, Huang et al. (2017) demonstrated that the possibility of reaching deep targets (as described in human subsection) might be possible thanks to the proximity of cerebrospinal fluid (CSF)-filled ventricles (Huang *et al.*, 2017). Indeed, CSF is hypothesized to drive part of the skull-shunted current into deep brain regions (Datta *et al.*, 2009; Huang *et al.*, 2017). It is thus critical to integrate computational models of tES with CSF distribution and quantify its effect on EF distribution. Indeed, models accounting for this information found different EF distributions in the interfaces of gray matter with either white matter or CSF (Miranda *et al.*, 2013). This result depended on the chosen conductivity values of white matter and CSF, insisting on the need of precise definition of conductivity values for better representing tissue heterogeneity. Studies on simultaneous tACS stimulation and invasive recordings in DRE patients or non-human primates also evaluated the accuracy of their individualized computational models of EF distributions. The simulations resulted in similar distributions than the actual recorded ones, with an accuracy of $r = 0.86$ for cortical electrodes and $r = 0.88$ for depth electrodes (Huang *et al.*, 2017). It is nevertheless important to notice that, in some locations and on average, the simulated fields were higher than the real ones because of the limited spatial sampling of intracranial electrodes (median values across all electrode locations of 0.08 V/m in contrast with 0.002 V/m for real data) (Lafon *et al.*, 2017; Opitz *et al.*, 2018), or because of potentially wrong conductivity values (Huang *et al.*, 2017; Opitz *et al.*, 2018). The effects of tDCS depend on its polarity (Ghai, Bikson and Durand, 2000; Lian *et al.*, 2003; Bikson *et al.*, 2004; Chang, Lu and Shyu, 2015). Thus, it is crucial to model the EF orientation to best predict the effects of stimulation. Indeed, although EF magnitude indicates the strength of the induced field, the same magnitude applied to different brain regions (thus, neuronal composition and orientation) can give rise to different tES effects. For these reasons, Miranda et al. (2013) modeled the EF components during a bipolar DC stimulation (1–2 mA), finding that the highest values of the EF normal component concentrate in the sulci just below the stimulating electrodes, whereas the highest values of the tangential component occur on the gyri between the cathode and anode electrodes (Miranda *et al.*, 2013). Taking this into account, Ruffini et al. (2014) designed a computational model of

possible tES montages aimed at maximizing the chosen EF component on the target areas (Ruffini *et al.*, 2014). Such an approach appears pivotal for the optimization of tES clinical effects and the characterization of the differential roles of the EF components.

Another important parameter in the efficacy of tES stimulation is the geometry and position of scalp electrodes. Although the most used electrodes were, until recently, large (25 $cm^2$ or more) bipolar patches, this solution might not optimize the spatial control and focality required for epilepsy treatment. A configuration using small (0.4 cm radius) electrodes in a ring is more suitable for reaching the desired focality of stimulation beneath the stimulating electrodes, avoiding potentially unwanted stimulation of non-targeted areas (Datta *et al.*, 2009). Nevertheless, despite the greater focality given using smaller electrodes, this configuration needed two times the current used with a rectangular patch to produce the same EF intensity in the targeted area. This highlights the importance of studying other electrode configurations and dimensions to achieve focality without the need of increasing the current intensity. To answer these questions, Ruffini et al. (2014) studied 26 different configurations of multifocal montages with small electrodes (1 cm radius, anode at Cz and cathode at one of the other 26 positions of the 10–20 system) and compared the results with a model using two circular sponge electrodes (25 $cm^2$) (Ruffini *et al.*, 2014). With the goal of defining the optimal montage to target extended brain areas, they used precise head models combined with detailed cortical target maps obtained by functional data such as resting-state fMRI, PET, and EEG. Due to the complex nature of drug-resistant epilepsy, assigning target weights to specific cortical regions can strongly improve the tES effects, for instance by differentially optimizing the magnitude of the normal or tangential components of the EF according to the individual cortical anatomy (Ruffini *et al.*, 2014). This study also confirmed the improvement of stimulation spatial focality when using multifocal montages with small electrodes *vs*. large-sponge bipolar montages (Figure II.1.A).

Additionally, the anode position in tDCS clinical protocols has been a matter of discussion (Bikson *et al.*, 2016). Although most montages with two electrodes place the anode on non-epileptogenic brain areas, some protocols (Auvichayapat *et al.*, 2013; Lin *et al.*, 2018) place it over the contralateral shoulder. Parazzini et al. (2014) used customized brain models to demonstrate that varying the anode position induces different EF intensity distributions not only at cortical level but also in the deeper brain regions (Parazzini *et al.*, 2014). More specifically, they showed that placing the anode over the shoulder significantly enhances the EF induced in deep brain regions (including thalamus and hippocampus) and strongly increases the spatial focality of cathodal stimulation with respect to an anode positioned on the contralateral cortex. Therefore, the risk of seizure induction in epilepsy patients during tDCS might be limited using an extracephalic anode, which could dramatically reduce the excitability levels induced beneath the anodal electrode. However, placing the anode on the upper arm could cause hardly predictable changes in the current flow, increasing the amount of current flowing in parietal regions even when the parietal cortex is not directly targeted. Moreover, extracephalic electrodes might lead to spurious currents in vital areas such as the heart, brainstem, and respiratory

system (Vandermeeren, Jamart and Ossemann, 2010). More safety and electric fields distribution studies are needed before employing extracephalic electrodes in a more consistent manner. Correct electrode placing is crucial; indeed, electrodes should be placed a minimum of 1 cm away from the optimal location given by simulations to achieve the predicted EF distribution (Opitz *et al.*, 2018). For more information on the possible implementation guidelines of tDCS, we refer the reader to the review by (Thair *et al.*, 2017).

In addition to providing useful information on EF distribution and optimal stimulation design, computational models allow to characterize the physiological mechanisms of tES on brain activity. To model the long-term effects of tDCS on epileptic activity, Giannakakis et al. (2020) investigated how the brain structural connectivity prior to stimulation can affect the changes induced during and after a stimulation session (Giannakakis *et al.*, 2020). With this aim, they used structural connectivity data from healthy and epileptic patients to create either healthy or epileptic network nodes, modeling tDCS effects up to 24 h after stimulation. The main findings were: (1) the simulated effects of tDCS differ between network models of either healthy controls and epilepsy patients; (2) the modeled stimulation of epileptogenic networks resulted in medium-term (5–6 h), connectivity decrease inside the targeted areas and in long-term connectivity increase inside some non-stimulated regions connected to the stimulated ones; (3) there was a high inter-subject variability in both short- and long- term effects of tDCS, given by the individual pre-stimulation connectivity matrices. Interestingly, when comparing the simulated data with the clinical outcomes of the patients used to create such models, there was a weak correlation between the connectivity increase in non-targeted areas and worsen surgery outcome. It is important to notice that the tDCS session was modeled as a 50% reduction of external input in the simulated amygdala, hippocampus and parahippocampus nodes. Despite the ability of tES in reaching such deep brain regions, the EF intensities found there correspond to a maximum of 0.49 V/m (see the paragraph on EF distributions and (Huang *et al.*, 2017; Lafon *et al.*, 2017; Louviot *et al.*, 2022)). It is thus arguable that tES could result in a decrease of deep structures activity of 50% with such a small EF modulation, but more studies are needed to define the precise activity reduction corresponding to the real EF intensities measured. Another computational study tried to shed light on the potential cellular mechanisms responsible for both acute and long-lasting effects of cathodal tDCS on epileptic activity (Denoyer *et al.*, 2020). To this aim, they developed a novel approach of computational models combining both cellular and neural mass features, designing an *in silico* thalamocortical column based on physiological data. To study the plasticity effects of tDCS, they inserted in the model glutamatergic excitatory cells and three types of GABA-ergic interneurons. In this model, the immediate effects of cathodal tDCS on a large (10.000 neurons) cortical column resulted in a small firing rate reduction in all cell types and tDCS effects were best explained by modulation of the presynaptic probability of release. The firing modulation was stronger in vasointestinal peptide expressing (VIP) interneurons, which are mostly present in the upper cortical layer. Regarding long-lasting effects, their model suggested that the decrease in epileptiform activity given by simulated cathodal tDCS is highly

influenced by the network size. More specifically, large networks of 10 thousand neurons showed the longer-lasting effects on ED decrease, while small networks of 250 neurons only showed immediate effects. Recently, following the work of (Wendling *et al.*, 2002) and (Lopez-Sola *et al.*, 2021) provide a laminar NMM capable of realistically reproducing the electrical activity recorded by SEEG in the epileptogenic zone during interictal to ictal states. A novel element in the model is a physiologically motivated algorithm for chloride dynamics: the gain of GABAergic post-synaptic potentials is modulated by the pathological accumulation of chloride in pyramidal cells due to high inhibitory input and/or dysfunctional chloride transport. By integrating pathophysiological mechanisms, such models can provide a better basis to understand the effects of tES EFs and optimize stimulation protocols.

In conclusion, computational models have been increasingly used for the design of tES protocols and showed crucial results for the optimization of stimulation montages targeting focal or extended brain regions. Within recent years, the creation of complex, personalized head and brain models resulted in the precise investigation of EF distributions inside the brain and the comparison with real data from which these models were generated. Moreover, the integration of personalized models with high resolution anatomical imaging (e.g., MRI, CT scan, and DTI) and with physiological data (e.g., EEG, iEEG, and PET) has allowed the design of high-resolution models (up to 1 $mm^3$) informed by patient-specific functional information on the epileptogenic network.

Nevertheless, there are still some main limitations. First, even though the studies highlight the importance of CSF in the EF propagation across deep brain areas, there is little account for CSF simulation parameters and distribution in individual head models. Additionally, the used conductivity values were almost exclusively based on relatively old *ex-vivo* studies, underlying the need for a better characterization of conductivity values based on *in vivo* studies. The further step in this direction would be the use of individual conductivity measures, especially important for epilepsy (Opitz *et al.*, 2016; Huang *et al.*, 2017, p. 2). Although it is generally thought that the neurons are influenced only by the EF component parallel to their axo-somatic axis (Bikson *et al.*, 2004), the precise impact of tangential and normal EF components on small neuronal networks in different brain regions has yet to be unraveled (Miranda *et al.*, 2013; Ruffini *et al.*, 2014). This is even more problematic when considering that cortical pyramidal neurons are mostly perpendicular to the cortical surface, but their axonal projections and cortical interneurons are often aligned tangentially to the surface (Fox *et al.*, 2014). Characterizing such effects is of fundamental importance for designing optimal stimulation montages depending on the local brain anatomy and axon orientation.

## 2.4. Discussion

We performed a systematic review of clinical and fundamental studies using tES as a therapeutic approach in epilepsy. First, clinical cases and clinical trials performing cathodal tDCS in patients suffering from DRE provided preliminary encouraging results regarding the clinical improvement of these untreatable patients, estimated by seizure frequency (SF) changes. Most studies (14/16 of clinical trials) reported a decrease in SF after one or several sessions of tDCS in patients suffering from DRE, with cumulative effects, compared to the baseline SF. Thus, one of the main clinical challenges of this technique is to prolong the beneficial after-effect due to tDCS. Studies with long-term follow-up interestingly showed that the repetition of stimulation and the length of the duration of the break between two stimulations are of major importance (Monte-Silva *et al.*, 2010; Yook *et al.*, 2011; Yang *et al.*, 2020; Kaufmann *et al.*, 2021). When tDCS is applied for several consecutive days, the resulting decrease in SF lasted for several weeks or months (Auvichayapat *et al.*, 2016; Tekturk, Erdogan, Kurt, Kocagoncu, *et al.*, 2016; Tekturk, Erdogan, Kurt, Vanli-yavuz, *et al.*, 2016; Lin *et al.*, 2018; Yang *et al.*, 2019; Kaye *et al.*, 2021). Another issue of using neuromodulation techniques as epilepsy treatment is to specifically target the EZ. In this view, the development of multichannel tDCS or HD-tDCS using several pairs of smaller electrodes than the two large electrodes conventionally used showed promising results. Multichannel tDCS makes it possible to optimize and personalize the electrode montage to target more precisely the epileptic focus while sparing the rest of the cortex from any effect (Ruffini *et al.*, 2014; Kaye *et al.*, 2021; Daoud *et al.*, 2022). Moreover, the use of more channels enables to target multiple foci and complex and complex brain networks distributed over wide regions of the cortex (Sanchez-Todo *et al.*, 2018). Another interest of using multichannel tDCS is the potential ability to reach deeper brain regions. Indeed, one of the main limitations of conventional tDCS is the very superficial diffusion of electrical field with the use of two large sponge electrodes and a very weak electrical current, making very difficult to reach deep brain structures. Recent evidence has shown that optimizing stimulation montage with several electrodes allows to achieve more focal stimulation for superficial targets and reach deep targets with more intense stimulation, mostly due to cerebro-spinal fluid guiding currents deep into the brain (Huang and Parra, 2019). An indirect modulation of deep brain regions might also be achieved targeting their related cortical functional brain network, as proposed by (Fox *et al.*, 2014). They used common targets of deep brain stimulation as seeds in functional connectivity-resting state MRI, to obtain a functional representation of the cortical areas positively or negatively correlated to them. Multichannel tES can be optimized to enhance positive or negative regions, inducing changes in their connectivity with the seed and possibly modulating its activity.

Moreover, regarding the safety of tES, no serious adverse effects have been reported after application of tDCS in both children and adults with epilepsy. The most common effects were the slight tingling and itching sensation during the stimulation. The use of tACS in epilepsy is promising but relatively under-examined. The safety of this technique

has been assessed in epileptic patients (Opitz *et al.*, 2016; Lafon *et al.*, 2017) and a recent study obtained interesting preliminary studies of tACS in epilepsy (Holmes *et al.*, 2019). To design optimal stimulation protocols for patients, it is necessary to investigate the underlying physiological mechanisms of tACS, via cell cultures, animal, or computational models. *In vitro* studies have demonstrated that the acute and long-term effects of tACS can differ from the ones observed in tDCS (Lian *et al.*, 2003; Bikson *et al.*, 2004). Nevertheless, this technique is often neglected in most *in vivo*, *in silico*, and clinical studies. Since the working hypothesis of tACS is that it can disrupt or amplify endogenous brain rhythms (Berényi *et al.*, 2012; Lafon *et al.*, 2017), it will be required to design individual protocols based on brain signals recordings for the definition of precise target frequencies. The use of online EEG, iEEG or MEG data, coupled with in silico studies using personalized head models and cortical target maps, might allow the closed loop tACS stimulation of epilepsy patients (Ruffini *et al.*, 2014).

Furthermore, electrophysiological measures are used to quantify the clinical outcome resulting from tDCS application. The most common technique applied in clinical trials studying tDCS effects on epileptic patients is to measure changes in interictal epileptiform activities using electrophysiological data (EEG and/or MEG). However, this approach is questionable because interictal activity is not a reliable marker of epilepsy efficacy or severity. The discrepancies observed between the different studies in this field led to open the path to new brain activity measures more suited for studying plasticity changes induced by tDCS. Indeed, considering epilepsy as a brain network disease, analyzing the functional alterations due to tDCS is highly relevant as a marker of epilepsy improvement. Recent studies focusing on functional brain network changes have highlighted interesting results between the response to tDCS therapy and functional disturbances in global brain networks (Lin *et al.*, 2018; Tecchio *et al.*, 2018; Daoud *et al.*, 2022). Measuring FC changes may thus be a possible predictor of the tES clinical efficacy in epileptic patients (Hao *et al.*, 2021). However, measuring changes in functional connectivity after tDCS in epilepsy has some limitations. One of the issues in studying FC changes is that DRE patients are taking several and different pharmacological treatments. Although they remained unchanged during the studies, they could affect the FC and the efficacy of tDCS. In addition, most studies using electrophysiological data measuring FC have employed EEG with low numbers of EEG channels, limiting the accuracy of localizing brain sources affected by functional changes. Finally, the functional changes observed over long periods of time are not known and this requires future studies on the long-term effects of tDCS. Thus, network effects are no doubt important, but they necessitate computational models combining physics and physiology to evaluate mechanistic implications and properly interpret data. In this view, by unraveling the underlying cellular and molecular mechanisms involved in the tES-induced electrophysiological plasticity, further studies could lead to more realistic computational models and to improved clinical stimulation protocols.

The reported physiological studies have demonstrated that tES induces concurrent and plastic effects that are relevant to epilepsy and its control. Overall, *in vitro* studies suggest that acute effects of both tDCS and tACS are likely related to membrane

polarization (Bikson *et al.*, 2004), with a major influence on spike timing and spike-timing-dependent plasticity (Reato *et al.*, 2010; Rahman *et al.*, 2017). However, stimulation effects are not limited to polarization. Crucial factors underlying tDCS are as well NMDA receptor-mediated synaptic strength modulation (Liebetanz *et al.*, 2006; Chang, Lu and Shyu, 2015; Sun *et al.*, 2020); reduction of mossy fiber sprouting (Kamida *et al.*, 2011; Wu *et al.*, 2020) and of hippocampal cell loss (Kamida *et al.*, 2011); modulation of GABAergic cortical inhibition (Dhamne *et al.*, 2015); modulation of neuroinflammation, neurotrophines, IL-1β, TNF-α, NGF, and BDNF (Regner *et al.*, 2020). Regarding tACS effects, studies have moreover showed a stimulation related increase of extracellular $K^+$ (Bikson *et al.*, 2001; Lian *et al.*, 2003), which might reflect a depolarization block. Indeed, the persistent membrane depolarization would lead to tonic inactivation of $Na^+$ channels, which in turn would lead to action potential's initiation. Another hypothesis on the mechanisms of tACS is that it could recruit subset of thalamic cells, which would be in their refractory phase during the spike and wave duty cycle, thus preventing the synchronous cell firing of the ongoing rhythm (Berényi *et al.*, 2012; Kozák and Berényi, 2017).

Later and sustained effects may be related to neurogenesis, cortical reorganization and likely to changes in synaptic plasticity (Chang, Lu and Shyu, 2015; Rahman *et al.*, 2017; Sun *et al.*, 2020). To better characterize tDCS effects on epilepsy, future studies should differentiate the pathophysiological plasticity induced by the epileptic activity itself leading to hyperexcitability (e.g., pathological LTP and NMDA receptor upregulation), and the physiological mechanisms of plasticity that might be induced by tDCS. It is unclear whether *in vitro* and *in vivo* findings obtained with EF magnitudes higher than 1 V/m are representative of real tES protocols. Most *in vitro* DC stimulation studies have so far involved electric field magnitudes of at least 20 V/m (20 times higher than the EF induced in the human brain for a 2 mA tDCS protocol). Even with the EF magnitudes used by Ghai et al. (2000) and Chang et al. (2015) (2–16 V/m), the membrane voltage changes induced by either DC or AC fields at low amplitudes are consistently lower than the action potential firing threshold (Ghai, Bikson and Durand, 2000; Chang, Lu and Shyu, 2015). Therefore, one needs to investigate how this effect can be amplified to modulate large networks. One hypothesis is that tDCS can increase the presynaptic firing rate and modulate spike timing, increasing synaptic integration and thus the coincidence of pre- and postsynaptic APs (Rahman *et al.*, 2017). However, it is not clear how might result in brain-wide effects as it happens during *in vivo* stimulation. To understand this, it is crucial to model the effects in neuronal network models. Although not included in most of the studies reported here, the endogenous neural activity is essential for obtaining realistic tES effects, as proved by the studies of (Ghai, Bikson and Durand, 2000) and (Chang, Lu and Shyu, 2015). The interaction between of tES exogenous fields with endogenous field mechanisms can give rise to further amplification effects, which could cause important firing activity changes at the network level (Fröhlich and McCormick, 2010; Weiss, 2010). Future *in vitro*, *in vivo*, and computational studies should thus model endogenous field effects (e.g., ephaptic coupling) in order to better

characterize the combined endogenous field and tES network effects (Fröhlich and McCormick, 2010; Reato *et al.*, 2010; Ruffini *et al.*, 2020).

Furthermore, the present studies emphasize the need for patient-tailored models, including functional and structural connectivity data (Ruffini *et al.*, 2013, 2018; Tecchio *et al.*, 2018), precise anatomical reconstruction with skull defects and CSF models (Datta *et al.*, 2009; Huang *et al.*, 2017; Louviot *et al.*, 2022), metal implants (Mercadal *et al.*, 2021) as well as detailed target mapping (Ruffini *et al.*, 2014). The strong inter-subject variability of tDCS-induced connectivity changes could cause the variability in the effectiveness of stimulation (Giannakakis *et al.*, 2020). The recent technique of transcranial Individual Neurodynamics Stimulation (tIDS), which mimics the endogenous dynamics of the target neuronal networks, might partially answer this issue through the characterization of individual local functional connectivity prior to stimulation (Cottone *et al.*, 2018). Other techniques also aim at restricting the tES spatial focus (for a recent review, the reader is referred to (Takeuchi and Berényi, 2020)). For instance, Intersectional Short Pulse Stimulation (Vöröslakos *et al.*, 2018) and concentric ring electrodes montages (Besio, Koka and Cole, 2007) increase spatial focality of tES and may be useful when the target area is confined to a small area. However, they do not improve tES ability to target deeper structures. The novel technique of Temporal Interference (TI) could tackle this issue by creating a constructive interference of high-frequency transcranial stimulation waves. Consequently, TI might reach deeper structures such as the hippocampus (Grossman *et al.*, 2017; Missey *et al.*, 2021), but it is still unclear how amplitude modulated kHz electric fields influence the areas inside or outside the target.

# 3. Chapter III: Personalized Multichannel tDCS Protocol in Drug-resistant Epilepsy: A Preliminary Study

This chapter was published in:

**Daoud, M**., Salvador, R., El Youssef, N., Fierain, A., Garnier, E., Biagi, M. C., Medina Villalon, S., Wendling, F., Benar, C., Ruffini, G., & Bartolomei, F. (2022). Stereo-EEG based personalized multichannel transcranial direct current stimulation in drug-resistant epilepsy. Clinical Neurophysiology, 137, 142–151. doi:10.1016/j.clinph.2022.02.023.

# Rationale

Study 2 served as the preliminary phase of the clinical trials of the SYNERGY GALVANI European project. Unlike previous studies using tDCS for epilepsy treatment, which typically employed generic bipolar montage with two large-sponge electrodes for one or a few treatment sessions and without personalization, our approach took into account the influence of individual brain anatomy on the impact of transcranial electrical current (Auvichayapat *et al.*, 2013; Miranda *et al.*, 2013; Ruffini *et al.*, 2014; Assenza *et al.*, 2017). We used a personalized multichannel stimulation protocol to accurately target each patient's epileptogenic zone, previously identified through intracerebral recordings (SEEG). Additionally, as previously mentioned, although tDCS shows promise in reducing seizure frequency in patients with drug-resistant epilepsy (DRE), its effects are temporary and reversible. When a treatment is effective, the ultimate goal is to prolong its benefits over time. Thus, drawing on prior research, we have developed a protocol involving repeated stimulation sessions interspersed with breaks to maintain the potential positive effects achieved through stimulation.

The primary objective of this preliminary study was to achieve a sustained decrease in seizure frequency among patients with DRE who were ineligible for surgery or had experienced surgical failure. Furthermore, as previously discussed, epilepsy affects brain networks, and tDCS may disrupt or restore them. This raises the following question: how does tDCS affect functional brain activity, and how are these changes related to therapeutic effects?

To investigate this question, we conducted a pilot study involving ten patients with DRE. They received repeated sessions using a personalized multichannel tDCS protocol. We then assessed potential changes in functional connectivity measured from scalp electroencephalography (EEG) recordings to link these changes to clinical outcomes.

# 3.1. Introduction

One-third of patients with epilepsy have seizures refractory to pharmacotherapy (Brodie and Kwan, 2002; Devinsky *et al.*, 2018). The only curative treatment is surgery and in this context stereoelectroencephalography (SEEG) is increasingly used in presurgical assessment (Jehi *et al.*, 2015; Baud *et al.*, 2018). However, epilepsy surgery is only possible in a limited number of cases (15–20%) and is associated with a relatively high number of failures (Baud *et al.*, 2018). Consequently, alternative treatments based on non-invasive brain stimulation methods aiming at decreasing cortical excitability represent a promising therapeutic. Transcranial direct current stimulation (tDCS) is an emerging non-invasive method of brain stimulation involving passing a weak current (1–2 mA) across the head tissue (scalp, skull, cortex) using scalp electrodes positioned on the head (San-juan *et al.*, 2015). This neuromodulatory technique could modulate brain excitability by subthreshold membrane depolarization or hyperpolarization. As the electric field under the anode is predominantly excitatory, and the one under the cathode is predominantly inhibitory (Nitsche and Paulus, 2000; Nitsche *et al.*, 2003), in epilepsy, the target region must be in the field of a cathode to achieve cerebral inhibition. tDCS effects depend on several factors including stimulation duration, current intensity, number of repetitions, duration of the interval between stimulation sessions, number, and localization of electrodes. Indeed, conventional tDCS montage employs only two large electrodes (one anode and one cathode) whereas multichannel tDCS, uses several smaller pairs of electrodes that potentially enhance and optimize stimulation focality (Villamar *et al.*, 2013). Furthermore, the current values and electrode positions can be determined from computational head models and account for the geometry and conductive properties of the head tissues in order to accurately calculate the induced electric field, making it possible to target brain regions with more accuracy (Sadleir *et al.*, 2012).

In this way, several human and animal studies have shown the efficacy of cathodal stimulation for decreasing the number of epileptiform discharges (Lian *et al.*, 2003; Fregni *et al.*, 2006; Yook *et al.*, 2011). However, the majority of previous studies employed generic bipolar montages with large sponges applied during one or a few treatment sessions and without personalization. Recently, a study involving drug resistant epilepsy patients employed multielectrode montages that were designed using a realistic head model-driven approach to drive an inhibitory electric field to the target cortical epileptic region (Kaye *et al.*, 2021). This study used a generic head model and a definition of the epileptogenic zone based solely on non-invasive recordings. Since tDCS electric-fields are affected by individual brain anatomy, a patientspecific approach is more suited to properly engage the targeted brain region (Miranda *et al.*, 2013; Ruffini *et al.*, 2014; Laakso *et al.*, 2015).

We report here a pilot study investigating the efficacy of anindividualized multichannel tDCS protocol based on the patient's anatomy and epileptogenic network. We selected a population of patients with focal epilepsy considered as inoperable (or

failing after surgery) and whose epileptogenic zone was clearly identified by prior SEEG recordings. This specific population was selected because the patients have severe epilepsy with no other therapeutic resources and they had SEEG procedure favoring optimal targeting for multichannel cathodal tDCS, especially for epilepsies with normal MRI or a complex epileptogenic zone exceeding lesion boundaries. Moreover, the neuromodulatory mechanisms associated with the application of a low-frequency electric field remain poorly understood. Drug-resistant focal epilepsies are associated with interictal alterations in functional connectivity (FC), characterized in particular by increased neural synchrony in most epileptogenic regions (Bettus *et al.*, 2008; Bartolomei *et al.*, 2017; Lagarde *et al.*, 2018). Thus, we sought to correlate the clinical efficacy of our tDCS protocol with changes in FC measured from scalp EEG recordings. We hypothesized that the efficacy of multichannel tDCS is associated with FC-specific changes.

# 3.2. Materials and methods

### *Patients*

Ten patients with drug-resistant focal epilepsy were enrolled in this study (seven males, three females); mean age 29.9 years; range 12–60 years). Inclusion criteria were the following: (1) ≥ 12 years of age; (2) diagnosed with focal drug-resistant epilepsy not operable or presenting a failure of previous epilepsy surgery with at least three seizures per month during the baseline (before the first session of tDCS treatment) for at least 3 months; (3) SEEG previously performed before inclusion with an adequate definition of unifocal epileptogenic zone; (4) have stable medications for epilepsy for the whole study duration (5) Total IQ > 55; (6) be able to understand, speak and write in French.

Exclusion criteria were the following: (1) skin conditions (e.g., eczema, lesions) on the scalp;(2) any cranial metal implant; (3) or implanted devices (i.e. cardiac pacemaker, deep brain stimulator, cochlear implant, medication infusion pump); (4) previous surgeries opening the skull leaving skull defects with a radius ≥ to 5 mm; (5) persons protected by articles L1121-5, L1121-6 and L1121-8 of Public Health Code (pregnant or breastfeeding woman, deprived of liberty by judicial decision, situations of social fragility, adults unable to express their consent). The general characteristics of the patients are summarized in Table III.1. This study was approved by the local ethics committee. Written informed consent was obtained from each patient or his or her legal representative before inclusion in the study.

| Patient | Gender | Age | SOZ defined by SEEG | SEEG electrodes (number) | Etiology | SZs type | ASM | Previous failed Surgery | tDCS target | Injected current (mA) | Desired E field in target (V/m) | Achieved average E field in target (V/m) | Number of electrodes | Response |
|---|---|---|---|---|---|---|---|---|---|---|---|---|---|---|
| 1 | F | 12 | Left paracentral lobule, Post SMA | 8 | Unknown | EPC, focal motor seizures | 2 | Premotor Cortectomy | Left paracentral | 1.99 | 0.5 | −0.070 | 8 | R |
| 2 | M | 60 | Left temporal lateral, mesial, Parietal infero-temporal | 15 | Infectious | Focal non motor, impaired awareness | 3 | No | Left temporo-basal | 1.99 | 0.25 | −0.016 | 8 | NR |
| 3 | M | 34 | Right parietal posterior, Precuneus, cuneus | 9 | Unknown | Focal non motor, SGTC | 5 | No (thermocoagulation) | Right posterior parietal | 1.99 | 0.5 | −0.011 | 6 | NR |
| 4 | M | 23 | Left temporal lateromesial | 9 | FCD | Focal non motor | 2 | Anterior anterior temporal lobectomy | Left temporo insular | 1.99 | 0.5 | −0.031 | 7 | NR |
| 5 | M | 41 | Left basal, lateral temporal | 16 | Unknown | Focal non motor, partial impaired awareness | 2 | No (thermocoagulation) | Left temporo-opercular | 1.99 | 0.5 | −0.017 | 7 | R |
| 6 | F | 29 | Left latero-mesial, Temporo-occipital | 13 | FCD | Focal non motor | 3 | No (thermocoagulation) | Left temporal | 1.99 | 0.25 | −0.008 | 7 | R |
| 7 | M | 20 | Right operculo-insular | 9 | Unknown | Focal sensitivi-motor, visual hallucination | 3 | Temporal lobectomy Operculectomy | Left temporo periylvian, Mesial occipital | 1.99 | 0.5 | −0.038 | 8 | NR |
| 8 | M | 29 | Left parietal, premotor | 12 | Prenatal stroke | Focal motor, impaired awareness | 4 | Left parietal cortectomy | Left fronto parietal sup | 1.99 | 0.25 | −0.023 | 7 | R |
| 9 | F | 38 | Left temporo-latero-mesial | 9 | FCD | Focal motor, impaired awareness | 3 | Anterior temporal lobectomy | Left temporal | 1.99 | 0.5 | −0.070 | 7 | NR |
| 10 | M | 14 | Right paracentral | 10 | Unknown | Focal motor, no impaired awareness | 4 | No | Right paracentral | 1.99 | 0.5 | −0.042 | 7 | R |

**Table III.1. Patient data**. Abbreviations: SOZ: Seizure onset zone; SEEG: Stereoelectroencephalography; SMA: Supplementary motor area; SZs: Seizures; FCD: Focal cortical dysplasia; SGTC: Seizure generalized tonico-clonic; ASM: Antiseizure medication; R: responder; NR: Non-responder.

### *Experimental design*

This is a prospective, open labelled, monocentric pilot study in patients with medically refractory epilepsy followed during 8 months with patients acting as their own internal control.

For each patient, after a baseline period of at least two months, the study started with a 1-h EEG exam (Electroencephalography) on day 1 of the week (before stimulation) in order to collect electrophysiological brain state right before stimulation treatment at the end of the baseline period. Then, each day of each stimulation cycle period (a cycle consisted of five consecutive days of stimulation), patients received tDCS treatment with a mean total injected current of 1.99 mA. The daily treatment was organized in two periods of 20 min of stimulation (a bi-session) each separated by 20 min off (i.e., with 40 min of cathodal stimulation in total). At the end of each cycle (on the 5th day), another EEG exam of 1 h was performed for comparison with the one obtained before tDCS treatment at the first day of the cycle. Each cycle was repeated every two months, for a total of three times (six months in total) (see Figure III.1).

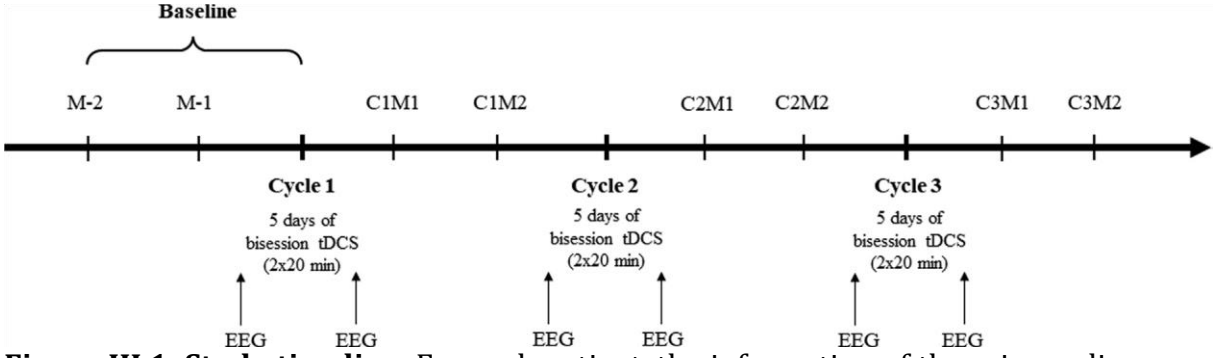


**Figure III.1. Study timeline**. For each patient, the information of the seizure diary was collected at each timepoint (C1M1, C1M2, C2M1, C2M2, C3M1, C3M2). Each cycle was composed of 5 days of two periods of 20 minutes stimulation separated by 20 minutes off (20 min tDCS – 20 min off – 20 min tDCS) with a 1-h EEG performed before the first day of stimulation and right after the last day of the cycle. Each session was renewed every 2 months. Abbreviations: tDCS: transcranial direct current stimulation; EEG: Electroencephalography; M-2, M-1: 2 and 1 months before the first stimulation cycle; C1M1: one month after the first cycle; C1M2: two months after the first cycle; C2M1: one month after the second cycle; C2M2: two months after the second cycle; C3M1: one month after the third cycle; C3M2: two months after the third cycle.

### *Personalized multichannel cathodal tDCS*

The electrode montage was determined individually based on a montage optimization pipeline. Biophysical head models were created from structural images of each patient (T1-weighted MRIs), using the methods described in (Fischer *et al.*, 2017). We used MRI acquisitions performed before the SEEG. These models included lesions such as previous corticectomies. Montage optimization was performed with the Stimweaver algorithm (Ruffini *et al.*, 2014). In short, this method takes as input a target E-field map, defined on the personalized cortical surface of the head model created for each patient. This target map contained information about the areas to inhibit (identified by SEEG recording previously acquired Figure III.2) and of areas to leave unaffected by stimulation. The latter corresponded to silent areas, defined as the cortical areas with normal EEG activity or with the smallest amount of epileptogenic activity. The region to be inhibited (target) was defined according to the definition of the epileptogenic zone obtained from SEEG. It was based on visual analysis according to classical rules of interpretation (Bartolomei, Chauvel and Wendling, 2008) and quantification using epileptogenicity index (EI). The EI combines analysis of both spectral and temporal features of SEEG signals, respectively, related to the propensity of a brain area to generate fast discharges (12.4–127 Hz), and to the earliness of involvement of this area in the seizure (see details in (Bartolomei, Chauvel and Wendling, 2008)).

The algorithm then automatically identified the positions of electrodes and associated currents that resulted in the E-field distribution that better approximates the target. This solution was constrained to a maximum number of electrodes (8), maximum current per

electrode (1.884 mA, in absolute value) and maximum total injected current (2.0 mA). The electrode positions were constrained to a subset of positions of the 10–10 EEG system. Typical montages involved cathodes over the areas to inhibit and anodes over the silent areas. Stimulation was applied via a multichannel tDCS system (Starstim8, Neuroelectrics Barcelona). The stimulation protocol was created and monitored using the NIC 2.0 software (https://www.neuroelectrics.com/products/software/nic2/). The electrodes (NG PiStim electrodes, 1 cm radius, cylindrical Ag/AgCl electrodes with a layer of conductive SIGMA gel underneath) were positioned in a neoprene cap with the 39 positions used in the montage optimization (Neuroelectric's Standard Cap). The current was gradually ramped-up over a period of 15 s until reaching an intensity up to 2.0 mA and delivered in two periods of 20 min separated by 20 min off. The break between sessions of tDCS may be crucial for optimizing cumulative effects and for prolongating the inhibitory neuroplastic effects of cathodal stimulation (Monte-Silva *et al.*, 2010). A recent study (Yang *et al.*, 2020) has found a superior significant effect using a protocol of 2 x 20 min stimulation per day with a 20 min interval, compared with a protocol using 40 min stimulation only (without interval).

At the end of each period, the currents ramped-down for a period of 15 s. These parameters have previously been shown to be well tolerated in healthy subjects and in other clinical conditions (Borckardt *et al.*, 2012; Yang *et al.*, 2020).

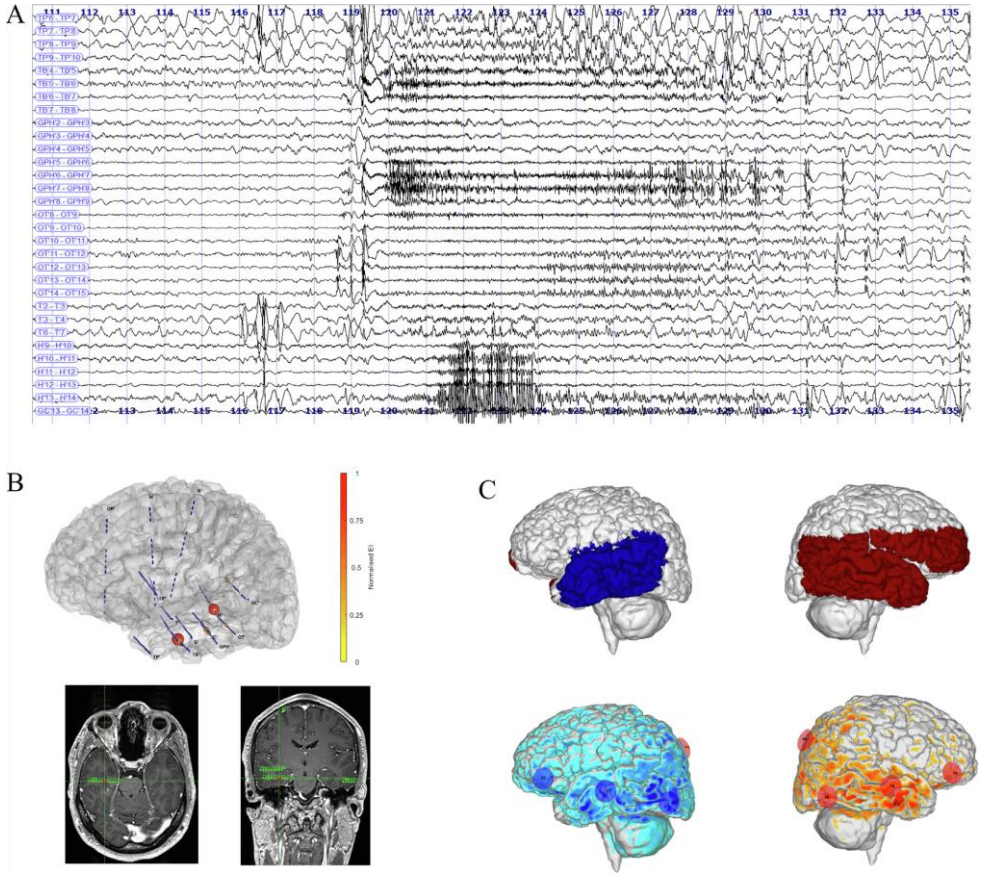


**Figure III.2. Example of epileptogenic zone identification using SEEG recordings for tDCS targeting using the optimization protocol of tDCS electrode's montage for the patient 5.** A. SEEG recordings during left temporal lobe ictal event. Seizure starts from

left temporo-basal area and left occipito-temporal area. Intra-cerebral electrodes are identified by letter (A, etc.) and the recordings' leads are numbered from 1 to 15, low numbers corresponding to the deepest structures (for example, leads TB' 1–2 recorded the electrical activity of the entorhinal cortex). TP': left temporal pole electrode, TB': left temporobasal electrode; GPH' left parahippocampal gyrus electrode, OT': left occipito temporal electrode; T' left superior temporal electrode; H' Heschl gyrus electrode. GC': electode reaching the posterior cingulate gyrus. Bipolar signals are obtained by substracting the signals recorded from two adjacent leads. B. The maximum epileptogenicity values (red sphere) are shown in a three-dimensional scheme of the patient 5 brain illustrated based on CT-MRI reconstruction of electrode tracks and epileptogenic index (EI). EI values were computed on a bipolar montage derivation. The diameter and position on the color scale are proportional to the normalized EI values. C. Optimization protocol used for patient 5 with tDCS electrode's positions and generated normal component of electrical fields (V/m). The blue area (left panel) corresponds to the epileptogenic zone and must be inhibited with cathodal electrodes (in blue below). The red part (right panel) is the area with the excitatory return current using anodal electrodes (in red below). Abbreviations: tDCS: transcranial direct current stimulation; SEEG: stereoelectroencephalography.

### *EEG recordings*

EEG was performed using 21 channels EEG cap using a Natus apparatus (Natus, France, sampling rate 256 Hz). Signals were acquired during 1 h with at least 10 min eyes-closed resting state, and at distance from seizures or post-ictal state (at least 3 h). EEG recording was obtained before the start of stimulations (baseline), before each cycle of personalized multichannel tDCS and at the last day of each cycle, immediately following the last stimulation period. The electrodes were arranged based on the international 10–20 system.

### *Clinical outcome*

The patients or their relatives were instructed to record the number and type of seizures in a calendar (seizure diary) two months before (the baseline) the beginning of the study until two months after the last stimulation-period of multichannel tDCS. The records were evaluated each month to count the number of seizures for each period (before, during, shortly after and a long-time period after each cycle of tDCS). Reduction and increase in the number of seizures were represented as a percentage compared to the baseline. Patients whose seizures were reduced by at least 50% in frequency after tDCS cycles were qualified as ''responders''. Others were qualified as ''non-responders''. Furthermore, patients were asked to notify any perceived adverse effect of tDCS, during and after each bi-session of 20-min stimulation. All adverse events (AEs) were recorded.

### *Data analysis and functional connectivity*

EEG recordings were analysed using AnyWave software (Colombet *et al.*, 2015). A post recording bandpass filter (notch) was applied to signals to remove 50 Hz noise (powerline frequency band in Europe), frequencies below 0.5 Hz and above 70 Hz. The sampling frequency was 256 Hz. We first removed artifacts using independent component analysis (ICA) (Barbati *et al.*, 2004). Then, the EEG recording was inspected visually, and all segments containing artifacts not identified by the ICA analysis were rejected (cardiac, muscles, and eye movement artefacts were eliminated). Interictal spikes were automatically quantified in AnyWave using Delphos (Detector of ElectroPhysiological Oscillations and Spikes) (Roehri *et al.*, 2016).

Then, we estimated the functional connectivity in the theta (4–8 Hz), alpha (8–13 Hz) and beta (13–30 Hz) frequency bands. We did not include gamma activity in this analysis because fast electrical rhythms recorded in the scalp (30–100 Hz) are predominantly due to electromyographic (EMG) activity (Goncharova *et al.*, 2003). Then, FC was computed on bipolar channels in such a way that there was no common electrode between all pairs of electrodes in order to avoid massive biases for the functional connectivity analysis (Fp2-F8, F4-C4, P4-O2, T8-P8, Fz-Pz, Fp1-F7, F3-C3, P3-O1, T7-P7).

Functional connectivity was estimated using linear regression analysis which quantifies the dependency of a signal x on a signal y, from signal samples only and independently of the type of relation between the two signals (Pijn and Lopes da Silva, 1993). The level of dependency can be characterized by the linear cross-correlation coefficient $r^2_{xy}$.

$$r_{xy}^2 = \frac{\mathrm{cov}^2(\mathrm{x}+\tau))}{(\sigma_{x(t)}\sigma_{(t+\tau)})^2}$$

Where σ and cov denote the standard deviation and the covariance, respectively, and s the delay between signals x and y. $r^2_{xy}$ will be simply denoted by $r^2$ in the following. Correlation values are contained between 0 (y is uncorrelated of x) and 1 (x and y are fully linearly dependent). The estimation of this parameter is performed on a temporal window of fixed duration and sliding in time in order to follow the temporal evolution of the linear statistical relationship between both signals (fixed window of 2 s, 1 s overlap, max lag of 100 ms). This statistical coupling between signals was recorded on each pair of the 21 electrodes over the selected resting-state period. In the present study, we summarized coupling at each bipolar electrode pair (node) by the sum of all values containing this node (this is the ‘‘node strength” in graph theory terminology). The strength values were computed on signals filtered in the EEG frequency sub-bands followed: theta (4–8 Hz), alpha (8–13 Hz) and beta (13–30 Hz).

### *Statistical analysis*

Changes in functional connectivity between the first and the last day of each cycle were assessed by linear mixed models (LMM) using the ‘‘lme4” package (version 1.1-26, (Bates *et al.*, 2015)) of the statistical software R version 4.0.3 (R Core Team, 2020). One LMM was computed for each frequency band with the responsiveness to the tDCS treatment (R or NR) and cycle as fixed effects. The by-subject intercept was included as a random factor as well as the effect of cycle. Restricted Maximum Likelihood (REML) was used to fit the LMM and Satterthwaite’s method was used to estimate the degrees of freedom. Post-hoc pairwise comparisons were performed with the Least Squares Means (LSM) method. In addition, the difference in seizure onset zones (temporal or extratemporal) and in gender between responder and non-responder patients were tested with Fisher’s exact test. Differences with p-values < 0.05 (two-sided) were considered as significant.

## 3.3. Results

### *Subjects*

Ten patients with various forms of focal refractory epilepsy were included in this study between December 2019 and April 2021. Their clinical characteristics are summarized in Table III.1.

### *Clinical outcome*

All patients regularly completed their seizure diary. The results are shown in Figure III.3. The mean number (±SD) of seizures, in the two months before stimulation, was 44 ± 91. After the first cycle of tDCS, the average seizure frequency had decreased by -32% (±44%) compared with baseline. After the second cycle of five days of stimulation, the average seizure frequency had decreased by -57% (±31) compared with baseline. Finally, after the last cycle (C3) of stimulation, the average seizure frequency had decreased by -48% (±39%). At this point, five patients (50%) had more than 50% decrease in their seizure frequency compared with baseline (R group mean of decrease: -74% ± 14%) and were considered as ‘‘responders” for the connectivity analysis (see below). The non-responder group (5/10) presented a mean seizure frequency reduction of -16% (±36%) compared to the baseline SF.

No significant difference in responsiveness to the stimulation protocol was found between patients suffering from temporal lobe epilepsy (5/10) and those suffering from extra-temporal lobe epilepsy (5/10) (Odd Ratio = 0.5; p = 1). No significant effect of

gender was found on the responsiveness to the treatment (Odd Ratio = 0.4; p = 1). We found no significant difference in the rate of interictal spikes per minute between cycles and the day of stimulation (before the first stimulation of the cycle: "pre" condition and after the last stimulation day of the cycle: "post" condition) ($F_{1,44.084}$ = 0.1012, p = 0.75) and between responder and non-responder patients ($F_{1,8.051}$ = 0.2326, p = 0.6424) (see in Appendix A).

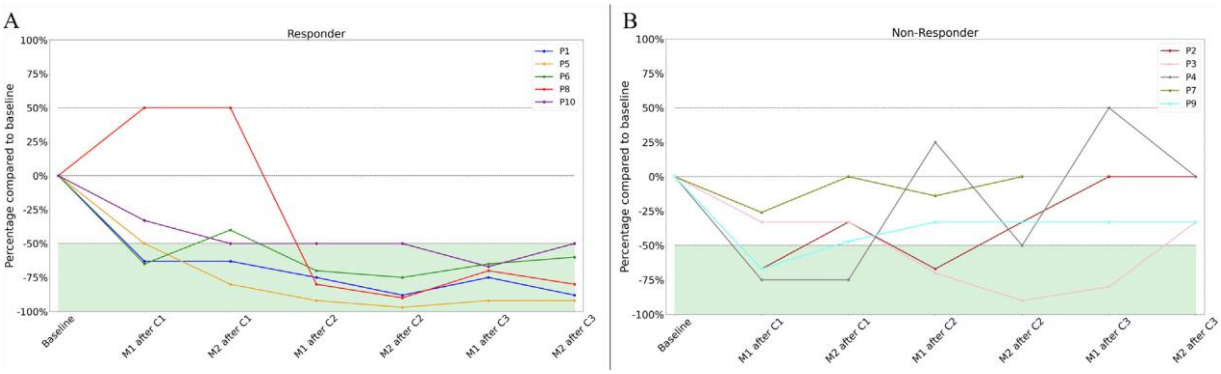


**Figure III.3. Evolution of seizure frequency over time after three stimulation cycles of responder and non-responder patients.** A. Evolution of seizure frequency for responder patients (N = 5). B. Evolution of seizure frequency for non-responder patients (N = 5). Y axis: percentage of SF evolution compared with baseline (%). X axis: time periods. Abbreviations: M1 after C1: one month after the first cycle; M2 after C1: two months after the first cycle; M1 after C2: one month after the second cycle; M2 after C2: two months after the second cycle; M1 after C3: one month after the third cycle; M2 after C3: two months after the third cycle; SF: seizure frequency.

### *Safety and tolerability*

Overall, all participants tolerated well tDCS treatment. A slight itching sensation under the stimulation electrodes was described by 7/10 of all patients during stimulation. A sensation of slight dizziness at the beginning of the stimulation was reported by two patients. None of the participants reported moderate nor severe side effects during or after the procedure. Two patients had an increase in seizures: one patient (P8) showed an increase in SF after the first cycle of stimulation (50% increase from baseline) but by the second 5-days cycle of stimulation, SF had dropped dramatically from baseline and P8 was considered a responder. Another patient in the non-responder group (P4) showed a moderate and transient increase in SF in the first month following the cycles 2 and 3 (25–50%).

### *Functional connectivity*

FC, estimated by $r^2$ strength, was first analyzed in EEG broadband signal (4–30 Hz). Results did not show a significant change for the cycles ($F_{2,7.1}$ = 0.9, p = 0.46) and for responder and non-responder patients ($F_{1,8.1}$ = 0.7, p = 0.43) (Figure III.4.A). For the theta

band (4–8 Hz) analysis, we did not find a significant change for the cycles ($F_{2,5.9} = 1.6$, $p = 0.28$) and the responsiveness to the tDCS treatment ($F_{1,8.02} = 0.2$, $p = 0.65$). However, we clearly identified a tendency to a decrease in the $r^2$ strength, between the cycles 1 and 3 for the responder patients (Figure III.4.B). The alpha band (8–13 Hz) analysis revealed no main effect (cycle: $F_{2,5.9} = 3.8$, $p = 0.09$; response $F_{1,8.3} = 0.1$, $p = 0.72$) but an interaction effect was present significantly ($F_{2,5.9} = 5.9$, $p = 0.04$). Post-hoc tests have shown a significant difference between cycles 1 and 2 ($t = 2.7$, $p = 0.04$) and between 1 and 3 ($t = 4.3$, $p = 0.009$) for the responder group. The mean strength in responders for the cycle 1 was 0.08 ± 0.09, in cycle two 0.01 ± 0.07 and -0.06 ± 0.08 for the third cycle (Figure III.4.C). The beta band (13–30 Hz) analysis revealed no main effect (cycle: $F_{2,6.8} = 0.9$, $p = 0.5$; response $F_{1,8.1} = 0.05$) but an interaction effect was present significantly ($F_{2,6.8} = 6.4$, $p = 0.03$). Post-hoc tests have shown a significant difference between cycles 1 and 3 for responder patients ($t = 3.4$, $p = 0.01$) (Figure III.4.D). Although there was no significant difference, we also observed a trend to a decrease in SF between cycles 1 and 2 for responder patients. Interestingly for the non-responder group, we observed a trend for an increase in FC at the end of the study compared to cycle 1 (non-significant). Finally, comparing FC at baseline (before any tDCS stimulation), we have found significant difference between responders and non-responders with higher value of $r^2$ strength in beta band in non-responder patients ($p < 0.001$).

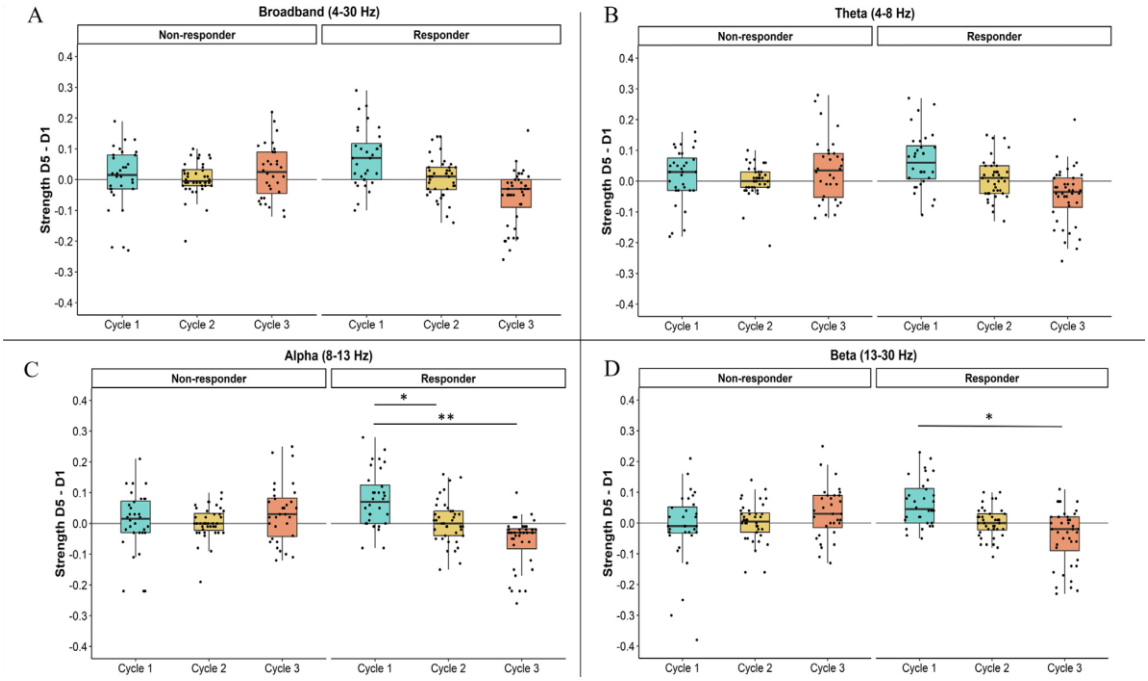


**Figure III.4. Multichannel cathodal tDCS induced a decrease in functional connectivity (FC) for responder patients in alpha (8–13 Hz) and beta (13–30 Hz) bands**. Variation of FC across cycles (6 months in total) calculated by the difference in strength before and after each cycle of 5 day's stimulation (D5-D1) in broadband filtered (4–30 Hz) (A), in theta (4–8 Hz) (B), in alpha (8–13 Hz) (C), and beta (13–30 Hz) (D) bands for non-responder and responder patients. Abbreviations: Strength D5-D1: Strength Day 5 – Strength Day 1 (after – before tDCS cycle); tDCS: transcranial direct current stimulation; FC: functional connectivity.

## 3.4. Discussion

In this open pilot study, we used for the first time a personalized multichannel tDCS protocol targeting the epileptogenic zone as defined on SEEG in a population of patients with drug-resistant focal epilepsy involving different anatomical regions.

### *Efficacy of multichannel tDCS*

Our study confirms that tDCS can lead to a significant reduction in seizures with a responder rate of about 50% and an average seizure reduction of 48% after the third treatment cycle. In responders, the reduction in seizure frequency was 74% (min -58.5%, max -92%). Importantly, and contrary to previous studies, the duration of patient follow-up (six months) was longer, and we performed three cycles of tDCS, whereas in previous studies, only short-term results were reported (Fregni *et al.*, 2006; Auvichayapat *et al.*, 2013; Tecchio *et al.*, 2018). The decrease in seizure frequency observed in our study agrees with previous trials in the field. Most previous studies of tDCS in epilepsy, making use of a generic set-up with a single pair of sponge electrodes, have highlighted the safety and the potential clinical benefit of this neuromodulation technique despite the heterogeneity of patient populations and methods. Three studies by Auvichayapat et al., Tekturk et al., and San-Juan et al. have found a significant reduction in seizure frequency of at least 50% after cathodal tDCS, respectively in patients with epilepsy compared with sham stimulation (Auvichayapat *et al.*, 2013; Tekturk, Erdogan, Kurt, Vanli-yavuz, *et al.*, 2016; San-Juan *et al.*, 2018). Another clinical report showed the importance of repeating the DCS session to achieve a cumulative and long-term decrease in seizure frequency (San-Juan *et al.*, 2018). Then, the study by Yang et al. used a 14-days stimulation protocol versus sham stimulation (Yang *et al.*, 2020, p. 202). They found a median seizure frequency reduction of 50% and 50% (the first 4-weeks of follow-up), as well as 25% and 45% (the second 4-weeks of follow-up), respectively, for patients who received 20-min of tDCS (group 2) and for patients from the group receiving 2 x 20-min of tDCS (group 3) as compared to a -12.50% change in the sham group (group 1).

Recently, Kaye et al reported a study using a methodology similar to the present study with regard to optimization (Kaye *et al.*, 2021). There were important differences with our study, however they used a single cycle of ten days and a 20-min single simulation session per day, defining the target area without SEEG, and without using an MRI-personalized brain model in all patients. In our study, we achieved a comparable result in terms of reduction in mean frequency (48% vs. 44%) but with a demonstrated effect over a longer term, using a multi-cycle approach.

Furthermore, the beneficial clinical effect in our study, lasted at least eight weeks after a 5-days cycle of tDCS. This could be explained by several new factors in our protocol. In

addition to SEEG target identification and model personalization, previous studies have shown that the duration of the clinical benefit depends on the repetition, duration, pause between stimulation sessions and current intensity (Monte-Silva *et al.*, 2010; Yang *et al.*, 2020). Yang et al. (2020) have found a greater effect in reducing seizure frequency using a protocol of 2 x 20 min stimulation per day with a 20 min interval, compared with a protocol using 40 min stimulation only (no interval) (Yang *et al.*, 2020).

### *Personalized tDCS protocol*

In the present work, we used an individualized montage targeting the epileptogenic focus identified by the SEEG recordings, which allowed for a more precise delineation of the patient-specific epileptogenic network. Thus, we sought to optimize current levels and orientation such that induced currents maximized inhibitory stimulation of the while minimizing excitatory anodal feedback in other potentially epileptogenic regions from return currents.

### *Safety*

This long-term study allowed us to confirm the safety of long-term multichannel inhibitory tDCS treatment for epilepsy (six months). Only mild side effects were reported in most of the participants, such as mild itching and dizziness at the beginning of the stimulation. However, we reported an increase in seizure frequency for one patient in the NR group (25–50%) but who returned to baseline at the end of the study. In addition, one patient in the responder group showed a transient increase in seizure frequency after the first cycle (50%) before a dramatic reduction of seizures after the second and third cycles.

### *Functional connectivity*

Despite the growing number of studies supporting the clinical interest of applying low-level electric fields using tDCS in epilepsy, the underlying neurophysiological mechanisms remain elusive. Some recent studies have suggested its role regarding transient and long-term effects on cortical excitability (Antal *et al.*, 2017; Cirillo *et al.*, 2017; Stagg, Antal and Nitsche, 2018; Lefaucheur and Wendling, 2019). Here, we performed a non-invasive measure of functional connectivity to characterize changes induced by several cycles of stimulation. The study of functional connectivity is justified because it is a classic measure of network brain activity and because several publications have shown that regions generating seizures are characterized by an increased FC compared to non-epileptic regions (Schevon *et al.*, 2007; Bettus *et al.*, 2008; Lagarde *et al.*,

2018). In the present study, the 6-month period of stimulation had induced a decrease in EEG FC in responder patients compared to their first cycle of tDCS. This profile of cumulative decrease observed in responders across cycles was not observed for non-responder patients. Conversely, for the latest, we observed a tendency to an increase of FC at the end of the study. In line with these findings, a recent study has used FC with fMRI as a quantitative measure of tDCS effects on brain activity in patients with epilepsy (Hao *et al.*, 2021). This study showed that the response to the cathodal tDCS was linked to functional network alterations with a decreasing FC in patients responding to the active cathodal tDCS.

Here, we observed a general tendency to a decrease in FC in the broad frequency band in the responder group, but this decrease was only significantly observed for the alpha and the beta bands. In line with our results, Lin and colleagues have shown that seizure reduction due to repeated application of cathodal tDCS was associated with a decrease in phase lag index synchrony measure in the alpha band without altering the number of epileptiform discharges (Lin *et al.*, 2018). The reduction of FC in epilepsy could be a general mechanism for the action of neuromodulation techniques in epilepsy. A decrease in FC in responding patients has been shown for example after vagus nerve stimulation (VNS) (Bodin *et al.*, 2015; Sangare *et al.*, 2020) in delta, after biofeedback (Ferri *et al.*, 2021), or thalamic stimulation (Deutschová *et al.*, 2021). The same trend has been also observed after epilepsy surgery (Ueda *et al.*, 2021).

On the contrary, Tecchio et al have shown that cathodal tDCS was able to increase FC in six patients suffering from epilepsy in the theta band most specifically (Tecchio *et al.*, 2018). These discrepancies between studies may be partially explained by the repetition of tDCS cycles and the use of different FC analysis methods.

### *Limitations*

This study has some limitations. First, our small sample size makes it difficult to generalize results regarding tDCS efficiency for all types of epilepsy disease. Another limitation is related to its open-ended design. We showed that it was possible to obtain a significant response both in terms of seizure frequency and in terms of number of responders (50% of patients with a mean response of -74%) but without comparison with a control group. However, neuromodulation studies, particularly in tDCS, have shown a response to placebo about 13–27% in terms of seizure frequency (Goldenholz and Goldenholz, 2020) and our results are much higher than this figure. Moreover, we have shown that the therapeutic response is linked to an objective marker of functional connectivity. Our estimation of FC was quite simple based on EEG scalp measurement with a limited number of electrodes. This did not allow us to study more precisely the brain changes induced by the stimulation. One of the emerging issues that remains to be demonstrated is the superiority of a customized multichannel tDCS protocol. Again, a

specific study comparing conventional bipolar tDCS and multichannel tDCS could be interesting in the future.

From the modelling perspective there are also several limitations. In this population of patients with scar tissue in the skull due to prior SEEG implantation and, sometimes, surgery, there can be significant changes in the E-field distribution in the brain when compared to a healthy case. This has been shown previously (Datta, Bikson and Fregni, 2010) and confirmed with our own results (see Supplementary material). However, in none of these studies have these changes in the modeled induced E-field values exceeded those reported in the literature as inducing lesions in animal model (Bikson *et al.*, 2016). Our own results (see again Supplementary material) show that when these factors are correctly modelled, the montage optimization algorithm can adjust the currents and electrode positions to account in part for the local increases of E-field under the skull defects. Such models can also be extended to include the effects of implants such as Ti plates (Mercadal *et al.*, 2021, 2021). It should be noticed, however, that it is hard to accurately segment accurately the scar tissue with MRI data alone, and the incorporation of CT data with robust segmentation algorithms for scar tissue would improve the models. That uncertainty, allied with the uncertainty on the dielectric properties of the tissues in the scar region remains as a source of uncertainty when predicting the E-field distribution in this population of subjects.

To conclude, this pilot study shows the feasibility, clinical efficiency and safety of a long-term (>6 months) multichannel cathodal tDCS with a personalized stimulation protocol in patients with drug-resistant epilepsy. We observed a substantial reduction in seizure frequency after three cycles of 5-days stimulation every two months. Half of the patients were responders with a mean seizure reduction of 74%. This clinical improvement for these difficult cases is cumulative with the stimulation cycles and was associated with a decrease in functional connectivity in alpha and beta bands.

## 3.5. Supplementary material

### *Effects of craniotomies on E-Field distribution in tDCS*

To assess the possible effects of a craniotomy on the E-field distribution induced by tDCS, we used a template head model based on data from Colin27's template (https://www.mcgill.ca/bic/software/tools-data-analysis/anatomical-mri/atlases/colin-27). The methods used to create the head model are described in (Miranda *et al.*, 2013). Electrodes representing Neuroelectrics' NG PiStim were added to the head model in a similar manner to what was done in the head models created for this study. The tissue conductivities were also set to the same values used in this study: 0.3 S/m for the skin, 0.008 S/m for the skull, 1.79 S/m for the CSF (including the ventricles),

0.4 S/m for the grey-matter (GM) and 0.15 S/m for the white-matter (WM). The gel under each electrode was modeled with a conductivity of 4.0 S/m.

Craniotomies were modeled as a central hole filled with CSF (representing an "acute-phase" lesion) with a radius of 1.0, 2.5 and 5.0 mm surrounded by a gap between the bone flap and the rest of the skull (radius of bone flap of 20 mm, distance between flap and skull of 2.0 mm). Since many of the targets in this study were in the temporal region of the brain, we place the central hole directly under electrode T7 in the template head model. The model of the craniotomy is represented in Figure III.S1.a. All calculations were performed in Comsol 5.3a (www.comsol.com).

To assess safety, we calculated the E-field distribution with a montage employing T7 as an anode (current of 1.884 mA, the maximum allowed per electrode in this study) and Cz as the cathode. The presence of the burr hole increased the E-field peak value from 1.22 V/m to 4.25 V/m (2.5 mm radius central hole). The increase with other hole sizes was smaller (see Figure III.S1.b). There was also an increase under the gap between the bone flap and the skull, but the peak value there was smaller.

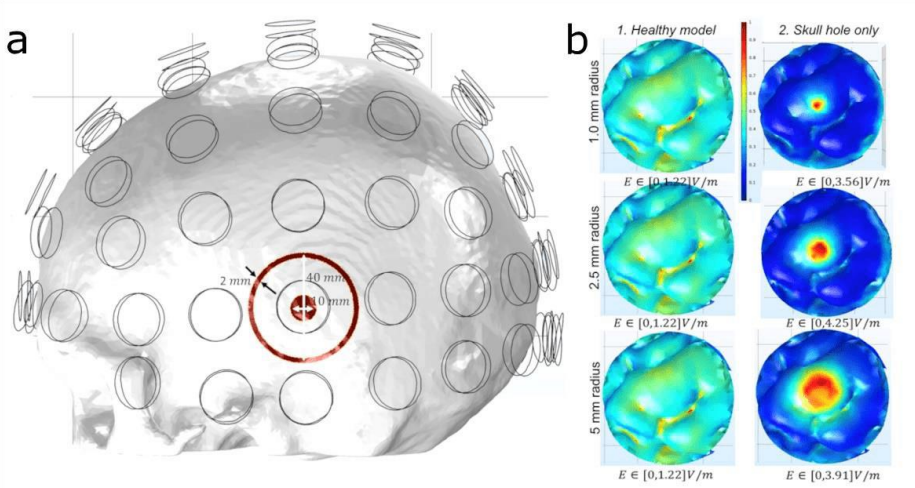


**Figure III.S1. Impact of a craniotomy of the magnitude of the E-field induced with tDCS**. a) Representation of the craniotomy consisting of a central whole inside a bone flap that is located at a 2 mm gap from the skull; b) E-field magnitude directly under the central hole for the healthy model (left column) and the models with central holes with increasing radius.

### *Effects of craniotomies on total injected current in optimized montage*

In order to test the influence of craniotomies in the results of montage optimization, we used the same head model as before, only now with the craniotomy located under electrode C3 (Figure III.S2). For simplicity we modeled the craniotomy in this case as a 1.0 cm radius cylindrical region with a conductivity equal to that of the CSF. The target for the optimization was defined by intersecting a cylinder with a radius of 1 cm to the cortical surface. We used three targets in this case: one under C3 (directly under the skull lesion), one under P3 and another one under T7. The target $En$ field was set to

+0.25 V/m in this cortical region and 0.0 V/m in the remaining areas. Weights for the optimization were set to 10 for the target region and 2 for the remaining areas. We ran optimizations with a maximum of two and six channels, and with current constraints set to 2.0 mA max per electrode and 4.0 mA max total injected current (double of what was used in the protocol followed for the patients, reported in the main manuscript). The optimizations conducted with the craniotomy were compared with optimizations conducted for an intact skull.

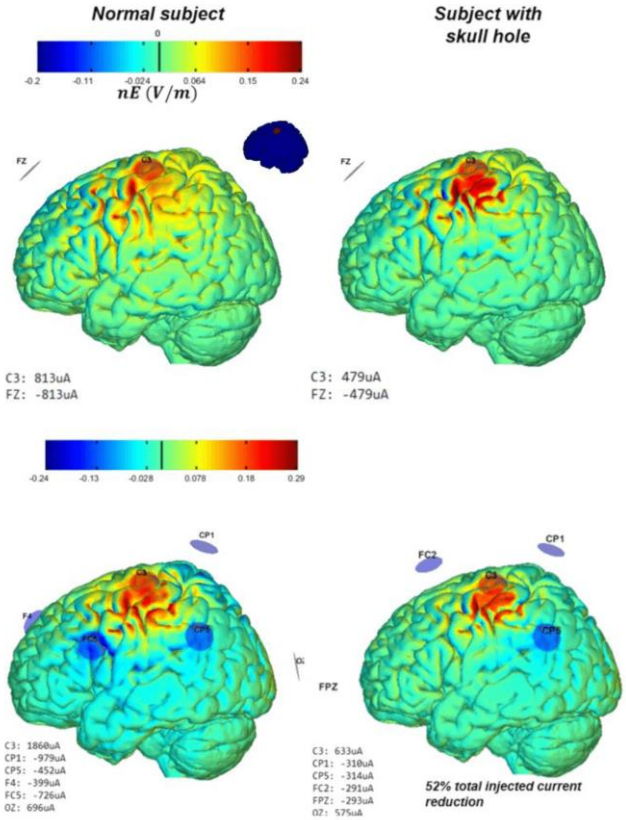


**Figure III.S2. Impact of a skull lesion in a montage optimization for a target directly under the hole**. Left column shows the results with the intact skull, whereas the right column shows the results with the skull hole. The top/bottom rows show the results of the optimization constrained with a maximum of 2/6 channels. The inset in the top-left figure shows the target used in the optimization.

For the optimizations conducted with the target under C3, the maximum value of the $En$-field was similar across models (0.23-0.29 V/m), however, the total injected current was much smaller in the model with the skull hole than in the model with the intact skull (42-52% reduction). Regarding the average $En$-field at the target, it was higher in the model with the skull hole in the two-channel montage (49% increase, relative to the model with the intact skull). In the six-channel optimization, this increase was much smaller: 0.44%. Table III.S1 presents a summary of the total injected current and the average $En$-field at the target for all the montages considered in this study.

| Target | Number of channels | Intact skull | | Skull hole | | Relative difference | |
|---|---|---|---|---|---|---|---|
| | | $\langle E_n \rangle$ $(V/m)$ | Total inj. $I$ $(mA)$ | $\langle E_n \rangle$ $(V/m)$ | Total inj. $I$ $(mA)$ | $\langle E_n \rangle$ | Total inj. $I$ |
| C3 | 2 | 0,027 | 0,813 | 0,040 | 0,479 | 49,0 | -41,1 |
| | 6 | 0,048 | 2,556 | 0,049 | 1,208 | 0,4 | -52,7 |
| P3 | 2 | 0,067 | 1,346 | 0,067 | 1,327 | -0,4 | -1,4 |
| | 6 | 0,077 | 2,417 | 0,078 | 2,398 | 0,2 | -0,8 |
| T7 | 2 | 0,016 | 0,732 | 0,016 | 0,732 | -0,2 | 0,0 |
| | 6 | 0,029 | 2,747 | 0,029 | 2,747 | -0,1 | 0,0 |

**Table III.S1. Average En at the target (V/m) and total injected current for all the montages and skull models in this study**. The last two columns show the differences between the skull hole values and the intact skull one as a percentage of the intact skull values.

The distribution of the $En$-field (Figure III.S3) was also much more focalized at the target for the skull hole model in the 2-channel montage (first row of Figure III.S3). But the impact of the skull hole in the 6-channel montage was much smaller (second row of Figure III.S3).

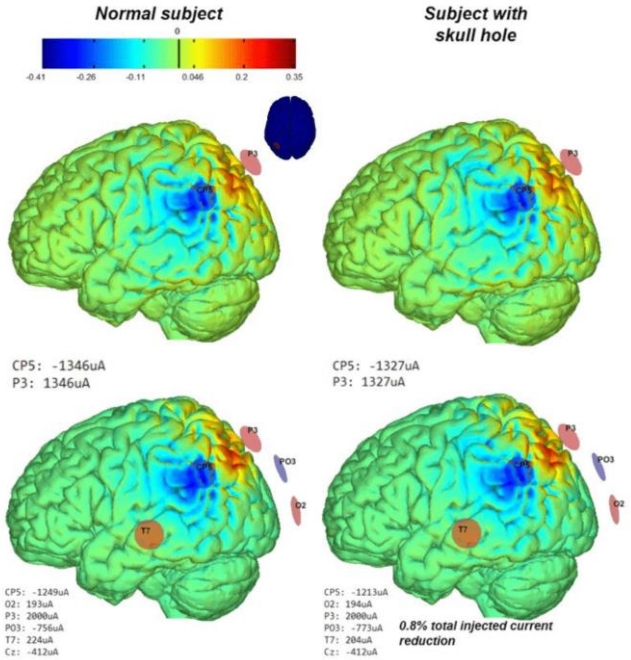


**Figure III.S3. Impact of a skull lesion in a montage optimization for a target under electrode P3.** Left column shows the results with the intact skull, whereas the right column shows the results with the skull hole. The top/bottom rows show the results of the optimization constrained with a maximum of 2/6 channels. The inset in the top-left figure shows the target used in the optimization.

For the optimizations conducted for the targets located over P3 and T7, the presence of the skull hole under C3 affected much less the results. This is shown in table III.S1 where the maximum relative difference between the injected currents is of only -1.4% and the maximum relative difference in the average $En$-field is only -0.8%. Even the positions and currents of each individual electrodes are very similar, as can be seen in Figure III.S4 which show the distribution of the component of the $En$-field for the

optimizations conducted with the targets under T7. As expected, the distribution of the $En$-field is almost unchanged with the presence of the skull hole.

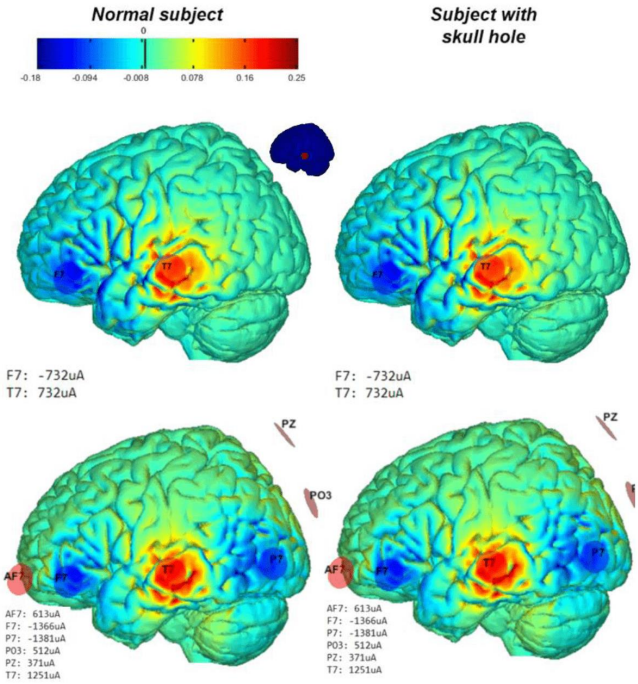


**Figure III.S4. Impact of a skull lesion in a montage optimization for a target under electrode T7.** Left column shows the results with the intact skull, whereas the right column shows the results with the skull hole. The top/bottom rows show the results of the optimization constrained with a maximum of 2/6 channels. The inset in the top-left figure shows the target used in the optimization.

### *Discussion*

The results presented here show that the presence of skull regions with higher conductivity can influence greatly the E-field distribution as expected. The observed increase in E-field is not, however, enough to reach peak values near the threshold for lesion generation according to animal models: 23 V/m for 60 minutes tDCS protocols and 61 V/m for 20 minutes protocols (Bikson *et al.*, 2016). Furthermore, if correctly segmented and represented in the head model, the montage optimization algorithm adjusts the currents and electrode positions to maintain a similar average $En$ on target.

# 4. Chapter IV: Local and Network Changes after Multichannel tDCS using MEG in Epilepsy

**Daoud, M**., Medina Villalon, S., Savlador, R., Fratello, M., Kanzari, K., Pizzo, F., Damiani, G., Garnier, E., Badier, J.M., Wendling, F., Ruffini, G., Bénar, C.G.*, Bartolomei, F*. Local and Network Changes after Multichannel Transcranial Direct Current Stimulation Using Magnetoencephalography in Patients with Refractory Epilepsy. *(In review)*

* Christian-George Bénar and Fabrice Bartolomei are co-last authors.

# Rationale

Study 3 aimed to evaluate the impact of tDCS on brain electrophysiology as measured with magnetoencephalography (MEG). We used the personalized multichannel tDCS protocol in DRE patients as proposed in the first study. This study was indeed designed to optimize current levels and orientation to ensure maximum inhibitory stimulation in the target area while minimizing excitatory anodal return current in other potentially epileptogenic regions.

This study employed advanced source reconstruction method on pre- and post-tDCS MEG recordings. The goal was to uncover local and network-level changes induced by tDCS and correlate them with clinical outcomes. Thus, study 3 aims to deepen our understanding of the neurophysiological effects of tDCS and to uncover predictive biomarkers for its clinical efficacy in DRE patients. This will advance the development of personalized treatment strategies in this challenging medical field.

# 4.1. Introduction

Transcranial direct current stimulation (tDCS) has emerged as a promising alternative in the treatment of focal drug-resistant epilepsies (DRE) (Simula *et al.*, 2022). This non-invasive brain stimulation technique delivers a low electrical current to the cortex through scalp electrodes. The electric field under the anodal electrode is typically excitatory, while the field under the cathodal electrode is inhibitory (Nitsche and Paulus, 2000, 2001), a property utilized in treating of epilepsy. Advanced methods, such as multichannel tDCS, which incorporates smaller electrode pairs, have emerged to target epileptogenic brain regions with greater precision. These advances include enhanced targeting accuracy through the integration of biophysical modeling, offering avenues for optimization (Ruffini *et al.*, 2014; Hannah, Iacovou and Rothwell, 2019).

To date, several clinical studies on tDCS have reported a decrease in the occurrence of seizures (review in (Simula *et al.*, 2022)). However, despite the therapeutic action of tDCS in epilepsy patients and the refinement of protocols, the underlying mechanisms driving clinical improvements remain poorly understood and are a topic of ongoing debate. Accumulating evidence from previous investigations underscores the need to characterize epilepsy as a large-scale brain network disorder (Pittau and Vulliemoz, 2015; Bartolomei *et al.*, 2017). In particular, interictal alterations in functional connectivity within the epileptogenic network have been shown (Lagarde *et al.*, 2018).

The main objective of this study was to evaluate the changes in local (power spectral density measures) and network (functional connectivity) brain activity induced by tDCS, as measured by magnetoencephalography (MEG), and to establish correlations with clinical outcomes. We also explored whether alterations were confined to the inhibited areas or extended more broadly across the brain. Finally, we analyzed data before transcranial stimulation with the objective of identifying predictive biomarkers of the clinical response to tDCS.

# 4.2. Materials and methods

### *Study design*

17 patients with drug-resistant epilepsy (DRE) were prospectively enrolled in this study. The protocol was approved by the national ethics committee (N°ID RCB 2020-A02861-38). The inclusion criteria comprised: (1) age ≥ 12 years; (2) diagnosed with focal drug-resistant epilepsy that is either inoperable or has experienced failure of prior epilepsy surgery, (3) with at least four seizures per month at baseline; (4) previous SEEG conducted before inclusion, providing an adequate definition of unifocal epileptogenic zone. Clinical and demographic data are summarized in Table IV.S1.

### *Multichannel tDCS sessions*

After a baseline period of two months for each patient, the patients received daily stimulation with an individualized multichannel tDCS protocol (see below) for five consecutive days, referred here as a tDCS 'cycle'. The daily treatment resulted in a total of 40 minutes of cathodal stimulation. Each cycle started and finished with a 1-hour magnetoencephalography exam (MEG). This tDCS cycle (including MEG and daily tDCS) was repeated every two months, for three tDCS cycles within six months (Figure IV.1.A).

The position of tDCS electrodes for each patient was personalized using an optimization process based on individual factors, including the location of the epileptogenic network and previous cortectomies or lesions (for details, see methodology in (Daoud *et al.*, 2022)). In brief, the personalized approach involved creating individual head models from MRI scans and optimizing electrode placement using the Stimweaver algorithm (Ruffini *et al.*, 2014). This algorithm determines the optimal electrode positions and currents to suppress the epileptogenic network, represented as a weighted target En-field map on the cortical surface. En influences cortical excitability (Galan-Gadea *et al.*, 2023). The optimization minimizes the ERNI function, a weighted difference between En induced by each candidate solution and the target weight map. Currents were limited to a maximum of 1.884 mA per stimulation channel and 2.0 mA total injected current. Stimulation was administered using the Starstim8 tDCS system, with NG PiStim electrodes positioned in a neoprene cap (Neuroelectrics Barcelona). The current intensity was delivered in two 20-minute sessions separated by a 20-minute break to prolong inhibitory effects (Monte-Silva *et al.*, 2010; Yang *et al.*, 2020).

### *MEG recordings*

On the first day of each cycle (prior to the first stimulation of the week), patients underwent a MEG recording to capture the electrophysiological brain state before stimulation. At the end of each tDCS cycle (on the 5th day), another MEG exam was performed for comparison with the pre-tDCS treatment recording.

The biomagnetic signals used in this study were acquired using a 4D Neuroimaging™ 3600 whole head system equipped with 248 magnetometers operating at a sampling rate of 2034.51 Hz (4D Neuroimaging Inc., San Diego CA) (Pizzo *et al.*, 2019). Each recording session consisted of five runs of 10 minutes during resting state (two runs with eyes closed). To co-register MEG recordings with patient's MRI images, three fiducial positions (nasion, left pre-auricular, and right pre-auricular) and head coil positions were determined.

### *Seizure frequency measures*

The patients or/and their caregivers were asked to record daily the number and the type of seizures in a seizure diary starting two months before the study onset (baseline) and continuing until two months after the final multichannel tDCS stimulation cycle (V4). Changes in seizure frequency (SF) were expressed as a percentage of baseline frequency. Patients experiencing at least 50% seizure reduction at the end of the study were categorized as 'responders' (R), while others were labeled as 'non-responders' (NR).

### *MEG data pre-processing and source reconstruction*

MEG data were analyzed using the AnyWave software (Colombet *et al.*, 2015) (http://meg.univ-amu.fr/wiki/AnyWave) and Matlab in-house scripts (The Mathworks Inc., MA, USA). The MEG signals were first bandpass filtered in the range [1-70 Hz] a notch-filtered at 50 Hz. All MEG channels were thoroughly examined, and channels displaying noise or flat signals were excluded from the analysis. We additionally removed artifacts using independent component analysis (ICA) (Barbati *et al.*, 2004) including those related to cardiac activity, muscle interference, and eye movements. Subsequently, the MEG signals were visually inspected, and any segments containing residual artifacts not identified by the ICA analysis were excluded.

Regarding the MEG source localization and reconstruction, we used the open-source FieldTrip toolbox (Oostenveld *et al.*, 2011). The forward model was computed using OpenMEEG (Kybic *et al.*, 2005; Gramfort *et al.*, 2010). For the inverse solutions, we used the linearly constrained minimum-variance beamformer (LCMV-BF) (Van Veen *et al.*, 1997). This method uses a spatial filter, linking the magnetic field measured by MEG sensors outside the brain to neural activities within the brain. It uses the covariance of recorded signals without requiring assumptions about the number of active sources. The beamformer calculation results in a time series for each target location within the brain, representing the activity of that source. We thus estimated the source activity at the centroids of the regions defined by the Virtual Epileptic Patient atlas (VEP Atlas) (Wang *et al.*, 2021). The analysis schema is reported in Figure IV.1.B.

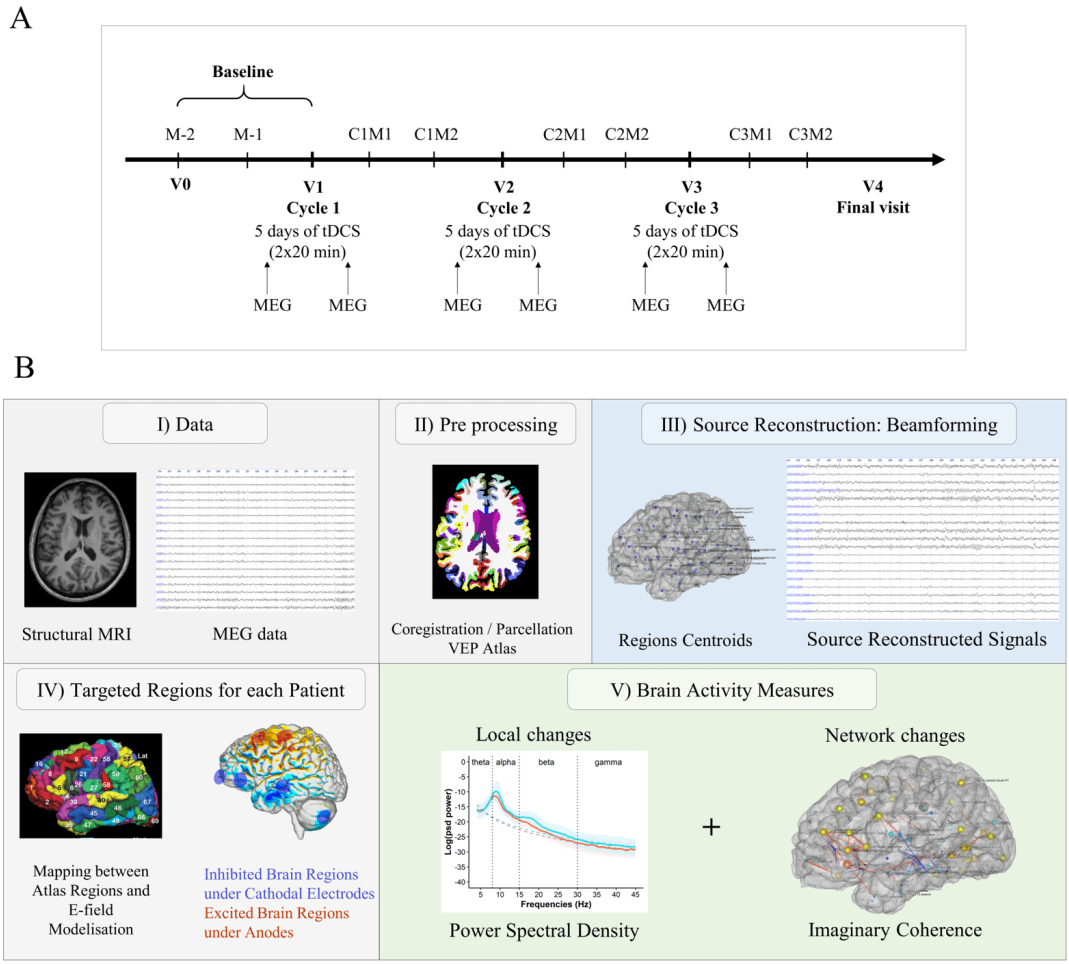


**Figure IV.1. Overview of study design and data analysis pipeline. A. Study timeline.** Seizure diary information was collected monthly for each cycle (C1M1, C1M2, C2M1, C2M2, C3M1, C3M2). Each tDCS cycle consisted of two 20-minute stimulation periods separated by a 20-minute off period (20 min tDCS – 20 min off – 20 min tDCS), with a 1-hour MEG recording performed before the first day of stimulation and immediately after the last day of the cycle. Cycles were repeated every 2 months for three times. B. Pipeline for MEG data analysis. After cleaning the MEG recordings (I) and performing the co-registration with patient's MRI (II), a linearly constrained minimum-variance beamformer (LCMV-BF) was used to estimate the MEG source times series at VEP regions level (following (Wang *et al.*, 2021)) (III). Then we identified the patient-specific regions of interest, that include inhibited brain regions in blue and excited brain regions (in red). Finally, we performed local (power spectral density) and network (functional connectivity estimated by imaginary coherence measures) source analyses before and after each tDCS cycle and summarized them separately for inhibitory and excitatory brain regions. Abbreviations: tDCS: Transcranial Direct Current Stimulation; MEG: Magnetoencephalography; M-2, M-1: 1 and 2 months before the first stimulation cycle (baseline period); V0: Visit 0 Inclusion; C1M1: 1 month (M1) after the first cycle (C1); C1M2: 2 months (M2) after the first cycle (C1); C2M1: 1 month (M1) after the second cycle (C2); C2M2: 2 months after the second cycle; C3M1: 1 month after the third cycle; C3M2: 2 months after the third cycle; V4: Visit 4, final visit; MRI: Magnetic Resonance Imaging; VEP: Virtual Epileptic Patient.

### *Local and network source analysis*

Using the electrical field map generated from the tDCS montage of each patient, we delineated the excited brain regions (linked to anodal electrodes) and inhibited brain regions containing cortical areas (including EZ) associated with cathodal electrodes. These patient-specific regions of interest are represented respectively in red and blue in Figure IV.1.B.

First, to assess the potential local changes induced by tDCS in the targeted brain regions, we computed the power spectral density (PSD) (using Hanning windows of 2 s, overlap of 1 s) before and after each tDCS cycle. To prepare the data for statistical analysis, we calculated the mean power in specific frequency bands (theta 4–8 Hz, alpha 8–15 Hz, beta 15–30 Hz, and gamma 30-45 Hz) for each FFT iteration, normalized by the total power in the broadband range (1-45 Hz).

Second, to evaluate the impact on network activity, we investigated functional connectivity (FC) changes at the source level following each tDCS cycle. An inherent challenge in interpreting source FC analysis is the emergence of spurious coherence due to the inevitable leakage of the inverse algorithm (Schoffelen and Gross, 2009). To mitigate this issue, we opted for the imaginary coherence measure (icoh, (Nolte *et al.*, 2004)). The imaginary part of coherence specifically detects synchronizations between processes that are time-lagged to each other. This approach quantifies the coupling of oscillatory phases in the activation dynamics between two brain sources, with a focus on minimizing crosstalk effects between the sources. To obtain a distribution of values for statistical analysis, we computed the metric across 15 trials, each comprising a 2-second window with a 50% overlap. This process was repeated throughout the entire recording, excluding artifact periods. Subsequently, multiple connectivity matrices were generated for each recording and frequency band (broadband, theta, alpha, beta, gamma). To summarize connectivity information for each region and frequency band, we calculated the normalized strength of the node. This was done by summing up all the links connected to the node and then dividing this sum by the number of connected nodes.

To investigate spectral changes between post and pre-stimulation, we performed a Wilcoxon rank sum test for each region and frequency band. This test was chosen due to the non-normal distribution of the data. We used Matlab ranksum function to compare all PSD values (as described above) of the two periods of interest (Day 5 – Day 1 for each cycle). Similarly, to investigate FC changes between day 5 and day 1 of each cycle (Day 5 – Day 1), per region and frequency band, we performed a Wilcoxon rank sum test between all the values of node strength of the two periods.

For each measure, we kept the values of the z-statistic (called Z-value in the manuscript) to assess any differences between R and NR, between tDCS cycles, and between brain regions.

### *Statistical analysis*

For each frequency band, Student t-tests were used to assess the changes of Z-values in local and network activity induced by tDCS across R and NR patients, tDCS cycles, and inhibited/excited brain regions. In addition, to attempt to predict favorable responses to tDCS treatment, differences in node strength values between R and NR patients at day 1 of the first cycle were also evaluated with Wilcoxon test as values were not normally distributed. All analyses were carried out using RStudio (version 4.2.2). To address multiple comparisons, we applied Bonferroni correction to the p-values. Effect sizes were computed using Cohen's d. A p-value less than 0.05 (after adjustment) was considered statistically significant.

## 4.3. Results

Seventeen patients with diverse forms of focal refractory epilepsy were enrolled between July 2021 and April 2023 (ten females, seven males; mean age 30.2; range 12-50). Three patients were excluded from the analysis pipeline. As a result, we have included a total of 14 patients in our study analysis.

### *Effects of tDCS on seizure frequency*

At the two-month follow-up after the last tDCS cycle, nine of the fourteen patients experienced a decrease in their seizure frequency (SF) compared to the baseline (mean decrease -46% ± 28%) (Figure IV.2). Among these patients, five were considered as responder (R) patients with a SF decrease >50% (mean reduction: -66% ± 20%). Patients 10 and 13 had to stop the tDCS stimulation after cycle 2 according to the safety protocol rules (SF increase >100%). Overall, only mild adverse events were reported, mostly characterized by mild itching (9/14) and tingling (4/14) sensation beneath the stimulation electrodes during the first 30 seconds of the stimulation period.

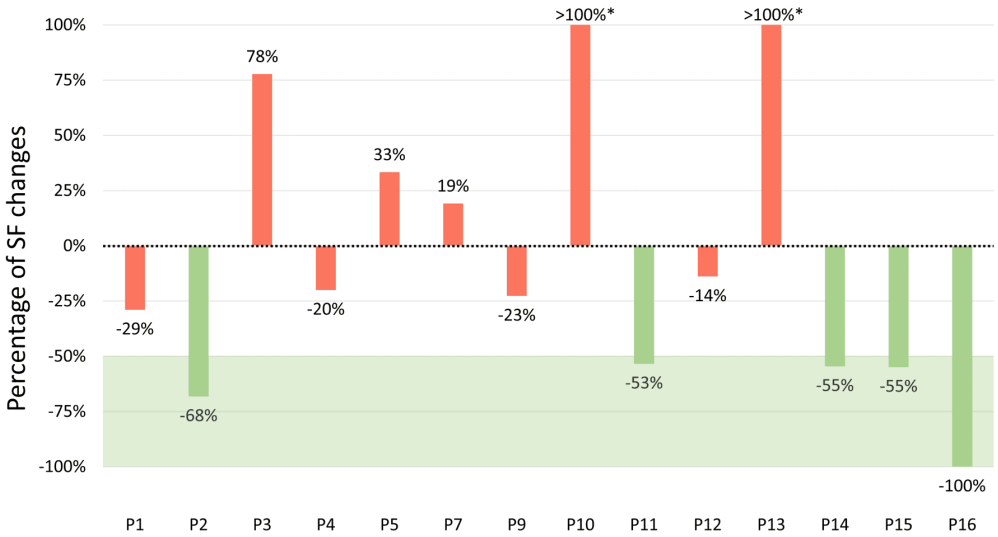


**Figure IV.2. Percentage change in seizure frequency compared to baseline after three tDCS cycles at the two-months follow-up (n=14 patients)**. *Patients 10 and 13 had to stop the study after the cycle 2 according to the safety rules of our protocol (increase in SF >100%).

### *Spectral activity changes after multichannel tDCS*

We first focused on PSD changes occurring between day 5 and day 1 of each cycle for R and NR patients in the whole brain (Figure IV.3). The results were found to vary significantly across different frequency bands (see details in Supplementary data Table IV.2). In the theta band (4-8 Hz), R patients exhibited a moderate and cumulative decrease in spectral power across cycles. Conversely, NR patients displayed a substantial and cumulative increase in PSD in the theta range across cycles, with the maximum increase observed in cycle 3. When comparing spectral power between R and NR groups, a significant and large decrease was observed in R patients in cycles 2 and 3 (Figure IV.3.A). Regarding changes in the alpha band (8-15 Hz) across cycles for both R and NR, a significant increase in power was observed between cycles 1 and 2. In NR patients, the observed increase in spectral power between cycles was smaller. R patients exhibited a significant increase in alpha spectral power in all cycles compared to NR patients (Figure IV.3.B). In the beta band (15-30 Hz), we noted a significant cumulative large decrease across stimulation cycles in NR patients and, conversely, an increase in the last tDCS cycle in R patients. Comparing the R and NR groups, the PSD changes varied at each tDCS cycle. After C1 and C2, R had a significantly lower PSD in the beta band than the NR group. After C3, R presented a significantly larger PSD in beta band than in NR group (Figure IV.3.C).

Regarding changes in PSD within the gamma band (30-45 Hz) across cycles for R patients, a small but significant increase in power was observed between the second and the last tDCS cycle. In NR patients, we observed a cumulative decrease in spectral power in the gamma range across cycles. When comparing R and NR groups across cycles, we obtained similar results to those of the beta band. After the first cycle (C1), R had a

significantly lower PSD than the NR group. After the third cycle (C3), R presented a significantly larger PSD in the gamma band than the NR group (Figure IV.3.D).

We then focused on PSD changes involving the specific targeted brain regions. Supplementary data Figure IV.S1 depicts the changes in PSD focusing on targeted and non-targeted regions in all frequency bands (theta, alpha, beta, gamma). We did not find significant differences in PSD changes between excited and inhibited brain regions.

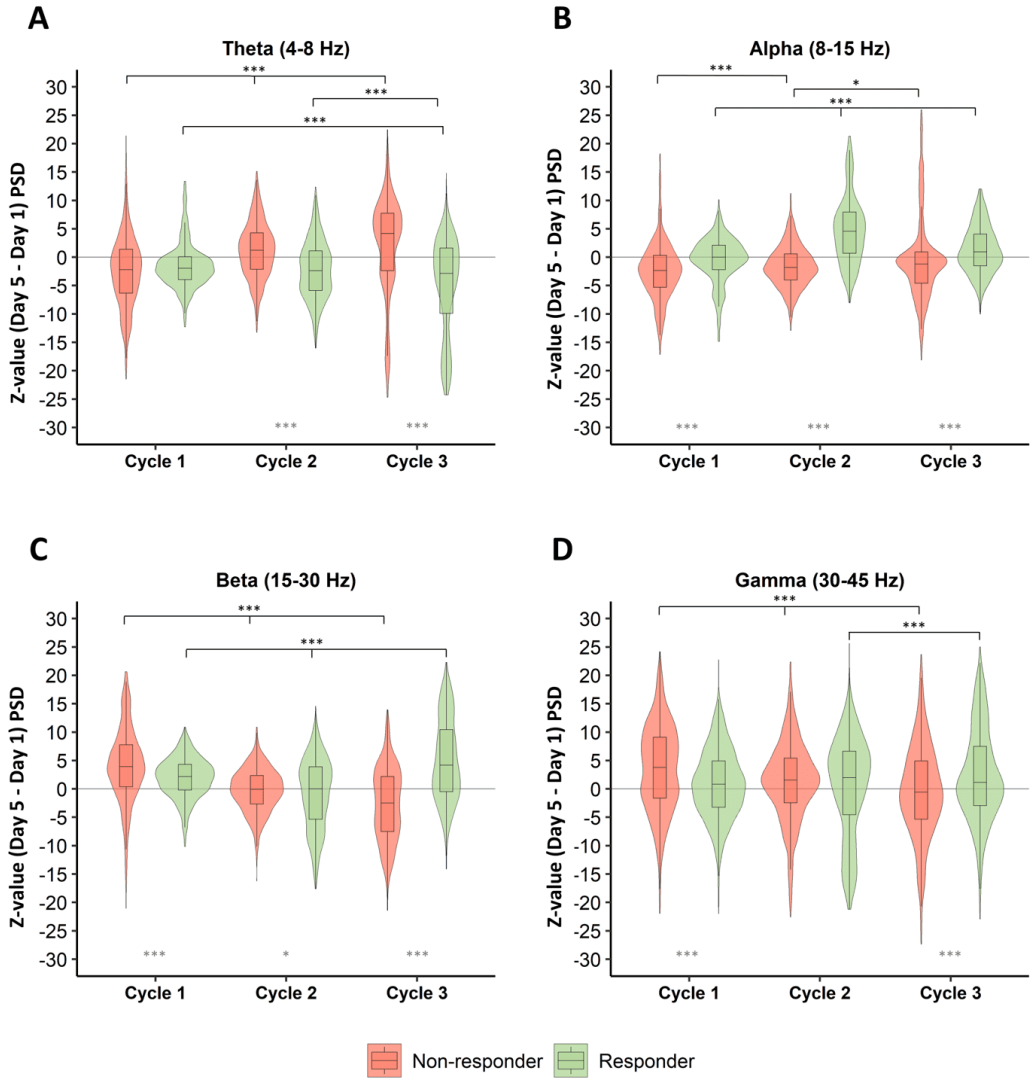


**Figure IV.3. Power spectral density (PSD) changes after each tDCS cycle in responder and non-responder patients.** A. Violin plots represent the power spectral density (PSD) induced changes after each tDCS cycle in all brain regions in responders (in green) and non-responders (in orange) in theta band (4-8 Hz). B. In alpha band (8-15 Hz). C. In beta band (15-30 Hz). D. In gamma band (30-45 Hz). Grey asterisks represent differences between responder and non-responder groups. P-values were corrected using Bonferroni correction and black bars with asterisks representing significant differences between PSD changes occurring in cycles (* $p < 0.01$, ** $p < 0.001$, *** $p < 0.0001$).

We also studied the PSD changes by decomposing the spectrum into periodic and aperiodic components using the Fitting Oscillations and One-Over-F (FOOOF) algorithm (Donoghue *et al.*, 2020). One example of this analysis is illustrated in Appendix B.

### *Functional connectivity changes after multichannel tDCS*

First, to gain a broader overview of potential functional changes, we examined global variations in FC by comparing node strength values of all regions between cycles and between R and NR groups (Figure IV.4). The statistical results are summarized in Supplementary data Table IV.S3. The overall FC change pattern observed between groups and cycles appears similar across the frequency bands studied. In the broadband range (Figure IV.4.A), R patients exhibited a global decrease in FC from the second cycle of stimulation. In contrast, the NR group showed either no modification or very slight changes in FC. The comparison of FC changes occurring after cycles 2 and 3 confirmed a significant decrease in FC for R compared to the NR group.

Sub-band analysis revealed that in the theta band (Figure IV.4.B), we also observed a cumulative, significant decrease in FC across all brain regions in R patients between cycles. In contrast, NR patients showed a slight increase in FC across cycles. When comparing FC changes between R and NR groups, R patients presented a significant decrease in FC compared to the NR group at the second and the last tDCS cycles. The findings for other frequency bands are detailed in Supplementary data Figure IV.S2 and Table IV.S3.

A significant reduction in FC in the broadband range within targeted inhibited and excited brain regions was observed after cycle 2 for R patients compared to NR patients (Inhibited regions in Cycle 2, R vs NR: $t(110) = -5.0422$, $p < 0.0001$, Cohen's $d = -0.85$ [-1.19 – -0.51]; Excited regions in Cycle 2, R vs NR: $t(99) = -3.8912$, $p < 0.001$, Cohen's $d = -0.75$ [-1.15 – -0.36]) (Figure IV.4.C). A similar trend was noted for the last tDCS cycle. We then analyzed whether FC changes were different in inhibited (targeted) and excited regions, and no difference was observed.

We also estimated these changes in frequency sub-bands. Figure IV.4.D displays as an example the findings related to theta band. We observed a similar trend with a reduction in FC within both inhibited and excited brain regions after C2 and C3 for R patients compared to NR patients (Inhibited regions in Cycle 2, R vs NR: $t(86) = -3.3525$, $p = 0.028$, Cohen's $d = -0.62$ [-0.95 – -0.28] ; Inhibited regions in Cycle 3, R vs NR: $t(105) = -4.2953$, $p<0.001$, Cohen's $d = -0.79$ [-1.19 – -0.39] ; Excited regions in Cycle 3, R vs NR: $t(79) = -4.6473$ $p<0.001$, Cohen's $d = -1.03$ [-1.49 – -0.56]). Finally, no significant variations between inhibited and excited regions were observed in other frequency bands (Supplementary data Figure IV.S2).

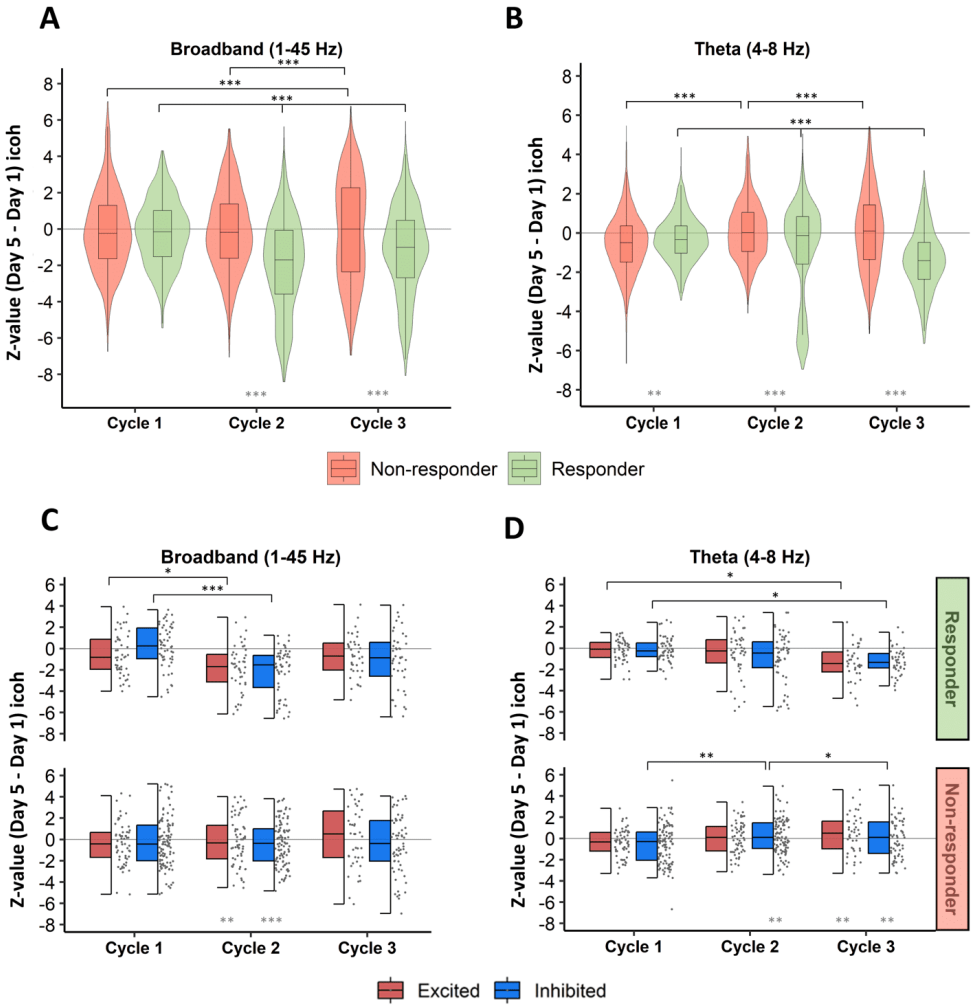


**Figure IV.4. Functional connectivity (FC) changes in responder and non-responder patients**. In panels A and B, violin plots represent FC changes after each tDCS cycle in all brain regions at source level in responder (in green) and non-responder patients (in orange) in broadband (A) and in theta band (B). In panels C and D, half-boxplots illustrate FC-induced changes in broadband (C) and in theta band (D) after each tDCS cycle within inhibited brain regions (under cathodal tDCS electrodes in blue) and within excited brain regions (under anodal tDCS electrodes in red) for responder and non-responder patients. Each data point represents the z-value of one source region (zero: no FC change after the tDCS cycle; negative/positive z-value: decrease/increase of FC after the tDCS cycle). Grey asterisks represent differences between responder and non-responder groups. P-values were corrected using Bonferroni correction, and black bars with asterisks represent the differences between FC changes occurring in cycles (* $p < 0.01$, ** $p < 0.001$, *** $p < 0.0001$).

### *Pre-stimulation brain network and relationship with therapeutic outcome*

We further investigated whether responders and non-responders had different properties in their brain networks before starting tDCS, potentially serving as predictors of the future response to tDCS. We used the node strength calculated from the initial MEG recording of the study— before the first stimulation in cycle 1. We found a higher global

FC in the broadband range in R patients compared to NR patients before any tDCS stimulation (W = 600165 , p<0.0001 , Cohen's d = 0.55 [0.45 – 0.64]) (Figure IV.5).

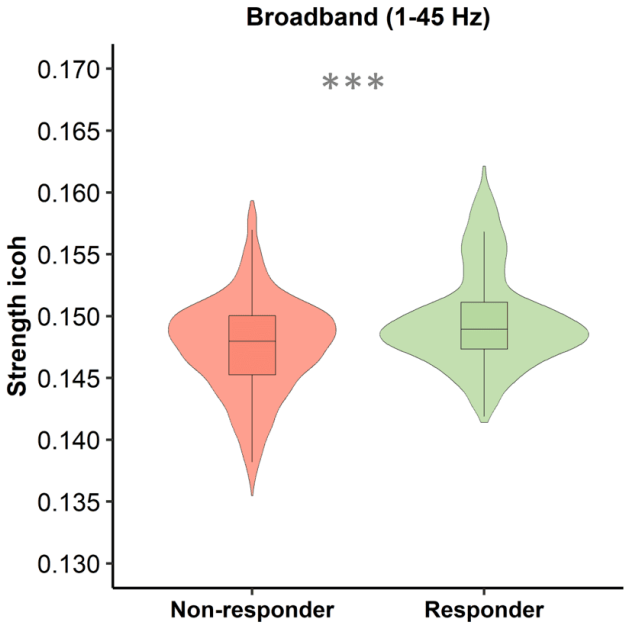


**Figure IV.5. Functional connectivity measured before the first tDCS stimulation in responder and non-responder patients.** The data represented by violin plots corresponds to the node strength changes in all source regions for the patients of each group (R vs NR). Grey asterisks represent differences between responder and non-responder groups (*** p < 0.0001).

# 4.4. Discussion

### *Multichannel tDCS induced changes in spectral power according to the clinical response*

Following previous studies (Kaye *et al.*, 2021; Daoud *et al.*, 2022), we used a personalized multichannel tDCS protocol guided by an SEEG-based definition of the target. This allowed us to optimize current levels to ensure that induced electric fields maximized inhibitory stimulation at the target site (Ruffini *et al.*, 2014; Hannah, Iacovou and Rothwell, 2019). Among the 14 patients, nine disclosed a seizure decrease after the three tDCS cycles and five were classified as responders (R), with a substantial mean SF decrease of -66% ± 20%. Examining power spectral changes at the source level, we found distinct patterns for the R and NR groups across different frequency bands following tDCS cycles.

Our findings indicate a cumulative decrease in spectral power in the theta band for R patients while NR patients displayed an inverse trend, with a significant increase, particularly after the third tDCS cycle. Previous studies identified an increased theta

power in the interictal waking state of patients with partial and generalized epilepsy, exhibiting a consistent distribution across all derivations in EEG signals (Clemens, Szigeti and Barta, 2000; Clemens, 2004; Douw *et al.*, 2010). At the same time, the clinical efficacy of antiepileptic interventions, including pharmacological treatments, has been demonstrated to reduce and restore this abnormal increase in theta activity (Clemens *et al.*, 2010; Biondi *et al.*, 2022). Additionally, our results indicated enhanced alpha band activity in R compared to NR patients after tDCS cycles. This observation aligns with a recent study conducted by Gin et al. (Ghin, O'Hare and Pavan, 2021), who reported amplified EEG PSD in the alpha band using high-frequency transcranial random noise stimulation (hf-RNS) in healthy subjects. The increase in alpha activity in R patients could play an inhibitory role, consequently reducing the occurrence of seizures. The rise in signal amplitude within the alpha band is commonly linked to cortical deactivation, and inhibition, reducing cortical excitability (Klimesch, Sauseng and Hanslmayr, 2007; Romei *et al.*, 2008; Sauseng *et al.*, 2009). In epilepsy patients, several studies have shown a decrease in peak frequency and reduced power in the alpha band in epileptic patients, reflecting inadequate control over seizure occurrence (Díaz *et al.*, 1998; Larsson and Kostov, 2005; Abela *et al.*, 2019).

We also observed that the spectral modifications induced by tDCS in the beta band differed between R and NR across stimulation cycles. R patients tended to have an increase in beta band power with successive cycles, whereas NR showed a power decrease. In line with the fluctuations observed during stimulation cycles, epilepsy studies examining the spectral features of the beta band have yielded contradictory outcomes. Some studies emphasized the inhibitory role of beta activity (Pellegrino *et al.*, 2021), highlighting heightened oscillatory activity in response to specific antiepileptic drugs (Marrosu *et al.*, 2005; Cho *et al.*, 2012). Conversely, other research revealed an abnormal increase in beta band power in epilepsy patients (Miyauchi *et al.*, 1991; Pegg, Taylor and Mohanraj, 2020), suggesting reduced beta activity following deep brain stimulation (DBS) as a potential clinical efficacy biomarker (Tong *et al.*, 2022).

Interestingly, no significant differences were observed when comparing PSD changes between excited and inhibited brain regions within the same patient group across all frequency bands. This suggests that the spectral content was altered uniformly throughout the entire brain and not specifically within the inhibited targeted regions, i.e., the areas around the epileptogenic zone. Another investigation using a high-definition protocol of responsive neurostimulation (hf-RNS) similarly reported this widespread phenomenon (Ghin, O'Hare and Pavan, 2021).

### *Multichannel tDCS induced whole brain functional changes based on clinical response*

Previous research has shown that heightened connectivity is observed in both the epileptogenic zone and the propagation zone when compared to the non-involved zone (NIZ) (Bettus *et al.*, 2008; Warren *et al.*, 2010; Bartolomei *et al.*, 2017; Lagarde *et al.*, 2022). It is reasonable to hypothesize that effective antiepileptic therapy could normalize functional connectivity, as it has already been shown in VNS (Bodin *et al.*, 2015; Sangare *et al.*, 2020; Vespa *et al.*, 2021), thalamic stimulation (Scherer *et al.*, 2020; Deutschová *et al.*, 2021), or after SEEG radiofrequency ablation (Simula, Garnier, *et al.*, 2023). To date, several recent studies have suggested an association between a tDCS-induced decrease in FC or in synchronization induced by tDCS and its clinical effectiveness, measured by seizure frequency reduction (Lin *et al.*, 2018; Luo *et al.*, 2021; Daoud *et al.*, 2022). However, the connectivity estimations in these studies were elementary, derived from simple scalp EEG with only a few channels. Our study showed that R patients, after the second and the third tDCS cycles, exhibited a decrease in overall source level-functional connectivity compared to NR across all frequency bands. Additionally, no significant differences were observed when comparing functional changes in brain regions involved in the epileptogenic zone (under cathodes) to non-involved regions (under anodes). This is consistent with the PSD results and supports the assumption that, despite being a focal method, tDCS exerts a widespread and robust influence on the whole brain networks. Previous research suggested the possibility of inducing effects affecting both local and network-to-network connectivity dynamics when applying multichannel tDCS in healthy subjects (Ruffini *et al.*, 2018; Mencarelli *et al.*, 2020).

### *Functional source connectivity as a predictive biomarker for clinical response to tDCS?*

We finally observed that individuals who later showed a positive clinical response to tDCS had a baseline FC level significantly higher than the FC level observed in NR patients, prior to the start of the first tDCS stimulation. The state of the brain networks before the start of the therapeutic procedure could be predictive of the treatment response. This has already been suggested with other types of neurostimulation. Before treatment with VNS, it has been shown that the network topology measured by MEG was different in R and NR patients (Babajani-Feremi *et al.*, 2018). A higher pre-intervention level of functional connectivity has also been found in patients responding to pulvinar-DBS compared to NR patients (Deutschová *et al.*, 2021). In a trial aimed at predicting the treatment outcome of cathodal tDCS in focal epilepsy, Hao and colleagues used graph theoretical analysis based on fMRI data (Hao *et al.*, 2021). By employing a support vector machine (SVM) prediction model, they achieved a promising mean accuracy of 68.3%, demonstrating the potential for clinical prediction of tDCS treatment outcomes in epilepsy patients.

### *Limitations*

The first limitation concerns to the small sample size; further studies should adopt a multicentric approach to enhance patient enrolment. Secondly, the absence of a sham control group in our study raises concerns about the robustness of the findings. However, earlier tDCS investigations have shown a notable placebo response of approximately 13–27% change in seizure frequency (Goldenholz and Goldenholz, 2020). When assessing R patients exhibiting a reduction in seizure frequency exceeding 50%, our findings exceed this range significantly.

To conclude, the acquisition of MEG data before and after multiple cycles of multichannel tDCS, coupled with source reconstruction analysis, enabled the identification of induced changes in power spectral density and in functional connectivity in whole brain networks. Notably, distinct patterns of brain changes were observed between responder and non-responder patients. The findings pave the way for future investigations, offering potential clinical applications and enhancing our understanding of tDCS effects on epileptic brain networks.

## 4.5. Supplementary data

| *Patient* | Gender | Age | Etiology | Seizure type | Number of ASM | SOZ defined by SEEG | Number of SEEG electrodes | Previous failed surgery | tDCS target | Injected Current (mA) | Desired E field in Target (V/ m) | Number of tDCS electrodes |
|---|---|---|---|---|---|---|---|---|---|---|---|---|
| *1* | F | 43 | Schizencephalia, heterotopia, polymicrogyria | Focal seizure, impaired awareness | 3 | Ltemporal mesial, Perisylvain deep, superficial, parietal lateral | 19 | Thermocoagulation, VNS | L MLa temporo-parietal | 1.998 | -0.5 | 7 |
| *2* | F | 31 | FCD 2 | Simple focal seizure | 1 | TLE, L frontal mesial, central mesial and lateral | 9 | Cortectomy L premotor cortex | L pericentral | 1.999 | -0.5 | 8 |
| *3* | M | 42 | Cavernoma | Complex left focal seizure, impaired awareness | 4 | L frontal mesial temporal mesial | 9 | No | L MLa, temporo-orbitofrontal | 1.998 | -0.25 | 7 |
| *4* | M | 48 | Cryptogenic | Complex focal seizure, impaired awareness | 4 | L Temporal mesial, left insula bilateral | 13 | Thermocoagulation, VNS (desactivated) | L MLa temporal | 1.999 | -0.034 | 6 |
| *5* | F | 50 | FCD 1 | Complex focal seizure, impaired awareness, SGTC | 5 | R temporal mesial, parietal mesial, lateral bilateral (R>L) | 13 | Thermocoagulation, resective surgery | R pericentral/ parietal and posterior temporal (carrefour) | 1.997 | -0.5 | 8 |
| *6* | F | 23 | Hippocampal sclerosis | Complex focal seizure, impared awareness | 3 | R mesio temporal | 11 | No | R MLa temporal | 1.999 | -0.014 | 7 |
| *7* | M | 32 | Gliosis | EPC, focal motor seizures | 4 | R paracentral lobule | 4 | Gamma-knife, VNS | R pericental extended | 1.998 | -0.055 | 6 |

| | | | | | | | | | | | | |
|---|---|---|---|---|---|---|---|---|---|---|---|---|
| *8* | M | 49 | FCD 2 | Complex focal seizure, impaired awareness | 5 | L mesio frontal, mesio central | 12 | VNS | L pericental | 1.999 | -0.055 | 4 |
| *9* | M | 31 | Cryptogenic | Simple focal seizure without loss of awareness, complex focal seizure with loss of awareness, SGTC | 2 | L temporo mesial | 16 | No | L MLa temporal | 1.998 | -0.25 | 7 |
| *10* | F | 15 | Cryptogenic | Focal seizure without loss of awareness, Paresthesia | 2 | R lateral mesial frontal, central mesial lateral | 15 | Cortectomy, residual lesionectomy | R perisylvian and post central | 1.999 | -0.11 | 8 |
| *11* | F | 16 | FCD 1 | Simple focal seizure, without loss of awareness | 3 | R frontal mesial lateral, central mesial lateral | 13 | Cortectomy R frontal | Bilat pericentral (R>L) | 1.998 | -0.25 | 8 |
| *12* | F | 23 | Cryptogenic | Focal sensitivo motor seizure without loss of awareness | 2 | R fronto lateral centro mesial, posterior | 13 | Thermocoagulation, VNS | R pericentral | 1.999 | -0.25 | 4 |
| *13* | M | 29 | Cryptogenic | Simple focal seizure without loss of awareness, complex focal seizure with loss of awareness, SGTC (<1/year) | 3 | L temporal mesial lateral | 15 | VNS | L MLa Temporal Plus dorso-lateral frontal | 1.999 | -0.02 | 8 |
| *14* | M | 16 | Infectious/trauma, MRI left hemispheric atrophy | Simple focal seizure, without loss of awareness, Paresthesia | 4 | L frontal lateral centro lateral parietal | 15 | No | L carrefour and dorso-lateral pre-frontal | 1.999 | -0.08 | 7 |
| *15* | F | 23 | Heterotopia | Visual impairement | 3 | L occipito temporal mesial | 10 | Thermocoagulation | L occipital plus posterior baso-temporal | 1.999 | Lat -0.029 Mesial -0.031 | 6 |
| *16* | F | 12 | Cryptogenic | EPC, focal motor seizures, generalized seizures | 3 | Left fronto mesio lateral | 8 | Thermocoagulation | L pericentral | 1.99 | -0.216 | 7 |
| *17* | F | 30 | FCD 2 | Complex focal seizure with loss of awareness, SGTC | 4 | L paracentral lobule | 9 | No | L pericentral | 1.999 | -0.25 | 8 |

**Table IV.S1. Demographic data and epilepsy characteristics of the patients.** Abbreviations: FCD: Focal Cortical Dysplasia; EPC: Epilepsia Partialis Continua; ASM: Antiseizure Medication; SOZ: Seizure Onset Zone; TLE: Temporal Lobe Epilepsy; SEEG: Stereoelectrocencephalography; VNS: Vagus Nerve Stimulation; L: Left; R: Right; MLa: Mesio-lateral. SGTC: Secondarily generalized tonic-clonic seizures.

| | Theta | Alpha | Beta | Gamma |
|---|---|---|---|---|
| | **t(dF)<br>pval<br>d(95% CI)** | **t(dF)<br>pval<br>d(95% CI)** | **t(dF)<br>pval<br>d(95% CI)** | **t(dF)<br>pval<br>d(95% CI)** |
| **Responder vs Non-Responders** | | | | |
| **C1** | *NS* | t(1902) = 10.092<br>p < 0.0001<br>d = 0.44 [0.35 – 0.53] | t(1965) = -9.5252<br>p < 0.0001<br>d = -0.38 [-0.47 – -0.29] | t(1901) = -8.8476<br>p < 0.0001<br>d = -0.38 [-0.48 – -0.29] |
| **C2** | t(1602) = -15.203<br>p < 0.0001<br>d = -0.7 [-0.79 – -0.61] | t(1139) = 27.383<br>p < 0.0001<br>d = 1.39 [1.29 – 1.49] | t(1147) = -2.5447<br>p = 0.011<br>d = -0.13 [-0.22 – -0.04] | *NS* |
| **C3** | t(1334) = -16.055<br>p < 0.0001<br>d = -0.83 [-0.94 – -0.73] | t(1514) = 6.56<br>p < 0.0001<br>d = 0.31 [0.21 – 0.41] | t(1224) = 22.201<br>p < 0.0001<br>d = 1.18 [1.07– 1.29] | t(1330) = 6.7123<br>p < 0.0001<br>d = 0.35 [0.25 – 0.45] |
| **Responders** | | | | |
| **C1 vs C2** | *NS* | t(773) = -21.438<br>p < 0.0001<br>d = -0.77 [-0.85 – -0.69] | *NS* | *NS* |
| **C1 vs C3** | t(618) = 11.563<br>p < 0.0001<br>d = 0.46 [0.38 – 0.55] | t(618) = -7.8357<br>p < 0.0001<br>d = -0.31 [-0.4 – -0.23] | t(618) = -11.186<br>p < 0.0001<br>d = -0.45 [-0.53 – -0.37] | *NS* |
| **C2 vs C3** | t(618) = 7.68<br>p < 0.0001<br>d = 0.31 [0.23 – 0.39] | *NS* | t(618) = -14.742<br>p < 0.0001<br>d = -0.59 [-0.68 – -0.51] | t(618) = -6.7187<br>p < 0.0001<br>d = -0.27 [-0.35 – -0.19] |
| **Non-responders** | | | | |
| **C1 vs C2** | t(1084) = -19.54<br>p < 0.0001<br>d = -0.59 [-0.66 – -0.53] | t(1084) = -5.4989<br>p < 0.0001<br>d = -0.17 [-0.23 – -0.11] | t(1084) = 22.434<br>p < 0.0001<br>d = 0.68 [0.61 – 0.75] | t(1084) = 12.256<br>p < 0.0001<br>d = 0.37 [0.31 – 0.43] |
| **C1 vs C3** | t(772) = -11.035<br>p < 0.0001<br>d = -0.4 [-0.47 – -0.32] | t(772) = -12.324<br>p < 0.0001<br>d = -0.44 [-0.52 – -0.37] | t(772) = 15.48<br>p < 0.0001<br>d = 0.56 [0.48 – 0.63] | t(772) = 10.996<br>p < 0.0001<br>d = 0.40 [0.32 – 0.47] |
| **C2 vs C3** | t(772) = -8.2263<br>p < 0.0001<br>d = -0.3 [-0.37 – -0.22] | t(772) = -3.2237<br>p = 0.0118<br>d = -0.12 [-0.19 – -0.05] | t(772) = 13.812<br>p < 0.0001<br>d = 0.5 [0.42 – 0.57] | t(772) = 19.408<br>p < 0.0001<br>d = 0.7 [0.62 – 0.78] |

**Table IV.S2. Statistical summary of power spectral density changes after each tDCS cycle for responder and non-responder patients in each frequency band (theta, alpha, beta and gamma).** Statistical analysis was conducted using Student t-tests with Bonferroni correction for multiple comparisons. Effect size measures are reported, including confidence intervals (CI) for Cohen's d estimates.

| | Broadband | Theta | Alpha | Beta | Gamma |
|---|---|---|---|---|---|
| | **t(dF)<br>pval<br>d(95% CI)** | **t(dF)<br>pval<br>d(95% CI)** | **t(dF)<br>pval<br>d(95% CI)** | **t(dF)<br>pval<br>d(95% CI)** | **t(dF)<br>pval<br>d(95% CI)** |
| **Responder vs Non-Responders** | | | | | |
| **C1** | *NS* | *NS* | t(1796) = 3.58<br>p = 0.003<br>d = 0.16 [0.07 – 0.25] | t(1505) = -3.53<br>p = 0.004<br>d = -0.17 [-0.26 – -0.08] | t(1586) = -7.8<br>p < 0.0001<br>d = -0.36 [-0.45 – -0.27] |
| **C2** | t(1445) = -16.51<br>p < 0.0001<br>d = -0.78 [-0.88 – -0.69] | t(1115) = -9.83<br>p < 0.0001<br>d = -0.5 [-0.59 – -0.41] | t(1082) = -10.33<br>p<0.0001<br>d = -0.53 [-0.63 – -0.44] | t(1580) = -22.28<br>p < 0.0001<br>d = -1.03 [-1.13 – -0.94] | t(1954) = -4.23<br>p < 0.0001<br>d = -0.18 [-0.27 – -0.09] |
| **C3** | t(1452) = -8.34<br>p < 0.0001<br>d = -0.42 [-0.52 – -0.32] | t(1504) = -16.329<br>p < 0.0001<br>d = -0.81 [-1.05 – -0.7] | *NS* | t(1504) = -4.07<br>p < 0.001<br>d = -0.2 [-0.3 – -0.1] | *NS* |
| **Responders** | | | | | |
| **C1 vs C2** | t(773) = 18.56<br>p < 0.0001<br>d = 0.67 [0.59 – 0.74] | t(773) = 6.2<br>p < 0.0001<br>d = 0.22 [0.15 – 0.29] | t(773) = 19.33<br>p < 0.0001<br>d = 0.69 [0.62 – 0.77] | t(773) = 25.02<br>p < 0.0001<br>d= 0.9 [0.82 – 0.98] | *NS* |
| **C1 vs C3** | t(618) =6.0064<br>p < 0.0001<br>d = 0.24 [0.16 – 0.32] | t(618) = 14.05<br>p < 0.0001<br>d = 0.56 [0.48 – 0.65] | t(618) = 5.025<br>p < 0.0001<br>d = 0.2 [0.12 – 0.28] | *NS* | *NS* |
| **C2 vs C3** | *NS* | t(618) = 3.3747<br>p < 0.0001<br>d = 0.14 [0.06 – 0.21] | t(618) = -9.559<br>p < 0.0001<br>d = -0.38 [-0.47 – -0.3] | t(618) = -10.55<br>p < 0.0001<br>d = -0.42 [-0.51 – -0.34] | t(618) = 3.34<br>p = 0.0078<br>d = 0.13 [0.06 – 0.21] |
| **Non-responders** | | | | | |
| **C1 vs C2** | *NS* | t(1084) = -12.19<br>p < 0.0001<br>d = -0.37 [-0.43 – -0.31] | *NS* | t(1084) = 4.48<br>p < 0.0001<br>d = 0.14 [0.08 – 0.2] | t(1084) = 4.48<br>p < 0.0001<br>d = 0.14 [0.08 – 0.2] |
| **C1 vs C3** | t(772) = 8.2<br>p < 0.0001<br>d = 0.29 [0.22 – 0.37] | *NS* | t(772) = 13.818<br>p < 0.0001<br>d = 0.5 [0.42 – 0.57] | t(772) = 8.32<br>p < 0.0001<br>d = 0.3 [0.23 – 0.37] | t(772) = 8.41<br>p < 0.0001<br>d = 0.3 [0.23 – 0.37] |
| **C2 vs C3** | t(772) = -6.88<br>p < 0.0001<br>d = -0.25 [-0.32 – -0.18] | t(772) = -10.97<br>p < 0.0001<br>d = -0.39 [-0.47 – -0.32] | t(772) = -5.73<br>p < 0.0001<br>d = -0.21 [-0.28 – -0.13] | t(772) = -6.84<br>p < 0.0001<br>d = -0.25 [-0.32 – -0.17] | t(772) = 4.78<br>p < 0.0001<br>d = 0.17 [0.1 – 0.24] |

**Table IV.S3. Statistical summary of functional connectivity changes after each tDCS cycle for responder and non-responder patients in each frequency band**. Statistical analysis was conducted using Student t-tests with Bonferroni correction for multiple comparisons. Effect size measures are reported, including confidence intervals (CI) for Cohen's d estimates.

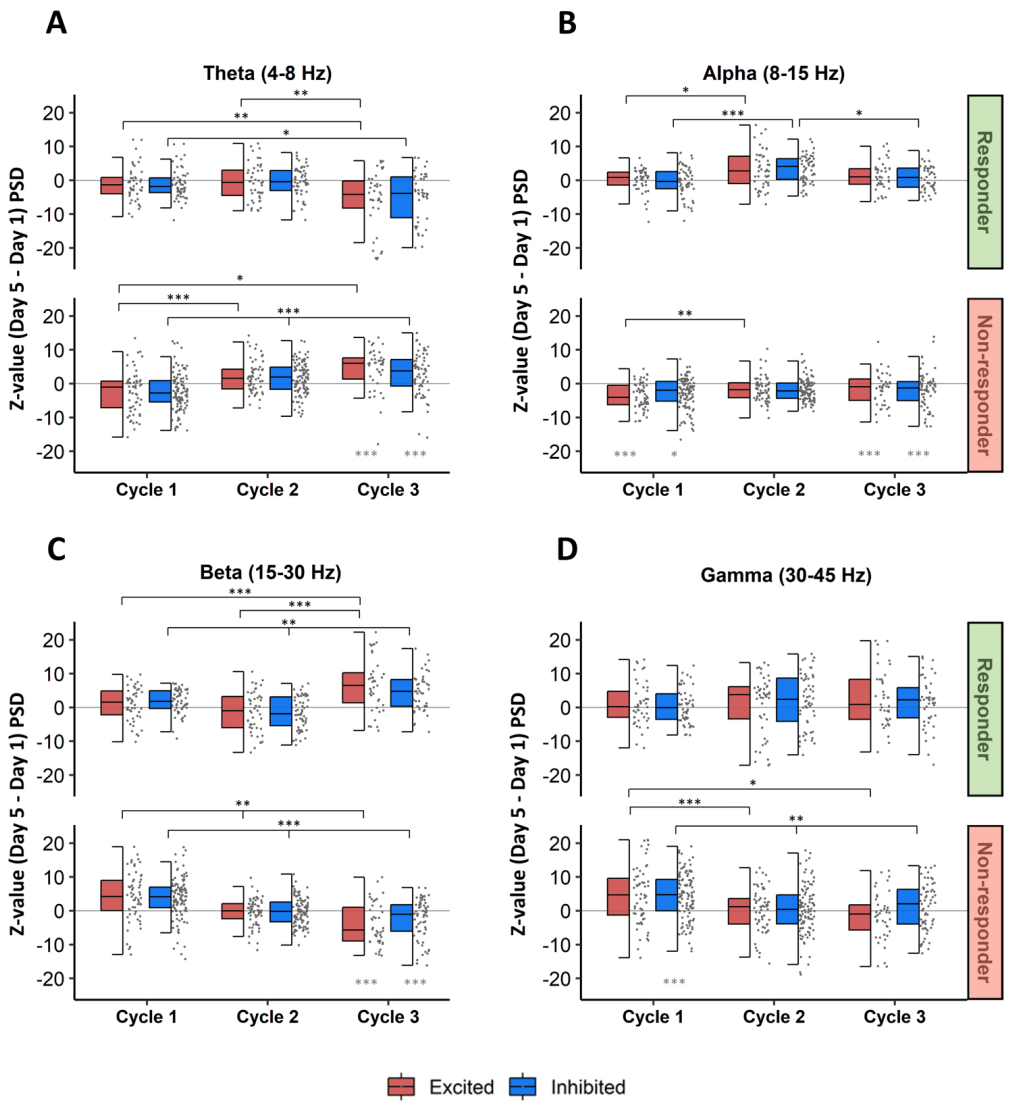


**Figure IV.S1. Power spectral changes in specific targeted brain regions under cathodal (inhibited) and anodal (excited) tDCS electrodes: Responder vs. Non-responder patients across tDCS cycles.** A. Half-boxplots illustrate PSD induced changes in the theta band after each tDCS cycle at the source level within inhibited brain regions (under cathodal tDCS electrodes in blue) and within excited brain regions (under anodal tDCS electrodes in red) for responder (in green) and non-responder patients (in orange). B. In alpha band. C. In beta band. D. In gamma band. Each data point represents the Z-value of one source region (zero: no spectral power change after tDCS cycle; negative/positive Z-value: decrease/increase of spectral power after tDCS cycle). Grey asterisks represent differences between responder and non-responder groups. P-values were corrected using Bonferroni correction and black bars with asterisks represent the differences between PSD changes occurring in cycles (* $p < 0.01$, ** $p < 0.001$, *** $p < 0.0001$).

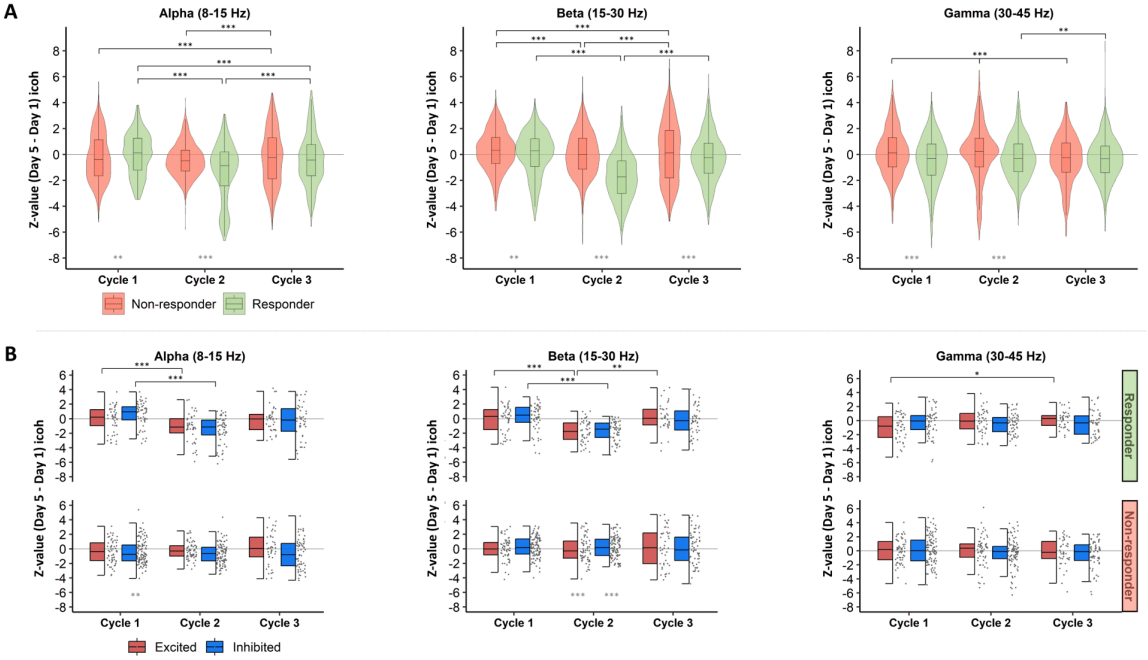


**Figure IV. S2. Functional connectivity (FC) changes in responder and non-responder patients in sub frequency bands**. In panel A violin plots represent FC changes after each tDCS cycle in all brain regions in responder (in green) and non-responder patients (in orange) in alpha, beta and gamma frequency bands. In panel B, half-boxplots illustrate FC changes in alpha, beta and gamma frequency bands after each tDCS cycle within inhibited brain regions (under cathodal tDCS electrodes in blue) and within excited brain regions (under anodal tDCS electrodes in red) for responder and non-responder patients. Each data point represents the Z-value of one source region (zero: no FC change after tDCS cycle; negative/positive Z-value: decrease/increase of FC after tDCS cycle). Grey asterisks represent differences between responder and non-responder groups. P-values were corrected using Bonferroni correction and black bars with asterisks represent the differences between FC changes occurring in cycles (* $p < 0.01$, ** $p < 0.001$, *** $p < 0.0001$).

# 5. Chapter V: Decoding tDCS Efficacy: Unraveling the Impact of Epileptogenic Zone Network Extent and Depth in Drug-resistant Epilepsy

**Daoud, M**., Medina Villalon, S., Garnier, E., Bratu, F., Damiani, G., Savlador, R., Wendling, F., Ruffini, G., Bénar, C.G., Pizzo, F.*, Bartolomei, F*. The Extent and Depth of the Epileptogenic Zone Network Impact the Response to Transcranial Direct Current Stimulation (tDCS). *(Submitted)*

* Francesca Pizzo and Fabrice Bartolomei are co-last authors.

# Rationale

Research conducted both within this thesis and in other clinical studies has consistently reported a notable reduction in seizure frequency following tDCS stimulation sessions. However, not all patients respond similarly. Approximately 40-50% of focal drug-resistant epilepsy (DRE) patients experience significant decrease (more than 50%) in seizure frequency after tDCS. At the same time, remaining patients may see minimal change or even a worsening in seizure frequency. Addressing this issue is crucial, necessitating efforts to understand and mitigate the variable response to tDCS treatment among patients. These concerns prompt the following question: Why does tDCS prove effective for certain patients while ineffective for others?

Typically, cathodal tDCS targets the epileptogenic zone, comprising a network of interconnected brain regions with high epileptogenicity (Bartolomei *et al.*, 2017; Lagarde *et al.*, 2018). Moreover, this epileptogenic zone network (EZN) is embedded within a broader network including the propagation zone. Computational research has investigated how the extent of the neural network stimulated by cathodal tDCS affects the duration of the stimulation (Denoyer *et al.*, 2020). However, this aspect has not yet been investigated in studies involving human patients with epilepsy. Understanding how the extent of the targeted network affects the efficacy and durability of induced changes could offer valuable insights for refining treatment approaches in epilepsy management.

One of the main challenges associated with tDCS is ensuring that low-intensity currents penetrate deep into brain tissues. Although modeling studies indicated that applying low-intensity electrical current may propagate the electric field to subcortical regions, its *in vivo* effects in humans, particularly in patients, remain uncertain.

Therefore, study 4 aims to retrospectively investigate how the anatomical characteristics of the epileptogenic networks, in terms of depth and extent, could affect the clinical outcome of tDCS. Acquiring knowledge of these anatomical characteristics serves a dual purpose. Firstly, it enhances our comprehension of how tDCS operates within patients, shedding light on the intricate mechanisms underlying its therapeutic effects. Secondly, it holds promise in clinical trial design, offering the potential to refine patient selection criteria.

# 5.1. Introduction

Epilepsy is a neurological condition with high prevalence, affecting over 50 million people worldwide. Despite the effectiveness of pharmacological treatments in controlling seizures for a portion of patients with epilepsy, one-third of patients still experience uncontrolled seizures (Devinsky *et al.*, 2018). For patients who have focal drug-resistant epilepsy (DRE), the surgical resection of the epileptogenic zone appears as a promising strategy to achieve lasting seizure control. However, this approach may not always be indicated and is associated with a non-negligible rate of failures (Baud *et al.*, 2018), leading to the search for alternative treatment solutions. Methods employing non-invasive brain stimulation to modulate brain excitability, such as transcranial direct current stimulation (tDCS), are promising therapeutic options (Simula *et al.*, 2022). In this neuromodulation technique, a weak current (1-2 mA) is delivered through the cortex using scalp electrodes (Ruffini *et al.*, 2013; San-juan *et al.*, 2015). It has been established that tDCS modulates neural activity through subthreshold membrane depolarization or hyperpolarization. This modulation occurs through the electric field generated by currents between the electrodes, which induce excitation or inhibition depending on field distribution relative to the cortical surface (Nitsche and Paulus, 2000; Nitsche *et al.*, 2003; Ruffini *et al.*, 2014). In epilepsy, precise targeting of the cathodal electrode on the epileptogenic zone is crucial for inducing cortical inhibition and alleviating the exacerbated neural activity that characterizes this pathological brain region.

Several controlled trials utilizing tDCS demonstrated favorable clinical outcomes in reducing seizure frequency in adult and pediatric patients with DRE (Fregni *et al.*, 2006; Auvichayapat *et al.*, 2013; Assenza *et al.*, 2017; San-Juan *et al.*, 2017). While tDCS is increasingly used for focal refractory epilepsy and has proven to be efficient in some patients, a substantial number of individuals with DRE do not respond positively to this treatment. Some studies have documented negative outcomes, without change in epileptic discharges nor improvement in seizure frequency after cathodal tDCS (Varga *et al.*, 2011; Lin *et al.*, 2018; Hao *et al.*, 2021). 50-60% of patients included in recent studies, including multichannel tDCS, are not responders (San-Juan *et al.*, 2017; Yang *et al.*, 2019; Kaye *et al.*, 2021; Daoud *et al.*, 2022). Moreover, some patients may even experience a transient worsening of seizures after repeated tDCS sessions (San-Juan *et al.*, 2017; Yang *et al.*, 2020; Daoud *et al.*, 2022). Considering the substantial risks associated with seizures, including increased mortality rates, injuries, and the development of related comorbidities, it is essential to address these challenges for non-responder patients. Efforts should focus on mitigating the induced worsening of seizure occurrence and investigating the factors underlying the variable response to tDCS treatment among patients.

Notably, the variability in clinical outcome may arise from the heterogeneity in stimulation parameters, including electrode placement, electrode size, current intensity, stimulation duration, and number of tDCS sessions (Lefaucheur *et al.*, 2017), but also from

patient heterogeneity (etiology, location, and the extent of the epileptogenic zone). The main challenge of tDCS lies in the ability of low-intensity current to penetrate tissues and reach deep brain regions. Indeed, several studies have highlighted the reduction of electric field magnitude due to the depth between scalp stimulation electrodes and the anatomical target (Datta *et al.*, 2009; Lafon *et al.*, 2017; Vöröslakos *et al.*, 2018; Huang and Parra, 2019). The use of multichannel tDCS, incorporating smaller electrode pairs and contrasting with conventional tDCS using two large rectangular electrodes, potentially enhances targeting precision while potentially reaching deeper brain regions (Ruffini *et al.*, 2014; Hannah, Iacovou and Rothwell, 2019). Incorporating multiple pairs of cathodal and anodal electrodes raises concerns about achieving precise targeting of the epileptogenic zone with inhibitory electric field while minimizing unintended excitation of non-target areas.

In current epilepsy research, it is widely recognized that focal DRE should be considered a large-scale brain network disorder, including both the epileptogenic zone network (EZN) and the propagation zone network (PZN) (Bartolomei *et al.*, 2017; Hashemi *et al.*, 2021). The specific brain regions involved in the epileptogenic zone EZN are identified through pre-surgical assessment using Stereoelectroencephalography (SEEG) recordings, and these regions differ among patients.

To our knowledge, no study has explored whether the EZN characteristics in terms of depth and extent impact the outcome of tDCS. Therefore, our study aimed to retrospectively examine how the characteristics of the epileptogenic network may influence the clinical response observed after multiple multichannel tDCS cycles in patients with focal DRE.

# 5.2. Materials and methods

### *Patients and data collection*

Between 2019 and 2023, 23 patients suffering from focal DRE participated in a clinical trial based on a personalized multichannel tDCS protocol. The protocol proceeded as follows: after a two-month baseline period, each patient received daily stimulation with an individualized multichannel tDCS treatment for five consecutive days, constituting a tDCS cycle, as described in (Daoud *et al.*, 2022). This cycle was repeated three times every two months for all patients. Each daily treatment consisted of two 20-minute stimulation sessions separated by a 20-minute break for a total of 40 minutes of stimulation. The average total injected current was approximately 2 mA. For each patient, personalized electrode positions were determined using an optimization pipeline based on individual factors and biophysical head models derived from patient T1-weighted MRIs (Miranda *et al.*, 2013). The Stimweaver algorithm (Ruffini *et al.*, 2014) produced the montage using a

target E-field map on the patient's neocortical surface, taking into account the regions to be inhibited based on SEEG recordings and identifying 'silent areas' without epileptogenic activity. Electrode positions were based on the 10-20 EEG system, typically with cathodes over the areas to inhibit and anodes over silent areas.

For this retrospective study, we collected and pre and post-surgical implantation data, including MRI and CT scans with SEEG electrodes. We used GARDEL (a Graphical User Interface for Automatic Registration and Depth Electrodes Localization), our in-house Matlab-based software (available at https://meg.univ-amu.fr/wiki/GARDEL:presentation). This tool performed the co-registration of MRI with CT scans, automating the segmentation and precise localization of intracranial electrode contacts using image processing techniques (Medina Villalon *et al.*, 2018). GARDEL accurately identifies the position of each SEEG contact within the grey and white matter, and assigns its anatomical location using a chosen atlas. In our study, we used the Virtual Epileptic Patient atlas (VEP Atlas) (Wang *et al.*, 2021). The VEP atlas subdivides brain regions from Destrieux atlas to better match with clinical practice (Destrieux *et al.*, 2010).

Clinical data were collected by extracting seizure counts from patients' seizure diaries. We categorized patients into two groups based on their response to the tDCS protocol. The responder group (R) consisted of patients who achieved a reduction of at least 50% in their seizure frequency at a 2-month follow-up after the third tDCS cycle compared to baseline while the non-responder group (NR) comprised patients who showed less improvement, no change, or an increase in seizure frequency.

### *Determining the extent of the epileptogenic zone and networks*

The SEEG analysis used a bipolar montage in the open-source AnyWave software (Colombet *et al.*, 2015). An expert clinician (F.P.) identified epileptogenic regions through a combination of visual and quantitative analysis of SEEG signals, in particular using the 'Epileptogenicity Index' (EI) method (Bartolomei, Chauvel and Wendling, 2008). This index evaluates the epileptogenicity of brain structures recorded with depth electrodes, considering spectral aspects (e.g., occurrence of fast oscillations replacing background activity) and temporal properties (e.g., delay of appearance with respect to seizure onset time) within intracerebral electroencephalography (EEG) signals (Bartolomei, Chauvel and Wendling, 2008)). Elevated EI values indicate structures involved early in the ictal process, generating rapid discharges at seizure onset. Normalized EI values ranging from 0 (indicating no epileptogenicity) to 1 (representing maximal epileptogenicity) were assigned to each brain region of interest, defined based on the VEP atlas (Wang *et al.*, 2021). Two clinical experts (F.P., F.Br.) classified these regions as part of the EZN or part of the PZN. Regions with an EI ≥ 0.4 were considered as EZN regions, whereas regions with $0.2 < EI < 0.4$ and sustained discharge during seizures were designated as PZN (Figure V.1). If two or more bipolar contacts sampled a region, the maximum EI value

obtained for that region was used. EZN and PZN regions defined for each patient are detailed in Supplementary data Table V.S1.

The extent of EZN and PZN was determined by counting the number of brain regions within these areas for each patient. A higher count of EZN regions (with a normalized EI of 0.4 or higher) indicates a more extensive EZN. The whole pathologic network is denoted as the epileptogenic and early propagation networks (EPZN). The EPZN extent was determined by summing the EZN and PZN regions (Figure V.1).

### *Assessment of EZ depth*

To assess the depth of epileptogenic regions for each patient, we concentrated on EZN regions (with EI ≥ 0.4) due to their close spatial proximity. Subsequently, the anatomical position of each VEP region on the patient's MRI was projected into a normalized MNI space for analysis. The MRI coordinates of the centroids were acquired using an in-house Matlab script (Mathworks, Naticks, MA). Using the centroids coordinates, we calculated the Euclidean distances in millimeters between the centroid of each region and the skull surface, retaining the minimal distance. Ultimately, to establish the depth of EZN, we averaged the distance from the surface across all centroids of regions within the EZN (Figure V.1).

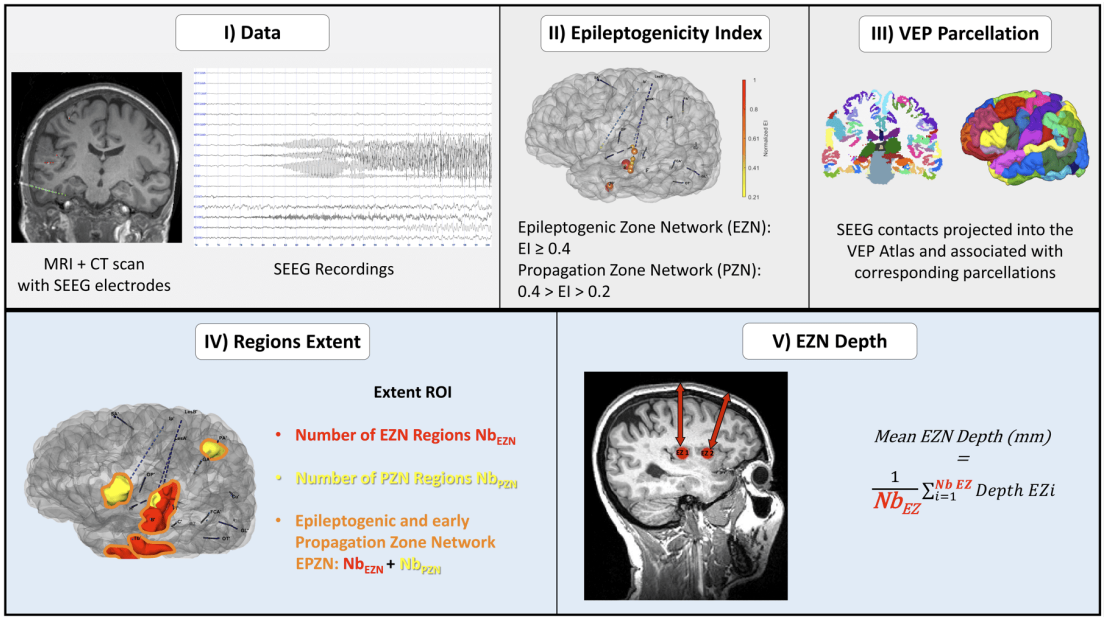


**Figure V.1. Overview of the data analysis pipeline.** For the presurgical assessment, each patient underwent SEEG well before the tDCS protocol. (I) The co-registration between the CT scan with SEEG electrodes and the patient's MRI was performed. (II) The epileptogenicity index (EI) was calculated from SEEG signals. SEEG contacts were labeled as belonging to the epileptogenic zone (EZN) if EI ≥ 0.4 and as part of the propagation zone (PZN) if 0.4 > EI > 0.2. (III) Then SEEG contacts were assigned to anatomical locations within the Virtual Epileptic Patient (VEP) atlas. (IV) The extent of EZN, PZN and Epileptogenic early propagation zone network EPZN (EZ+PZ) was determined by

counting the number of brain regions within these areas for each patient. (V) EZN depth was determined by averaging the distance from the scalp to all centroids of epileptogenic zones (EZ).

### *Statistical analysis*

We investigated differences in epileptogenic region characteristics between responder (R) and non-responder (NR) groups, focusing on their extent and depth. We evaluated the significance of differences in the number of EZN, PZN and EPZN (EZ + PZ) regions between R and NR groups. Additionally, we compared the mean depth of EZN for R and NR using a Wilcoxon test, with a correction for false discovery rate (FDR) applied to P-values. P-values below 0.05 after FDR correction were considered statistically significant.

The second analysis was based on the Spearman correlation coefficient computed between the change in seizure frequency (SF) after tDCS cycles and the number of EZN, PZN, and EPZN regions. Additionally, we examined the correlation between SF change and the mean depth of epileptogenic zone regions. Statistical analyses were performed using RStudio (version 4.2.2), considering a p-value of less than 0.05 (after correction) as statistically significant.

## 5.3. Results

Clinical information for the 23 included patients is provided in Table V.1. Due to a substantial increase (100%) in their SF after the second tDCS cycle compared to the baseline, two patients (patients 21 and 22) underwent only two cycles (two weeks) of tDCS instead of the initially planned three cycles. This event led to their exclusion from the last stimulation cycle based on safety protocol guidelines, resulting in their categorization as non-responder patients. Nonetheless, their SF levels returned to baseline after two months of follow-up.

| *Patients* | Gender | Age | SZs type | Etiology | Number SEEG electrodes | Number EZ regions | Number PZ regions | ASM | tDCS target | Response |
|---|---|---|---|---|---|---|---|---|---|---|
| *Pat 1* | M | 20 | Focal sensitivity, Visual hallucination | Cryptogenic | 9 | 9 | 2 | 3 | Left temporo-sylvian, mesio-occipital | NR |
| *Pat 2* | F | 23 | Visual impairment | Heterotopia | 10 | 2 | 6 | 3 | Left occipital plus posterior baso-temporal | R |

| | | | | | | | | | | |
|---|---|---|---|---|---|---|---|---|---|---|
| *Pat 3* | M | 23 | Focal non motor | FCD | 9 | 10 | 5 | 2 | Left temporo-insular | NR |
| *Pat 4* | M | 31 | Simple focal without loss of awareness, complex focal seizure with loss of awareness, SGTC | Cryptogenic | 16 | 2 | 2 | 2 | Left mesio-lateral, temporal | NR |
| *Pat 5* | M | 41 | Focal non motor, partial impaired awareness | Cryptogenic | 16 | 9 | 4 | 2 | Left temporo opercular | R |
| *Pat 6* | F | 50 | Complex focal, impaired awareness, SGTC | FCD 1 | 13 | 9 | 3 | 5 | Right pericentral/ parietal and posterior temporal (Carrefour) | NR |
| *Pat 7* | M | 42 | Complex focal, impaired awareness | Cavernoma | 9 | 3 | 2 | 4 | Left Mesio-lateral, Temporo-orbitofrontal | NR |
| *Pat 8* | M | 60 | Focal non motor, impaired awareness | Infectious | 15 | 8 | 5 | 3 | Left temporo basal | NR |
| *Pat 9* | M | 32 | EPC, focal motor seizures | Gliosis | 4 | 6 | 3 | 4 | Right pericental extended | NR |
| *Pat 10* | M | 29 | Focal motor, impaired awareness | Pre-natal stroke | 12 | 9 | 1 | 4 | Left fronto parietal sup | R |
| *Pat 11* | F | 43 | Focal, impaired awareness | Schizencephalia, heterotopia, polymicrogyria | 19 | 6 | 3 | 3 | Left mesio-lateral, temporo-parietal | NR |
| *Pat 12* | M | 14 | Focal motor | Cryptogenic | 10 | 4 | 1 | 4 | Right paracentral | R |
| *Pat 13* | F | 16 | Complex focal with loss of awareness, SGTC | FCD 1 | 13 | 6 | 3 | 3 | Bilat pericentral (R>L) | R |
| *Pat 14* | F | 12 | Focal motor, EPC | Cryptogenic | 8 | 2 | 6 | 2 | Left paracentral | R |
| *Pat 15* | M | 16 | Simple focal, without loss of awareness, paresthesia | Infectious/trauma, MRI left hemispheric atrophy | 15 | 5 | 2 | 4 | Left carrefour and dorso-lateral pre-frontal | R |
| *Pat 16* | F | 23 | Focal sensitive motor without loss of awareness | Cryptogenic | 13 | 3 | 5 | 2 | Right pericentral | R |
| *Pat 17* | F | 29 | Focal non motor | FCD | 13 | 9 | 5 | 3 | Left temporal | NR |
| *Pat 18* | F | 12 | EPC, focal motor, generalized seizures | Cryptogenic | 8 | 5 | 1 | 3 | Left pericentral | R |
| *Pat 19* | F | 30 | Complex focal with loss of awareness, SGTC | FCD 2 | 9 | 8 | 1 | 4 | Left pericentral | NR |
| *Pat 20* | M | 48 | Complex focal, impaired awareness | Cryptogenic | 13 | 5 | 6 | 4 | Left mesio-lateral, temporal | NR |

| | | | | | | | | | | |
|---|---|---|---|---|---|---|---|---|---|---|
| *Pat 21* | F | 15 | Focal motor without loss of awareness, Paresthesia | Cryptogenic | 15 | 9 | 5 | 2 | Right perisylvian and post central | NR |
| *Pat 22* | M | 29 | Simple focal without loss of awareness, complex focal with loss of awareness, SGTC | Cryptogenic | 15 | 16 | 2 | 3 | Left mesio-lateral, Temporal Plus dorso-lateral frontal | NR |
| *Pat 23* | F | 31 | Focal motor | FCD 2 | 9 | 9 | 1 | 1 | Left pericentral | R |

**Table V.1. Demographic data and epilepsy characteristics of the patients.**

The clinical results (Figure V.2) illustrate the SF change at two months following the last tDCS cycle compared to each patient's baseline. Specifically, 10 patients were classified as responder patients (R), demonstrating a SF decrease exceeding 50% (mean change -67% ± 19%). The remaining 13 patients, who exhibited either an SF decrease of less than 50% or an increase compared to baseline, were classified as non-responder patients (NR) (mean change 17% ± 47%).

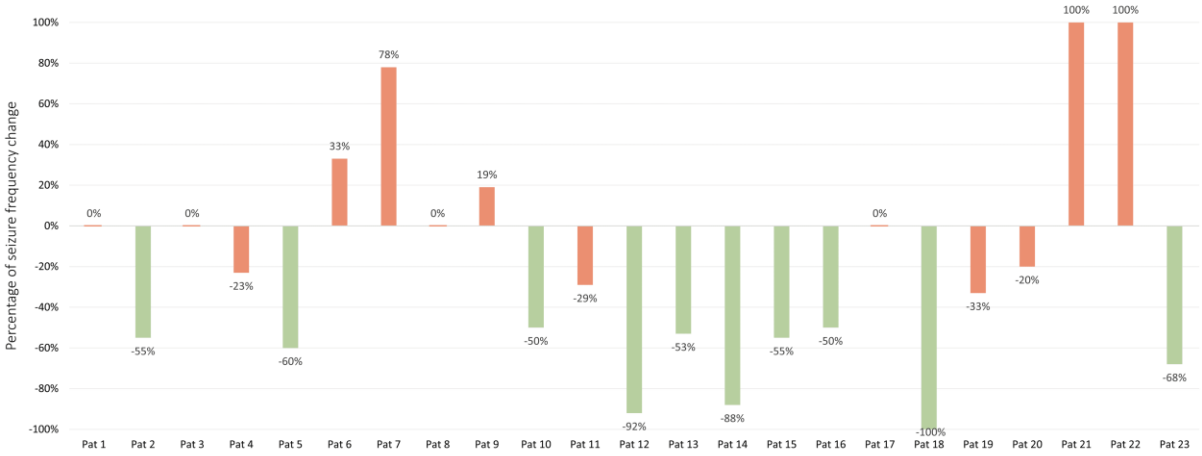


**Figure V.2. Percentage change in seizure frequency compared to baseline two months after multichannel tDCS cycles (n=23 patients).** The responder patients are represented in green and the non-responder patients are in red.

### *Effects of epileptogenic regions' extent*

We investigated how the extent of epileptogenic areas, as determined by the epileptogenicity index, might affect the clinical response to tDCS. We estimated this extent by counting the brain regions involved in epileptogenic regions (EZN, PZN and EPZN) and targeted by inhibitory stimulation.

Comparing R and NR groups, no significant difference was observed in the number of EZN regions or in the number of PZN regions (Figure V.3.A and V.3.B). However, when considering the total extent of the EPZN, calculated by combining EZN and PZN values, we observed a trend indicating a greater extent of the whole epileptogenic and early

propagation network in NR patients compared to R (*pval* = 0.053 ; Wilcoxon test) (Figure V.3.C).

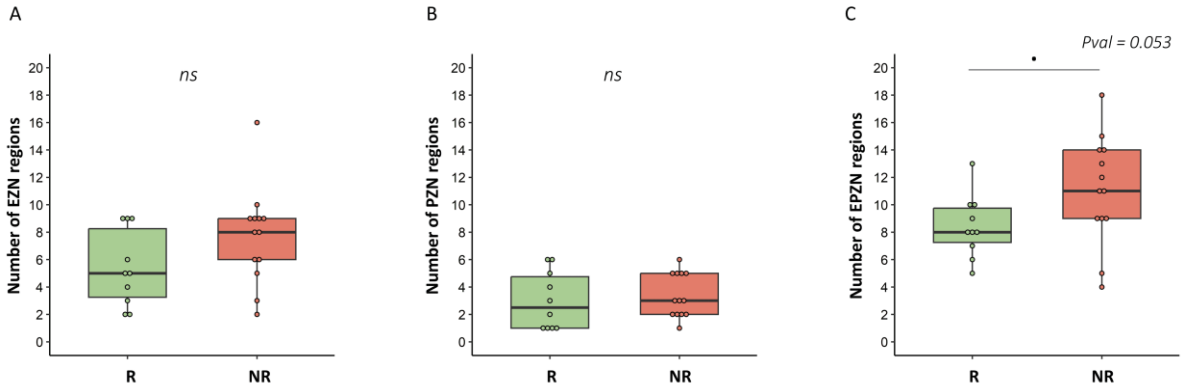


**Figure V.3. Comparing the extent of epileptogenic regions in responder (R) and non-responder (NR) patients.** A. Boxplots illustrate EZN extent determined by the number of EZN regions for R (in green) and NR (in red) groups (respectively n=10 and n=13). B. For PZN regions. C. For epileptogenic and early propagation network regions (EPZN) (EZN + PZN). Each data point corresponds to the number of the specific brain regions considered for each patient (EZN, PZN and both). The black bar and black point represent the difference (but not significant *pval* = 0.053) between R and NR groups using the Wilcoxon test. '*ns*' refers to a non-significant difference between the groups.

In the light of this trend, we further investigated the correlation between the SF change and the extent of epileptogenic regions. A significant positive correlation was observed between the SF changes and the extent of EZN regions (Spearman correlation R = 0.43 , *pval* = 0.04) (Figure V.4.A). This suggested that when the EZN was smaller, the tDCS was more effective, resulting in a substantial reduction in SF. Conversely, with a larger EZN, patients tended to have no change or even an increase in the number of seizures compared to the baseline. No correlation was found between the change in SF and the extent of the PZN area (Figure V.4.B). However, when the entire EPZN (comprising EZN and PZN) was taken into account, a significant positive correlation was observed between SF changes and the extent of the EPZN (Spearman correlation R = 0.52 , *pval* = 0.01) (Figure V.4.C).

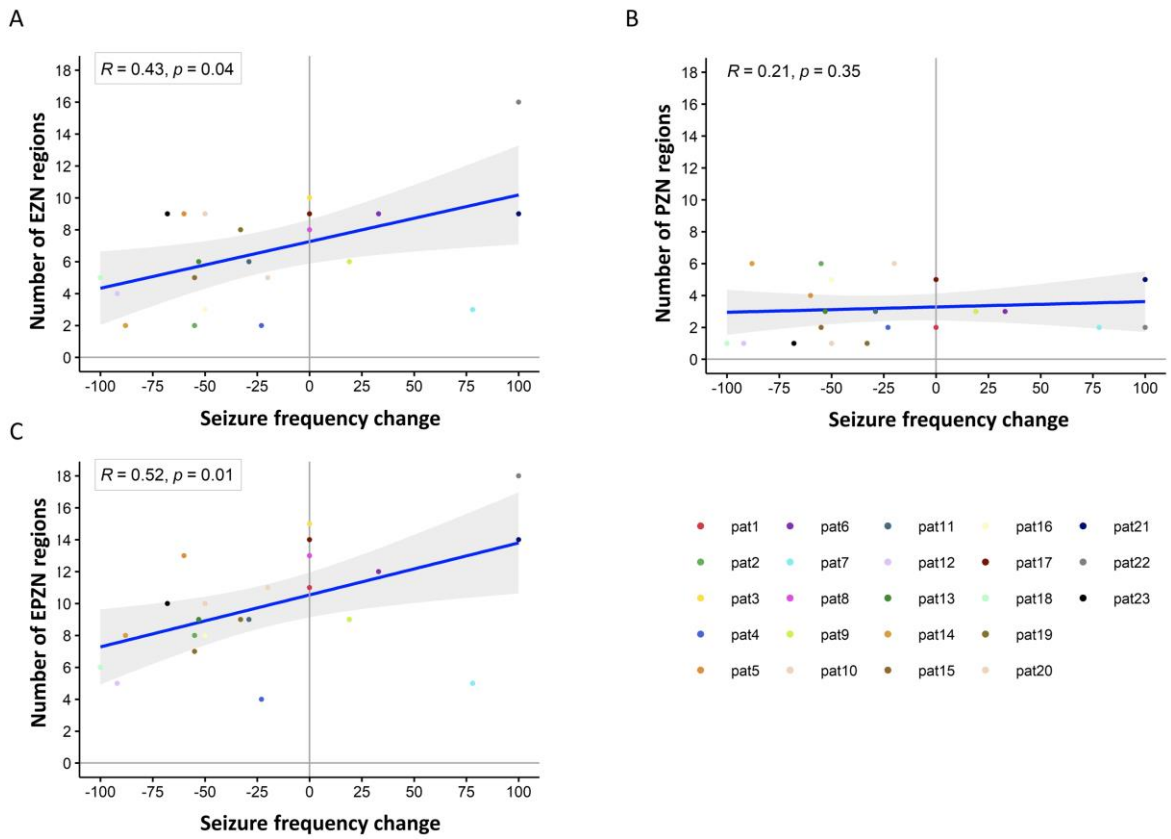


**Figure V.4. Correlation between number of epileptogenic regions and changes in seizure frequency in patients with epilepsy after repeated sessions of tDCS.** A. The scatter plot represents the regression of the number of EZN regions on the SF change after multiple cycles of multichannel tDCS in 23 patients with epilepsy. B. Regression of the number of PZN regions on SF changes. C. Correlation between the number of EPZN regions and SF changes.

### *Effects of the depth of the EZN on tDCS response*

Subsequently, we examined whether the mean distance to the scalp of the EZN could influence the clinical efficacy of multichannel tDCS. Following the calculation of EZN depth, we compared this measurement between the R and NR groups.

We found that the EZN was significantly deeper in the NR group than in the R group (*pval* = 0.025 ; Wilcoxon test) (Figure V.5.A). This finding strongly suggests a potential association between the depth of the epileptogenic zone (targeted by our tDCS protocol) and the treatment response. The correlation analysis between the depth of EZN and the SF changes following tDCS cycles did not demonstrate statistical significance (Spearman correlation R = 0.23 , *pval* = 0.28) (Figure V.5.B).

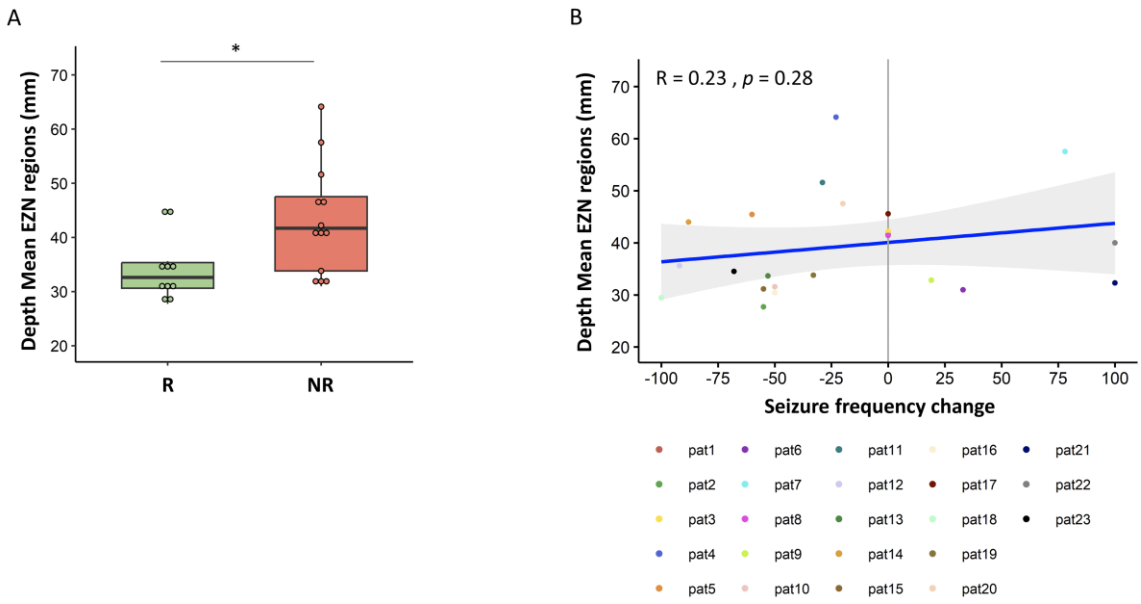


**Figure V.5. Influence of EZ depth on clinical response to multichannel tDCS.** A. Boxplots illustrate EZN depth determined by averaging the depth of each EZ regions (regions with normalized EI ≥ 0.4) for the responder (R) (in green) and non-responder (NR) (in red) groups (n=10 and n=13, respectively). Each data point corresponds to the mean depth of EZ regions for each patient. The black bar with an asterisk marks a significant difference (pval = 0.025) between R and NR groups using the Wilcoxon test. B. The scatter plot represents the Spearman correlation coefficient (R = 0.23) between the mean depth of EZ regions and the SF change after multiple cycles of multichannel tDCS.

# 5.4. Discussion

The main objective of this study was to explore how the extent of the epileptogenic network and the depth of the epileptogenic zone impact the clinical response to a multichannel tDCS protocol. The primary finding was a positive correlation between the extent of the epileptogenic network and the changes in seizure frequency after three tDCS cycles. Additionally, R and NR patients exhibited a significant difference in the mean depth of the epileptogenic zone.

### *The clinical efficacy of tDCS is influenced by the extent of the epileptogenic network*

This retrospective analysis included 23 patients diagnosed with DRE. They underwent three weeks of daily stimulation over a six-month period using a personalized multichannel protocol targeting their epileptogenic zone (Daoud *et al.*, 2022). Among these patients, 10 were classified as 'responders' due to a reduction in SF of over 50% two months after the last stimulation compared to baseline. Overall, nearly half of the patients

experienced substantial clinical improvement (mean change -67% ± 19%). This ratio aligns with findings from other studies using tDCS in epilepsy (Yang *et al.*, 2019; Kaye *et al.*, 2021; Daoud *et al.*, 2022; San-Juan *et al.*, 2022). In our study, we observed a difference in the extent of the epileptogenic network (grouping the EZN and the PZN) between R and NR groups, which approached statistical significance. Specifically, the EPZN appeared more extended in NR compared to R. This finding was reinforced by the significant positive correlation we found between the extent of the EZN and EPZN and the changes in seizure frequency. In particular, when the epileptogenic regions were more focal, the tDCS was more efficient. Conversely, when the targeted regions for tDCS were extensive, this technique failed to reduce seizure occurrences. At the extreme, the broadest epileptogenic zones may lead to an increase in seizure frequency. The extension of epileptogenic networks is a proven limitation in surgical therapies, whether at the level of EZN (Aubert *et al.*, 2009) or the PZN (Lagarde *et al.*, 2018). Large-scale simulation studies show that it is more difficult to stop seizures when the network is more densely connected (Olmi *et al.*, 2019). It is possible that these network parameters are also limitations on the effectiveness of tDCS. These findings agree with a recent study (Yu *et al.*, 2023) that found that when the epileptogenic zone and whole network were widely extended across both hemispheres, cathodal tDCS demonstrated reduced therapeutic benefits. Finally, large epileptic networks may expose certain nodes to the risk of accidental excitation (anodes), thus exacerbating seizures. Therefore, it may be advisable to incorporate specific characteristics of the targeted anatomical zones to refine patient selection and potentially mitigate tDCS-related exacerbations observed in some NR patients. For instance, one could consider including the extent of the epileptogenic network in the criteria for patient inclusion.

### *The effectiveness of tDCS in epilepsy is constrained by the depth of the EZN*

Previous studies have highlighted the potential difficulty in reaching deep brain regions with low-intensity stimulation due to the distance between the electrodes and the targeted area (Datta *et al.*, 2009; Lafon *et al.*, 2017; Vöröslakos *et al.*, 2018; Huang and Parra, 2019). Our findings support this view, indicating a significant difference in the depth of the EZN in the brain in NR patients compared to R. These results diverge from computational studies developing epilepsy models to explore the spread of electric fields in the brain through various parameters of low-intensity stimulation application (Peterchev *et al.*, 2012). Indeed, modeling studies have suggested that adjusting the number and positioning of scalp electrodes during tDCS could improve both the intensity and the focus of stimulation, even for deep brain targets (Sadleir *et al.*, 2012; Ruffini *et al.*, 2014; Wagner, Burger and Wolters, 2016; Huang and Parra, 2019). Human studies have corroborated these results using transcranial electrical stimulation during intracranial recordings (Huang *et al.*, 2017; Louviot *et al.*, 2022). These latter studies proposed that transcranial electrical stimulation could induce an electric field capable of reaching deep structures like the hippocampus. Nevertheless, it is crucial to emphasize that the electric

field detected in deep brain regions was relatively weak. Louviot et al., reported mean EF magnitudes of 0.21, 0.17 and 0.07 $V.m^{-1}$ in the amygdala, hippocampus, and cingulate gyrus, respectively, in a study combining SEEG recordings with transcranial electrical stimulation (Louviot *et al.*, 2022). Recently, our group also found a remarkably low magnitude of effects on deep brain structures in epileptic patients who underwent simultaneous SEEG recording (Simula, Damiani, *et al.*, 2023). To date, none of these studies have been clinically validated (Huang *et al.*, 2017; Louviot *et al.*, 2022). These rare investigations involved a relatively small number of patients, reflecting the challenges inherent in conducting protocols with both transcranial stimulation and intracranial recordings. Notably, the potential clinical benefits of tDCS, such as reduced seizure frequency, are believed to arise from both immediate and from plasticity effects (for a more comprehensive review, see (Liu *et al.*, 2018; Simula *et al.*, 2022)). These complex mechanisms involve functional changes within brain networks, which could be crucial for mitigating epileptic activity (Lin *et al.*, 2018; Tecchio *et al.*, 2018; Hao *et al.*, 2021; Daoud *et al.*, 2022). However, our results suggest that targeting deep brain regions with tDCS can be challenging. This difficulty arises from the reduced strength of the electrical field as the distance from the scalp increases, and from the inability to control the direction of the electric field when targeting deep brain areas. New stimulation paradigms could be of interest in this context. A novel stimulation technique, known as temporal interference (TI) has proven ability to reach and stimulate deep brain regions by generating interferences at points located distant from the surface electrodes (Grossman *et al.*, 2017). A recent investigation conducted on cadavers revealed superior penetration of TI fields into the human hippocampus compared to transcranial current stimulation without affecting the surrounding tissues (Acerbo *et al.*, 2022).

To conclude, the retrospective nature of this study and the relatively small number of subjects included are limitations of our study. However, we are able to show that both the extension of epileptogenic networks and their depth relative to the surface are factors limiting the effectiveness of tDCS. This underscores the need to explore alternative methods of stimulation and/or optimize the current method.

## 5.5. Supplementary data

| PATIENTS | EPILEPTOGENIC HEMISPHERE | EZ REGIONS | PZ REGIONS |
|---|---|---|---|
| ***PAT 1*** | Right hemisphere | T1 planum temporale, Parietal operculum, STS anterior, Thalamus, Insula gyri longi, Central sulcus upper limb, Caudate nucleus, F3 pars opercularis, Central operculum | Gyrus of Heschl, Putamen |
| ***PAT 2*** | Left hemisphere | Cuneus, O2 | Hippocampus-posterior, O1, STS posterior, Lingual sulcus, Collateral sulcus, Precuneus |

| | | | |
|---|---|---|---|
| ***PAT 3*** | **Bilateral** | Left T1 lateral posterior, Left insula gyri longi, Left STS anterior, Left hippocampus posterior, Left STS posterior, Left T2 posterior, Left Collateral sulcus, Left temporal pole, Left T3 posterior, Left lingual gyrus | Right parahippocampal cortex, Right rhinal cortex, Left parahippocampal cortex, Left O2, Left calcarine sulcus |
| ***PAT 4*** | **Left hemisphere** | Parahippocampal cortex, Collateral sulcus | Insula gyri brevi, F3 pars opercularis |
| ***PAT 5*** | **Left hemisphere** | Hippocampus anterior, Rhinal cortex, Hippocampus posterior, Occipito-temporal sulcus, T1 planum temporale, Gyrus of Heschl, T1 lateral posterior, STS posterior, Calcarine sulcus | T3 posterior, T2 posterior, Insula gyri longi, T1 lateral anterior |
| ***PAT 6*** | **Right hemisphere** | STS posterior, Intraparietal sulcus, Supramarginal posterior, Angular gyrus, T3 posterior, T1 planum temporale, Gyrus of Heschl, STS anterior, T1 lateral posterior | Postcentral sulcus, Intraparietal sulcus, Occipito-temporal sulcus |
| ***PAT 7*** | **Left hemisphere** | Amygdala, Hippocampus anterior, Fusiform-gyrus | F2 rostral, Orbito-frontal cortex |
| ***PAT 8*** | **Bilateral** | Left temporal pole, Left T1 planum polare, Left T2 anterior, Left parahippocampal cortex, Left Insula gyri brevi, Left T2 posterior, Left STS posterior, Left Orbito-frontal cortex | Left ITS anterior, Left T3 posterior, Left F2 caudal Right orbito-frontal cortex, Left STS anterior |
| ***PAT 9*** | **Right hemisphere** | Intraparietal sulcus, Superior parietal lobule P1, Middle cingulate cortex posterior, Central sulcus upper limb, Precentral gyrus upper limb, Supramarginal posterior | Middle frontal sulcus, Postcentral sulcus, Anterior-cingulate cortex |
| ***PAT 10*** | **Bilateral** | Right-SMA, Left-SMA, Left SFS caudal, Left paracentral lobule, Left central sulcus upper limb, Left superior parietal lobule P1, Left O1, Left O2, Right STS posterior | Left intraparietal sulcus |
| ***PAT 11*** | **Left hemisphere** | Thalamus, Ventral DC, Rhinal cortex, Temporal pole, Parietal operculum, T3 anterior | Insula gyri brevi, STS anterior, Intraparietal sulcus |
| ***PAT 12*** | **Right hemisphere** | Precentral sulcus inferior part, Middle cingulate cortex posterior, Paracentral lobule, Postcentral gyrus | F2 caudal |
| ***PAT 13*** | **Bilateral** | Right SFS caudal, Right F2 caudal, Right SMA, Right precentral sulcus superior, Right paracentral lobule, Right insula gyri brevi | Right postcentral gyrus, Right anterior cingulate cortex, Left Middle cingulate cortex anterior |
| ***PAT 14*** | **Left hemisphere** | SMA, Marginal branch of the cingulate sulcus | Middle cingulate cortex posterior, Central sulcus upper limb, Precentral gyrus upper limb, Precuneus, Paracentral lobule, Posterior cingulate cortex dorsal |
| ***PAT 15*** | **Left hemisphere** | Postcentral sulcus, Supramarginal posterior, Central sulcus head face, Precentral gyrus upper limb, Precentral sulcus inferior | F2 caudal, Central sulcus upper limb |
| ***PAT 16*** | **Right hemisphere** | Paracentral lobule, Central-sulcus upper limb, Precentral gyrus upper limb | Insula gyri brevi, F3 pars opercularis, Parietal operculum, Parieto-occipital sulcus, Precentral sulcus superior |
| ***PAT 17*** | **Left hemisphere** | Temporal pole, Hippocampus anterior, Hippocampus posterior, Occipito-temporal sulcus, Middle frontal sulcus, Collateral sulcus, Fusiform gyrus, T3 posterior, T1 lateral anterior | Amygdala, T2 anterior, T3 anterior, STS anterior, Orbito-frontal cortex |
| ***PAT 18*** | **Left hemisphere** | Precentral gyrus upper limb, Precentral gyrus head face, Central | Middle cingulate cortex posterior |

| | | | |
|---|---|---|---|
| | | sulcus upper limb, Postcentral gyrus, Precentral sulcus superior | |
| ***PAT 19*** | **Left hemisphere** | Paracentral lobule, F1 lateral premotor, Precentral gyrus upper limb, Central sulcus upper limb, Postcentral gyrus, Marginal branch of the cingulate sulcus, Postcentral sulcus, SMA | Central sulcus head face |
| ***PAT 20*** | **Bilateral** | Left temporal pole, Left T1 planum polare, Left ITS anterior, Left amygdala, Left insula gyri longi | Left T1 lateral anterior, Left rhinal cortex, Left T3 anterior, Left hippocampus posterior, Left insula gyri brevi, Right rhinal cortex |
| ***PAT 21*** | **Right hemisphere** | Precentral sulcus superior, Central sulcus upper limb, Central sulcus head face, Postcentral gyrus, T1 planum temporal, Supramarginal anterior, Intraparietal sulcus, Marginal branch of the cingulate sulcus, Superior parietal lobule P1 | Precentral gyrus upper limb, Middle cingulate cortex posterior, Parietal operculum, Paracentral-lobule, Postcentral-sulcus |
| ***PAT 22*** | **Left hemisphere** | STS anterior, T2-anterior, Amygdala, Hippocampus anterior, ITS anterior, ITS-posterior, T2-posterior, Gyrus of Heschl, T1 lateral posterior, Insula gyri longi, Insula gyri brevi, Inferior frontal sulcus, Left F3, pars-triangularis, T3-anterior, Rhinal-cortex, Temporal-pole | Orbito-frontal cortex, T1 planum polare |
| ***PAT 23*** | **Left hemisphere** | Middle cingulate cortex posterior, SFS caudal, Precentral sulcus superior, Central sulcus upper limb, Precentral gyrus upper limb, Postcentral gyrus, Insula gyri brevi, Precentral gyrus head face, Paracentral lobule | Postcentral sulcus |

**Table V.S1. Comprehensive listing of EZ and PZ regions for each patient.**

# 6. Chapter VI: Long-term tDCS in Epilepsia Partialis Continua Cases

This chapter was published in:

**Daoud, M**.,* Durelle, C.,* Fierain, A., Wendling, F., Ruffini, G., Benquet, P., Bartolomei, F. (2024). Long-term Effect of Multichannel tDCS Protocol in Patients with Central Cortex Epilepsies Associated with Epilepsia Partialis Continua. *Brain Topography*, 10.1007/s10548-024-01045-3

* These authors share first authorship

# Rationale

Studies 2 and 3 have shown a substantial decrease in seizure frequency for some patients with drug-resistant epilepsy. However, since patients may experience different seizure types, which can vary from one individual to another, our studies did not investigate the effects of multichannel tDCS on different seizure types within individual patients. One type of epilepsy with distinct seizures types is Epilepsia partialis continua (EPC), a rare and challenging form of epilepsy (Engel, 2001). It is characterized by persistent and continuous myoclonus affecting a specific part of the body (Obeso, Rothwell and Marsden, 1985; Guerrini, 2009). EPC is also associated with more severe seizures such as the secondarily generalized tonic-clonic seizures (Cockerell *et al.*, 1996). In most cases, this condition is resistant to pharmacotherapy. Moreover, resection surgery is not feasible regarding the location of the epileptogenic zone around cortical motor areas.

In study 5, we aim to assess the clinical effects of prolonged tDCS protocols on different seizure types associated with EPC. Specifically, we will focus on the clinical outcomes of a personalized multichannel tDCS, using the same stimulation parameters as in studies 2 and 3. This protocol is administered over several months to three patients with drug-resistant EPC with various etiologies (Rasmussen's Encephalitis, focal cortical dysplasia, and cryptogenic).

# 6.1. Introduction

Epilepsia partialis continua (EPC) is a form of epilepsy that is rare and challenging to manage (Engel, 2001). It is characterized by persistent and continuous myoclonus that affect a specific part of the body (Obeso, Rothwell and Marsden, 1985; Guerrini, 2009). Typically, EPC is accompanied by more severe seizures, such as focal motor seizures or focal to bilateral tonic-clonic seizure (Cockerell *et al.*, 1996). In the ILAE task force report on status epilepticus (Trinka *et al.*, 2015), EPC appears as a subclass of focal motor status. This condition is often associated with significant functional impairment (in particular motor deficits) and has a major impact on the quality of life of the affected individuals. The main causes of EPC include structural brain abnormalities (such as cortical dysplasia or tumors), autoimmune processes (Rasmussen's encephalitis), infectious or inflammatory conditions, and, in rare cases, genetic factors (Cockerell *et al.*, 1996; Mameniškienė and Wolf, 2017). Accurate diagnosis of EPC is crucial for appropriate management. The cortical origin of EPC was described by an analysis of intracerebral recordings (Bancaud *et al.*, 1970; Wieser *et al.*, 1978; Chauvel *et al.*, 1986) or scalp electroencephalography (EEG) studies, particularly using "back averaging" (Pandian *et al.*, 2002).

The treatment of EPC is often challenging. In most cases, the condition is resistant to drug therapy. Furthermore, resective surgery is generally not an option, given the location of the epileptogenic zone (EZ) in cortical motor areas. In this context, alternative methods of neuromodulation may be considered. Invasive methods using direct stimulation have been reported in a few cases of EPC with positive results (Valentin *et al.*, 2015; Yang *et al.*, 2021). Non-invasive brain stimulation techniques are also potentially applicable, with the advantage of being safe, well-tolerated, and reversible. This includes repetitive transcranial magnetic stimulation (rTMS) and vagus nerve stimulation (VNS), which have been proposed in a few cases of EPC (Rotenberg *et al.*, 2009; De Benedictis *et al.*, 2013). Another method is transcranial direct current stimulation (tDCS), which allows the modulation of brain excitability by the application of cur- rents of low intensity (< 2 mA) on the brain via scalp electrodes (Nitsche and Paulus, 2000, 2001; Antal, Nitsche and Paulus, 2001). Most *in vitro* studies employing direct current fields have demonstrated their ability in controlling epileptogenic bio- markers and seizure features (Gluckman *et al.*, 1996; Ghai, Bikson and Durand, 2000; Bikson *et al.*, 2001). These results have been supported by human studies, illustrating the spread and the impact of electric field on epileptiform activity (Opitz *et al.*, 2016; Huang *et al.*, 2017; Louviot *et al.*, 2022). Furthermore, several clinical studies on tDCS have reported promising results for several epileptic syndromes by reducing seizure frequency (SF) (Auvichayapat *et al.*, 2013; San-juan *et al.*, 2015; Assenza *et al.*, 2017; San-Juan *et al.*, 2017; Koessler *et al.*, 2023), for a more exhaustive review, see (Lefaucheur, 2016; Lefaucheur *et al.*, 2017; Fregni *et al.*, 2021; Simula *et al.*, 2022). Among the patient population in these studies, some cases with Rasmussen's Encephalitis have been reported to benefit from tDCS (San-Juan *et al.*, 2011; Tekturk, Erdogan, Kurt, Kocagoncu, *et al.*, 2016).

Only very few studies have explored the impact of tDCS on EPC and their findings are incomplete and contradictory. Indeed, in a single-case report, tDCS demonstrated no efficacy in a patient with POLG-related mitochondrial disease experiencing severe multifocal epilepsia partialis continua (Marquardt *et al.*, 2019). However, the research landscape lacks comprehensive studies on prolonged tDCS protocols addressing diverse seizure types associated with EPC. Our study contributes by presenting the clinical outcomes of personalized tDCS protocols administered over several months to three patients with drug-resistant EPC.

# 6.2. Materials and methods

### *Patients*

From 2019 to 2023, three patients with drug-resistant epilepsy associated with EPC were admitted and followed a tDCS protocol at the Epileptology department of Timone's Hospital, Marseille, France. Throughout the study, seizure data was collected from two months before the first tDCS cycle and regularly every month. Additionally, a clinical evaluation was conducted every two months at each visit. The patients' general characteristics are summarized in Table VI.1. This study was approved by the local ethics committee, and written informed consent was obtained from each patient or their legal representative before they were included in the study.

| Patient | Gender | Age | Etiology | Seizure type | Number of ASM | SOZ defined by SEEG | Number of SEEG electrodes | Previous failed surgery | tDCS target | Injected Current (mA) | Desired E field in Target (V/ m) | Achieved average E field in target (V/m) | Number of tDCS electrodes |
|---|---|---|---|---|---|---|---|---|---|---|---|---|---|
| 1 | M | 26 | Rasmussen's encephalitis | EPC, Hemibody seizures | 7 | Left mesio temporal, insular cortex | 13 | No surgery | Left centro-insular cortex | 2 | 0.25 | -0.04 | 8 |
| 2 | F | 13 | FCD | EPC, focal motor seizures | 2 | Left paracentral lobule, Post SMA | 8 | Premotor cortectomy, thermocoagulation | Left paracentral | 2 | 0.5 | -0.07 | 8 |
| 3 | F | 13 | Unknown | EPC | 4 | Left fronto mesio lateral | 8 | Thermocoagulation central gyrus | Left mesio latero central | 2 | 0.22 | -0.03 | 7 |

**Table VI.1. Demographic data and epilepsy characteristics of the three cases of EPC.** E-field refers to the component of the E-field perpendicular to the cortical surface (En). Negative En hyperpolarizes pyramidal cell membranes, causing transient and potentially long-term decreases in cortical excitability. The term Desired E field refers to the target E field (En_Target) that was used in the optimization algorithm (Stimweaver algorithm (Ruffini *et al.*, 2014)). The achieved average E field is the surface average of En induced by the optimized montage in the target region. It is lower than En_Target due to the convoluted nature of the cortical surface, preventing consistent orientation across different regions.

### *General scheme of tDCS protocols*

After a baseline period of two months, each patient received daily stimulation of an individualized multichannel tDCS protocol for five consecutive days, called a cycle of tDCS. The protocol has already been described in detail in (Daoud *et al.*, 2022). The tDCS cycle

was repeated multiple times every two months. Patient 1 underwent eleven cycles, patient 2 had nine cycles, and patient 3 had three cycles at the time of last follow-up.

The daily treatment consisted of two 20-minute stimulation periods, referred to as a *bi-session*, with a 20-minute break in between for a total of 40 min of personalized stimulation. The duration of the break between tDCS sessions may be crucial to optimize cumulative effects and to prolong the inhibitory neuroplastic effects of inhibitory stimulation (Monte-Silva *et al.*, 2010; Yang *et al.*, 2020). The average total injected current in our study was about 2 mA. The current intensity was gradually increased over a period of 30 s until reaching that level. Similarly, at the end of the stimulation period, the currents ramped down for a period of 30 s.

### *Personalization of multichannel tDCS electrode positions*

Personalized electrode montages for each patient were determined using an optimization pipeline considering individual factors, such as previous cortectomies or lesions, based on biophysical head models derived from patient T1-weighted MRIs (Miranda *et al.*, 2013). The Stimweaver algorithm (Ruffini *et al.*, 2014) was employed to optimize the montage based on a target E-field map defined on the patient's personalized neocortical surface. The target map included information about specific areas to be inhibited based on SEEG recordings, as well as "silent areas" with normal SEEG activity or minimal epileptogenic activity. The determination of the target region to be inhibited was based on the identification of the potential EZ. In two patients, the determination was guided by previous SEEG recordings. As the localization of the EPC is the primary (sensori)motor cortex, this region was always included in the cathodal area of stimulation.

The algorithm (Ruffini *et al.*, 2014) was used to automatically determine the position of active (anodal) and reference (cathodal) electrodes and the associated currents that result in the most effective distribution of the electric field (E-field) reaching the target region. Several constraints were imposed on this solution, including a maximum of 8 electrodes, a maximum current per electrode of 1.884 mA (in absolute value), and a maximum total injected current of 2.0 mA. The electrode positions were based on the 10–20 EEG system, with cathodes placed over the areas to be inhibited and anodes over silent areas (example of the target optimization of patient 2 in Figure VI.1). Stimulation was applied via a multichannel tDCS system (Starstim8, Neuroelectrics Barcelona). Stimulation was delivered using the Starstim8 multichannel tDCS system, controlled by NIC 2.0 software (https://www.neuroelectrics.com/products/software/nic2/). The electrodes used (Neuroelectrics NG PiStim electrodes, 1 cm radius, cylindrical Ag/AgCl electrodes with a layer of conductive SIGMA gel underneath) were positioned in a neoprene cap with the 39 positions used in the montage optimization (Neuroelectrics

Standard Cap). The optimization of the tDCS electrode's positions is illustrated for the three patients (Figure VI.1.C).

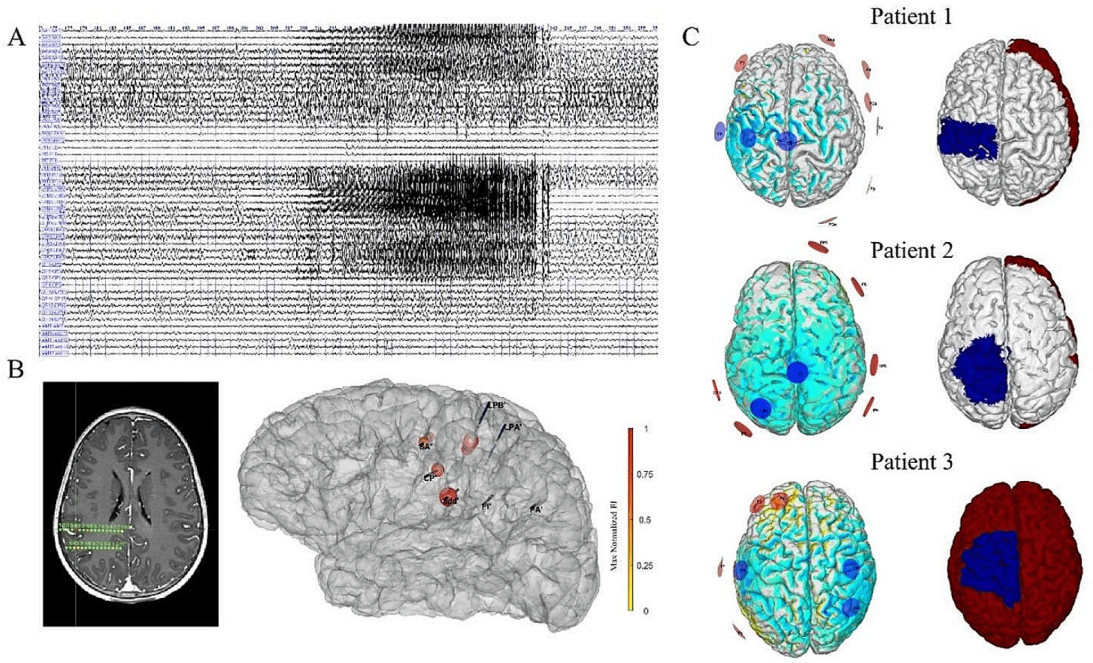


**Figure VI.1. Illustration of the epileptogenic zone identification process using SEEG recordings and the optimization protocol for tDCS electrode's montage for the three patients.** (A) SEEG recordings during left centro-parietal and left motor area for the patient 2. Intracerebral electrodes are identified by letter and the recordings' leads are numbered from 1 to 15, low numbers corresponding to the deepest structures. Bipolar signals are obtained by subtracting the signals recorded from two adjacent leads. (B) The maximum epileptogenicity values (red and orange spheres) are shown in a three-dimensional scheme of the patient 2 brain illustrated based on CT-MRI reconstruction of electrode tracks and epileptogenic index (EI). The diameter and the position on the color scale are proportional to the normalized EI values. (C) Optimization protocols used for the three patients (numbered 1 to 3 from top to bottom) with tDCS electrode's positions and generated normal component of electrical fields (V/m). The blue area corresponds to the epileptogenic zone and must be inhibited with cathodal electrodes (in blue circles on the left). The red electrodes on the left correspond to the anodal electrodes delivering the excitatory return current (red circles). The non-involved zone is colored in white or red on the right side.

### *Clinical outcome*

A seizure diary was used to monitor seizure frequency (SF) before (two months baseline) and during the study, completed by patients and/or their relatives. The diaries were analyzed by month to count the number of seizures for each period (before, during, shortly after, and a long period after each cycle of tDCS). Decreases and increases in the number of seizures were expressed as a percentage compared to the baseline. Furthermore, patients were also asked to notify any perceived adverse effect of tDCS during and after each bi-session.

## 6.3. Results

Patient 1 is 26 years old and was diagnosed with Rasmussen's encephalitis at 7. The disease primarily affects the right upper limb, causing focal clonic seizures of the right hemi- body and, in some cases, leading to bilateral motor seizures. The EPC occurred early in the course of the disease and was characterized by sub-continuous jerks in the extremity of the right upper limb. The patient has experienced generalized motor status epilepticus three times a year over the past five years, requiring intensive care management. Antiseizure medication (ASM) polytherapy and various immunomodulatory treatments have been tried, including corticosteroids, intravenous immunoglobulins, anti-TNF alpha, and azathioprine. Neurologically, there was a slight deficit in the patient's right hand. Cognitive alteration, mainly in the form of language production deficit and marked executive function disorders, was observed. Surgery was not recommended as there was no significant motor deficit observed. MRI scans showed atrophy of the left hemisphere, predominantly in the perisylvian region and the deep nuclei, worsening over the first few years. Fluorodeoxyglucose positron emission tomography (FDG-PET) showed diffuse left hemispheric hypometabolism. Different video-EEG recordings showed slowed background activity in the left hemisphere and recorded motor seizures associated with left central discharge. The patient experienced three motor seizures of the right hemibody per week prior to tDCS. However, after starting the protocol, the patient displayed a noteworthy decrease in SF compared to the baseline (-42%). As the treatment progressed, this reduction continued to accumulate with each cycle of tDCS. By cycle 7 to cycle 11, seizures reduced to only one per month, indicating a massive reduction of 92% (Figure VI.2). In addition, the patient has not experienced status epilepticus since the second cycle of tDCS. While the patient reported no side effects following the stimulation, the treatment had little effect on the EPC itself, with continuous myoclonus of the right upper limb remaining largely unchanged (Figure VI.2.B). The ASM (carbamazepine, levetiracetam and perampanel) remained unchanged during follow-up. Prednisone was progressively reduced from 20 mg/d to 5 mg/d at the last follow-up.

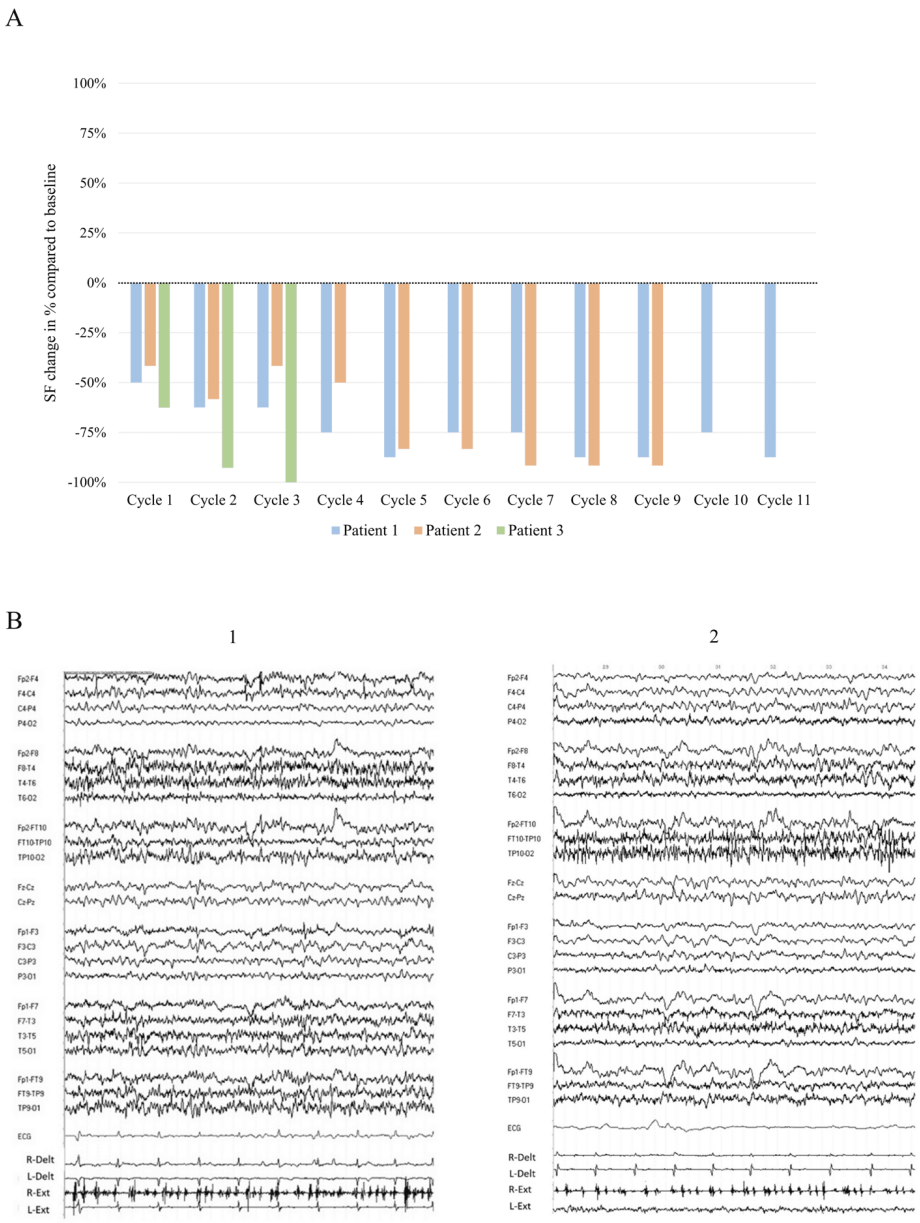


**Figure VI. 2. Seizure frequency changes across the study compared to the baseline**. A. Seizure frequency changes of secondarily generalized seizures. The seizure frequency has been estimated from the seizure diary count. We averaged the number of seizures at each month after each tDCS cycle (corresponded to the cycle value) for each patient represented as a percentage of change compared to the baseline. B Polygraphic interictal EEG -EMG recordings before (1) and after (2) eleven tDCS cycle in patient 1. The EPC is still visible with continuous myoclonus on the right hand extensor muscle EMG recording Abbreviation: Delt: deltoide muscle, Ext: extensor muscle R : right L : left.

Patient 2 is a young girl, with no notable history other than epilepsy, aged 12 at the time of her first tDCS sessions. She presented with drug-resistant epilepsy that started at the age of 5. The first seizures were characterized by isolated and rare clonic jerks of the right foot, followed after a few months by more marked seizures with tonic contraction of the right foot, followed by clonic jerks and a transient motor deficit, occurring several times a month. Stronger nocturnal seizures could extend to the entire right hemibody and become bilateral. After a few months of evolution, EPC of the right foot appeared,

characterized by sub-continuous clonic jerking. The seizures were resistant to ASM, and the patient underwent pre-surgical evaluation. A 3T-MRI scan showed images compatible with focal cortical dysplasia (FCD) in the left paracentral lobule (Flair hypersignal). Fluorodeoxyglucose positron emission tomography (FDG- PET) showed a left paracentral metabolic defect with moderate striatal and left thalamic hypometabolism. Video-EEG recorded ictal events with motor seizures of the right upper limb associated with a scalp EEG discharge over the left fronto-central channels and continuous clonic jerking of the right foot, characterizing EPC. A pre-surgical SEEG examination was performed (2015) with 7 implanted electrodes. Interictal activity was maximal in the left paracentral lobule, with rhythmic slow waves and sharp waves characterizing the FCD lesion. A seizure was recorded during the examination, originating in the left paracentral lobule and superior motor area (Figure VI.1. A. B). Thermocoagulation of the mesial part of the left paracentral lobule was performed but had no effect on SF. The patient underwent partial surgical resection of the EZ located in the left paracentral lobule. This surgical procedure had no effect on seizures (approximately two per week) or EPC. Multichannel tDCS was performed, targeting the residual volume of the left primary motor cortex and SMA (Figure VI.1.C). After the initial cycle, SF was reduced by half (-50% compared with baseline). Thereafter, the patient showed a progressive reduction in SF throughout subsequent stimulation cycles until reaching a frequency of one (-88% decrease) or two seizures (-75% decrease) per month from cycle 4 through to cycle 9 (Figure VI.2). Stimulation had no adverse effects, with the exception of mild tingling reported by the patient at the start of each session. Although our protocol had a beneficial effect on the most disabling and severe seizures, it had no major effect on the jerking EPC component, which persisted. ASM (carbamazepine and topiramate) remained unchanged during the follow up.

Patient 3, a 13-year-old girl, was referred to our center for the management of drug-resistant epilepsy affecting the left motor cortex. Epilepsy began at the age of 10, with recurrent contractions of the right labial commissure. Focal motor seizures and focal to bilateral tonic-clonic seizures occurred early in the course of the disease. Several ASM in association failed to control seizures. Brain MRI was normal, and CSF study showed no inflammatory process. A few months after the onset of seizures, the patient developed EPC in the form of continuous jerking of the right lower leg associated with a mild distal deficit of the right foot. Video-EEG exploration revealed a permanent clonus of the right foot associated with paroxysms in the left fronto-rolandic region. An SEEG was performed (2022) with 8 depth electrodes. Interictal activity was maximal in the left central gyrus, with extension to the premotor and cingulate regions (Figure VI.1.C). A typical motor seizure (episode of right-sided clonus) was recorded, characterized by discharges in the left central gyrus. Extensive thermocoagulation of the mesial part of the central gyrus was performed, with no effect on EPC or SF. Prior to the start of tDCS, the patient presented with a permanent myoclonus of the right foot (EPC) and two focal motor seizures per day. She also experienced focal to bilateral tonic-clonic seizures, occurring at a rate of approximately three per week. After the first cycle of tDCS, the daily focal motor seizures were reduced to seven per week, without bilateral tonic-clonic seizures. After the second

cycle, she only had two focal motor seizures per week until the last stimulation cycle, when she no longer had any motor seizures or secondarily generalized tonic-clonic seizures (Figure VI.2). Despite this considerable clinical improvement, after three cycles of stimulation, the patient still presented continuous muscular movements in the foot (EPC), making walking difficult. Throughout the protocol, the patient reported only a slight transient itching at the start of stimulation. ASM (topiramate, oxcarbazepine, clonazepam, lacosamide) remained unchanged during the follow up.

## 6.4. Discussion

This case report series examines the efficacy of prolonged (6–22 months) multichannel personalized tDCS protocols in the treatment of central cortical epilepsy associated with EPC, in three patients with different causes (Rasmussen's Encephalitis, FCD, and unknown origin). We were able to reach a significant reduction (over 75% in SF, and, in one patient, a complete absence of the most debilitating motor seizures. However, our protocols did not have a noticeable positive effect on the jerking component of the EPC in any of the three cases.

The first case involved a patient suffering from Rasmussen's encephalitis. Repeated and sustained application of tDCS in this patient resulted in a significant reduction in secondarily motor seizures (-92% reduction in FS from baseline after five cycles of tDCS). It is noteworthy that the long-term effect of tDCS (22 months of protocol) resulted in the disappearance of recurrent episodes of convulsive status epilepticus. Some previous reports have highlighted the potential benefits of tDCS for patients with this syndrome, especially in cases where surgery poses a significant functional risk. A study was conducted to investigate the impact of four cathodal tDCS sessions on two patients with Rasmussen's encephalitis (San-Juan *et al.*, 2011). In that study, one patient experienced a substantial reduction in SF, while the other was completely seizure-free by the end of the protocol. In contrast with our present study, they also reported a mild improvement in EPC. Another study examined the impact and safety of tDCS on five patients diagnosed with Rasmussen's Encephalitis (Tekturk, Erdogan, Kurt, Kocagoncu, *et al.*, 2016). Four out of five patients experienced a reduction of more than 50% in SF after three consecutive days of cathodal tDCS. However, this study did not report any information regarding the EPC itself. Furthermore, these studies confirmed the absence of side effects and showed a high tolerance to tDCS. A recent case report has brought attention to the short-term effective- ness of tDCS, specifically its impact on the EPC component (Bangel, Pang and Baker, 2023). They reported a suppression of continuous partial seizures for 18 weeks after 8 daily tDCS in a young patient with Rasmussen's Encephalitis, enabling her to walk unassisted.

The second case in the present study involved a patient who likely had FCD and who did not experience any improvement after previous surgery that was not fully effective due to functional limitations. Over the course of 18 months and 9 cycles, the use of multichannel tDCS resulted in an 88% decrease in motor SF. Other clinical studies involving patients with brain tumors have suggested that tDCS should be considered when resection surgery has failed or is not a viable option (Fregni *et al.*, 2006; Yook *et al.*, 2011). Methodological studies, employing computational modeling, have underscored the impact and safety of tDCS electrical field distribution in cases involving craniotomies and skull lesions (Bikson *et al.*, 2016; Daoud *et al.*, 2022).

The third case involved EPC-associated seizures in the central region and received a shorter course of tDCS cycles compared to the others. The patient underwent three weeks of stimulation within a six-month period. The impact on motor seizures and secondarily generalized tonic-clonic seizures was significant and quickly noticeable. Following the second cycle of tDCS, there was a substantial decrease of 93% in seizure episodes. Eventually, the seizures ceased completely after the third cycle within the next two months. These outcomes are encouraging since, to date, only limited number of studies have achieved such results, especially by using a non-invasive method of neuromodulation (San-Juan *et al.*, 2011, 2017).

Based on the presented cases, repeated cycles of tDCS appear to have a positive impact on overall clinical outcomes for patients. As the treatment progresses, the patient's SF stabilizes. Several other studies have also noted the potential for long-term effects of cathodal tDCS on epileptic-like activity (Monte-Silva *et al.*, 2010; Lin *et al.*, 2018; Yang *et al.*, 2020; Daoud *et al.*, 2022). While the current results show promise in reducing seizure frequency, this study has certain limitations to consider. Firstly, the study's reliance on a small sample size, consisting of three patients with different etiologies of EPC, raises concerns about the broader applicability of the findings. Additionally, the inherent diversity among the patients further complicates the ability to draw universal conclusions. In addition, only two patients had more than five tDCS sessions. Furthermore, the absence of a control group limits our ability to make direct comparisons and fully attribute the observed effects to the long-term multichannel tDCS protocol. These limitations underscore the need for caution in extrapolating the results and emphasize the necessity for larger, more homogenous studies with proper control groups to validate the effectiveness of tDCS in EPC. Finally, despite maintaining stable ASM doses throughout the study, the influence of ASMs on the observed outcomes remains unclear and needs careful consideration.

From a neurophysiological viewpoint, the precise mechanism through which weak fields modulate cortical excitability remains enigmatic, particularly in the context of epilepsy. It remains uncertain whether transcranial current stimulation impacts the EZ itself or the surrounding tissue. A recent clinical case report attempted to elucidate the acute neuromodulatory effects of tDCS in the human epileptic brain (Koessler *et al.*, 2023). By simultaneously applying tDCS and recording intracranial EEG, the study demonstrated

that tDCS completely eliminated low-amplitude fast discharges, alleviating the most debilitating clinical symptoms. While there is a prevailing consensus that tDCS effects involve physiological synaptic plasticity mechanisms like long-term potentiation (LTP) and long-term depression (LTD) (Modolo *et al.*, 2018; Simula *et al.*, 2022), our study, indicated by the persistence of continuous myoclonic activity, suggests that tDCS had minimal influence on the central motor cortex's excitability, possibly due to altered LTD mechanisms within the core of the EZ in certain cases. Indeed, previous studies conducted at cell levels have suggested that typical physiological plasticity processes responsible for LTD and LTP, governed by NMDA and calcium-related mechanisms linked to synaptic AMPA receptors, can be severely disrupted or absent in EZ (Zhou and Roper, 2012; Naylor *et al.*, 2013; Kurbatova *et al.*, 2016; Chen *et al.*, 2017; Burman *et al.*, 2019). Instead, these situations might involve pathological plasticity, including heightened NMDA receptor activity and impaired GABA-ergic inhibition (Zhou and Roper, 2012; Naylor *et al.*, 2013; Kurbatova *et al.*, 2016; Chen *et al.*, 2017; Burman *et al.*, 2019). On the other hand, we observed a significant and sustained reduction in the number of motor seizures, suggesting that repeated tDCS cycles could affect the excitability of the larger epileptogenic network. In this view, tDCS might induce LTD in the surrounding synapses, decreasing the recruitment of remote nodes and potentially preventing seizure generation within the larger epileptogenic network (Wenzel *et al.*, 2019). From a biophysical viewpoint, these results suggest that the localization of the EZ (sensorimotor neocortex) has an impact on the beneficial therapeutic effect of tDCS. It is likely that low-intensity currents injected at the scalp electrodes induce electric fields that reach the target brain regions and modulate their activity despite their low magnitude.

Finally, an important limitation of tDCS is the short-term effect and the need to repeat sessions to maintain the protective effect (see review in (Simula *et al.*, 2022)). This led us to repeat the personalized tDCS protocol over time. However, this is cumbersome and requires inpatient sessions. In the future, home tDCS is likely to be a satisfactory solution. tDCS is a relatively simple and portable technology, particularly well-suited to remotely supervised home treatment. To date, this technology has been tested for the treatment of several neurological conditions, including neuropathic pain (Lefaucheur *et al.*, 2017) and Alzheimer's disease (Bréchet *et al.*, 2021). In a systematic review, Palm et al. identified 22 original research articles, trial protocols or trial recordings concerning home tDCS (Palm *et al.*, 2018). They were able to show that adherence to treatment was high and side effects were minimal, and therefore concluded that remotely controlled and supervised home tDCS was feasible and promising.

To conclude, long-term multichannel tDCS reduced or even eliminated the most severe and disabling seizures in three patients with EPC. This highlights the potential efficacy of our approach in the management of this challenging condition although tDCS had little or no impact on the EPC itself.

# 7. Chapter VII: General Discussion and Perspectives

# Summary of studies' findings

This thesis resulted in five scientific articles—three published, one under review and one submitted—addressing the clinical and fundamental effects of tDCS on patients with drug-resistant epilepsy.

In the first study (Simula†, Daoud† et al., 2022), we conducted a systematic review of transcranial current stimulation in epilepsy, exploring its biological, neurophysiological, functional and clinical effects. The studies referenced in this review have served to design and develop our stimulation protocol. Moreover, the analysis sheds light on the underlying mechanisms and biomarkers linked to tDCS efficacy.

In the second study (Daoud et al., 2022), we clinically validated a personalized multichannel tDCS protocol targeting the epileptogenic zone in patients with DRE based on SEEG data. This approach achieved a 50% response rate, with a notable reduction in seizures for half of the patients. Additionally, responder patients showed reduced EEG functional connectivity following stimulation cycles, suggesting a potential underlying mechanism for tDCS efficacy.

Study 3 (Daoud et al., under review in Epilepsia) aimed to uncover tDCS-induced changes at local and network levels and their correlation with clinical outcomes in DRE patients. Using MEG data and source reconstruction, we identified distinct power spectral density changes across frequency bands, with responders and non-responders showing opposite trends. Responders exhibited reduced functional connectivity, while non-responders showed increased connectivity at the source level. Interestingly, these changes occurred across whole brain networks rather than specifically within targeted regions. Additionally, higher baseline functional connectivity levels were observed in responders, indicating its potential as a predictive biomarker for clinical response.

In study 4 (Daoud et al., submitted), we investigated the clinical response to tDCS by analyzing the influence of epileptogenic zone characteristics. Results demonstrated that the extent and depth of the targeted epileptogenic zone significantly affect tDCS efficacy in refractory focal epilepsy patients, with responders typically having a smaller and shallower epileptogenic zone than non-responders. It opens the door for machine learning studies to use extent and depth parameters, potentially identifying thresholds and improving patient selection criteria to prevent seizure worsening in some patients.

In study 5 (Daoud et al., 2024), we studied the effects of prolonged tDCS protocols on various seizure types in three patients with epilepsia partialis continua (EPC). While the treatment significantly reduced or eliminated the most severe seizures in patients, it had minimal impact on the continuous myoclonus characterizing EPC. These findings underscore the potential efficacy of repeated tDCS in managing challenging conditions

like EPC and emphasize the importance of considering seizure types when analyzing changes in seizure frequency.

## 7.1. A personalized protocol of multichannel tDCS to decrease the seizure frequency

Clinical trials in studies 2 and 3 evaluated changes in seizure frequency after three cycles of multichannel tDCS. In study 2, half of the patients showed a reduction in seizures exceeding 50% (classified as responders). In contrast, in study 3, 36% achieved a similar reduction (Figure VII.1). These results suggest that tDCS, a non-invasive method, holds substantial promise in improving refractory epilepsy, even when other traditional or invasive treatments have fallen short. Developed as part of the Galvani project, the stimulation protocol used in these studies stands out for its personalized approach, based on anatomical data and SEEG. Customization is essential for optimal delivery of inhibitory current to the epileptogenic zone (Miranda *et al.*, 2013; Ruffini *et al.*, 2014; Laakso *et al.*, 2015). Since tDCS electric fields are influenced by neuron orientations, adopting patient-specific strategies that consider patient-specific brain anatomy becomes imperative for precise targeting. While this Ph.D. thesis confirmed the safety and the clinical efficacy of our optimized multichannel tDCS protocol, it did not demonstrate superior clinical effectiveness in reducing seizure frequency compared to conventional protocols employing two large sponge electrodes. In contrast, computational studies suggest that using multiple small electrodes leads to achieve more targeted and more effective results (Ruffini *et al.*, 2014; Liu *et al.*, 2018; Hannah, Iacovou and Rothwell, 2019) (Figure VII.2). In the same line, previous studies on healthy subjects and other medical conditions have indicated that optimized multichannel protocols may surpass conventional bipolar tDCS montages in terms of efficacy (Khan *et al.*, 2023; Salehinejad *et al.*, 2024). Thus, to address these conflicting results, further investigations should focus on direct comparisons of these protocols specifically in patients with epilepsy.

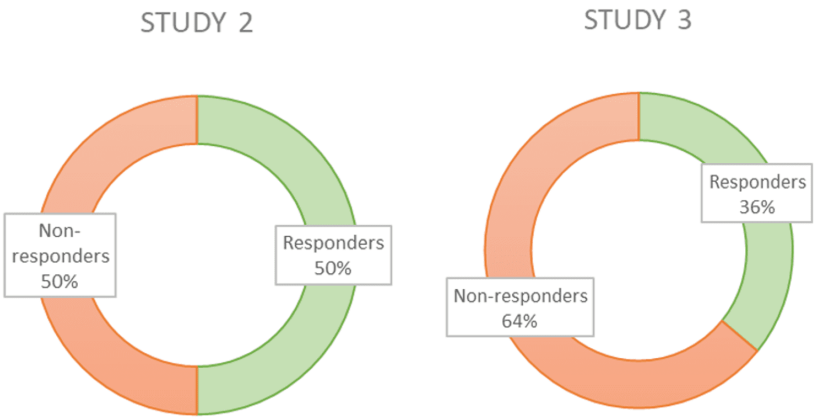


**Figure VII.1. Clinical response rates in patients from studies 2 and 3.**

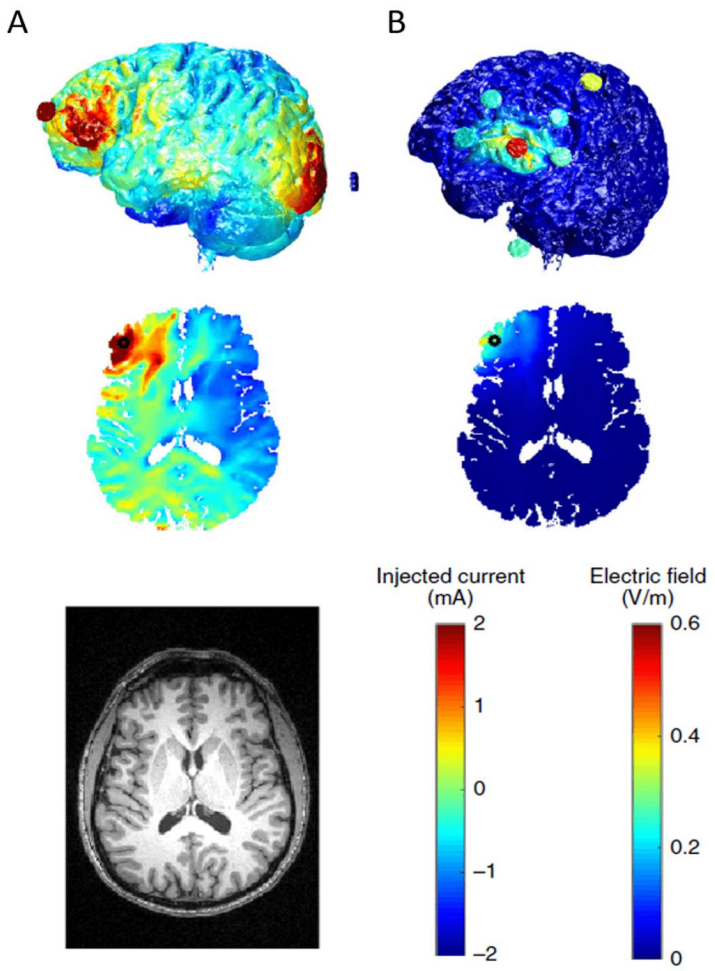


**Figure VII.2. Computational models for optimizing electrode placement to maximize stimulation of a targeted brain region**. A. Model of Subject 1 with 2 mA current injected at electrode Fp1 and return from electrode P3. B. Model of Subject 1 with another electrode configuration attempting to achieve more focal stimulation. Note that stimulation B is more focal but achieves weaker fields compared to A, due to increased current shunting through the skin between nearby electrodes. Adapted from (Liu *et al.*, 2018)).

The main limitation of our studies was the absence of a sham group, complicating the attribution of specific effects to the tDCS stimulation and increasing the risk of confounding variables. Placebo response rates in epilepsy clinical trials using similar devices typically hover around 21% of reduction in seizure frequency (Goldenholz and Goldenholz, 2020; Kaye *et al.*, 2021). Although the response rates in our studies—50% and 36%—might seem low, they must be interpreted in the context of our patient population, which comprised pharmacoresistant patients who either had failed surgery or were ineligible for it. Approximately half of the patients had previously undergone VNS therapy without meaningful improvement. Despite these challenges, tDCS, a completely safe and non-invasive technique, greatly improved the clinical condition of some patients, offering renewed hope to those with limited treatment options. Higher response rates might be achievable with tDCS in patients with less severe forms of epilepsy, where it could potentially replace or complement existing medication instead of requiring additional drugs.

As part of the ERC Galvani project, this Ph.D. thesis, along with computational simulations of electric fields in epilepsy models conducted by collaborating centers has significantly influenced the design of the project's final clinical trial. Entitled *'Model-based multichannel tDCS in refractory epilepsy: A cross-over study of efficacy*,' this multicentric, randomized, double-blind study aims to evaluate the clinical effects of personalized multichannel tDCS compared to sham stimulation. The primary focus is on changes in seizure frequency, related comorbidities, and quality of life in DRE patients. The study protocol is illustrated in Figure VII.3. In this clinical trial, patients will be monitored for eight months, with a 2-month washout period, acting as their internal controls. The tDCS treatment involves two 20-minute stimulation sessions per day, with a 20-minute break in between, over ten non-consecutive days. Patients will alternate between two phases: sham and active stimulation.

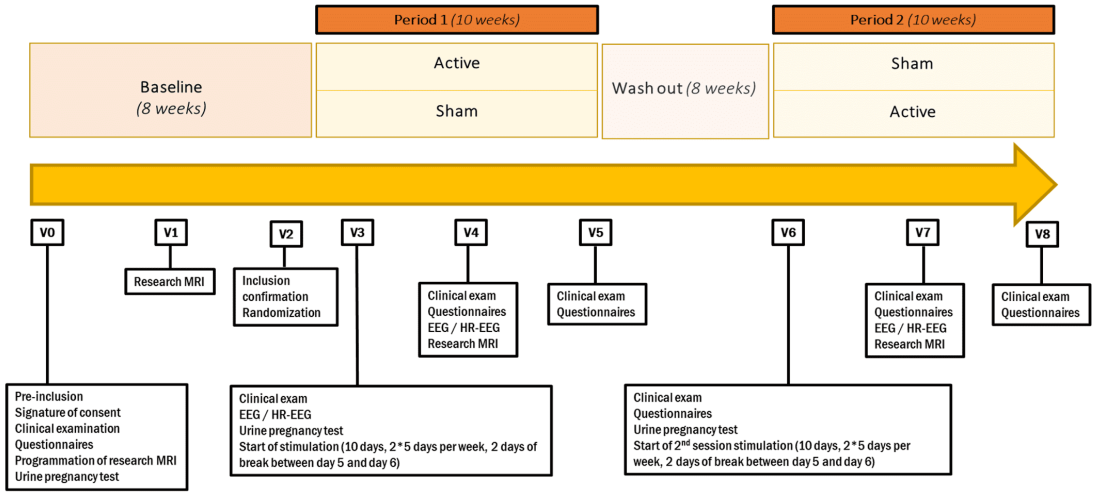


**Figure VII.3. Milestones of clinical investigation of the final Galvani clinical trial** (ID-RCB: 2023-A02482-43).

Our optimized protocol also aimed to prolong the positive after-effects of tDCS, marking a significant and innovative objective in non-invasive neuromodulation studies. Previous studies have shown that the duration of tDCS effects depends on the number of repetitions, stimulation duration, and the interval between sessions. Recently, Yang et al., (2020) found a significantly higher reduction in seizure frequency in patients with refractory focal epilepsy using a protocol of 2x20 min stimulation per day, with a 20 min interval, compared to a single 40-minute session without a break (Yang *et al.*, 2020). Based on these findings, we adopted a protocol with a 20-minute interval between two 20-minute sessions to achieve prolonged beneficial effects. As a result, responder patients experienced a reduction in seizure frequency of over 50% two months after the last tDCS cycle. However, since tDCS effects are reversible, seizure frequency tends to return to baseline if the interval between cycles exceeds two months. This suggests the need for regular hospital visits for ongoing treatment, highlighting a potential benefit of developing home-based stimulation devices. The feasibility of home-based protocols has been proven in other neurological conditions, such as chronic pain. Thus, Garcia-Larrea et al., (2019) assessed the feasibility and pilot efficacy of an internet-based, at-home

transcranial motor cortex stimulation (H-tDCS) system for treating neuropathic pain that was refractory to standard drug therapy (Garcia-Larrea *et al.*, 2019). To date, no study has considered home devices as a treatment option for epilepsy.

## 7.2. Functional changes in whole brain networks are related to tDCS efficacy

Several studies demonstrated that tDCS can change brain connectivity. For instance, Keeser et al. showed that tDCS can modulate resting-state connectivity, while Polanía et al. found that tDCS enhances communication between task-related areas while reducing it between other areas (Keeser *et al.*, 2011; Polanía *et al.*, 2011). This Ph.D. thesis aimed to investigate how repeated cycles of tDCS impact brain excitability, measured through changes in functional connectivity, in patients with DRE. These effects were assessed using non-invasive electrophysiological recordings (EEG and MEG) before and after each tDCS cycle. This study is unique in its use of long-term daily stimulation—lasting at least three weeks over six months—with regular brain activity measurements throughout. Although our protocol required significant effort to implement, it provided valuable insights into the mechanisms underlying the clinical efficacy of tDCS in epilepsy. Overall, our studies showed a decrease in functional connectivity after several cycles of tDCS in responder patients—those who experienced over a 50% reduction in seizure frequency. Conversely, non-responders showed increased connectivity as tDCS cycles progressed. These findings, observed at both sensor and source levels, suggest that brain network modulation might be a critical mechanism driving the effectiveness of tDCS. Other studies on cathodal tDCS for epilepsy patients also reported functional network changes associated with stimulation. For instance, Lin et al. (2018) showed that reduced seizure frequency after tDCS correlated with lower global synchronization in epilepsy patients, as measured by the Phase Lag Index (PLI) derived from EEG (Lin *et al.*, 2018). Similarly, Luo et al. (2021) observed decreased neural transfer efficiency after cathodal tDCS using graph-based EEG analysis (Luo *et al.*, 2021). An imaging study revealed reduced connectivity in responder patients based on fMRI graph theory. In our studies, using EEG and MEG, we explored the dynamic changes in network connectivity throughout the protocol. In the future, it would also be valuable to investigate the structural impact of stimulation on the physical connections between neuronal populations. The final Galvani clinical trial will investigate such impact, using fMRI to measure changes in connectivity four weeks after the stimulation period, compared to baseline.

Furthermore, Study 3, based on source-level analysis, investigated whether tDCS effects were confined to specific targeted areas or spread more widely across the brain. Surprisingly, the study found no significant difference in functional connectivity changes between regions exposed to excitatory (anodal) current and those exposed to inhibitory (cathodal) current. This suggests that even with a highly focal approach, the effects of

tDCS are distributed throughout the brain. This finding raises questions about the mechanisms of the focused approach. For instance, one study demonstrated dynamic interaction between networks induced by multichannel tDCS in healthy subjects, suggesting its influence at the whole brain level (Mencarelli *et al.*, 2020). Additionally, when considering these observations within the scope of epilepsy—a syndrome affecting large-scale cerebral networks—it becomes less surprising that individuals responding positively to stimulation exhibit decreased functional connectivity across the brain. This global effect may help modulating exacerbated epileptic networks that are distributed across the brain (Lagarde *et al.*, 2022), potentially reducing network hyperexcitability and, consequently, seizure occurrence.

Lastly, our protocol facilitated pre-stimulation recording of brain activity, enabling investigation of baseline functional connectivity as a predictive biomarker for tDCS response. We found that individuals who later responded positively to tDCS had higher baseline functional connectivity levels compared to non-responders before the first tDCS session. This suggests that the state of brain networks prior to treatment could predict the response to stimulation. Further exploration of machine-learning approaches focusing on this biomarker will be interesting for advancing research in the field. This is supported by studies using similar methodologies in patients with epilepsy. For example, Hao et al. achieved a notable mean accuracy of 68.3% in predicting the outcome of cathodal tDCS in focal epilepsy using graph theoretical analysis and a support vector machine (SVM) prediction model (Hao *et al.*, 2021). Similarly, pioneering VNS studies have explored predictive models for responder screening in patients with DRE. Ma et al. (2022) established the first prediction model for preoperative VNS responder screening in children with DRE, emphasizing the potential for effective identification of responders before VNS implantation (Ma *et al.*, 2022). In another VNS study, the authors extracted brain connectivity features from scalp EEG during seizures, revealing significant differences in VNS responders and non-responders (Chen *et al.*, 2023). Their predictive support vector machine (SVM) model accurately identified VNS responders in patient-level cross-validation and on an independent testing cohort. Using tDCS as an antiepileptic intervention introduces uncertainty about its effectiveness for individual patients. Early anticipation of treatment outcome is essential for clinicians, facilitating timely decisions and limiting risks. Further research into predictive biomarkers and machine learning models will be crucial for improving the precision and efficacy of tDCS in treating epilepsy.

Another important concern is the intra- and inter-individual variability of brain activity. Our research required repeated recordings, at the beginning and at the end of each tDCS cycle, inevitably resulting in different brain state independently of the impact of stimulation. Previous studies have explored the variability of intrinsic brain activity across time. They pointed to the complexity of the mechanisms underlying this variability and to the many factors that may interfere with the measured effects, even in healthy subjects (genetic variance, changes in neural networks, differences in cognitive and physiological processes, age of subjects) (MacDonald, Nyberg and Bäckman, 2006; Smit *et al.*, 2012; Haegens *et al.*, 2014; Díaz, M *et al.*, 2019). The investigation of neural oscillations

through the standard power spectral density analysis poses challenges due to potential confounding effects arising from changes in aperiodic activity. To address this, estimating the $1/f$ component of the spectrum has recently been suggested (Donoghue *et al.*, 2020). This component is referred as "scale-free" activity and is composed by the exponent and the offset. In study 3 (see in section 4.2), we used the Fitting Oscillations and One-Over-F (FOOOF) method to observe tDCS-induced changes (Donoghue *et al.*, 2020). While our findings regarding periodic activity were consistent with our PSD results, we observed significant inter-individual variability in aperiodic components, which complicates comparisons across groups. It would therefore be interesting to study the intrinsic variability of brain activity (bot inter- and intra-individual) from one period to another by repeated measurements, specifically in patients with epilepsy. To date, only one case study has examined the separation of periodic and aperiodic spectral components in an epileptic patient (Gerster *et al.*, 2022). The study of aperiodic components, which are thought to reflect the excitation-inhibition balance (Gao, Peterson and Voytek, 2017), remains to be performed in a larger epileptic population in which spike and non-spike periods would be separated to minimize the impact of sharp spikes on spectral power (Bénar *et al.*, 2010). This exploration could contribute valuable insights to clinical trials by associating aperiodic activity with treatment response and advancing our understanding of tDCS efficacy.

## 7.3. Why do patients respond differently to tDCS effectiveness?

Previous literature, including findings from Studies 2 and 3, indicates that around 50-60% of patients with DRE do not respond to repeated sessions of cathodal tDCS. This thesis project aimed to elucidate why patients exhibit differential responses to tDCS effectiveness. One parameter could be the type of seizures experienced by a given patient. Importantly, neither Studies 2 and 3, nor existing tDCS research in epilepsy clearly addresses whether tDCS affects all seizure types. Typically, tDCS studies combine all seizure types when evaluating changes in seizure count or frequency, overlooking the diversity of seizure types. Understanding how tDCS affects different seizure types and their associated brain networks is essential for enhancing patient selection. Study 5 thus focused on the impact of tDCS on different seizure types from a specific epileptic syndrome, epilepsia partialis continua (EPC). This syndrome typically presents two seizure types: continuous partial focal seizures affecting the primary motor cortex (illustrated in Figure VII.4) and secondarily generalized seizures involving a broader epileptogenic network. Study 5 reported a notable reduction in the frequency of severe seizures, specifically secondarily generalized seizures, following repeated sessions of multichannel tDCS. However, no impact was observed on continuous partial seizures, which are typical of this syndrome. One explanation for the persistence of continuous

myoclonic activity is that tDCS had minimal influence on the central motor cortex's excitability, the core of the epileptogenic zone in these patients, possibly due to altered long-term depression (LTD) mechanisms in the epileptogenic zone. The sustained reduction in secondarily motor seizures suggests that repeated tDCS cycles may decrease the excitability of the more extensive epileptogenic network by inducing LTD in surrounding synapses, thereby preventing seizure generation (Wenzel *et al.*, 2019). These results suggest that the localization of the epileptogenic zone (sensorimotor neocortex), as well as the potential degree of biological alteration in the epileptogenic zone, affects the therapeutic efficacy of tDCS. This novel insight highlights the varying impact of tDCS on different types of focal epilepsy seizures, providing a valuable contribution to our understanding of tDCS mechanisms.

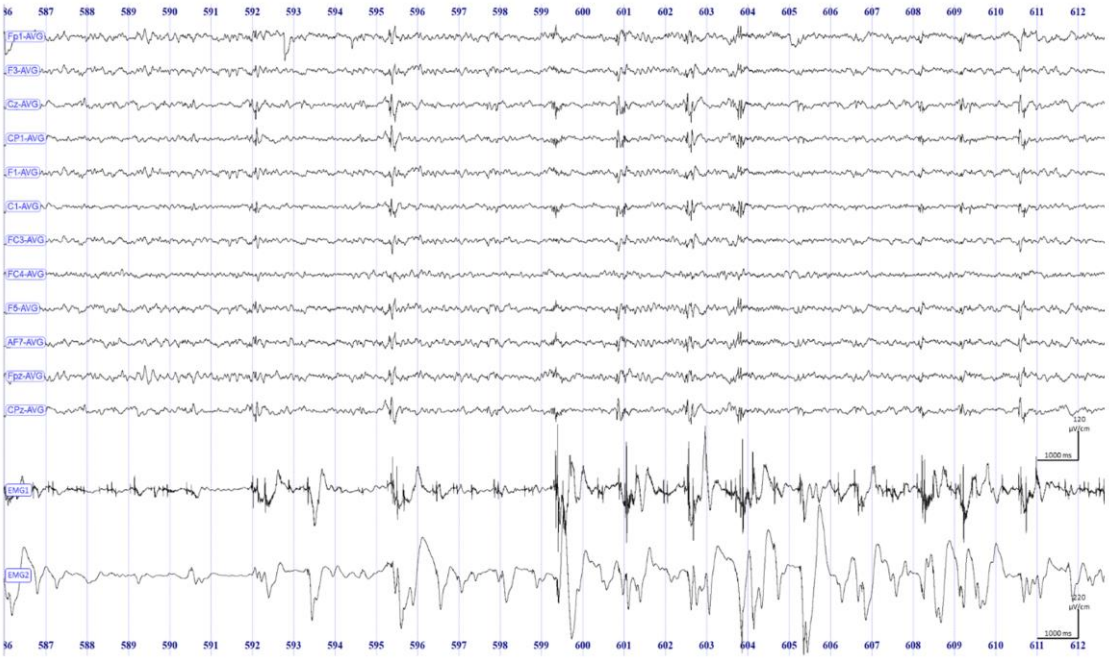


**Figure VII.4. Polygraphic recording from case 3 with EPC in right leg before the first tDCS session as a typical example of electrophysiological recordings characterizing continuous partial seizures in patients with EPC**. The left EEG shows periodic epileptiform activities, correlated with right leg myoclonias. Polyspikes are mainly over the left and central mesio-frontolateral regions. EMG1 and EMG2 being over the right soleus and the right extensor digitorum longus.

Additionally, in our quest to understand the clinical effectiveness of tDCS in epilepsy, we explored how the characteristics of the epileptogenic zone, targeted by the inhibitory electric field during stimulation, might influence treatment outcomes. Study 4 showed a significant positive correlation between the extent of the epileptogenic zone and changes in seizure frequency. Notably, tDCS demonstrated greater efficacy when epileptogenic regions were focal, whereas extensive epileptogenic zones either resulted in no reduction or even in an increase in seizure frequency. These findings suggest that targeting large epileptogenic areas with tDCS may cause excitatory return currents from the anodal electrodes, interfering with brain regions associated with the epileptogenic

network. This aligns with a recent study by Yu et al., which observed reduced therapeutic benefits of cathodal tDCS when the epileptogenic zone and network were widespread across both hemispheres (Yu *et al.*, 2023). To refine patient selection and potentially mitigate tDCS-related exacerbations in non-responders, it might be advisable to include only patients with a smaller extent of the epileptogenic network in tDCS trials.

Finally, one major challenge with transcranial stimulation lies in accurately targeting deep brain regions. Study 4, a retrospective analysis of DRE patients completing three stimulation cycles from Studies 2 and 3, revealed a limitation in the efficacy of this approach, constrained by the depth of the epileptogenic network. Notably, non-responder patients exhibited significantly deeper epileptogenic zones compared to responders, questioning previous computational studies showing that optimized multielectrode montages could effectively stimulate both superficial and deep regions (Sadleir *et al.*, 2012; Ruffini *et al.*, 2014; Wagner, Burger and Wolters, 2016; Huang and Parra, 2019). Our findings echo previous research confirming that the electric field weakens as the distance between the scalp electrode and the deep target increases, reducing its impact (Datta *et al.*, 2009; Lafon *et al.*, 2017; Vöröslakos *et al.*, 2018). At the core of the Galvani project lies the investigation of the immediate effects of applying transcranial current to patients undergoing SEEG recording. One study within this project has indicated minimal impact on deep brain structures (Simula, Damiani, *et al.*, 2023). Another solution for targeting deep sources is the temporal interference (TI) technique, which is capable of reaching and stimulating deep brain regions by generating interferences at a focal point very distant from the surface electrodes (Grossman *et al.*, 2017). TI operates by delivering multiple electric fields to the brain at different kHz frequencies, which are too high to induce neural firing. The envelope amplitude of the combined field is modulated at a difference frequency low enough to drive neural activity. Stimulation occurs at the targeted region where the modulation amplitude is higher (Violante *et al.*, 2023) (see Figure VII.5). Recent investigations in epileptic mouse models and human cadavers have shown that TI fields penetrate the human hippocampus more effectively than traditional transcranial current stimulation, with minimal impact on surrounding tissues (Acerbo *et al.*, 2022).

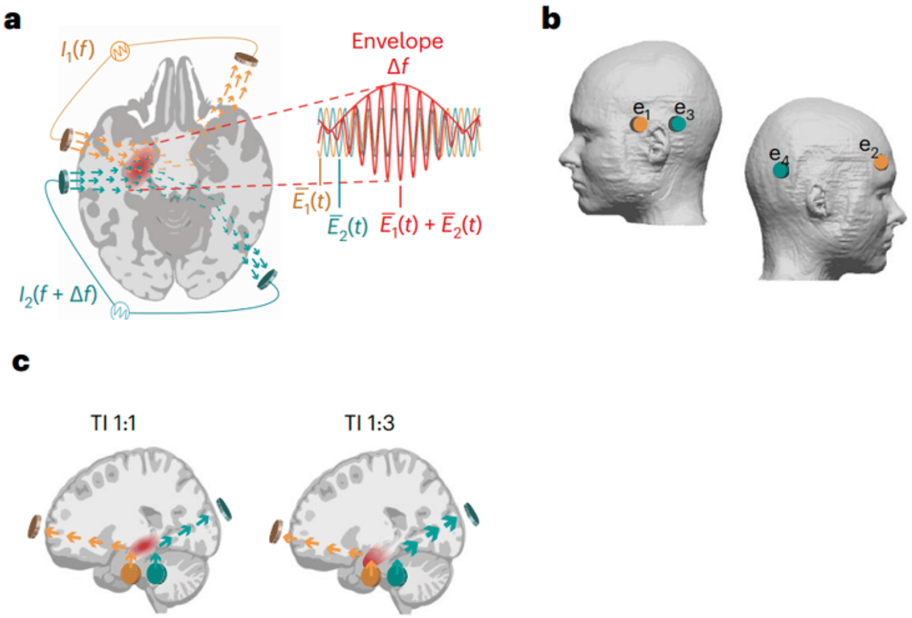


**Figure VII.5. Fundamentals of temporal interference hippocampal stimulation**. a. Concept of TI hippocampal stimulation: Two current sources, I1 and I2, applied via scalp electrodes (orange and green) at kHz frequencies f1 and f2, with frequency difference Δf = f1 − f2. Electric fields E1(t) and E2(t) combine to modulate envelope amplitude at Δf, focusing peak amplitude in deep structures like the hippocampus (red). b. Electrode configuration targeting left hippocampus: Electrodes e1/e2 (orange) and e3/e4 (green) are positioned above the hippocampus and right eyebrow. Sizes: 1.5 cm × 1.5 cm squares (ex vivo/in vivo) and 2 cm diameter circles (modeling). c. Steering TI stimulation along the hippocampal axis: With 1:1 current ratio ('TI 1:1'), stimulation at middle region; with 1:3 ratio ('TI 1:3'), anterior region. Adjusting current amplitudes in each pair directs stimulation locus. From (Violante *et al.*, 2023).

In future investigations, it would be essential to take into account the extent and depth of the epileptogenic network as targeted by tDCS in order to refine patient selection criteria. Machine learning algorithms could play a crucial role in this process, by identifying specific thresholds for the extent and depth of the epileptogenic zone associated with treatment responsiveness. By establishing such thresholds, it would be possible to prevent the inclusion of ineligible patients, potentially avoiding exacerbation of seizure activity as observed in our studies. Further research should also make efforts to correlate clinical outcomes with the actual electric field distribution in targeted brain regions for each patient. This can be achieved by exploring deeper brain areas using SEEG recordings during transcranial stimulation. Such investigations may provide valuable insights into the effects of stimulation on brain activity, potentially refining tDCS protocols for improved epilepsy management.

# General conclusion

This Ph.D. thesis investigated the effects of multichannel tDCS on patients with refractory epilepsy. Clinical trials conducted during the Ph.D. have shown that tDCS, a non-invasive neuromodulatory technique, has the potential to reduce seizure frequency. We obtained a 50% response rate in Study 2 and a 36% response rate in Study 3. This suggests that tDCS is a promising option for patients unresponsive to traditional treatments. Our personalized stimulation protocol, based on individual anatomical data and SEEG, emphasized the importance of tailored treatment strategies. Further studies should compare optimized and conventional tDCS protocols.

Investigating the dynamic changes in brain connectivity induced by tDCS revealed decreased functional connectivity in responders and increased connectivity in non-responders, suggesting that network modulation is key to tDCS efficacy. Surprisingly, tDCS effects were widespread throughout the brain. Future research should evaluate whether this is a network effect arising from focal stimulation or from difficulties on targeting focal region. Elucidating tDCS influence on brain networks should enhance our understanding of epilepsy pathophysiology and treatment responses.

In addition, baseline functional connectivity emerged as a predictor of tDCS response, paving the way for future machine learning approaches in patient selection. Moreover, tDCS showed greater efficacy for focal epileptogenic regions than for larger zones. This could be due to potential unwanted excitation of epileptogenic regions. Our findings also indicate that deeper epileptogenic zones constrain tDCS efficacy. Other methods like temporal interference could be investigated.

In summary, this research underscores the importance of refining patient selection criteria and optimizing stimulation protocols for future studies. The integration of machine learning algorithms offers promising avenues for enhancing treatment precision through the identification of predictive biomarkers and patient-specific factors. Despite all these challenges, ongoing exploration and refinement of tDCS protocols, along with advances in machine learning and home-based technologies, hold great promise for improving epilepsy treatment outcomes and enhancing patients' quality of life. Through collaborative efforts and innovative research, future research should maximize the therapeutic potential of tDCS for individuals with epilepsy.

# References


Abela, E. *et al.* (2019) 'Slower alpha rhythm associates with poorer seizure control in epilepsy', *Annals of Clinical and Translational Neurology*, 6(2), pp. 333–343. Available at: https://doi.org/10.1002/acn3.710.

Acerbo, E. *et al.* (2022) 'Focal non-invasive deep-brain stimulation with temporal interference for the suppression of epileptic biomarkers', *Frontiers in Neuroscience*, 16, p. 945221. Available at: https://doi.org/10.3389/fnins.2022.945221.

Akiyama, T. *et al.* (2011) 'Focal resection of fast ripples on extraoperative intracranial EEG improves seizure outcome in pediatric epilepsy: Interictal HFOs and Seizure Outcome', *Epilepsia*, 52(10), pp. 1802–1811. Available at: https://doi.org/10.1111/j.1528-1167.2011.03199.x.

Allen, P.J., Fish, D.R. and Smith, S.J.M. (1992) 'Very high-frequency rhythmic activity during SEEG suppression in frontal lobe epilepsy', *Electroencephalography and Clinical Neurophysiology*, 82(2), pp. 155–159. Available at: https://doi.org/10.1016/0013-4694(92)90160-J.

Anderson, D.E., Madhavan, D. and Swaminathan, A. (2020) 'Global brain network dynamics predict therapeutic responsiveness to cannabidiol treatment for refractory epilepsy', *Brain Communications*, 2(2), p. fcaa140. Available at: https://doi.org/10.1093/braincomms/fcaa140.

Antal, A. *et al.* (2017) 'Low intensity transcranial electric stimulation: Safety, ethical, legal regulatory and application guidelines', *Clinical Neurophysiology*, 128(9), pp. 1774–1809. Available at: https://doi.org/10.1016/j.clinph.2017.06.001.

Antal, A. *et al.* (2022) 'Non-invasive brain stimulation and neuroenhancement', *Clinical Neurophysiology Practice*, 7, pp. 146–165. Available at: https://doi.org/10.1016/j.cnp.2022.05.002.

Antal, A., Nitsche, M.A. and Paulus, W. (2001) 'External modulation of visual perception in humans':, *Neuroreport*, 12(16), pp. 3553–3555. Available at: https://doi.org/10.1097/00001756-200111160-00036.

Assenza, G. *et al.* (2017) 'Cathodal transcranial direct current stimulation reduces seizure frequency in adults with drug-resistant temporal lobe epilepsy: A sham controlled study', *Brain Stimulation*, 10(2), pp. 333–335. Available at: https://doi.org/10.1016/j.brs.2016.12.005.

Aubert, S. *et al.* (2009) 'Local and remote epileptogenicity in focal cortical dysplasias and neurodevelopmental tumours', *Brain*, 132(11), pp. 3072–3086. Available at: https://doi.org/10.1093/brain/awp242.

Auvichayapat, N. *et al.* (2013) 'Transcranial Direct Current Stimulation for Treatment of Refractory Childhood Focal Epilepsy', *Brain Stimulation*, 6(4), pp. 696–700. Available at: https://doi.org/10.1016/j.brs.2013.01.009.

Auvichayapat, N. *et al.* (2016) 'Transcranial Direct Current Stimulation for Treatment of Childhood Pharmacoresistant Lennox–Gastaut Syndrome: A Pilot Study', *Frontiers in Neurology*, 7. Available at: https://doi.org/10.3389/fneur.2016.00066.

Ayala, G.F. *et al.* (1973) 'Genesis of epileptic interictal spikes. New knowledge of cortical feedback systems suggests a neurophysiological explanation of brief paroxysms', *Brain Research*, 52, pp. 1–17. Available at: https://doi.org/10.1016/0006-8993(73)90647-1.

Ayala, M. *et al.* (2011) 'Subdural EEG Classification Into Seizure and Nonseizure Files Using Neural Networks in the Gamma Frequency Band', *Journal of Clinical Neurophysiology*, 28(1), pp. 20–29. Available at: https://doi.org/10.1097/WNP.0b013e31820512ee.

Azeem, A. *et al.* (2021) 'Interictal spike networks predict surgical outcome in patients with drug-resistant focal epilepsy', *Annals of Clinical and Translational Neurology*, 8(6), pp. 1212–1223. Available at: https://doi.org/10.1002/acn3.51337.

Babajani-Feremi, A. *et al.* (2018) 'Predicting seizure outcome of vagus nerve stimulation using MEG-based network topology', *NeuroImage: Clinical*, 19, pp. 990–999. Available at: https://doi.org/10.1016/j.nicl.2018.06.017.

Baillet, S. (2014) 'Forward and Inverse Problems of MEG/EEG', in D. Jaeger and R. Jung (eds) *Encyclopedia of Computational Neuroscience*. New York, NY: Springer New York, pp. 1–8. Available at: https://doi.org/10.1007/978-1-4614-7320-6_529-1.

Balatskaya, A. *et al.* (2020) 'The "Connectivity Epileptogenicity Index " (cEI), a method for mapping the different seizure onset patterns in StereoElectroEncephalography recorded seizures', *Clinical Neurophysiology*, 131(8), pp. 1947–1955. Available at: https://doi.org/10.1016/j.clinph.2020.05.029.

Bancaud, J. *et al.* (1970) 'Kojewnikow syndrome and somato-motor attacks (clinical, E.E.G., E.M.G. and S.E.E.G. study)', *Encephale*, pp. 391–438.

Bancaud, J. and Talairach, J. (1965) 'L'électroencéphalographie de profondeur (Stéréo-électro-encéphalographie dans l'épilepsie)', *Epilepy. Mod. Probl. Pharmacopsychiat.*, 4, pp. 29–41.

Bandarabadi, M. *et al.* (2015) 'Epileptic seizure prediction using relative spectral power features', *Clinical Neurophysiology*, 126(2), pp. 237–248. Available at: https://doi.org/10.1016/j.clinph.2014.05.022.

Bangel, K.A., Pang, K. and Baker, M.R. (2023) 'Cathodal Transcranial Direct Current Stimulation for Treatment of Rasmussen Encephalitis', *Neurology*, 100(10), pp. 484–485. Available at: https://doi.org/10.1212/WNL.0000000000201644.

Barbati, G. *et al.* (2004) 'Optimization of an independent component analysis approach for artifact identification and removal in magnetoencephalographic signals', *Clinical Neurophysiology*, 115(5), pp. 1220–1232. Available at: https://doi.org/10.1016/j.clinph.2003.12.015.

Bartolomei, F. *et al.* (2002) 'Les investigations prechirurgicales des epilepsies', *Revue Neurologique*, (158), pp. 4S55-4S64.

Bartolomei, F. *et al.* (2004) 'EEG and video-EEG explorations in refractory partial epilepsy', *Revue Neurologique*, 160(Spec No1), pp. 5S81-90.

Bartolomei, F. *et al.* (2016) 'How does vagal nerve stimulation (VNS) change EEG brain functional connectivity?', *Epilepsy Research*, 126, pp. 141–146. Available at: https://doi.org/10.1016/j.eplepsyres.2016.06.008.

Bartolomei, F. *et al.* (2017) 'Defining epileptogenic networks: Contribution of SEEG and signal analysis', *Epilepsia*, 58(7), pp. 1131–1147. Available at: https://doi.org/10.1111/epi.13791.

Bartolomei, F., Chauvel, P. and Wendling, F. (2008) 'Epileptogenicity of brain structures in human temporal lobe epilepsy: a quantified study from intracerebral EEG', *Brain*, 131(7), pp. 1818–1830. Available at: https://doi.org/10.1093/brain/awn111.

Bartolomei, F., Guye, M. and Wendling, F. (2013) 'Abnormal binding and disruption in large scale networks involved in human partial seizures', *EPJ Nonlinear Biomedical Physics*, 1(1), p. 4. Available at: https://doi.org/10.1140/epjnbp11.

Bassett, D.S. and Sporns, O. (2017) 'Network neuroscience', *Nature Neuroscience*, 20(3), pp. 353–364. Available at: https://doi.org/10.1038/nn.4502.

Bastos, A.M. and Schoffelen, J.-M. (2016) 'A Tutorial Review of Functional Connectivity Analysis Methods and Their Interpretational Pitfalls', *Frontiers in Systems Neuroscience*, 9. Available at: https://doi.org/10.3389/fnsys.2015.00175.

Bates, D. *et al.* (2015) 'Fitting Linear Mixed-Effects Models Using lme4', *Journal of Statistical Software*, 67(1). Available at: https://doi.org/10.18637/jss.v067.i01.

Baud, M.O. *et al.* (2018) 'European trends in epilepsy surgery', *Neurology*, 91(2), pp. e96–e106. Available at: https://doi.org/10.1212/WNL.0000000000005776.

Begley, C. *et al.* (2022) 'The global cost of epilepsy: A systematic review and extrapolation', *Epilepsia*, 63(4), pp. 892–903. Available at: https://doi.org/10.1111/epi.17165.

Benar, C.-G. *et al.* (2005) 'Statistical Maps for EEG Dipolar Source Localization', *IEEE Transactions on Biomedical Engineering*, 52(3), pp. 401–413. Available at: https://doi.org/10.1109/TBME.2004.841263.

Bénar, C.G. *et al.* (2010) 'Pitfalls of high-pass filtering for detecting epileptic oscillations: A technical note on "false" ripples', *Clinical Neurophysiology*, 121(3), pp. 301–310. Available at: https://doi.org/10.1016/j.clinph.2009.10.019.

Berényi, A. *et al.* (2012) 'Closed-Loop Control of Epilepsy by Transcranial Electrical Stimulation', *Science*, 337(6095), pp. 735–737. Available at: https://doi.org/10.1126/science.1223154.

Bertram, E.H. *et al.* (2001) 'The Midline Thalamus: Alterations and a Potential Role in Limbic Epilepsy', *Epilepsia*, 42(8), pp. 967–978. Available at: https://doi.org/10.1046/j.1528-1157.2001.042008967.x.

Besio, W.G., Koka, K. and Cole, A.J. (2007) 'Effects of Noninvasive Transcutaneous Electrical Stimulation via Concentric Ring Electrodes on Pilocarpine-induced Status Epilepticus in Rats', *Epilepsia*, 48(12), pp. 2273–2279. Available at: https://doi.org/10.1111/j.1528-1167.2007.01202.x.

Bettus, G. *et al.* (2008) 'Enhanced EEG functional connectivity in mesial temporal lobe epilepsy', *Epilepsy Research*, 81(1), pp. 58–68. Available at: https://doi.org/10.1016/j.eplepsyres.2008.04.020.

Bikson, M. *et al.* (2001) 'Suppression of epileptiform activity by high frequency sinusoidal fields in rat hippocampal slices', *The Journal of Physiology*, 531(1), pp. 181–191. Available at: https://doi.org/10.1111/j.1469-7793.2001.0181j.x.

Bikson, M. *et al.* (2004) 'Effects of uniform extracellular DC electric fields on excitability in rat hippocampal slices *in vitro*', *The Journal of Physiology*, 557(1), pp. 175–190. Available at: https://doi.org/10.1113/jphysiol.2003.055772.

Bikson, M. *et al.* (2016) 'Safety of Transcranial Direct Current Stimulation: Evidence Based Update 2016', *Brain Stimulation*, 9(5), pp. 641–661. Available at: https://doi.org/10.1016/j.brs.2016.06.004.

Bikson, M. *et al.* (2019) 'Transcranial electrical stimulation nomenclature', *Brain Stimulation*, 12(6), pp. 1349–1366. Available at: https://doi.org/10.1016/j.brs.2019.07.010.

Biondi, A. *et al.* (2022) 'Spontaneous and TMS-related EEG changes as new biomarkers to measure anti-epileptic drug effects', *Scientific Reports*, 12(1), p. 1919. Available at: https://doi.org/10.1038/s41598-022-05179-x.

Bodin, C. *et al.* (2015) 'Responders to vagus nerve stimulation (VNS) in refractory epilepsy have reduced interictal cortical synchronicity on scalp EEG', *Epilepsy Research*, 113, pp. 98–103. Available at: https://doi.org/10.1016/j.eplepsyres.2015.03.018.

Borckardt, J.J. *et al.* (2012) 'A Pilot Study of the Tolerability and Effects of High-Definition Transcranial Direct Current Stimulation (HD-tDCS) on Pain Perception', *The Journal of Pain*, 13(2), pp. 112–120. Available at: https://doi.org/10.1016/j.jpain.2011.07.001.

Bouwens Van Der Vlis, T.A.M. *et al.* (2019) 'Deep brain stimulation of the anterior nucleus of the thalamus for drug-resistant epilepsy', *Neurosurgical Review*, 42(2), pp. 287–296. Available at: https://doi.org/10.1007/s10143-017-0941-x.

Bragin, A. *et al.* (2002) 'Local Generation of Fast Ripples in Epileptic Brain', *The Journal of Neuroscience*, 22(5), pp. 2012–2021. Available at: https://doi.org/10.1523/JNEUROSCI.22-05-02012.2002.

Brazier, M.A.B. (1966) 'A Study of the Electrical Fields at the Surface of the Head', *American Journal of EEG Technology*, 6(4), pp. 114–128. Available at: https://doi.org/10.1080/00029238.1966.11080676.

Bréchet, L. *et al.* (2021) 'Patient-Tailored, Home-Based Non-invasive Brain Stimulation for Memory Deficits in Dementia Due to Alzheimer's Disease', *Frontiers in Neurology*, 12, p. 598135. Available at: https://doi.org/10.3389/fneur.2021.598135.

Brodie, M.J. and Kwan, P. (2002) 'Staged approach to epilepsy management', *Neurology*, 58(Issue 8, Supplement 5), pp. S2–S8. Available at: https://doi.org/10.1212/WNL.58.8_suppl_5.S2.

Brookes, M.J., Woolrich, M.W. and Barnes, G.R. (2012) 'Measuring functional connectivity in MEG: A multivariate approach insensitive to linear source leakage', *NeuroImage*, 63(2), pp. 910–920. Available at: https://doi.org/10.1016/j.neuroimage.2012.03.048.

Brovelli, A. *et al.* (2004) 'Beta oscillations in a large-scale sensorimotor cortical network: Directional influences revealed by Granger causality', *Proceedings of the National Academy of Sciences*, 101(26), pp. 9849–9854. Available at: https://doi.org/10.1073/pnas.0308538101.

Bullmore, E. and Sporns, O. (2009) 'Complex brain networks: graph theoretical analysis of structural and functional systems', *Nature Reviews Neuroscience*, 10(3), pp. 186–198. Available at: https://doi.org/10.1038/nrn2575.

Bullmore, E. and Sporns, O. (2012) 'The economy of brain network organization', *Nature Reviews Neuroscience*, 13(5), pp. 336–349. Available at: https://doi.org/10.1038/nrn3214.

Burman, R.J. *et al.* (2019) 'Excitatory GABAergic signalling is associated with benzodiazepine resistance in status epilepticus', *Brain*, 142(11), pp. 3482–3501. Available at: https://doi.org/10.1093/brain/awz283.

Buzsáki, G., Anastassiou, C.A. and Koch, C. (2012) 'The origin of extracellular fields and currents — EEG, ECoG, LFP and spikes', *Nature Reviews Neuroscience*, 13(6), pp. 407–420. Available at: https://doi.org/10.1038/nrn3241.

Buzsaki, G. and Draguhn, A. (2004) 'Neuronal Oscillations in Cortical Networks', 304. Available at: https://doi.org/10.1126/science.1099745.

Cabral, J., Kringelbach, M.L. and Deco, G. (2017) 'Functional connectivity dynamically evolves on multiple time-scales over a static structural connectome: Models and mechanisms', *NeuroImage*, 160, pp. 84–96. Available at: https://doi.org/10.1016/j.neuroimage.2017.03.045.

Cardinale, F. *et al.* (2019) 'Stereoelectroencephalography: retrospective analysis of 742 procedures in a single centre', *Brain*, 142(9), pp. 2688–2704. Available at: https://doi.org/10.1093/brain/awz196.

Cascino, G.D. (2002) 'Video-EEG Monitoring in Adults', *Epilepsia*, 43(s3), pp. 80–93. Available at: https://doi.org/10.1046/j.1528-1157.43.s.3.14.x.

Centeno, M. and Carmichael, D.W. (2014) 'Network Connectivity in Epilepsy: Resting State fMRI and EEGâ€"fMRI Contributions', *Frontiers in Neurology*, 5. Available at: https://doi.org/10.3389/fneur.2014.00093.

Cerf, R. and El Ouasdad, E.H. (2000) 'Spectral analysis of stereo-electroencephalograms: preictal slowing in partial epilepsies', *Biological Cybernetics*, 83(5), pp. 399–405. Available at: https://doi.org/10.1007/s004220000178.

Chadwick, D. (1990) 'Diagnosis of epilepsy', *The Lancet*, 336, pp. 291–295.

Chang, W.-P., Lu, H.-C. and Shyu, B.-C. (2015) 'Treatment with direct-current stimulation against cingulate seizure-like activity induced by 4-aminopyridine and bicuculline in an in vitro mouse model', *Experimental Neurology*, 265, pp. 180–192. Available at: https://doi.org/10.1016/j.expneurol.2015.02.002.

Chauvel, P. *et al.* (1986) 'Distinction between the myoclonus-related potential and the epileptic spike in epilepsia partialis continua', *Electroencephalography and Clinical Neurophysiology*, 64(4), pp. 304–307. Available at: https://doi.org/10.1016/0013-4694(86)90154-9.

Chauvel, P. *et al.* (1993) 'Electrical stimulation with intracerebral electrodes to evoke seizures', *Adv. Neurol*, 63, pp. 115–121.

Chen, H. *et al.* (2023) 'Brain functional connectivity-based prediction of vagus nerve stimulation efficacy in pediatric pharmacoresistant epilepsy', *CNS Neuroscience & Therapeutics*, 29(11), pp. 3259–3268. Available at: https://doi.org/10.1111/cns.14257.

Chen, J. *et al.* (2021) 'Can Spectral Power Be Used as a Candidate Seizure Marker of the Periodic Discharges Pattern?', *Frontiers in Neurology*, 12, p. 642669. Available at: https://doi.org/10.3389/fneur.2021.642669.

Chen, L. *et al.* (2017) 'KCC2 downregulation facilitates epileptic seizures', *Scientific Reports*, 7(1), p. 156. Available at: https://doi.org/10.1038/s41598-017-00196-7.

Chen, Z. *et al.* (2018) 'Treatment Outcomes in Patients With Newly Diagnosed Epilepsy Treated With Established and New Antiepileptic Drugs: A 30-Year Longitudinal Cohort Study', *JAMA Neurology*, 75(3), p. 279. Available at: https://doi.org/10.1001/jamaneurol.2017.3949.

Cho, J.R. *et al.* (2012) 'Effect of levetiracetam monotherapy on background EEG activity and cognition in drug-naïve epilepsy patients', *Clinical Neurophysiology*, 123(5), pp. 883–891. Available at: https://doi.org/10.1016/j.clinph.2011.09.012.

Cirillo, G. *et al.* (2017) 'Neurobiological after-effects of non-invasive brain stimulation', *Brain Stimulation*, 10(1), pp. 1–18. Available at: https://doi.org/10.1016/j.brs.2016.11.009.

Clemens, B. (2004) 'Pathological theta oscillations in idiopathic generalised epilepsy', *Clinical Neurophysiology*, 115(6), pp. 1436–1441. Available at: https://doi.org/10.1016/j.clinph.2004.01.018.

Clemens, B. *et al.* (2010) 'Theta EEG source localization using LORETA in partial epilepsy patients with and without medication', *Clinical Neurophysiology*, 121(6), pp. 848–858. Available at: https://doi.org/10.1016/j.clinph.2010.01.020.

Clemens, B. *et al.* (2011) 'EEG functional connectivity of the intrahemispheric cortico-cortical network of idiopathic generalized epilepsy', *Epilepsy Research*, 96(1–2), pp. 11–23. Available at: https://doi.org/10.1016/j.eplepsyres.2011.04.011.

Clemens, B. *et al.* (2014) 'Valproate treatment normalizes EEG functional connectivity in successfully treated idiopathic generalized epilepsy patients', *Epilepsy Research*, 108(10), pp. 1896–1903. Available at: https://doi.org/10.1016/j.eplepsyres.2014.09.032.

Clemens, B., Szigeti, G. and Barta, Z. (2000) 'EEG frequency profiles of idiopathic generalised epilepsy syndromes', *Epilepsy Research*, 42(2–3), pp. 105–115. Available at: https://doi.org/10.1016/S0920-1211(00)00167-4.

Cockerell, O.C. *et al.* (1996) 'Clinical and physiological features of epilepsia partialis continua: Cases ascertained in the UK', *Brain*, 119(2), pp. 393–407. Available at: https://doi.org/10.1093/brain/119.2.393.

Coito, A. *et al.* (2015) 'Dynamic directed interictal connectivity in left and right temporal lobe epilepsy', *Epilepsia*, 56(2), pp. 207–217. Available at: https://doi.org/10.1111/epi.12904.

Coito, A. *et al.* (2016) 'Altered directed functional connectivity in temporal lobe epilepsy in the absence of interictal spikes: A high density EEG study', *Epilepsia*, 57(3), pp. 402–411. Available at: https://doi.org/10.1111/epi.13308.

Colombet, B. *et al.* (2015) 'AnyWave: A cross-platform and modular software for visualizing and processing electrophysiological signals', *Journal of Neuroscience Methods*, 242, pp. 118–126. Available at: https://doi.org/10.1016/j.jneumeth.2015.01.017.

Cottone, X.C. *et al.* (2018) 'A New, High-Efficacy, Noninvasive Transcranial Electric Stimulation Tuned to Local Neurodynamics', *Journal of Neuroscience*, 38, pp. 586–594. Available at: https://doi.org/10.1523/JNEUROSCI.2521-16.2017.

Courtens, S. *et al.* (2016) 'Graph Measures of Node Strength for Characterizing Preictal Synchrony in Partial Epilepsy', *Brain Connectivity*, 6(7), pp. 530–539. Available at: https://doi.org/10.1089/brain.2015.0397.

Dale, A.M. and Sereno, I. (1993) 'Improved Localizadon of Cortical Activity by Combining EEG and MEG with MRI Cortical Surface Reconstruction: A Linear Approach', *J Cogn Neurosci.*, 5(2), pp. 162–176. Available at: https://doi.org/10.1162/jocn.1993.5.2.162.

Daoud, M. *et al.* (2022) 'Stereo-EEG based personalized multichannel transcranial direct current stimulation in drug-resistant epilepsy', *Clinical Neurophysiology*, 137, pp. 142–151. Available at: https://doi.org/10.1016/j.clinph.2022.02.023.

Datta, A. *et al.* (2009) 'Gyri-precise head model of transcranial direct current stimulation: Improved spatial focality using a ring electrode versus conventional rectangular pad', *Brain Stimulation*, 2(4), pp. 201-207.e1. Available at: https://doi.org/10.1016/j.brs.2009.03.005.

Datta, A., Bikson, M. and Fregni, F. (2010) 'Transcranial direct current stimulation in patients with skull defects and skull plates: High-resolution computational FEM study of factors altering cortical current flow', *NeuroImage*, 52(4), pp. 1268–1278. Available at: https://doi.org/10.1016/j.neuroimage.2010.04.252.

David, O. *et al.* (2008) 'Identifying Neural Drivers with Functional MRI: An Electrophysiological Validation', *PLoS Biology*. Edited by P. Valdes-Sosa, 6(12), p. e315. Available at: https://doi.org/10.1371/journal.pbio.0060315.

De Benedictis, A. *et al.* (2013) 'Vagus nerve stimulation for drug-resistant Epilepsia Partialis Continua: Report of four cases', *Epilepsy Research*, 107(1–2), pp. 163–171. Available at: https://doi.org/10.1016/j.eplepsyres.2013.07.010.

Denoyer, Y. *et al.* (2020) 'Modelling acute and lasting effects of tDCS on epileptic activity', *Journal of Computational Neuroscience*, 48(2), pp. 161–176. Available at: https://doi.org/10.1007/s10827-020-00745-6.

Destrieux, C. *et al.* (2010) 'Automatic parcellation of human cortical gyri and sulci using standard anatomical nomenclature', *NeuroImage*, 53(1), pp. 1–15. Available at: https://doi.org/10.1016/j.neuroimage.2010.06.010.

Deutschová, B. *et al.* (2021) 'Ictal connectivity changes induced by pulvinar stimulation correlate with improvement of awareness', *Brain Stimulation*, 14(2), pp. 344–346. Available at: https://doi.org/10.1016/j.brs.2021.01.021.

Devinsky, O. *et al.* (2018) 'Epilepsy', *Nature Reviews Disease Primers*, 4(1), p. 18024. Available at: https://doi.org/10.1038/nrdp.2018.24.

Dhamne, S.C. *et al.* (2015) 'Acute seizure suppression by transcranial direct current stimulation in rats', *Annals of Clinical and Translational Neurology*, 2(8), pp. 843–856. Available at: https://doi.org/10.1002/acn3.226.

Díaz, M, H. *et al.* (2019) 'Intra and inter-individual variability in the chaotic component and functional connectivity of the EEG signal in basal eyes closed condition', *Procedia Computer Science*, 162, pp. 966–973. Available at: https://doi.org/10.1016/j.procs.2019.12.077.

van Diessen, E. *et al.* (2013) 'Functional and structural brain networks in epilepsy: What have we learned?', *Epilepsia*, 54(11), pp. 1855–1865. Available at: https://doi.org/10.1111/epi.12350.

Ding, L. *et al.* (2007) 'Ictal source analysis: Localization and imaging of causal interactions in humans', *NeuroImage*, 34(2), pp. 575–586. Available at: https://doi.org/10.1016/j.neuroimage.2006.09.042.

Díaz, G.F. *et al.* (1998) 'Generalized background qEEG abnormalities in localized symptomatic epilepsy', *Electroencephalography and Clinical Neurophysiology*, 106(6), pp. 501–507. Available at: https://doi.org/10.1016/S0013-4694(98)00026-1.

Donoghue, T. *et al.* (2020) 'Parameterizing neural power spectra into periodic and aperiodic components', *Nature Neuroscience*, 23(12), pp. 1655–1665. Available at: https://doi.org/10.1038/s41593-020-00744-x.

Douw, L. *et al.* (2010) '"Functional Connectivity" Is a Sensitive Predictor of Epilepsy Diagnosis after the First Seizure', *PLoS ONE*. Edited by O. Sporns, 5(5), p. e10839. Available at: https://doi.org/10.1371/journal.pone.0010839.

Ekhtiari, H. *et al.* (2019) 'Transcranial electrical and magnetic stimulation (tES and TMS) for addiction medicine: A consensus paper on the present state of the science and the road ahead', *Neuroscience & Biobehavioral Reviews*, 104, pp. 118–140. Available at: https://doi.org/10.1016/j.neubiorev.2019.06.007.

El Tahry, R. and Wang, I.Z. (2017) 'Failed epilepsy surgery: is this the end?', *Acta Neurologica Belgica*, 117(2), pp. 433–440. Available at: https://doi.org/10.1007/s13760-017-0769-8.

Engel, J. *et al.* (1982) 'Pathological findings underlying focal temporal lobe hypometabolism in partial epilepsy', *Annals of Neurology*, 12(6), pp. 518–528. Available at: https://doi.org/10.1002/ana.410120604.

Engel, J. (2001) 'A Proposed Diagnostic Scheme for People with Epileptic Seizures and with Epilepsy: Report of the ILAE Task Force on Classification and Terminology', *Epilepsia*, 42(6), pp. 796–803. Available at: https://doi.org/10.1046/j.1528-1157.2001.10401.x.

Englot, D.J. *et al.* (2011) 'Vagus nerve stimulation for epilepsy: a meta-analysis of efficacy and predictors of response', *J Neurosurg*, 115, pp. 1248–1255.

Englot, D.J. *et al.* (2015) 'Global and regional functional connectivity maps of neural oscillations in focal epilepsy', *Brain*, 138(8), pp. 2249–2262. Available at: https://doi.org/10.1093/brain/awv130.

Englot, D.J. *et al.* (2017) 'Quality-of-life metrics with vagus nerve stimulation for epilepsy from provider survey data', *Epilepsy & Behavior*, 66, pp. 4–9. Available at: https://doi.org/10.1016/j.yebeh.2016.10.005.

Fahoum, F. *et al.* (2022) 'VNS parameters for clinical response in Epilepsy', *Brain Stimulation*, 15(3), pp. 814–821. Available at: https://doi.org/10.1016/j.brs.2022.05.016.

Faria, P. *et al.* (2012) 'Feasibility of focal transcranial DC polarization with simultaneous EEG recording: Preliminary assessment in healthy subjects and human epilepsy', *Epilepsy & Behavior*, 25(3), pp. 417–425. Available at: https://doi.org/10.1016/j.yebeh.2012.06.027.

Ferri, L. *et al.* (2021) 'Is beta band desynchronization related to skin conductance biofeedback effectiveness in drug resistant focal epilepsy?', *Epilepsy Research*, 169, p. 106528. Available at: https://doi.org/10.1016/j.eplepsyres.2020.106528.

Fiest, K.M. *et al.* (2016) 'Prevalence and incidence of epilepsy'.

Fischer, D.B. *et al.* (2017) 'Multifocal tDCS targeting the resting state motor network increases cortical excitability beyond traditional tDCS targeting unilateral motor cortex', *NeuroImage*, 157, pp. 34–44. Available at: https://doi.org/10.1016/j.neuroimage.2017.05.060.

Fisher, R. *et al.* (2010) 'Electrical stimulation of the anterior nucleus of thalamus for treatment of refractory epilepsy', *Epilepsia*, 51(5), pp. 899–908. Available at: https://doi.org/10.1111/j.1528-1167.2010.02536.x.

Fisher, R.S. *et al.* (2005) 'Epileptic Seizures and Epilepsy: Definitions Proposed by the International League Against Epilepsy (ILAE) and the International Bureau for Epilepsy (IBE)', *Epilepsia*, 46(4), pp. 470–472. Available at: https://doi.org/10.1111/j.0013-9580.2005.66104.x.

Fisher, R.S. *et al.* (2017) 'Operational classification of seizure types by the International League Against Epilepsy: Position Paper of the ILAE Commission for Classification and Terminology', *Epilepsia*, 58(4), pp. 522–530. Available at: https://doi.org/10.1111/epi.13670.

Fisher, R.S. (2023) 'Deep brain stimulation of thalamus for epilepsy', *Neurobiology of Disease*, 179, p. 106045. Available at: https://doi.org/10.1016/j.nbd.2023.106045.

Fox, M.D. *et al.* (2014) 'Resting-state networks link invasive and noninvasive brain stimulation across diverse psychiatric and neurological diseases', *Proceedings of the National Academy of Sciences*, 111(41). Available at: https://doi.org/10.1073/pnas.1405003111.

Francis, J.T., Gluckman, B.J. and Schiff, S.J. (2003) 'Sensitivity of Neurons to Weak Electric Fields', *The Journal of Neuroscience*, 23(19), pp. 7255–7261. Available at: https://doi.org/10.1523/JNEUROSCI.23-19-07255.2003.

Frank, E. (1952) 'Electric Potential Produced by Two Point Current Sources in a Homogeneous Conducting Sphere', *Journal of Applied Physics*, 23(11), pp. 1225–1228. Available at: https://doi.org/10.1063/1.1702037.

Fraschini, M. *et al.* (2013) 'VNS induced desynchronization in gamma bands correlates with positive clinical outcome in temporal lobe pharmacoresistant epilepsy', *Neuroscience Letters*, 536, pp. 14–18. Available at: https://doi.org/10.1016/j.neulet.2012.12.044.

Frauscher, B. *et al.* (2017) 'High-frequency oscillations: The state of clinical research', *Epilepsia*, 58(8), pp. 1316–1329. Available at: https://doi.org/10.1111/epi.13829.

Fregni, F. *et al.* (2006) 'A Controlled Clinical Trial of Cathodal DC Polarization in Patients with Refractory Epilepsy', *Epilepsia*, 47(2), pp. 335–342. Available at: https://doi.org/10.1111/j.1528-1167.2006.00426.x.

Fregni, F. *et al.* (2021) 'Evidence-Based Guidelines and Secondary Meta-Analysis for the Use of Transcranial Direct Current Stimulation in Neurological and Psychiatric Disorders', *International Journal of Neuropsychopharmacology*, 24(4), pp. 256–313. Available at: https://doi.org/10.1093/ijnp/pyaa051.

Friston, K.J. (2011) 'Functional and Effective Connectivity: A Review', *Brain Connectivity*, 1(1), pp. 13–36. Available at: https://doi.org/10.1089/brain.2011.0008.

Fröhlich, F. and McCormick, D.A. (2010) 'Endogenous Electric Fields May Guide Neocortical Network Activity', *Neuron*, 67(1), pp. 129–143. Available at: https://doi.org/10.1016/j.neuron.2010.06.005.

Galan-Gadea, A. *et al.* (2023) 'Spherical harmonics representation of the steady-state membrane potential shift induced by tDCS in realistic neuron models', *Journal of Neural Engineering*, 20(2), p. 026004. Available at: https://doi.org/10.1088/1741-2552/acbabd.

Gallotto, S. and Seeck, M. (2023) 'EEG biomarker candidates for the identification of epilepsy', *Clinical Neurophysiology Practice*, 8, pp. 32–41. Available at: https://doi.org/10.1016/j.cnp.2022.11.004.

Gao, R., Peterson, E.J. and Voytek, B. (2017) 'Inferring synaptic excitation/inhibition balance from field potentials', *NeuroImage*, 158, pp. 70–78. Available at: https://doi.org/10.1016/j.neuroimage.2017.06.078.

Garcia-Larrea, L. *et al.* (2019) 'At-Home Cortical Stimulation for Neuropathic Pain: a Feasibility Study with Initial Clinical Results', *Neurotherapeutics*, 16(4), pp. 1198–1209. Available at: https://doi.org/10.1007/s13311-019-00734-3.

Gavaret, M., Badier, J.M. and Chauvel, P. (2008) 'High-resolution EEG (HR-EEG) and magnetoencephalography (MEG)', *Neurochirurgie*, 54, pp. 185–190.

Geller, E.B. (2018) 'Responsive neurostimulation: Review of clinical trials and insights into focal epilepsy', *Epilepsy & Behavior*, 88, pp. 11–20. Available at: https://doi.org/10.1016/j.yebeh.2018.06.042.

Gerster, M. *et al.* (2022) 'Separating Neural Oscillations from Aperiodic 1/f Activity: Challenges and Recommendations', *Neuroinformatics*, 20(4), pp. 991–1012. Available at: https://doi.org/10.1007/s12021-022-09581-8.

Ghai, R.S., Bikson, M. and Durand, D.M. (2000) 'Effects of Applied Electric Fields on Low-Calcium Epileptiform Activity in the CA1 Region of Rat Hippocampal Slices', *Journal of Neurophysiology*, 84(1), pp. 274–280. Available at: https://doi.org/10.1152/jn.2000.84.1.274.

Ghin, F., O'Hare, L. and Pavan, A. (2021) 'Electrophysiological aftereffects of high-frequency transcranial random noise stimulation (hf-tRNS): an EEG investigation', *Experimental Brain Research*, 239(8), pp. 2399–2418. Available at: https://doi.org/10.1007/s00221-021-06142-4.

Giannakakis, E. *et al.* (2020) 'Computational modelling of the long-term effects of brain stimulation on the local and global structural connectivity of epileptic patients', *PLOS ONE*. Edited by T. Wennekers, 15(2), p. e0221380. Available at: https://doi.org/10.1371/journal.pone.0221380.

Gluckman, B.J. *et al.* (1996) 'Electric field suppression of epileptiform activity in hippocampal slices', *Journal of Neurophysiology*, 76(6), pp. 4202–4205. Available at: https://doi.org/10.1152/jn.1996.76.6.4202.

Gnatkovsky, V. *et al.* (2011) 'Identification of reproducible ictal patterns based on quantified frequency analysis of intracranial EEG signals: Quantified Analysis of Intracranial EEG', *Epilepsia*, 52(3), pp. 477–488. Available at: https://doi.org/10.1111/j.1528-1167.2010.02931.x.

Goldenholz, D.M. and Goldenholz, S.R. (2020) 'Placebo in epilepsy', in *International Review of Neurobiology*. Elsevier, pp. 231–266. Available at: https://doi.org/10.1016/bs.irn.2020.03.033.

Goncharova, I.I. *et al.* (2003) 'EMG contamination of EEG: spectral and topographical characteristics', *Clinical Neurophysiology*, 114(9), pp. 1580–1593. Available at: https://doi.org/10.1016/S1388-2457(03)00093-2.

Gotman, J. (1983) 'Measurement of small time differences between EEG channels: method and application to epileptic seizure propagation', *Electroencephalogr Clin Neurophysiol*, 56(5), pp. 501–514. Available at: https://doi.org/10.1016/0013-4694(83)90235-3.

Gramfort, A. *et al.* (2010) 'OpenMEEG: opensource software for quasistatic bioelectromagnetics', *BioMedical Engineering OnLine*, 9(1), p. 45. Available at: https://doi.org/10.1186/1475-925X-9-45.

Greiner, H.M. *et al.* (2016) 'Should spikes on post-resection ECoG guide pediatric epilepsy surgery?', *Epilepsy Research*, 122, pp. 73–78. Available at: https://doi.org/10.1016/j.eplepsyres.2016.02.011.

Grinenko, O. *et al.* (2018) 'A fingerprint of the epileptogenic zone in human epilepsies', *Brain*, 141(1), pp. 117–131. Available at: https://doi.org/10.1093/brain/awx306.

Grossman, N. *et al.* (2017) 'Noninvasive Deep Brain Stimulation via Temporally Interfering Electric Fields', *Cell*, 169(6), pp. 1029-1041.e16. Available at: https://doi.org/10.1016/j.cell.2017.05.024.

Guerrini, R. (2009) 'Physiology of epilepsia partialis continua and subcortical mechanisms of status epilepticus', *Epilepsia*, 50, pp. 7–9. Available at: https://doi.org/10.1111/j.1528-1167.2009.02356.x.

Guye, M. (2006) 'The role of corticothalamic coupling in human temporal lobe epilepsy', *Brain*, 129(7), pp. 1917–1928. Available at: https://doi.org/10.1093/brain/awl151.

Hachem, L.D., Wong, S.M. and Ibrahim, G.M. (2018) 'The vagus afferent network: emerging role in translational connectomics', *Neurosurgical Focus*, 45(3), p. E2. Available at: https://doi.org/10.3171/2018.6.FOCUS18216.

Haegens, S. *et al.* (2014) 'Inter- and intra-individual variability in alpha peak frequency', *NeuroImage*, 92, pp. 46–55. Available at: https://doi.org/10.1016/j.neuroimage.2014.01.049.

Hallez, H. *et al.* (2007) 'Review on solving the forward problem in EEG source analysis', *Journal of NeuroEngineering and Rehabilitation*, 4(1), p. 46. Available at: https://doi.org/10.1186/1743-0003-4-46.

Hannah, R., Iacovou, A. and Rothwell, J.C. (2019) 'Direction of TDCS current flow in human sensorimotor cortex influences behavioural learning', *Brain Stimulation*, 12(3), pp. 684–692. Available at: https://doi.org/10.1016/j.brs.2019.01.016.

Hao, J. *et al.* (2021) 'Functional Network Alterations as Markers for Predicting the Treatment Outcome of Cathodal Transcranial Direct Current Stimulation in Focal Epilepsy', *Frontiers in Human Neuroscience*, 15, p. 637071. Available at: https://doi.org/10.3389/fnhum.2021.637071.

Hashemi, M. *et al.* (2021) 'On the influence of prior information evaluated by fully Bayesian criteria in a personalized whole-brain model of epilepsy spread', *PLOS Computational Biology*. Edited by P.N. Taylor, 17(7), p. e1009129. Available at: https://doi.org/10.1371/journal.pcbi.1009129.

He, B. *et al.* (1987) 'Electric Dipole Tracing in the Brain by Means of the Boundary Element Method and Its Accuracy', *IEEE Transactions on Biomedical Engineering*, BME-34(6), pp. 406–414. Available at: https://doi.org/10.1109/TBME.1987.326056.

He, B. and Musha, T. (1992) 'Equivalent dipole estimation of spontaneous EEG alpha activity: two-moving dipole approach', *Med Biol Eng Comput.*, 30(3), pp. 324–332. Available at: https://doi.org/10.1007/BF02446971.

He, B.J. *et al.* (2010) 'The Temporal Structures and Functional Significance of Scale-free Brain Activity', *Neuron*, 66(3), pp. 353–369. Available at: https://doi.org/10.1016/j.neuron.2010.04.020.

Heck, C.N. *et al.* (2014) 'Two-year seizure reduction in adults with medically intractable partial onset epilepsy treated with responsive neurostimulation: Final results of the RNS System Pivotal trial', *Epilepsia*, 55(3), pp. 432–441. Available at: https://doi.org/10.1111/epi.12534.

Helmholtz, H. (1853) 'Ueber einige Gesetze der Vertheilung elektrischer Ströme in körperlichen Leitern, mit Anwendung auf die thierisch-elektrischen Versuche', *Ann. Phys. Chem.*, 89, pp. 211-233,353-377.

Hillebrand, A. *et al.* (2005) 'A new approach to neuroimaging with magnetoencephalography', *Human Brain Mapping*, 25(2), pp. 199–211. Available at: https://doi.org/10.1002/hbm.20102.

Holmes, M.D. *et al.* (2019) 'Safety of slow-pulsed transcranial electrical stimulation in acute spike suppression', *Annals of Clinical and Translational Neurology*, 6(12), pp. 2579–2585. Available at: https://doi.org/10.1002/acn3.50934.

Huang, Y. *et al.* (2017) 'Measurements and models of electric fields in the in vivo human brain during transcranial electric stimulation', *eLife*, 6, p. e18834. Available at: https://doi.org/10.7554/eLife.18834.

Huang, Y. and Parra, L.C. (2019) 'Can transcranial electric stimulation with multiple electrodes reach deep targets?', *Brain Stimulation*, 12(1), pp. 30–40. Available at: https://doi.org/10.1016/j.brs.2018.09.010.

Inaji, M. *et al.* (2020) 'Responsive Neurostimulation as a Novel Palliative Option in Epilepsy Surgery', *Neurologia medico-chirurgica*, 61(1), pp. 1–11. Available at: https://doi.org/10.2176/nmc.st.2020-0172.

Isnard, J. *et al.* (2018) 'French guidelines on stereoelectroencephalography (SEEG)', *Neurophysiologie Clinique*, 48(1), pp. 5–13. Available at: https://doi.org/10.1016/j.neucli.2017.11.005.

Jackson, M.P. *et al.* (2016) 'Animal models of transcranial direct current stimulation: Methods and mechanisms', *Clinical Neurophysiology*, 127(11), pp. 3425–3454. Available at: https://doi.org/10.1016/j.clinph.2016.08.016.

Jacobs, J. *et al.* (2010) 'High-frequency electroencephalographic oscillations correlate with outcome of epilepsy surgery', *Annals of Neurology*, 67(2), pp. 209–220. Available at: https://doi.org/10.1002/ana.21847.

Jasper, H.H. (1958) 'The Ten-Twenty Electrode System of the International Federation', *Electroencephalography and Clinical Neurophysiology*, 10, pp. 371–375.

Jehi, L. *et al.* (2015) 'The evolution of epilepsy surgery between 1991 and 2011 in nine major epilepsy centers across the United States, Germany, and Australia', *Epilepsia*, 56(10), pp. 1526–1533. Available at: https://doi.org/10.1111/epi.13116.

Jiruska, P. *et al.* (2013) 'Synchronization and desynchronization in epilepsy: controversies and hypotheses', *The Journal of Physiology*, 591(4), pp. 787–797. Available at: https://doi.org/10.1113/jphysiol.2012.239590.

Job, A.-S. *et al.* (2019) 'Epileptogenicity Maps of Intracerebral Fast Activities (60–100 Hz) at Seizure Onset in Epilepsy Surgery Candidates', *Frontiers in Neurology*, 10, p. 1263. Available at: https://doi.org/10.3389/fneur.2019.01263.

Jonmohamadi, Y. *et al.* (2014) 'Source-space ICA for EEG source separation, localization, and time-course reconstruction', *NeuroImage*, 101, pp. 720–737. Available at: https://doi.org/10.1016/j.neuroimage.2014.07.052.

Jung, T. *et al.* (2000) 'Removing electroencephalographic artifacts by blind source separation', *Psychophysiology*, 37(2), pp. 163–178. Available at: https://doi.org/10.1111/1469-8986.3720163.

Kahane, P. *et al.* (2006) 'The Bancaud and Talairach view on the epileptogenic zone: a working hypothesis', *Epileptic Disorders*, 8(S2). Available at: https://doi.org/10.1684/j.1950-6945.2006.tb00206.x.

Kamida, T. *et al.* (2011) 'Transcranial direct current stimulation decreases convulsions and spatial memory deficits following pilocarpine-induced status epilepticus in immature rats', *Behavioural Brain Research*, 217(1), pp. 99–103. Available at: https://doi.org/10.1016/j.bbr.2010.08.050.

Karvigh, S.A. *et al.* (2017) 'HD-tDCS in refractory lateral frontal lobe epilepsy patients', *Seizure*, 47, pp. 74–80. Available at: https://doi.org/10.1016/j.seizure.2017.03.005.

Kaufmann, E. *et al.* (2021) 'Acute effects of spaced cathodal transcranial direct current stimulation in drug resistant focal epilepsies', *Clinical Neurophysiology*, 132(7), pp. 1444–1451. Available at: https://doi.org/10.1016/j.clinph.2021.03.048.

Kaye, H.L. *et al.* (2021) 'Personalized, Multisession, Multichannel Transcranial Direct Current Stimulation in Medication-Refractory Focal Epilepsy: An Open-Label Study', *Journal of Clinical Neurophysiology*, Publish Ahead of Print. Available at: https://doi.org/10.1097/WNP.0000000000000838.

Keeser, D. *et al.* (2011) 'Prefrontal Transcranial Direct Current Stimulation Changes Connectivity of Resting-State Networks during fMRI', *The Journal of Neuroscience*, 31(43), pp. 15284–15293. Available at: https://doi.org/10.1523/JNEUROSCI.0542-11.2011.

Khan, A. *et al.* (2023) 'Can individually targeted and optimized multi-channel tDCS outperform standard bipolar tDCS in stimulating the primary somatosensory cortex?', *Brain Stimulation*, 16(1), pp. 1–16. Available at: https://doi.org/10.1016/j.brs.2022.12.006.

Klimesch, W., Sauseng, P. and Hanslmayr, S. (2007) 'EEG alpha oscillations: The inhibition–timing hypothesis', *Brain Research Reviews*, 53(1), pp. 63–88. Available at: https://doi.org/10.1016/j.brainresrev.2006.06.003.

Kobayashi, K. *et al.* (1999) 'Isolation of epileptiform discharges from unaveraged EEG by independent component analysis', *Clinical Neurophysiology*, 110(10), pp. 1755–1763. Available at: https://doi.org/10.1016/S1388-2457(99)00134-0.

Koessler, L. *et al.* (2023) 'Transcranial direct current stimulation reduces intracerebrally-recorded epileptic seizures and behavioral disturbances', *Brain Stimulation*, 16(2), pp. 667–669. Available at: https://doi.org/10.1016/j.brs.2023.03.040.

Kotsopoulos, I.A.W. *et al.* (2002) 'Systematic Review and Meta-analysis of Incidence Studies of Epilepsy and Unprovoked Seizures', *Epilepsia*, 43(11), pp. 1402–1409. Available at: https://doi.org/10.1046/j.1528-1157.2002.t01-1-26901.x.

Kozák, G. and Berényi, A. (2017) 'Sustained efficacy of closed loop electrical stimulation for long-term treatment of absence epilepsy in rats', *Scientific Reports*, 7(1), p. 6300. Available at: https://doi.org/10.1038/s41598-017-06684-0.

Kuba, R. *et al.* (2009) 'Vagus nerve stimulation: Longitudinal follow-up of patients treated for 5 years', *Seizure*, 18(4), pp. 269–274. Available at: https://doi.org/10.1016/j.seizure.2008.10.012.

Kural, M.A. *et al.* (2020) 'Criteria for defining interictal epileptiform discharges in EEG: A clinical validation study', *Neurology*, 94(20). Available at: https://doi.org/10.1212/WNL.0000000000009439.

Kurbatova, P. *et al.* (2016) 'Dynamic changes of depolarizing GABA in a computational model of epileptogenic brain: Insight for Dravet syndrome', *Experimental Neurology*, 283, pp. 57–72. Available at: https://doi.org/10.1016/j.expneurol.2016.05.037.

Kuzniecky, R.I. (2005) 'Neuroimaging of epilepsy: Therapeutic implications', 2(2).

Kwan, P. *et al.* (2010) 'Definition of drug resistant epilepsy: Consensus proposal by the ad hoc Task Force of the ILAE Commission on Therapeutic Strategies', *Epilepsia*, 51(6), pp. 1069–1077. Available at: https://doi.org/10.1111/j.1528-1167.2009.02397.x.

Kybic, J. *et al.* (2005) 'A common formalism for the Integral formulations of the forward EEG problem', *IEEE Transactions on Medical Imaging*, 24(1), pp. 12–28. Available at: https://doi.org/10.1109/TMI.2004.837363.

Kybic, J. *et al.* (2006) 'Generalized head models for MEG/EEG: boundary element method beyond nested volumes', *Physics in Medicine and Biology*, 51(5), pp. 1333–1346. Available at: https://doi.org/10.1088/0031-9155/51/5/021.

Laakso, I. *et al.* (2015) 'Inter-subject Variability in Electric Fields of Motor Cortical tDCS', *Brain Stimulation*, 8(5), pp. 906–913. Available at: https://doi.org/10.1016/j.brs.2015.05.002.

Lafon, B. *et al.* (2017) 'Low frequency transcranial electrical stimulation does not entrain sleep rhythms measured by human intracranial recordings', *Nature Communications*, 8(1), p. 1199. Available at: https://doi.org/10.1038/s41467-017-01045-x.

Lagarde, S. *et al.* (2018) 'Interictal stereotactic-EEG functional connectivity in refractory focal epilepsies', *Brain*, 141(10), pp. 2966–2980. Available at: https://doi.org/10.1093/brain/awy214.

Lagarde, S. *et al.* (2019) 'The repertoire of seizure onset patterns in human focal epilepsies: Determinants and prognostic values', *Epilepsia*, 60(1), pp. 85–95. Available at: https://doi.org/10.1111/epi.14604.

Lagarde, S. *et al.* (2022) 'Interictal Functional Connectivity in Focal Refractory Epilepsies Investigated by Intracranial EEG', *Brain Connectivity*, 12(10), pp. 850–869. Available at: https://doi.org/10.1089/brain.2021.0190.

Lamusuo, S. *et al.* (2001) '[18F]FDG-PET Reveals Temporal Hypometabolism in Patients With Temporal Lobe Epilepsy Even When Quantitative MRI and Histopathological Analysis Show Only Mild Hippocampal Damage', *Archives of Neurology*, 58(6), p. 933. Available at: https://doi.org/10.1001/archneur.58.6.933.

Larsson, P. and Kostov, H. (2005) 'Lower frequency variability in the alpha activity in EEG among patients with epilepsy', *Clinical Neurophysiology*, 116(11), pp. 2701–2706. Available at: https://doi.org/10.1016/j.clinph.2005.07.019.

Laufs, H. (2012) 'Functional imaging of seizures and epilepsy: evolution from zones to networks', *Current Opinion in Neurology*, 25(2), pp. 194–200. Available at: https://doi.org/10.1097/WCO.0b013e3283515db9.

Lee, K.J., Shon, Y.M. and Cho, C.B. (2012) 'Long-Term Outcome of Anterior Thalamic Nucleus Stimulation for Intractable Epilepsy', *Stereotactic and Functional Neurosurgery*, 90(6), pp. 379–385. Available at: https://doi.org/10.1159/000339991.

Lefaucheur, J.-P. (2016) 'A comprehensive database of published tDCS clinical trials (2005–2016)', *Neurophysiologie Clinique/Clinical Neurophysiology*, 46(6), pp. 319–398. Available at: https://doi.org/10.1016/j.neucli.2016.10.002.

Lefaucheur, J.-P. *et al.* (2017) 'Evidence-based guidelines on the therapeutic use of transcranial direct current stimulation (tDCS)', *Clinical Neurophysiology*, 128(1), pp. 56–92. Available at: https://doi.org/10.1016/j.clinph.2016.10.087.

Lefaucheur, J.-P. and Wendling, F. (2019) 'Mechanisms of action of tDCS: A brief and practical overview', *Neurophysiologie Clinique*, 49(4), pp. 269–275. Available at: https://doi.org/10.1016/j.neucli.2019.07.013.

Lian, J. *et al.* (2003) 'Local Suppression of Epileptiform Activity by Electrical Stimulation in Rat Hippocampus *In Vitro*', *The Journal of Physiology*, 547(2), pp. 427–434. Available at: https://doi.org/10.1113/jphysiol.2002.033209.

Liebetanz, D. *et al.* (2006) 'Anticonvulsant Effects of Transcranial Direct-current Stimulation (tDCS) in the Rat Cortical Ramp Model of Focal Epilepsy', *Epilepsia*, 47(7), pp. 1216–1224. Available at: https://doi.org/10.1111/j.1528-1167.2006.00539.x.

Lin, F. *et al.* (2006) 'Distributed current estimates using cortical orientation constraints', *Human Brain Mapping*, 27(1), pp. 1–13. Available at: https://doi.org/10.1002/hbm.20155.

Lin, L.-C. *et al.* (2018) 'Cumulative effect of transcranial direct current stimulation in patients with partial refractory epilepsy and its association with phase lag index-A preliminary study', *Epilepsy & Behavior*, 84, pp. 142–147. Available at: https://doi.org/10.1016/j.yebeh.2018.04.017.

Liu, A. *et al.* (2018) 'Immediate neurophysiological effects of transcranial electrical stimulation', *Nature Communications*, 9(1), p. 5092. Available at: https://doi.org/10.1038/s41467-018-07233-7.

Lopez-Sola, E. *et al.* (2021) 'An individualized neural mass model of ictal activity based on gaba-a pathology for personalization of brain stimulation protocols in epilepsy', *Brain Stimulation*, 14, p. 1677. Available at: https://doi.org/10.1016/j.brs.2021.10.282.

Louviot, S. *et al.* (2022) 'Transcranial Electrical Stimulation generates electric fields in deep human brain structures', *Brain Stimulation*, 15(1), pp. 1–12. Available at: https://doi.org/10.1016/j.brs.2021.11.001.

Lu, Y. *et al.* (2012) 'Seizure source imaging by means of FINE spatio-temporal dipole localization and directed transfer function in partial epilepsy patients', *Clinical Neurophysiology*, 123(7), pp. 1275–1283. Available at: https://doi.org/10.1016/j.clinph.2011.11.007.

Luft, C.D.B. *et al.* (2014) 'Best of both worlds: promise of combining brain stimulation and brain connectome', *Frontiers in Systems Neuroscience*, 8. Available at: https://doi.org/10.3389/fnsys.2014.00132.

Luo, W.-Y. *et al.* (2021) 'Efficacy of cathodal transcranial direct current stimulation on electroencephalographic functional networks in patients with focal epilepsy: Preliminary findings', *Epilepsy Research*, 178, p. 106791. Available at: https://doi.org/10.1016/j.eplepsyres.2021.106791.

Ma, J. *et al.* (2022) 'A prediction model integrating synchronization biomarkers and clinical features to identify responders to vagus nerve stimulation among pediatric patients with drug-resistant epilepsy', *CNS Neuroscience & Therapeutics*, 28(11), pp. 1838–1848. Available at: https://doi.org/10.1111/cns.13923.

MacDonald, S.W.S., Nyberg, L. and Bäckman, L. (2006) 'Intra-individual variability in behavior: links to brain structure, neurotransmission and neuronal activity', *Trends in Neurosciences*, 29(8), pp. 474–480. Available at: https://doi.org/10.1016/j.tins.2006.06.011.

Malinowska, U. *et al.* (2014) 'Interictal networks in Magnetoencephalography', *Human Brain Mapping*, 35(6), pp. 2789–2805. Available at: https://doi.org/10.1002/hbm.22367.

Mameniškienė, R. and Wolf, P. (2017) 'Epilepsia partialis continua: A review', *Seizure*, 44, pp. 74–80. Available at: https://doi.org/10.1016/j.seizure.2016.10.010.

Manning, J.R. *et al.* (2009) 'Broadband Shifts in Local Field Potential Power Spectra Are Correlated with Single-Neuron Spiking in Humans', *The Journal of Neuroscience*, 29(43), pp. 13613–13620. Available at: https://doi.org/10.1523/JNEUROSCI.2041-09.2009.

Marquardt, L. *et al.* (2019) 'No effect of electrical transcranial direct current stimulation adjunct treatment for epilepsia partialis continua in POLG disease', *Epilepsy & Behavior Reports*, 12, p. 100339. Available at: https://doi.org/10.1016/j.ebr.2019.100339.

Marrosu, F. *et al.* (2005) 'Increase in 20–50Hz (gamma frequencies) power spectrum and synchronization after chronic vagal nerve stimulation', *Clinical Neurophysiology*, 116(9), pp. 2026–2036. Available at: https://doi.org/10.1016/j.clinph.2005.06.015.

McCormick, D.A. and Bal, T. (1997) 'SLEEP AND AROUSAL: Thalamocortical Mechanisms', *Annual Review of Neuroscience*, 20(1), pp. 185–215. Available at: https://doi.org/10.1146/annurev.neuro.20.1.185.

McGonigal, A., Bartolomei, F. and Chauvel, P. (2021) 'On seizure semiology', *Epilepsia*, 62(9), pp. 2019–2035. Available at: https://doi.org/10.1111/epi.16994.

Meador, K.J. *et al.* (2015) 'Quality of life and mood in patients with medically intractable epilepsy treated with targeted responsive neurostimulation', *Epilepsy & Behavior*, 45, pp. 242–247. Available at: https://doi.org/10.1016/j.yebeh.2015.01.012.

Medina Villalon, S. *et al.* (2018) 'EpiTools, A software suite for presurgical brain mapping in epilepsy: Intracerebral EEG', *Journal of Neuroscience Methods*, 303, pp. 7–15. Available at: https://doi.org/10.1016/j.jneumeth.2018.03.018.

Mégevand, P. and Seeck, M. (2018) 'Electroencephalography, magnetoencephalography and source localization: their value in epilepsy', *Current Opinion in Neurology*, 31(2), pp. 176–183. Available at: https://doi.org/10.1097/WCO.0000000000000545.

Meiron, O. *et al.* (2018) 'High-Definition transcranial direct current stimulation in early onset epileptic encephalopathy: a case study', *Brain Injury*, 32(1), pp. 135–143. Available at: https://doi.org/10.1080/02699052.2017.1390254.

Mencarelli, L. *et al.* (2020) 'Impact of network-targeted multichannel transcranial direct current stimulation on intrinsic and network-to-network functional connectivity', *Journal of Neuroscience Research*, 98(10), pp. 1843–1856. Available at: https://doi.org/10.1002/jnr.24690.

Meng, F.-G. *et al.* (2015) 'Vagus Nerve Stimulation for Pediatric and Adult Patients with Pharmaco-resistant Epilepsy', *Chinese Medical Journal*, 128(19), pp. 2599–2604. Available at: https://doi.org/10.4103/0366-6999.166023.

Mercadal, B., Salvador, Ricardo, *et al.* (2021) 'Modeling implanted metals in electrical stimulation applications', *bioRxiv*, p. 2021.12.04.471211. Available at: https://doi.org/10.1101/2021.12.04.471211.

Mercadal, B., Salvador, R, *et al.* (2021) 'Modeling transcranial electrical current stimulation-induced electric fields in patients with skull plates', *Brain Stimulation*, 14(6), pp. 1683–1684. Available at: https://doi.org/10.1016/j. brs.2021.10.304.

Mercier, M.R. *et al.* (2022) 'Advances in human intracranial electroencephalography research, guidelines and good practices', *NeuroImage*, 260, p. 119438. Available at: https://doi.org/10.1016/j.neuroimage.2022.119438.

Miranda, P.C. *et al.* (2013) 'The electric field in the cortex during transcranial current stimulation', *NeuroImage*, 70, pp. 48–58. Available at: https://doi.org/10.1016/j.neuroimage.2012.12.034.

Missey, F. *et al.* (2021) 'Orientation of Temporal Interference for Non-invasive Deep Brain Stimulation in Epilepsy', *Frontiers in Neuroscience*, 15, p. 633988. Available at: https://doi.org/10.3389/fnins.2021.633988.

Miyauchi, T. *et al.* (1991) 'Computerized Analysis of EEG Background Activity in Epileptic Patients', *Epilepsia*, 32(6), pp. 870–881. Available at: https://doi.org/10.1111/j.1528-1157.1991.tb05544.x.

Modolo, J. *et al.* (2018) 'Physiological effects of low-magnitude electric fields on brain activity: Advances from in vitro, in vivo and in silico models', *Current Opinion in Biomedical Engineering*, 8, pp. 38–44. Available at: https://doi.org/10.1016/j.cobme.2018.09.006.

Monte-Silva, K. *et al.* (2010) 'Shaping the Optimal Repetition Interval for Cathodal Transcranial Direct Current Stimulation (tDCS)', *Journal of Neurophysiology*, 103(4), pp. 1735–1740. Available at: https://doi.org/10.1152/jn.00924.2009.

Mormann, F. *et al.* (2005) 'On the predictability of epileptic seizures', *Clinical Neurophysiology*, 116(3), pp. 569–587. Available at: https://doi.org/10.1016/j.clinph.2004.08.025.

Morrell, M.J. (2011) 'Responsive cortical stimulation for the treatment of medically intractable partial epilepsy', *Neurology*, 77(13), pp. 1295–1304. Available at: https://doi.org/10.1212/WNL.0b013e3182302056.

Mosher, J.C., Lewis, P.S. and Leahy, R.M. (1992) 'Multiple dipole modeling and localization from spatio-temporal MEG data', *IEEE Transactions on Biomedical Engineering*, 39(6), pp. 541–557. Available at: https://doi.org/10.1109/10.141192.

Næss, S. *et al.* (2017) 'Corrected Four-Sphere Head Model for EEG Signals', *Frontiers in Human Neuroscience*, 11, p. 490. Available at: https://doi.org/10.3389/fnhum.2017.00490.

Nascimento, F.A. *et al.* (2023) 'Focal epilepsies: Update on diagnosis and classification', *Epileptic Disorders*, 25(1), pp. 1–17. Available at: https://doi.org/10.1002/epd2.20045.

Nascimento, F.A. and Beniczky, S. (2023) 'Teaching the 6 Criteria of the International Federation of Clinical Neurophysiology for Defining Interictal Epileptiform Discharges on EEG Using a Visual Graphic', *Neurology Education*, 2(2), p. e200073. Available at: https://doi.org/10.1212/NE9.0000000000200073.

Naylor, D.E. *et al.* (2013) 'Rapid surface accumulation of NMDA receptors increases glutamatergic excitation during status epilepticus', *Neurobiology of Disease*, 54, pp. 225–238. Available at: https://doi.org/10.1016/j.nbd.2012.12.015.

Nissen, I.A. *et al.* (2016) 'Brain areas with epileptic high frequency oscillations are functionally isolated in MEG virtual electrode networks', *Clinical Neurophysiology*, 127(7), pp. 2581–2591. Available at: https://doi.org/10.1016/j.clinph.2016.04.013.

Nitsche, M.A. *et al.* (2003) 'Pharmacological Modulation of Cortical Excitability Shifts Induced by Transcranial Direct Current Stimulation in Humans', *The Journal of Physiology*, 553(1), pp. 293–301. Available at: https://doi.org/10.1113/jphysiol.2003.049916.

Nitsche, M.A. *et al.* (2007) 'Shaping the Effects of Transcranial Direct Current Stimulation of the Human Motor Cortex', *Journal of Neurophysiology*, 97(4), pp. 3109–3117. Available at: https://doi.org/10.1152/jn.01312.2006.

Nitsche, M.A. *et al.* (2008) 'Transcranial direct current stimulation: State of the art 2008', *Brain Stimulation*, 1(3), pp. 206–223. Available at: https://doi.org/10.1016/j.brs.2008.06.004.

Nitsche, M.A. and Paulus, W. (2000) 'Excitability changes induced in the human motor cortex by weak transcranial direct current stimulation', *The Journal of Physiology*, 527(3), pp. 633–639. Available at: https://doi.org/10.1111/j.1469-7793.2000.t01-1-00633.x.

Nitsche, M.A. and Paulus, W. (2001) 'Sustained excitability elevations induced by transcranial DC motor cortex stimulation in humans', *Neurology*, 57(10), pp. 1899–1901. Available at: https://doi.org/10.1212/WNL.57.10.1899.

Nolte, G. *et al.* (2004) 'Identifying true brain interaction from EEG data using the imaginary part of coherency', *Clinical Neurophysiology*, 115(10), pp. 2292–2307. Available at: https://doi.org/10.1016/j.clinph.2004.04.029.

Obeso, J.A., Rothwell, C. and Marsden, C.D. (1985) 'THE SPECTRUM OF CORTICAL MYOCLONUS: FROM FOCAL REFLEX JERKS TO SPONTANEOUS MOTOR EPILEPSY', *Brain*, 108(1), pp. 193–224. Available at: https://doi.org/10.1093/brain/108.1.193.

Ochi, A. *et al.* (2007) 'Dynamic Changes of Ictal High-Frequency Oscillations in Neocortical Epilepsy: Using Multiple Band Frequency Analysis', *Epilepsia*, 48(2), pp. 286–296. Available at: https://doi.org/10.1111/j.1528-1167.2007.00923.x.

Oh, Y.-S. *et al.* (2012) 'Cognitive improvement after long-term electrical stimulation of bilateral anterior thalamic nucleus in refractory epilepsy patients', *Seizure*, 21(3), pp. 183–187. Available at: https://doi.org/10.1016/j.seizure.2011.12.003.

Olmi, S. *et al.* (2019) 'Controlling seizure propagation in large-scale brain networks', *PLOS Computational Biology*. Edited by J. Daunizeau, 15(2), p. e1006805. Available at: https://doi.org/10.1371/journal.pcbi.1006805.

Oostenveld, R. *et al.* (2011) 'FieldTrip: Open Source Software for Advanced Analysis of MEG, EEG, and Invasive Electrophysiological Data', *Computational Intelligence and Neuroscience*, 2011, pp. 1–9. Available at: https://doi.org/10.1155/2011/156869.

Opitz, A. *et al.* (2016) 'Spatiotemporal structure of intracranial electric fields induced by transcranial electric stimulation in humans and nonhuman primates', *Scientific Reports*, 6(1), p. 31236. Available at: https://doi.org/10.1038/srep31236.

Opitz, A. *et al.* (2018) 'On the importance of precise electrode placement for targeted transcranial electric stimulation', *NeuroImage*, 181, pp. 560–567. Available at: https://doi.org/10.1016/j.neuroimage.2018.07.027.

Ossadtchi, A. *et al.* (2004) 'Automated interictal spike detection and source localization in magnetoencephalography using independent components analysis and spatio-temporal clustering', *Clinical Neurophysiology*, 115(3), pp. 508–522. Available at: https://doi.org/10.1016/j.clinph.2003.10.036.

Ou, W., Hämäläinen, M.S. and Golland, P. (2009) 'A distributed spatio-temporal EEG/MEG inverse solver', *NeuroImage*, 44(3), pp. 932–946. Available at: https://doi.org/10.1016/j.neuroimage.2008.05.063.

Page, M.J. *et al.* (2021) 'The PRISMA 2020 statement: an updated guideline for reporting systematic reviews', *BMJ*, p. n71. Available at: https://doi.org/10.1136/bmj.n71.

Palm, U. *et al.* (2018) 'Home Use, Remotely Supervised, and Remotely Controlled Transcranial Direct Current Stimulation: A Systematic Review of the Available Evidence', *Neuromodulation: Technology at the Neural Interface*, 21(4), pp. 323–333. Available at: https://doi.org/10.1111/ner.12686.

Palva, J.M., Palva, S. and Kaila, K. (2005) 'Phase Synchrony among Neuronal Oscillations in the Human Cortex', *The Journal of Neuroscience*, 25(15), pp. 3962–3972. Available at: https://doi.org/10.1523/JNEUROSCI.4250-04.2005.

Pan, J.W. *et al.* (2009) 'Intracranial EEG power and metabolism in human epilepsy', *Epilepsy Research*, 87(1), pp. 18–24. Available at: https://doi.org/10.1016/j.eplepsyres.2009.07.006.

Pandian, J.D. *et al.* (2002) 'Epilepsia partialis continua—a clinical and electroencephalography study', *Seizure*, 11(7), pp. 437–441. Available at: https://doi.org/10.1053/seiz.2001.0646.

Parazzini, M. *et al.* (2014) 'Computational modeling of transcranial direct current stimulation in the child brain: implications for the treatment of refractory childhood focal epilepsy', *International Journal of Neural Systems*, 24(02), p. 1430006. Available at: https://doi.org/10.1142/S012906571430006X.

Park, Y. *et al.* (2011) 'Seizure prediction with spectral power of EEG using cost-sensitive support vector machines: Seizure Prediction with Spectral Power of EEG', *Epilepsia*, 52(10), pp. 1761–1770. Available at: https://doi.org/10.1111/j.1528-1167.2011.03138.x.

Patriarca, C. *et al.* (2021) 'Ugo Cerletti, Pathologica and electroconvulsive therapy', *Pathologica*, pp. 1–7. Available at: https://doi.org/10.32074/1591-951X-263.

Pegg, E.J., Taylor, J.R. and Mohanraj, R. (2020) 'Spectral power of interictal EEG in the diagnosis and prognosis of idiopathic generalized epilepsies', *Epilepsy & Behavior*, 112, p. 107427. Available at: https://doi.org/10.1016/j.yebeh.2020.107427.

Pellegrino, G. *et al.* (2020) 'Effects of Independent Component Analysis on Magnetoencephalography Source Localization in Pre-surgical Frontal Lobe Epilepsy Patients', *Frontiers in Neurology*, 11, p. 479. Available at: https://doi.org/10.3389/fneur.2020.00479.

Pellegrino, G. *et al.* (2021) 'How cerebral cortex protects itself from interictal spikes: The alpha/beta inhibition mechanism', *Human Brain Mapping*, 42(11), pp. 3352–3365. Available at: https://doi.org/10.1002/hbm.25422.

Pelletier, S.J. and Cicchetti, F. (2015) 'Cellular and Molecular Mechanisms of Action of Transcranial Direct Current Stimulation: Evidence from In Vitro and In Vivo Models', *International Journal of Neuropsychopharmacology*, 18(2), pp. pyu047–pyu047. Available at: https://doi.org/10.1093/ijnp/pyu047.

Peterchev, A.V. *et al.* (2012) 'Fundamentals of transcranial electric and magnetic stimulation dose: Definition, selection, and reporting practices', *Brain Stimulation*, 5(4), pp. 435–453. Available at: https://doi.org/10.1016/j.brs.2011.10.001.

Pevzner, A. *et al.* (2016) 'Making Waves in the Brain: What Are Oscillations, and Why Modulating Them Makes Sense for Brain Injury', *Frontiers in Systems Neuroscience*, 10. Available at: https://doi.org/10.3389/fnsys.2016.00030.

Pfurtscheller, G. and Lopes Da Silva, F.H. (1999) 'Event-related EEG/MEG synchronization and desynchronization: basic principles', *Clinical Neurophysiology*, 110(11), pp. 1842–1857. Available at: https://doi.org/10.1016/S1388-2457(99)00141-8.

Pijn, J.P. and Lopes da Silva, F. (1993) 'Propagation of Electrical Activity: Nonlinear Associations and Time Delays between EEG Signals', in S. Zschocke and E.-J. Speckmann (eds) *Basic Mechanisms of the EEG*. Boston, MA: Birkhäuser Boston, pp. 41–61. Available at: https://doi.org/10.1007/978-1-4612-0341-4_4.

Pitkänen, A. *et al.* (2017) 'Models of Seizures and Epilepsy', *Amsterdam: Elsevier* [Preprint].

Pittau, F. and Vulliemoz, S. (2015) 'Functional brain networks in epilepsy: recent advances in noninvasive mapping', *Current Opinion in Neurology*, 28(4), pp. 338–343. Available at: https://doi.org/10.1097/WCO.0000000000000221.

Pizzo, F. *et al.* (2019) 'Deep brain activities can be detected with magnetoencephalography', *Nature Communications*, 10(1), p. 971. Available at: https://doi.org/10.1038/s41467-019-08665-5.

Pizzo, F. *et al.* (2021) 'The Ictal Signature of Thalamus and Basal Ganglia in Focal Epilepsy: A SEEG Study', *Neurology*, 96(2). Available at: https://doi.org/10.1212/WNL.0000000000011003.

Polanía, R. *et al.* (2011) 'Introducing graph theory to track for neuroplastic alterations in the resting human brain: A transcranial direct current stimulation study', *NeuroImage*, 54(3), pp. 2287–2296. Available at: https://doi.org/10.1016/j.neuroimage.2010.09.085.

Polanía, R., Nitsche, M.A. and Ruff, C.C. (2018) 'Studying and modifying brain function with non-invasive brain stimulation', *Nature Neuroscience*, 21(2), pp. 174–187. Available at: https://doi.org/10.1038/s41593-017-0054-4.

Priori, A. *et al.* (1998) 'Polarization of the human motor cortex through the scalp', *Neuroreport*, 9, pp. 2257–2260.

Priori, A. (2003) 'Brain polarization in humans: a reappraisal of an old tool for prolonged non-invasive modulation of brain excitability', *Clinical Neurophysiology*, 114(4), pp. 589–595. Available at: https://doi.org/10.1016/S1388-2457(02)00437-6.

Rahman, A. *et al.* (2013) 'Cellular effects of acute direct current stimulation: somatic and synaptic terminal effects', *The Journal of Physiology*, 591(10), pp. 2563–2578. Available at: https://doi.org/10.1113/jphysiol.2012.247171.

Rahman, A. *et al.* (2017) 'Direct current stimulation boosts synaptic gain and cooperativity *in vitro*', *The Journal of Physiology*, 595(11), pp. 3535–3547. Available at: https://doi.org/10.1113/JP273005.

Ramantani, G. *et al.* (2023) 'Passive and active markers of cortical excitability in epilepsy', *Epilepsia*, 64(S3). Available at: https://doi.org/10.1111/epi.17578.

Rampp, S. and Stefan, H. (2007) 'Magnetoencephalography in presurgical epilepsy diagnosis', *Expert Review of Medical Devices*, 4(3), pp. 335–347. Available at: https://doi.org/10.1586/17434440.4.3.335.

Reato, D. *et al.* (2010) 'Low-Intensity Electrical Stimulation Affects Network Dynamics by Modulating Population Rate and Spike Timing', *The Journal of Neuroscience*, 30(45), pp. 15067–15079. Available at: https://doi.org/10.1523/JNEUROSCI.2059-10.2010.

Reato, D. *et al.* (2013) 'Effects of weak transcranial alternating current stimulation on brain activity—a review of known mechanisms from animal studies', *Frontiers in Human Neuroscience*, 7. Available at: https://doi.org/10.3389/fnhum.2013.00687.

Regner, G.G. *et al.* (2020) 'Transcranial direct current stimulation (tDCS) affects neuroinflammation parameters and behavioral seizure activity in pentylenetetrazole-induced kindling in rats', *Neuroscience Letters*, 735, p. 135162. Available at: https://doi.org/10.1016/j.neulet.2020.135162.

Reithler, J., Peters, J.C. and Sack, A.T. (2011) 'Multimodal transcranial magnetic stimulation: Using concurrent neuroimaging to reveal the neural network dynamics of noninvasive brain stimulation', *Progress in Neurobiology*, 94(2), pp. 149–165. Available at: https://doi.org/10.1016/j.pneurobio.2011.04.004.

Roehri, N. *et al.* (2016) 'Time-Frequency Strategies for Increasing High-Frequency Oscillation Detectability in Intracerebral EEG', *IEEE Transactions on Biomedical*

*Engineering*, 63(12), pp. 2595–2606. Available at: https://doi.org/10.1109/TBME.2016.2556425.

Roehri, N. and Bartolomei, F. (2019) 'Are high-frequency oscillations better biomarkers of the epileptogenic zone than spikes?', *Current Opinion in Neurology*, 32(2), pp. 213–219. Available at: https://doi.org/10.1097/WCO.0000000000000663.

Romei, V. *et al.* (2008) 'Spontaneous Fluctuations in Posterior -Band EEG Activity Reflect Variability in Excitability of Human Visual Areas', *Cerebral Cortex*, 18(9), pp. 2010–2018. Available at: https://doi.org/10.1093/cercor/bhm229.

Rotenberg, A. *et al.* (2009) 'Repetitive transcranial magnetic stimulation in the treatment of epilepsia partialis continua', *Epilepsy & Behavior*, 14(1), pp. 253–257. Available at: https://doi.org/10.1016/j.yebeh.2008.09.007.

Roy, A., Baxter, B., and Bin He (2014) 'High-Definition Transcranial Direct Current Stimulation Induces Both Acute and Persistent Changes in Broadband Cortical Synchronization: A Simultaneous tDCS–EEG Study', *IEEE Transactions on Biomedical Engineering*, 61(7), pp. 1967–1978. Available at: https://doi.org/10.1109/TBME.2014.2311071.

Roy, T. and Pandit, A. (2011) 'Neuroimaging in epilepsy', *Annals of Indian Academy of Neurology*, 14(2), p. 78. Available at: https://doi.org/10.4103/0972-2327.82787.

Ruffini, G. *et al.* (2013) 'Transcranial Current Brain Stimulation (tCS): Models and Technologies', *IEEE Transactions on Neural Systems and Rehabilitation Engineering*, 21(3), pp. 333–345. Available at: https://doi.org/10.1109/TNSRE.2012.2200046.

Ruffini, G. *et al.* (2014) 'Optimization of multifocal transcranial current stimulation for weighted cortical pattern targeting from realistic modeling of electric fields', *NeuroImage*, 89, pp. 216–225. Available at: https://doi.org/10.1016/j.neuroimage.2013.12.002.

Ruffini, G. *et al.* (2018) 'Targeting brain networks with multichannel transcranial current stimulation (tCS)', *Current Opinion in Biomedical Engineering*, 8, pp. 70–77. Available at: https://doi.org/10.1016/j.cobme.2018.11.001.

Ruffini, G. *et al.* (2020) 'Realistic modeling of mesoscopic ephaptic coupling in the human brain', *PLOS Computational Biology*. Edited by D. Marinazzo, 16(6), p. e1007923. Available at: https://doi.org/10.1371/journal.pcbi.1007923.

Ryvlin, P. *et al.* (2014) 'The long-term effect of vagus nerve stimulation on quality of life in patients with pharmacoresistant focal epilepsy: The PuLsE (Open Prospective Randomized Long-term Effectiveness) trial', *Epilepsia*, 55(6), pp. 893–900. Available at: https://doi.org/10.1111/epi.12611.

Sadleir, R.J. *et al.* (2012) 'Target Optimization in Transcranial Direct Current Stimulation', *Frontiers in Psychiatry*, 3. Available at: https://doi.org/10.3389/fpsyt.2012.00090.

Salehinejad, M.A. *et al.* (2024) 'Optimized multichannel tDCS protocol for clinical use in patients with major depressive disorder: A randomized, controlled trial'. Available at: https://doi.org/10.31219/osf.io/tms4h.

Sanchez-Todo, R. *et al.* (2018) 'Personalization of hybrid brain models from neuroimaging and electrophysiology data', *bioRxiv* [Preprint]. Available at: https://doi.org/10.1101/461350.

Sangare, A. *et al.* (2020) 'The Effectiveness of Vagus Nerve Stimulation in Drug-Resistant Epilepsy Correlates with Vagus Nerve Stimulation-Induced Electroencephalography Desynchronization', *Brain Connectivity*, 10(10), pp. 566–577. Available at: https://doi.org/10.1089/brain.2020.0798.

San-Juan, D. *et al.* (2011) 'Transcranial direct current stimulation in adolescent and adult Rasmussen's encephalitis', *Epilepsy & Behavior*, 20(1), pp. 126–131. Available at: https://doi.org/10.1016/j.yebeh.2010.10.031.

San-juan, D. *et al.* (2015) 'Transcranial Direct Current Stimulation in Epilepsy', *Brain Stimulation*, 8(3), pp. 455–464. Available at: https://doi.org/10.1016/j.brs.2015.01.001.

San-Juan, D. *et al.* (2017) 'Transcranial Direct Current Stimulation in Mesial Temporal Lobe Epilepsy and Hippocampal Sclerosis', *Brain Stimulation*, 10(1), pp. 28–35. Available at: https://doi.org/10.1016/j.brs.2016.08.013.

San-Juan, D. *et al.* (2018) 'Successful Treatment of a Drug-Resistant Epilepsy by Long-term Transcranial Direct Current Stimulation: A Case Report', *Frontiers in Neurology*, 9, p. 65. Available at: https://doi.org/10.3389/fneur.2018.00065.

San-Juan, D. *et al.* (2022) 'Safety and efficacy of cathodal transcranial direct current stimulation in patients with Lennox Gastaut Syndrome: An open-label, prospective, single-center, single-blinded, pilot study', *Seizure: European Journal of Epilepsy*, 100, pp. 44–50. Available at: https://doi.org/10.1016/j.seizure.2022.06.009.

Sarmiento, C.I., San-Juan, D. and Prasath, V.B.S. (2016) 'Letter to the Editor: Brief history of transcranial direct current stimulation (tDCS): from electric fishes to microcontrollers', *Psychological Medicine*, 46(15), pp. 3259–3261. Available at: https://doi.org/10.1017/S0033291716001926.

Sauseng, P. *et al.* (2009) 'Spontaneous locally restricted EEG alpha activity determines cortical excitability in the motor cortex', *Neuropsychologia*, 47(1), pp. 284–288. Available at: https://doi.org/10.1016/j.neuropsychologia.2008.07.021.

Scheffer, I.E. *et al.* (2017) 'Classification of the epilepsies: Position paper of the Commission for Classification and Terminology', *Epilepsia*, 58(4), pp. 512–521. Available at: https://doi.org/10.1111/epi.13709.

Scherer, M. *et al.* (2020) 'Desynchronization of temporal lobe theta-band activity during effective anterior thalamus deep brain stimulation in epilepsy', *NeuroImage*, 218, p. 116967. Available at: https://doi.org/10.1016/j.neuroimage.2020.116967.

Schevon, C.A. *et al.* (2007) 'Cortical abnormalities in epilepsy revealed by local EEG synchrony', *NeuroImage*, 35(1), pp. 140–148. Available at: https://doi.org/10.1016/j.neuroimage.2006.11.009.

Schneider, M. and Gerin, P. (1970) 'Une méthode de localisation des dipôles cérébraux', *Electroencephalography and Clinical Neurophysiology*, 28(1), pp. 69–78.

Schoffelen, J. and Gross, J. (2009) 'Source connectivity analysis with MEG and EEG', *Human Brain Mapping*, 30(6), pp. 1857–1865. Available at: https://doi.org/10.1002/hbm.20745.

Seidenberg, M., Pulsipher, D.T. and Hermann, B. (2009) 'Association of Epilepsy and Comorbid Conditions', *Future Neurology*, 4(5), pp. 663–668. Available at: https://doi.org/10.2217/fnl.09.32.

Simula, S. *et al.* (2022) 'Transcranial current stimulation in epilepsy: A systematic review of the fundamental and clinical aspects', *Frontiers in Neuroscience*, 16, p. 909421. Available at: https://doi.org/10.3389/fnins.2022.909421.

Simula, S., Garnier, E., *et al.* (2023) 'Changes in local and network brain activity after stereotactic thermocoagulation in patients with DRUG-RESISTANT epilepsy', *Epilepsia*, 64(6), pp. 1582–1593. Available at: https://doi.org/10.1111/epi.17613.

Simula, S., Damiani, G., *et al.* (2023) 'Short-term Impact of Transcranial Current Stimulation on Brain Networks Measured by Simultaneous Stereoelectroencephalography Recordings in Drug-Resistant Focal Epilepsy Patients', *AES 2023 Annual Meeting Abstract Database*, p. AESnet.org.

Skarpaas, T.L., Jarosiewicz, B. and Morrell, M.J. (2019) 'Brain-responsive neurostimulation for epilepsy (RNS® System)', *Epilepsy Research*, 153, pp. 68–70. Available at: https://doi.org/10.1016/j.eplepsyres.2019.02.003.

Smit, D.J.A. *et al.* (2012) 'Individual Differences in EEG Spectral Power Reflect Genetic Variance in Gray and White Matter Volumes', *Twin Research and Human Genetics*, 15(3), pp. 384–392. Available at: https://doi.org/10.1017/thg.2012.6.

Stagg, C.J., Antal, A. and Nitsche, M.A. (2018) 'Physiology of Transcranial Direct Current Stimulation', *The Journal of ECT*, 34(3), pp. 144–152. Available at: https://doi.org/10.1097/YCT.0000000000000510.

Stam, C.J., Nolte, G. and Daffertshofer, A. (2007) 'Phase lag index: Assessment of functional connectivity from multi channel EEG and MEG with diminished bias from common sources', *Human Brain Mapping*, 28(11), pp. 1178–1193. Available at: https://doi.org/10.1002/hbm.20346.

Stam, C.J. and Van Straaten, E.C.W. (2012) 'The organization of physiological brain networks', *Clinical Neurophysiology*, 123(6), pp. 1067–1087. Available at: https://doi.org/10.1016/j.clinph.2012.01.011.

Stefan, H. (2009) 'Magnetic source imaging', *Revue Neurologique*, 165(10), pp. 742–745. Available at: https://doi.org/10.1016/j.neurol.2009.07.014.

Sudbrack-Oliveira, P. *et al.* (2021) 'Transcranial direct current stimulation (tDCS) in the management of epilepsy: A systematic review', *Seizure*, 86, pp. 85–95. Available at: https://doi.org/10.1016/j.seizure.2021.01.020.

Sun, Y. *et al.* (2020) 'Drug-Responsive Inhomogeneous Cortical Modulation by Direct Current Stimulation', *Annals of Neurology*, 88(3), pp. 489–502. Available at: https://doi.org/10.1002/ana.25822.

Takeuchi, Y. and Berényi, A. (2020) 'Oscillotherapeutics – Time-targeted interventions in epilepsy and beyond', *Neuroscience Research*, 152, pp. 87–107. Available at: https://doi.org/10.1016/j.neures.2020.01.002.

Talairach, J. and Bancaud, J. (1966) 'Lesion, "irritative" Zone and Epileptogenic Focus', *Confin. neurol.*, 27, pp. 91–94.

Tecchio, F. *et al.* (2018) 'Brain Functional Connectivity Changes After Transcranial Direct Current Stimulation in Epileptic Patients', *Frontiers in Neural Circuits*, 12, p. 44. Available at: https://doi.org/10.3389/fncir.2018.00044.

Tekturk, P., Erdogan, E.T., Kurt, A., Vanli-yavuz, E.N., *et al.* (2016) 'The effect of transcranial direct current stimulation on seizure frequency of patients with mesial temporal lobe epilepsy with hippocampal sclerosis', *Clinical Neurology and Neurosurgery*, 149, pp. 27–32. Available at: https://doi.org/10.1016/j.clineuro.2016.07.014.

Tekturk, P., Erdogan, E.T., Kurt, A., Kocagoncu, E., *et al.* (2016) 'Transcranial direct current stimulation improves seizure control in patients with Rasmussen encephalitis', *Epileptic Disorders*, 18(1), pp. 58–66. Available at: https://doi.org/10.1684/epd.2016.0796.

Tergau, F. *et al.* (1999) 'Low-frequency repetitive transcranial magnetic stimulation improves intractable epilepsy', *The Lancet*, 353(9171), p. 2209. Available at: https://doi.org/10.1016/S0140-6736(99)01301-X.

Thair, H. *et al.* (2017) 'Transcranial Direct Current Stimulation (tDCS): A Beginner's Guide for Design and Implementation', *Frontiers in Neuroscience*, 11, p. 641. Available at: https://doi.org/10.3389/fnins.2017.00641.

Thomas, S. and Nair, A. (2011) 'Confronting the stigma of epilepsy', *Annals of Indian Academy of Neurology*, 14(3), p. 158. Available at: https://doi.org/10.4103/0972-2327.85873.

Thurman, D.J. *et al.* (2017) 'The burden of premature mortality of epilepsy in high-income countries: A systematic review from the Mortality Task Force of the International League Against Epilepsy', *Epilepsia*, 58(1), pp. 17–26. Available at: https://doi.org/10.1111/epi.13604.

Tong, X. *et al.* (2022) 'Analysis of power spectrum and phase lag index changes following deep brain stimulation of the anterior nucleus of the thalamus in patients with drug-resistant epilepsy: A retrospective study', *Seizure*, 96, pp. 6–12. Available at: https://doi.org/10.1016/j.seizure.2022.01.004.

Touma, L. *et al.* (2022) 'Neurostimulation in people with drug-resistant epilepsy: Systematic review and meta-analysis from the ILAE Surgical Therapies Commission', *Epilepsia*, 63(6), pp. 1314–1329. Available at: https://doi.org/10.1111/epi.17243.

Trinka, E. *et al.* (2015) 'A definition and classification of status epilepticus - Report of the ILAE Task Force on Classification of Status Epilepticus', *Epilepsia*, 56(10), pp. 1515–1523. Available at: https://doi.org/10.1111/epi.13121.

Trinka, E. *et al.* (2023) 'Mortality, and life expectancy in Epilepsy and Status epilepticus—current trends and future aspects', *Frontiers in Epidemiology*, 3, p. 1081757. Available at: https://doi.org/10.3389/fepid.2023.1081757.

Tsuboyama, M., Kaye, H.L. and Rotenberg, A. (2020) 'Review of Transcranial Magnetic Stimulation in Epilepsy', *Clinical Therapeutics*, 42(7), pp. 1155–1168. Available at: https://doi.org/10.1016/j.clinthera.2020.05.016.

Ueda, R. *et al.* (2021) 'Improvement of brain function after surgery in infants with posterior quadrant cortical dysplasia', *Clinical Neurophysiology*, 132(2), pp. 332–337. Available at: https://doi.org/10.1016/j.clinph.2020.11.020.

Valentin, A. *et al.* (2015) 'Epilepsia partialis continua responsive to neocortical electrical stimulation', *Epilepsia*, 56(8), pp. e104–e109. Available at: https://doi.org/10.1111/epi.13067.

Van Mierlo, P. *et al.* (2014) 'Functional brain connectivity from EEG in epilepsy: Seizure prediction and epileptogenic focus localization', *Progress in Neurobiology*, 121, pp. 19–35. Available at: https://doi.org/10.1016/j.pneurobio.2014.06.004.

Van Mierlo, P. *et al.* (2019) 'Network Perspectives on Epilepsy Using EEG/MEG Source Connectivity', *Frontiers in Neurology*, 10, p. 721. Available at: https://doi.org/10.3389/fneur.2019.00721.

Van Veen, B.D. *et al.* (1997) 'Localization of brain electrical activity via linearly constrained minimum variance spatial filtering', *IEEE Transactions on Biomedical Engineering*, 44(9), pp. 867–880. Available at: https://doi.org/10.1109/10.623056.

Vandermeeren, Y., Jamart, J. and Ossemann, M. (2010) 'Effect of tDCS with an extracephalic reference electrode on cardio-respiratory and autonomic functions', *BMC Neuroscience*, 11(1), p. 38. Available at: https://doi.org/10.1186/1471-2202-11-38.

VanHaerents, S. *et al.* (2020) 'Noninvasive Brain Stimulation in Epilepsy', *Journal of Clinical Neurophysiology*, 37(2), pp. 118–130. Available at: https://doi.org/10.1097/WNP.0000000000000573.

Varga, E.T. *et al.* (2011) 'Transcranial direct current stimulation in refractory continuous spikes and waves during slow sleep: A controlled study', *Epilepsy Research*, 97(1–2), pp. 142–145. Available at: https://doi.org/10.1016/j.eplepsyres.2011.07.016.

Verger, A. *et al.* (2018) 'Brain molecular imaging in pharmacoresistant focal epilepsy: Current practice and perspectives', *Revue Neurologique*, 174(1–2), pp. 16–27. Available at: https://doi.org/10.1016/j.neurol.2017.05.001.

Vespa, S. *et al.* (2021) 'Vagus Nerve Stimulation Elicits Sleep EEG Desynchronization and Network Changes in Responder Patients in Epilepsy', *Neurotherapeutics*, 18(4), pp. 2623–2638. Available at: https://doi.org/10.1007/s13311-021-01124-4.

Vigário, R.N. (1997) 'Extraction of ocular artefacts from EEG using independent component analysis', *Electroencephalography and Clinical Neurophysiology*, 103(3), pp. 395–404. Available at: https://doi.org/10.1016/S0013-4694(97)00042-8.

Villamar, M.F. *et al.* (2013) 'Technique and Considerations in the Use of 4x1 Ring High-definition Transcranial Direct Current Stimulation (HD-tDCS)', *Journal of Visualized Experiments*, (77), p. 50309. Available at: https://doi.org/10.3791/50309.

Violante, I.R. *et al.* (2023) 'Non-invasive temporal interference electrical stimulation of the human hippocampus', *Nature Neuroscience*, 26(11), pp. 1994–2004. Available at: https://doi.org/10.1038/s41593-023-01456-8.

Vöröslakos, M. *et al.* (2018) 'Direct effects of transcranial electric stimulation on brain circuits in rats and humans', *Nature Communications*, 9(1), p. 483. Available at: https://doi.org/10.1038/s41467-018-02928-3.

Wagner, S., Burger, M. and Wolters, C.H. (2016) 'An optimization approach for well-targeted transcranial direct current stimulation'. arXiv. Available at: http://arxiv.org/abs/1506.07744 (Accessed: 18 March 2024).

Walton, D. *et al.* (2021) 'Transcranial magnetic stimulation for the treatment of epilepsy (Review)', *Cochrane Database of Systematic Reviews*, 4(CD011025). Available at: https://doi.org/10.1002/14651858.CD011025.pub3.

Wang, H.E. *et al.* (2021) 'VEP atlas: An anatomic and functional human brain atlas dedicated to epilepsy patients', *Journal of Neuroscience Methods*, 348, p. 108983. Available at: https://doi.org/10.1016/j.jneumeth.2020.108983.

Wang, M. *et al.* (2017) 'Identification of the epileptogenic zone of temporal lobe epilepsy from stereo-electroencephalography signals: A phase transfer entropy and graph theory approach', *NeuroImage: Clinical*, 16, pp. 184–195. Available at: https://doi.org/10.1016/j.nicl.2017.07.022.

Wang, Z. *et al.* (2022) 'Separating the aperiodic and periodic components of neural activity in Parkinson's disease', *European Journal of Neuroscience*, 56(6), pp. 4889–4900. Available at: https://doi.org/10.1111/ejn.15774.

Warren, C.P. *et al.* (2010) 'Synchrony in Normal and Focal Epileptic Brain: The Seizure Onset Zone is Functionally Disconnected', *Journal of Neurophysiology*, 104(6), pp. 3530–3539. Available at: https://doi.org/10.1152/jn.00368.2010.

Warsi, N.M. *et al.* (2023) 'Vagus Nerve Stimulation Modulates Phase-Amplitude Coupling in Thalamic Local Field Potentials', *Neuromodulation: Technology at the Neural Interface*, 26(3), pp. 601–606. Available at: https://doi.org/10.1016/j.neurom.2022.05.001.

Weiss (2010) 'Field effects in the CNS play functional roles', *Frontiers in Neural Circuits* [Preprint]. Available at: https://doi.org/10.3389/fncir.2010.00015.

Wendling, F. *et al.* (2002) 'Epileptic fast activity can be explained by a model of impaired GABAergic dendritic inhibition', *European Journal of Neuroscience*, 15(9), pp. 1499–1508. Available at: https://doi.org/10.1046/j.1460-9568.2002.01985.x.

Wendling, F. *et al.* (2003) 'Epileptic fast intracerebral EEG activity: evidence for spatial decorrelation at seizure onset', *Brain*, 126(6), pp. 1449–1459. Available at: https://doi.org/10.1093/brain/awg144.

Wendling, F. *et al.* (2010) 'From Intracerebral EEG Signals to Brain Connectivity: Identification of Epileptogenic Networks in Partial Epilepsy', *Frontiers in Systems Neuroscience*, 4. Available at: https://doi.org/10.3389/fnsys.2010.00154.

Wenzel, M. *et al.* (2019) 'Acute Focal Seizures Start As Local Synchronizations of Neuronal Ensembles', *The Journal of Neuroscience*, 39(43), pp. 8562–8575. Available at: https://doi.org/10.1523/JNEUROSCI.3176-18.2019.

Wieser, H.G. *et al.* (1978) 'Quantitative analysis of intracerebral recordings in epilepsia partialis continua', *Electroencephalography and Clinical Neurophysiology*, 44(1), pp. 14–22. Available at: https://doi.org/10.1016/0013-4694(78)90101-3.

Wolters, C.H. *et al.* (2006) 'Influence of tissue conductivity anisotropy on EEG/MEG field and return current computation in a realistic head model: A simulation and visualization study using high-resolution finite element modeling', *NeuroImage*, 30(3), pp. 813–826. Available at: https://doi.org/10.1016/j.neuroimage.2005.10.014.

Wu, J.Y. *et al.* (2010) 'Removing interictal fast ripples on electrocorticography linked with seizure freedom in children', *Neurology*, 75(19), pp. 1686–1694. Available at: https://doi.org/10.1212/WNL.0b013e3181fc27d0.

Wu, T. *et al.* (2014) 'Neuromagnetic coherence of epileptic activity: An MEG study', *Seizure*, 23(6), pp. 417–423. Available at: https://doi.org/10.1016/j.seizure.2014.01.022.

Wu, Y.-J. *et al.* (2020) 'Transcranial direct current stimulation alleviates seizure severity in kainic acid-induced status epilepticus rats', *Experimental Neurology*, 328, p. 113264. Available at: https://doi.org/10.1016/j.expneurol.2020.113264.

Yan, H. *et al.* (2023) 'Deep brain stimulation for patients with refractory epilepsy: nuclei selection and surgical outcome', *Frontiers in Neurology*, 14, p. 1169105. Available at: https://doi.org/10.3389/fneur.2023.1169105.

Yan, Y., Nunez, P.L. and Hart, R.T. (1991) 'Finite-element model of the human head: scalp potentials due to dipole sources', *Medical & Biological Engineering & Computing*, 29(5), pp. 475–481. Available at: https://doi.org/10.1007/BF02442317.

Yang, D. *et al.* (2019) 'Transcranial Direct Current Stimulation for Patients With Pharmacoresistant Epileptic Spasms: A Pilot Study', *Frontiers in Neurology*, 10, p. 50. Available at: https://doi.org/10.3389/fneur.2019.00050.

Yang, D. *et al.* (2020) 'Transcranial direct current stimulation reduces seizure frequency in patients with refractory focal epilepsy: A randomized, double-blind, sham-controlled, and three-arm parallel multicenter study', *Brain Stimulation*, 13(1), pp. 109–116. Available at: https://doi.org/10.1016/j.brs.2019.09.006.

Yang, J.C. *et al.* (2021) 'Responsive neurostimulation for focal motor status epilepticus', *Annals of Clinical and Translational Neurology*, 8(6), pp. 1353–1361. Available at: https://doi.org/10.1002/acn3.51318.

Yook, S.-W. *et al.* (2011) 'Suppression of Seizure by Cathodal Transcranial Direct Current Stimulation in an Epileptic Patient - A Case Report -', *Annals of Rehabilitation Medicine*, 35(4), p. 579. Available at: https://doi.org/10.5535/arm.2011.35.4.579.

Yu, Y. *et al.* (2023) 'Transcranial direct current stimulation inhibits epileptic activity propagation in a large-scale brain network model', *Science China Technological Sciences*, 66(12), pp. 3628–3638. Available at: https://doi.org/10.1007/s11431-022-2341-x.

Zaveri, H.P. *et al.* (2001) 'Distinguishing Subtypes of Temporal Lobe Epilepsy with Background Hippocampal Activity', *Epilepsia*, 42(6), pp. 725–730. Available at: https://doi.org/10.1046/j.1528-1157.2001.00500.x.

Zhou, F.-W. and Roper, S.N. (2012) 'Impaired hippocampal memory function and synaptic plasticity in experimental cortical dysplasia: Impaired Synaptic Plasticity in Experimental Cortical Dysplasia', *Epilepsia*, 53(5), pp. 850–859. Available at: https://doi.org/10.1111/j.1528-1167.2012.03431.x.

Zijlmans, M. *et al.* (2011) 'Ictal and interictal high frequency oscillations in patients with focal epilepsy', *Clinical Neurophysiology*, 122(4), pp. 664–671. Available at: https://doi.org/10.1016/j.clinph.2010.09.021.

Zijlmans, M. *et al.* (2012) 'High-frequency oscillations as a new biomarker in epilepsy', *Annals of Neurology*, 71(2), pp. 169–178. Available at: https://doi.org/10.1002/ana.22548.

Zijlmans, M. *et al.* (2017) 'How to record high-frequency oscillations in epilepsy: A practical guideline', *Epilepsia*, 58(8), pp. 1305–1315. Available at: https://doi.org/10.1111/epi.13814.

Zobeiri, M. and Van Luijtelaar, G. (2013) 'Noninvasive transcranial direct current stimulation in a genetic absence model', *Epilepsy & Behavior*, 26(1), pp. 42–50. Available at: https://doi.org/10.1016/j.yebeh.2012.10.018.

Zoghi, M. *et al.* (2016) 'Cathodal transcranial direct-current stimulation for treatment of drug-resistant temporal lobe epilepsy: A pilot randomized controlled trial', *Epilepsia Open*, 1(3–4), pp. 130–135. Available at: https://doi.org/10.1002/epi4.12020.

# Appendices

# Appendix A

### *Study 2: Changes in epileptiform discharges rates after tDCS cycles*

One objective of study 2 was to investigate the impact of tDCS on spike rates, measured from EEG recordings. The protocol and the signal analysis are described in 3.2 section. First, we used Independent Component Analysis (ICA) to decompose the EEG signal into epileptic and background components. We then performed automatic spike detection using DELPHOS (Detector of ElectroPhysiological Oscillations and Spikes) (Roehri *et al.*, 2016) on the independent components presenting spikes.

Our analysis revealed no significant difference in spike rate per minute between cycles of stimulation ("pre-stim": before the first stimulation of the cycle, and "post-stim": after the last stimulation of the cycle) ($F_{1,44.084}$=0.1012, p=0.75). Similarly, there was no significant difference between responder and non-responder patients ($F_{1,8.051}$=0.2326, p=0.6424).

Figure A.1. provides an example of the results from the first tDCS cycle, showing the spike rate (per minute) before the first stimulation on day 1 ("pre") compared to the spike rate measured after the last tDCS session on day 5 ("post"), for both responder and non-responder patients. These results are in line with previous studies showing no significant change in interictal epileptiform discharges (IEDs) after tDCS (Varga *et al.*, 2011; Assenza *et al.*, 2017; Lin *et al.*, 2018; San-Juan *et al.*, 2018; Marquardt *et al.*, 2019).

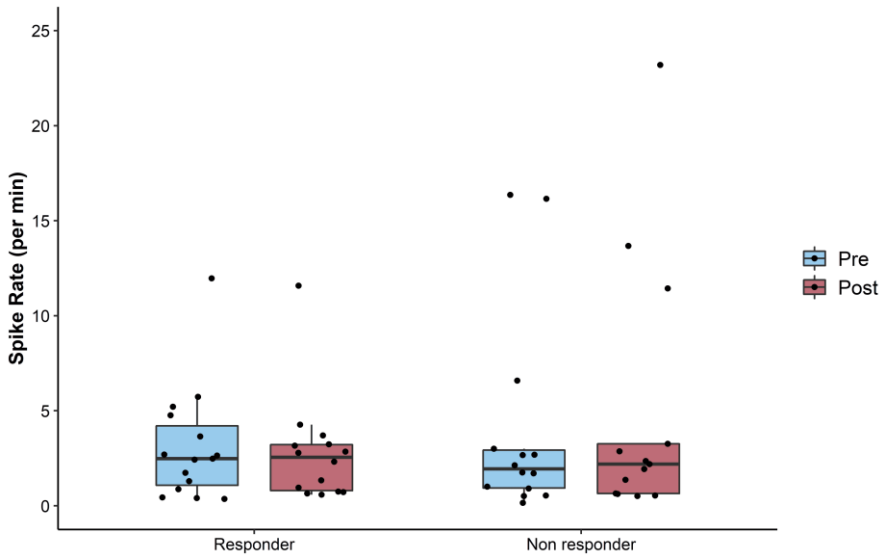


**Figure A.1. Comparison of spike rates before and after tDCS treatment cycle for responder and non-responder epilepsy patients.**

# Appendix B

## *Study 3: Periodic and aperiodic features of PSD changes after tDCS*

In study 3, we investigated the changes in power spectral density (PSD) before and after each tDCS cycle per region and per frequency band in patients. The results were presented in 4.3. Our aim was to investigate the changes after tDCS of both periodic and aperiodic spectrum components, including exponent and offset, using the Fitting Oscillations and One-Over-F (FOOOF) method in Matlab (Donoghue *et al.*, 2020). While the periodic component results were in line with PSD findings at the group level, substantial inter-individual variability was observed in the aperiodic component. This variability complicated interpretations for group comparisons, especially between Responder and Non-responder groups. Specifically, in study 3, there were five responder patients and nine non-responders. Consequently, we conducted individual-level analyses. Here, we illustrate one specific responder case (patient 15). We compared periodic and aperiodic components separately before and after the study—specifically, before the initial tDCS stimulation and after the final tDCS session of the third cycle (Figure B1).

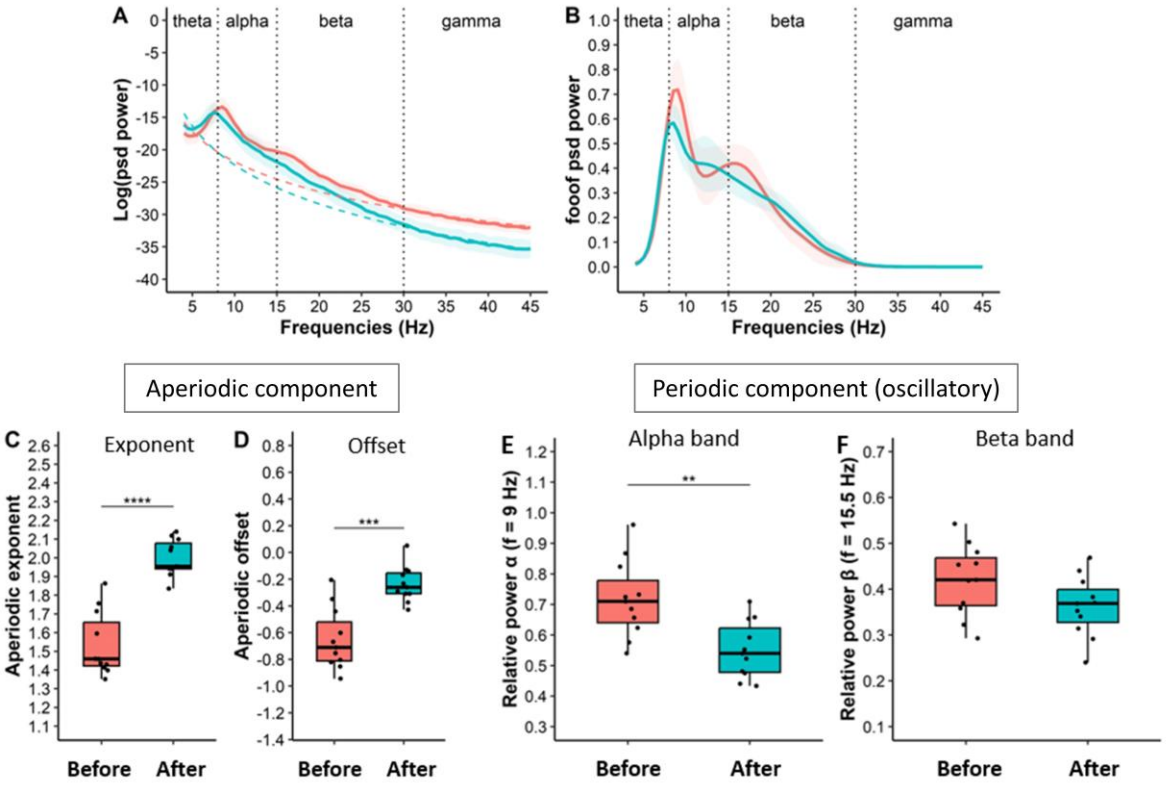


**Figure B1. Individual analysis of spectral components before and after the tDCS protocol in inhibited brain regions (patient 15)**. A: PSD curve. Mean and standard variation of PSD in inhibited regions with aperiodic fitting curve (dotted) from the Fitting Oscillations and One-Over F (FOOOF) algorithm. B: Oscillatory component in which aperiodic activity has been removed. Peaks in alpha and beta bands are present in this

case. C and D: Aperiodic exponent and offset. Boxplots representing exponent (C) and offset components of the FOOOF aperiodic fit. Comparisons were done via Wilcoxon rank-sum test with a false discovery rate correction. E and F represents the relative power differences between before and after the tDCS protocol, respectively in alpha and beta bands.

It would be interesting to study the intrinsic variability of brain activity (bot inter- and intra-individual) from one period to another by repeated measurements. In addition, only one case study has examined the decomposition of the spectrum separating periodic and aperiodic components in an epileptic patient (Gerster *et al.*, 2022). The study of aperiodic components, which are thought to reflect the excitation-inhibition balance, remains to be performed in a larger epileptic population in which spike and non-spike periods would be separated to minimize their effect on spectral power.

# Index

*Beamforming, 40*

*biomarker, 21, 52, 118, 155, 160*

*connectivity, 7, 46, 47, 48, 49, 50, 51, 52, 66, 67, 68, 79, 81, 82, 84, 86, 88, 93, 94, 96, 98, 99, 100, 107, 110, 111, 116, 117, 119, 120, 123, 125, 155, 159, 160, 165*

*EEG, 4, 18, 19, 20, 22, 31, 35, 36, 37, 38, 39, 40, 41, 42, 43, 44, 45, 46, 47, 48, 49, 50, 51, 63, 64, 65, 66, 67, 68, 74, 78, 80, 82, 85, 86, 88, 89, 90, 91, 92, 93, 95, 99, 118, 119, 130, 144, 146, 148, 149, 150, 152, 155, 159, 160, 162, 198*

*electric field, 28, 29, 30, 31, 32, 34, 35, 56, 57, 60, 65, 69, 83, 87, 88, 107, 127, 128, 129, 138, 144, 146, 162, 163, 164*

*electrical stimulation, 21, 23, 24, 26, 27, 32, 55, 58, 138*

*Epilepsy, 4, 5, 15, 16, 18, 19, 22, 23, 30, 35, 42, 53, 55, 56, 63, 66, 85, 105, 121, 126, 128, 138, 150*

*epileptogenic zone, 4, 17, 19, 21, 48, 54, 55, 56, 66, 80, 86, 87, 88, 90, 91, 97, 107, 118, 119, 127, 128, 129, 131, 132, 136, 137, 143, 144, 147, 155, 156, 162, 164*

*epileptogenicity, 17, 21, 44, 45, 49, 51, 60, 90, 92, 127, 130, 131, 134, 147*

*Epileptogenicity, 21, 130*

*Focal, 15, 16, 17, 89, 121, 150*

*FOOOF, 45, 115*

*hyperpolarization, 28, 29, 30, 33, 58, 70, 71, 87, 128*

*ICA, 41, 93, 109, 198*

*IEDs, 18, 30, 31, 38, 42, 44, 63, 64, 65, 67*

*machine learning, 21, 155, 160, 165*

*MEG, 5, 20, 36, 37, 38, 39, 41, 43, 46, 47, 48, 51, 66, 82, 105, 106, 107, 108, 109, 110, 116, 119, 120, 155, 159*

*Multichannel, 4, 5, 31, 32, 68, 81, 85, 90, 96, 97, 105, 108, 113, 115, 117, 119, 142, 146, 150, 156*

*network, 4, 16, 17, 23, 24, 26, 35, 46, 47, 48, 50, 55, 59, 66, 67, 68, 79, 80, 81, 82, 83, 87, 98, 106, 107, 108, 110, 111, 112, 119, 127, 129,*

*131, 135, 137, 138, 153, 155, 159, 160, 161, 163, 164, 165*

*neuromodulation, 22, 23, 24, 27, 54, 55, 65, 81, 97, 99, 128, 144, 152, 158*

*neurostimulation, 18, 25, 28, 30, 55, 67, 118, 119*

*Non-invasive, 19, 25, 27, 35, 144*

*propagation, 17, 21, 23, 32, 47, 48, 49, 50, 66, 68, 69, 75, 80, 119, 127, 129, 131, 135*

*PSD, 45, 111, 113, 114, 118, 119, 124*

*safety, 24, 26, 30, 32, 60, 65, 74, 79, 81, 97, 98, 100, 101, 112, 113, 132, 151, 152, 156*

*SEEG, 5, 20, 21, 22, 34, 42, 49, 50, 51, 56, 65, 66, 76, 80, 86, 87, 88, 89, 90, 91, 97, 98, 100, 107, 117, 119, 121, 129, 130, 131, 139, 146, 147, 150, 155, 156, 163, 164, 165*

*seizure, 16, 17, 18, 19, 21, 22, 23, 24, 25, 26, 30, 31, 42, 45, 49, 51, 52, 54, 55, 59, 61, 65, 66, 68, 69, 71, 73, 74, 75, 78, 81, 86, 90, 92, 94, 95, 97, 98, 99, 100, 109, 112, 113, 117, 118, 119, 120, 127, 128, 130, 132, 134, 136, 137, 138, 139, 143, 144, 145, 147, 149, 150, 151, 152, 153, 155, 156, 157, 158, 159, 160, 161, 162, 164, 165*

*source, 38, 39, 40, 41, 42, 49, 50, 51, 55, 100, 106, 109, 110, 111, 116, 117, 119, 120, 124, 125, 130, 155, 159*

*Source reconstruction, 40*

*spikes, 18, 38, 43, 44, 93, 95*

*surgery, 18, 20, 21, 22, 25, 44, 55, 79, 86, 87, 88, 99, 100, 107, 143, 144, 151, 152, 157*

*synchronization, 41, 42, 45, 46, 47, 48, 66, 67, 119, 159*

*tACS, 26, 27, 28, 29, 33, 51, 56, 63, 64, 65, 74, 75, 76, 77, 81, 82*

*target, 23, 24, 30, 31, 32, 34, 35, 41, 57, 60, 76, 78, 81, 82, 84, 86, 87, 90, 97, 98, 101, 102, 103, 104, 106, 107, 108, 109, 117, 129, 130, 145, 146, 163*

*tDCS, 4, 5, 7, 26, 27, 28, 29, 30, 31, 32, 33, 34, 51, 52, 54, 56, 59, 60, 61, 62, 63, 64, 65, 67, 68, 70, 71, 73, 74, 77, 78, 79, 81, 82, 83, 84, 85, 86, 87, 88, 89, 90, 91, 92, 94, 95, 96, 97, 98, 99, 100, 101, 104, 105, 106, 107, 108, 109, 110, 111, 112, 113, 114, 115, 116, 117, 118, 119, 120, 122, 123, 124, 125, 126, 127, 128, 129, 130, 131, 132, 134, 135, 136, 137, 138, 139, 142, 143, 144, 145, 146, 147, 148, 149, 150, 151, 152, 153, 155, 156, 157, 158, 159, 160, 161, 162, 164, 165, 198*

*tES, 26, 27, 28, 29, 30, 32, 33, 34, 35, 51, 54, 55, 56, 57, 58, 59, 61, 63, 64, 65, 67, 68, 69, 70, 71, 73, 74, 75, 76, 77, 78, 79, 80, 81, 82, 83, 84*